Cellulose Based Novel Coating System

Cameron Tristram

A thesis submitted in fulfilment of the requirements for the degree of PhD in Chemical and Materials Engineering, The University of Auckland 2014

Abstract

Cellulose esters (CEs) were investigated as binders for use in a water-based, architectural coating application. A series of per-esterified CEs were synthesised incorporating levulinic acid onto the cellulosic backbone. Levulinic acid is a keto acid which can be derived from carbohydrate biomass and is recognised as a platform molecule to support "green chemistry". Incorporation of the levulinyl species onto the cellulose chain proceeded *via* an unexpected esterification pathway, involving a series of γ-valerolactones. The rate of incorporation of levulinic acid (C_5) was unexpectedly high compared with that of similar short chain aliphatic acids (C_4-C_6) when using equivalent reaction conditions.

From the series of mixed levulinyl cellulose ester (levulinyl-CE) derivatives prepared, a lead candidate was chosen based on the combination of desirable physical attributes, ease of manufacture and cost-effective production. This lead candidate was butyryl levulinyl acetyl cellulose (BLAC) – a novel tri-functionalised CE, the first of these to be reported. The scalable nature and applicability of the process to industrial manufacture was demonstrated by the production of a levulinyl-CE at the 1 kg scale.

The presence of the levulinate functionality provided a ketone moiety that was amenable to further chemical modification. This unusual feature in a CE was utilised to further modify the physical attributes of the polymer. Short chain polyethylene glycol moieties were attached not only to demonstrate the utility of the ketone functionality, but also to internally plasticise the polymer, thereby lowering the T_g. These plasticising groups were linked onto the levulinyl-CE *via* an oxime linkage.

Carboxyl functionality was introduced onto levulinyl-CEs using an *O*-(carboxymethyl)hydroxyl amine to generate ionisable functionality on the polymer which enabled the formation of stable aqueous dispersions. These dispersions were produced using a high energy T-mixer, designed specifically for this project. This generated surfactant-free aqueous dispersions consisting of a self-stabilised polymer colloid, with a typical average particle size of 150-200 nm and a solids content of ≤ 29 wt%. The stable dispersions formed coherent films at room temperature when plasticised with sucrose acetate isobutyrate (a high renewable content plasticiser), and conformed to the Environmental Choice New Zealand specifications for a low volatile organic content binder. These dispersions were ultimately formulated into a low-sheen interior coating, indicating that the novel polymers generated have the potential to be incorporated as a binder in a new commercial line of renewable architectural paints.

Declaration and Copyright

1. M. Glenny, C. Gooch, S. Hinkley, J. Mason, C. Tristram, D. Williams. *Organic compounds.* Patent application WO2013085397 A1, PCT/NZ2012/000228.
2. C. Tristram, G. Gainsford, S. Hinkley. *Acetoxy-γ-valerolactone*. Acta Cryst. (2013). E69, 0952.
3. S. Hinkley, C. Tristram. *Novel renewable polymers for coating applications*. Conference proceeding, Surface Coatings Association New Zealand (2013).
4. C. Tristram, S. Hinkley, J. Mason, I. Sims, D. Williams. *Novel renewable architectural coating*. Conference proceeding, 34th Australasian Polymer Symposium (2013).
5. S. Hinkley, M. Glenny, C. Tristram. *Waterborne compositions*. New Zealand Patent Application No. 615465.
6. C. Tristram, J. Mason, I. Sims, D. Williams, S. Hinkley. *Doubly renewable cellulose polymer for water-based architectural coatings*. Article under review with ChemSusChem.

Acknowledgements

I would firstly like to thank Simon Hinkley for his time, effort and guidance over the course of this project and in the preparation of the final document - I am eternally grateful for all of your advice and support. Thanks to Mark Glenny at Resene Paints Ltd for his technical support throughout the project and Ashton Partridge (University of Auckland) for his contribution.

Finally, I would like to thank the entire Carbohydrate Chemistry staff (Callaghan Innovation) and in particular the people that have worked on the renewable coatings program for the positive and enjoyable working environment and for helping out when called upon.

Table of Contents

List of Tables

List of Figures

List of Acronyms

AGU – Anhydroglucose unit
AMP-95 – 2-Amino-2-methyl-1-propanol
α-AL – Alpha-angelica lactone
β-AL – Beta-angelica lactone
ASTM – American society for testing and materials
b.p. – Boiling point
BLAC – Butyryl levulinyl acetyl cellulose
CA – Cellulose acetate
CAB – Cellulose acetate butyrate
CAP – Cellulose acetate propionate
CAH – Cellulose acetate hexanoate
CE – Cellulose ester
CMC – Carboxyl methyl cellulose
CMCE – Carboxy methyl cellulose ester
CMCAB – Carboxy methyl cellulose acetate butyrate
CTA – Cellulose triacetate
CTB – Cellulose tributyrate
CTH – Cellulose trihexanoate
CTLev – Cellulose trilevulinate
DP – Degree of polymerisation
DCE – Dichloroethane
DCM – Dichloromethane
DEG – Diethylene glycol
DMAc – Dimethylacetamide
DMEA – Dimethylethanolamine
DMSO – Dimethyl sulfoxide
DMF – Dimethylformamide
DMTA – Dynamic mechanical thermal analysis
DSC – Differential scanning calorimetry
DS – Degree of substitution
DS-Ac – Degree of substitution - acetate
DS-But – Degree of substitution - butyrate
DS-Lev – Degree of substitution - levulinate
DS-Prop – Degree of substitution - propionate
DS-Total – Degree of substitution - total
DS-OH – Degree of substitution - hydroxyl
ECNZ – Environmental Choice New Zealand
Eq|OH – Equivalents per hydroxyl
GC – Gas chromatography
T_g – Glass transition temperature
HA – Hexanoic acid
OH – Hydroxyl
HMF – 5-Hydroxymethylfurfural
HMBC – Heteronuclear multiple-bond correlation
HPLC – High-performance liquid chromatography
HSQC – Heteronuclear single quantum correlation
LA – Levulinic acid
LAC – Levulinyl acetyl cellulose
LBC – Levulinyl butyryl cellulose
LVC – Levulinyl valeryl cellulose
MSA – Methane sulfonic acid
MTHF – Methyltetrahydrofuran
MIBK – Methyl isobutyl ketone
MFFT – Minimum film forming temperature
NMR – Nuclear magnetic resonance
O/W – Oil in Water
PSD – Particle size distribution
PEG – Polyethylene glycol
PTFE – Polytetrafluoroethylene
PU – Polyurethane
PnB – Propylene glycol n-butyl ether
RB – Round bottom
RT – Room temperature
SAIB – Sucrose acetate isobutyrate
SEM – Scanning electron microscopy
TEA – Triethylamine
TFA – Trifluoroacetic acid
THF – Tetrahydrofuran
pTSA – Para-toluenesulfonic acid
TPA – Total peak area
VA – Valeric acid
VOC – Volatile organic compound
WYPNZ – What's your problem New Zealand

List of Key Terms

Architectural coating – paint systems for use as an interior and/or exterior house paint
Binder or binder system – film forming component of a paint
High-performance coating – coating system with additional benefits such as high gloss, extreme wear capability, fire retardance, etc

1 Introduction

1.1 Project origin

In 2009 Industrial Research Limited (IRL) ran a competition entitled "What's your problem New Zealand?" (WYPNZ). The aim of this competition was to raise the profile of research and development in New Zealand. Businesses were invited to submit research proposals for the development of high value products, where the winning contender would receive $1,000,000 to develop their research concept. Of the 108 entrants, Resene Paints Ltd won with the concept to develop a water-based paint binder, of high renewable content, that could be formulated into an architectural coating suitable for interior applications. Resene Paints Ltd had identified a significant market opportunity for the development of such a coatings binder, with the long-term goal of producing a high-performance product capable of competing with acrylic binder systems. Waterborne acrylic binders are the industry standard for water-based architectural coatings owing to their ease of use, cost-effective manufacture and versatility in a range of applications. A major obstacle to overcome, aside from the technical challenges for all new products entering a competitive market place, is customer acceptance. Acrylic polymer water-based coatings are a proven technology experiencing unrivalled market confidence; they can deliver the performance and properties required in the specific application for which the paint system has been designed, and in a cost-effective manner. However, as the world becomes more concerned with depleting oil reserves and greenhouse gas emissions, there is a growing demand for products derived from renewable resources. Resene Paints Ltd therefore believed that the increasing levels of consumer awareness presented a significant market opportunity, and planned to use product renewability as the main marketing tool to gain consumer acceptance.

1.2 Project targets

At the time when the work detailed in this thesis began, research on the WYPNZ project was already underway at IRL. Two specific restrictions were in place regarding the development of a novel, high renewable content polymer for use as the binder, or "glue", in a paint formulation. The first constraint was specified by Resene Paints Ltd who had already pre-chosen cellulose as the renewable raw material for the project. Secondly, initial

research into derivatisation of the cellulose chain had identified levulinic acid (LA) as a useful functional group to incorporate into the cellulose backbone, for reasons that will be discussed.

At the start of this project, the following question was postulated: "What would replace petrochemical-based polymers if world production stopped tomorrow?" Resene Paints Ltd had the foresight to initiate research into developing alternative polymers that were not derived from petrochemical sources. The concept driving this project hinged on the proposition that cellulose-derived polymers had stalled in their development as a result of the effectiveness and cost-competitive nature of acrylics. This work therefore reassesses the potential of new cellulose-derived polymers as an alternative to existing polymer technologies being used as water-based paint binders. In addition, the potential utilisation of waste streams could provide a low-cost source of the cellulose starting materials providing an opportunity to create value-added products.

As this research progressed, a series of novel cellulose esters (CEs) were developed as polymer binders that were formulated into water-based architectural coatings. Levulinic acid (LA) was incorporated into the cellulose ester structure using a unique esterification method to generate a novel range of mixed levulinyl cellulose esters (levulinyl-CEs). The use of LA was advantageous as the structure provided an additional reactive centre for further derivatisation. Furthermore, LA is also a renewable material derived from carbohydrate biomass and can be directly produced from cellulose (discussed further in Section 1.9).

The goal of this program was to demonstrate that a novel cellulose derivative could function as a water-based paint binder. The development targets to reach this objective were as follows:

- Understanding and developing the reaction chemistry involved in generating levulinyl-CEs, allowing precise product control and to reproducibly generate a consistent product. The levulinyl-CE specifications are given in Section 4.1.
- Synthesis of a levulinyl-CE at pilot plant scale to demonstrate the scalability of the chemistry in a manufacturing environment.

- Develop an aqueous dispersion of a levulinyl-CE that could be utilised as a coatings binder in a composition, further criteria given in Section 8.2.
- Formulate a proof of concept architectural ceiling or wall coating.

Environmental and personal exposure concerns related to the detrimental effects of volatile organic compounds (VOCs) have led to the demand and formulation of low VOC architectural coatings. A requirement set out by our industry partners (Resene Paints Ltd) was to formulate the coating to meet the New Zealand low VOC coatings standard. Environmental Choice New Zealand (ECNZ) provides product specifications for a range of industries to ensure acceptable environmental performance. Products that meet their specifications receive the "Eco-label" which can be used as a marketing tool to attract the environmentally aware consumer market. The ECNZ specification for a low VOC interior architectural coating was < 50 g of VOCs per litre of paint [1], a standard applied in paint formulations by our industry partner. A VOC classified by ECNZ is an organic compound which has a vapour pressure of > 0.1 mm Hg at 25 °C; compounds that have a boiling point of > 250 °C at 101.3 kPa are not considered to be VOCs [2]. Therefore, in order to meet the low VOC specification it was critical that this project delivered a water-based paint formulation.

1.3 Waterborne acrylic binders

Waterborne acrylic latexes are the industry standard for water-based interior architectural coating binders. Eleven billion litres of both waterborne and solventborne acrylic binders are produced for the architectural paint market annually [3]. However, the proportion of waterborne acrylics is continuously increasing as new markets adopt waterborne technology. Commercially, water-based interior architectural coatings are, with limited exceptions, formulated using waterborne acrylic latexes as the paint binder. An acrylic latex is a stable polymer colloid in a continuous water phase [4] with a typical particle size in the range of 0.1-3.0 μm. The colloid suspension is maintained by Brownian motion and is typically stabilised by surfactants to inhibit particle agglomeration [5]. The raw acrylic latexes are usually formulated in the range of 45-55 wt% solids.

Since 1953, when the first acrylic latex was produced, there have been considerable advances in acrylic technology. One of the defining characteristics of the technology is the ability to tailor the properties of an acrylic polymer binder to a specific application [5]. This is a function of the range of acrylic monomers available and the development of the polymerisation technology that permits control of the particle structure and morphology. The ability to control both the polymer and particle architecture, combined with the variety of the monomers available creates the manifold opportunities for waterborne acrylics.

A basic acrylic latex has an average sale price of NZD$ 3 per litre which gives them a high performance to cost ratio in comparison to other binder systems [3]. However, this price can increase greatly depending on the monomer types used and their relative level of incorporation. The cost of the generic acrylic monomer building blocks, methyl methacrylate and butyl acrylate, has risen sharply over the last 18-24 months due to increasing oil prices although work on developing renewable acrylic monomers is currently underway [6, 7]. Due to the increased raw material cost for acrylics and consumer demand for more environmentally friendly products, it is timely to develop a novel and renewable binder system to compete with waterborne acrylics. However, in order to rival the acrylic binder market the proposed cellulose-based system must perform as well if not better than the current technology.

1.3.1 General preparation of an acrylic latex

Acrylic latex dispersions are produced by emulsion polymerisation as discussed by Penboss [5] and require four key components: monomer (e.g. methylmethacrylate, Figure 1-1), surfactant, initiator and water. An oil in water (O/W) emulsion is formed with the monomer (discontinuous phase) and water (continuous phase) using a high speed disperser, and the emulsion is generally stabilised with a mixture of non-ionic and anionic surfactants. The surfactant is also present to generate micelles which stabilise the growing acrylic polymer particles. A free-radical initiator is then added to start the polymerisation process within the micelles. As the polymer grows the monomer migrates from the monomer droplet into the micelle, generating a high molecular weight acrylic-polymer latex particle (Figure 1-2).

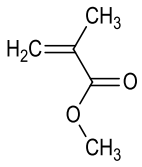

Figure 1-1 Methylmethacrylate monomer, an example of a common monomer used in acrylic latex production.

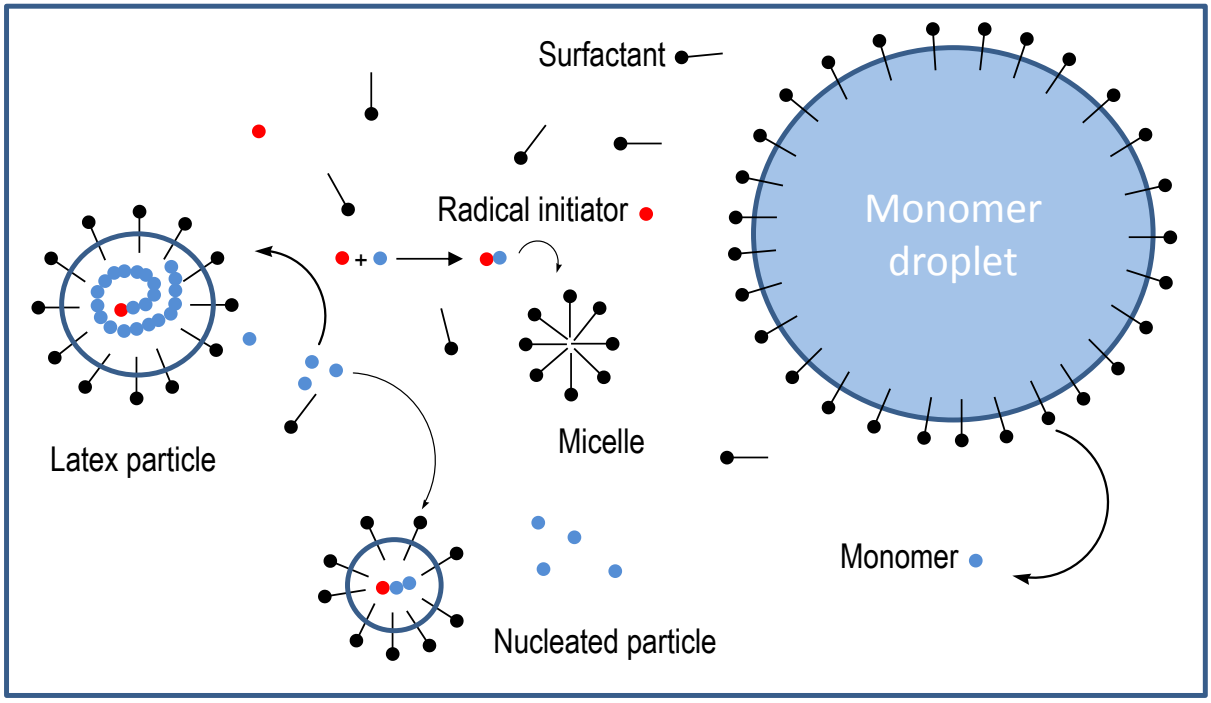

Figure 1-2 Emulsion polymerisation schematic.

1.3.2 Waterborne polymer latex film forming mechanism

The mechanism for polymer latex film formation is covered in detail by Keddie and Routh [4, 8], and is displayed graphically in Figure 1-3. The film formation process is completely reliant on overcoming the repulsive forces associated with polymer latex particles and begins with the evaporation of the continuous phase forcing the latex particles into a random close packed state, ultimately to a volume fraction of 0.64 (mono dispersed spheres, randomly close packed) [9]. This is followed by particle coalescence to form a continuous polymer film where the driving force is the reduction of surface area or free energy created by the close packing of the polymer particles. Based on the capillary theory of Brown [5, 10] the capillary forces generated by the evaporation of the continuous

phase from the interstitial voids causes polymer particle deformation and filling of the void space. At this point the film becomes optically transparent since light is no longer scattered by regions of inhomogeneity.

The glass transition temperature (T_g) is a second order thermal transition where an amorphous polymer moves from a glassy to a rubber state and is fundamental to coalescence. The process of film formation is resisted by the viscous and elastic deformation of the polymer particle. At temperatures below the T_g of the polymer, the forces involved in film formation are insufficient to deform the hard polymer particle resulting in a powdery residue on evaporation of the continuous phase. The minimum film forming temperature (MFFT) is the minimum temperature required for coalescence to occur and for the film to become optically transparent. At a temperature above the T_g of the polymer the particles will deform and coalesce, and the polymer chains will diffuse across the grain boundaries by the reptation[1] process [4] thus forming a homogeneous continuous film.

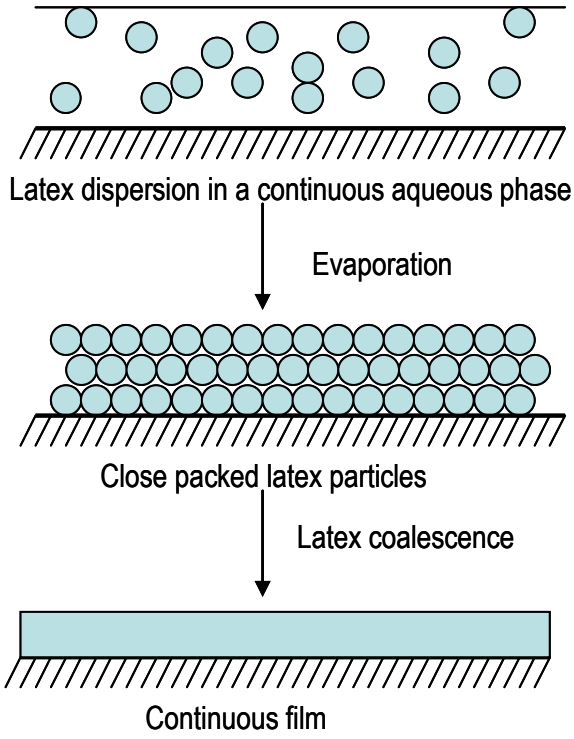

Figure 1-3 General latex film formation mechanism.

[1] Reptation is the process where intertwined and entangled polymer chains diffuse in a molten state.

As discussed above, the T_g of a polymer and the MFFT of the associated polymer latex are closely related. When a latex is generated using a high T_g polymer the MFFT can be artificially lowered using a number of methods [5]. Plasticisers may be used to lower the T_g of the polymer; these are small polymer-miscible compounds which are retained within the polymer, disrupting the polymer's structure and generating an increase in free volume, thereby increasing chain flexibility and movement. Plasticisers permanently lower the polymer's T_g and therefore the corresponding dried film will also remain in a softened state. In contrast to this, coalescing solvents have a temporary effect of softening the polymer particles (reducing the T_g) and permitting film formation at a lower temperature than the polymer alone. Over time these solvents diffuse and evaporate out of the film and therefore do not decrease the ultimate hardness of the film. In addition to using plasticisers or coalescing solvents, reducing the particle size of the polymer latex increases the capillary forces on the polymer particles during coalescence, which also serves to reduce the MFFT.

1.4 Cellulose

Cellulose was chosen as the raw material for this project. It is a renewable bio-polymer, with an estimated global annual production of 10^{11}-10^{12} tons [11]. Since first being discovered by French chemist Anselme Payen in 1838, the research into cellulose and cellulose-derived products is expansive [11-13]. Modern polymer science can be traced back to cellulose and some of the first synthetic coatings, fibres and films were based on cellulose derivatives [14]. The majority of the early research focussed on the synthesis of cellulose derivatives for material processing and product manufacture.

Cellulose is a component of all plant material. The most common commercial sources of cellulose are lignocellulose (forestry material, hard and soft woods) and cotton. Lignocellulose is a structural composite material consisting of cellulose, hemicellulose and lignin. Cellulose is a linear polymer, the structure of which is discussed below in Section 1.4.1, while hemicellulose is a branched polysaccharide, largely comprised of xylans and glucomannans, and is based on pentose and hexose sugars units [15, 16]. Lignin is a three-dimensional amorphous polymer comprised of methoxylated phenylpropane monomer units [17]. The lignocellulose

composite is formed by groups of cellulose chains forming microfibrils which are bound by lignin; this component is responsible for the strength, rigidity and protection of plants. The relative amounts of cellulose, hemicellulose and lignin varies between plant types, for example cotton has a cellulose content of 95% compared to wheat straws which have only 30% cellulose [11]. An alternative less abundant, but chemically pure, source of cellulose is bacterial cellulose [18, 19].

1.4.1 Cellulose structure

Cellulose is a linear polysaccharide with the chain length depending on the source material. The degree of polymerisation (DP) for the cellulose chain can be as high as 15,000 monomer units giving a molecular weight of $2.4x10^6$ g/mol (cotton) [12]. The cellulose chain is a homo-polymer comprised of repeating D-anhydroglucopyranose monomer units linked by β-1,4 glucosidic bonds (Figure 1-4) [11]. The anhydroglucose unit (AGU) monomer is a 6 carbon, 6 membered hemi-acetal ring containing a primary hydroxyl at the C-6 position and two secondary hydroxyls at C-2 and C-3, while C-1 and C-4 are the glucosidic linkage sites. The end groups of the polymer are classed as non-reducing at the C-4 position (terminated by a secondary hydroxyl) or reducing at the C-1 position, terminated by an unsubstituted anomeric hemi-acetal, which may have α- or β-orientation at this anomeric position. For the hemi-acetal α-anomer the hydroxyl is in the axial position while for the β anomer the hydroxyl is in the equatorial position.

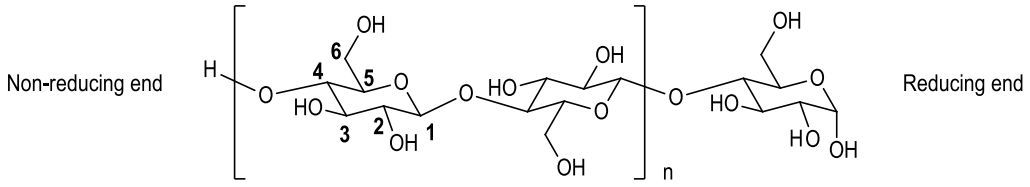

Figure 1-4 Cellulose structure and numbering; reducing end shown as the α anomer.

The free pendent hydroxyl groups along the cellulose chain are hydrogen bonding sites. An extensive inter- and intra-molecular hydrogen bonding network is formed between cellulose chains generating a rigid organised structure. As a result, cellulose contains both crystalline and amorphous regions. There are six crystalline polymorphs (I, II, III_I, III_{II}, IV_I, IV_{II}) some of which can be interconverted (Figure 1-5) [11, 12]. Polymorph I, which

exists as both an α and β form, and is the native crystalline structure of cellulose, can be irreversibly converted to the more thermodynamically stable polymorph II by both regeneration (see Section 1.5.1) and mercerisation[2] processes [12]. Cellulose I and II have different crystal structures as a result of unique hydrogen bonding arrangements as discussed in the literature [20-22]. Treatment of native crystalline cellulose with liquid ammonia reversibly converts polymorph I and II into III_I and III_{II} respectively, and further treatment of these two polymorphs with glycerol (206 °C) converts them to the corresponding crystalline polymorphs IV_I and IV_{II} (Figure 1-5). The amorphous region of cellulose is mainly found at the surface of the microfibril [23]. The percentage this region represents of the microfibril is a function of fibril dimension; thinner fibrils contain a higher proportion of amorphous cellulose and therefore the levels of amorphous cellulose present will vary from source to source.

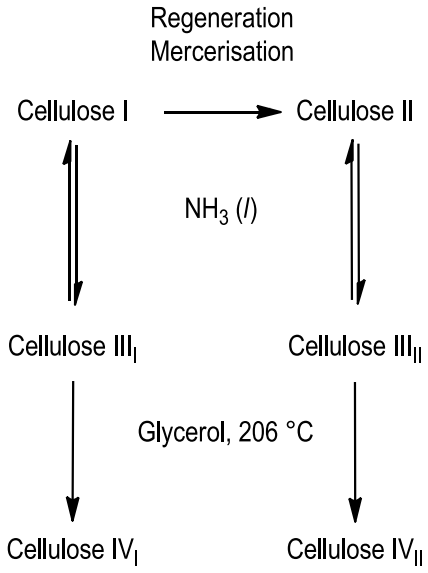

Figure 1-5 Crystalline cellulose polymorph conversions.

Cellulose is a highly polar polymer which is insoluble in most solvent systems, including water, due to the strong intra- and inter-molecular hydrogen bonding network. In spectacular contrast, the amylopectin portion of starch is a water-soluble polymer, but only differs by a α-1,4 glucosidic linkage and structural branching [24]. Thus the highly ordered, tightly hydrogen bonded structure of cellulose creates an inherently unreactive polymer.

[2] Mercerisation is the process of steeping cellulose in a sodium hydroxide solution.

1.5 Derivatised cellulose

To utilise the polymeric structure of cellulose, it must be processable into fibres, films, or mouldable components. However, due to the strong hydrogen bonding network within cellulose, conventional polymer processing techniques such as melts or solution processing cannot be used. The decomposition temperature of cellulose is lower than its melting temperature and it is only soluble in a very limited set of complex solvent systems such as ionic liquids and traditional solvents for cellulose dissolution such as LiCl and DMAc [25-27].

Chemical derivatisation of cellulose can be readily completed by reaction of the free hydroxyl groups on the cellulose chain. The degree of substitution (DS) refers to the number of hydroxyl sites that have been chemically modified and the value is an average per AGU. Each cellulose AGU monomer unit has three free hydroxyl sites that can be chemically modified and therefore the DS can range from 0 to 3. The DS is an important factor as many of the properties of cellulose derivatives are a function of the DS as well as the substituent being incorporated. There are three common commercial methods used to derivatise cellulose: regeneration, etherification and esterification. It is of note that these processes have remained largely unchanged since they were discovered [28].

1.5.1 Regenerated cellulose

The viscose process was developed as a method to provide cellulose in a form suitable for re-processing and was first reported by Cross *et al.* in 1892 and is discussed in detail by Kline [29]. The process begins with steeping the cellulose fibres in a strong caustic solution (15% NaOH), followed by the reaction of cellulose with carbon disulfide (CS_2) generating cellulose xanthate (Figure 1-6). Approximately one xanthate group is incorporated per two AGUs generating a cellulose product with a DS of 0.5 [14].

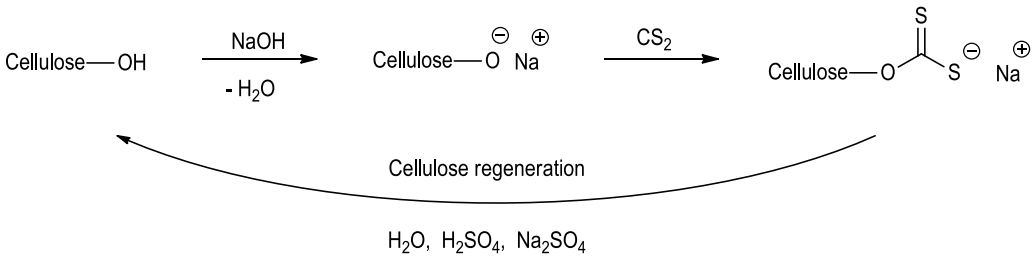

Figure 1-6 Regenerated cellulose using the viscose method.

The xanthate material is then spun into fibres (rayon) or cast into films (cellophane), where cellulose is regenerated by hydrolysis of the xanthate groups. The rayon produced can be spun and woven using conventional natural fibre techniques. Regenerated cellulose has been used in a wide range of applications; one of the more interesting being sausage casings [30].

At present, the viscose process has lost favour due to the safety and environmental concerns caused by using the highly flammable and toxic reactant CS_2. Since the early 1990s the Tencel and Lenzing Lyocell processes have been used for regenerated cellulose fibre production [31]. These methods are based on the dissolution of cellulose in *N*-methylmorpholine-*N*-oxide (NMMO) as discussed by Diener and Raouzeos [32] and the current global production is 120,000 tons per year.

1.5.2 Etherification of cellulose

Chemical derivatisation of cellulose to form cellulose ethers was first described at the turn of the 20th century and since their inception they have found their way into many commercial niches. They are generated by the reaction of cellulose with an alkylating agent under basic conditions (Figure 1-7) and can be prepared using both heterogeneous and homogeneous reaction conditions. In heterogeneous reactions the cellulose remains as a slurry (insoluble) for the entire process [33], while in a homogeneous reaction, the cellulose is pre-dissolved prior to reaction. The main advantage of the homogeneous process is product uniformity.

Commercially the heterogeneous process is used to manufacture cellulose ethers. The cellulose is first activated by steeping the fibres in a caustic solution and then slurried with the alkylating agents. A non-reactive diluent

may also be used to aid suspension of the cellulose fibres in the reaction media. Once the reaction is complete, the fibrous cellulose ether is collected and washed to remove residual reagents and salts. A particular point to note for this process is that apart from alkylation, there is no modification of the molecular size of the original polymer. Hence, the reaction product and its physical characteristics, specifically viscosity, are very strongly dependent on the raw material and thus the preparation of the cellulosic feed stock is strictly controlled, down to the month the trees are harvested [34].

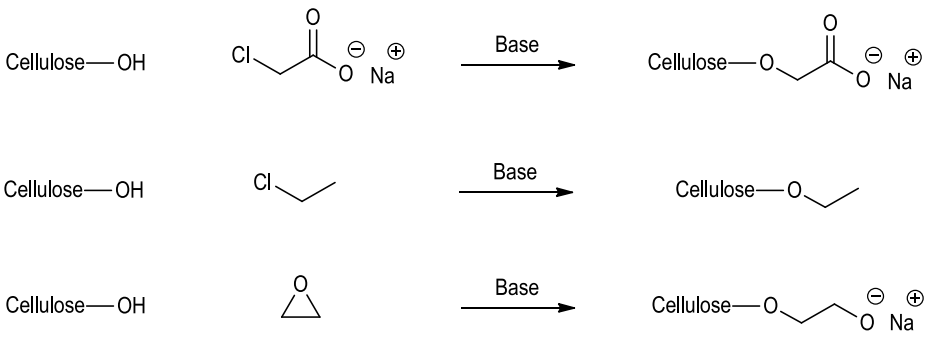

Figure 1-7 Cellulose ester alkylating agents and their products.

1.5.3 Esterification of cellulose

Cellulose esters were among the first synthetic polymers to be manufactured on a commercial scale. Polysaccharide nitrates are reported to have first been prepared by Braconnot in 1832 with the reaction of starch and concentrated nitric acid [35]. Following this, cellulose nitrates were developed and enjoyed widespread application as solventborne lacquers, explosives and films. Celluloid has long been regarded as the first synthetic thermoplastic. Made from cellulose nitrate plasticised with camphor, this produced an easily mouldable product [36, 37]. Celluloid also has wide ranging applications and has been extensively used to manufacture consumer products such as toys and hair combs.

Cellulose acetate (CA) was first made by Schutzenberger in 1865 by heating cellulose in a sealed glass tube at 130-140°C with acetic anhydride [14]. The general chemistry has not changed since 1879 when Franchimont

used sulfuric acid as a catalyst allowing the reaction to proceed at room temperature [14]. Acetic acid itself displays very limited capability for direct esterification of the cellulose fibre; after a reaction time of 500 hours, an average of only one hydroxyl in every four AGUs had been esterified [28, 38]. In contrast, formic acid will esterify cellulose directly, although the formate group is relatively labile and will be completely hydrolysed in water at 100 °C after 10 hours [39]. Therefore, for all practical purposes, acetic acid is unreactive towards cellulose and, apart from the aforementioned formic acid, no other organic acid will esterify cellulose directly.

Since the commercial manufacture of CA began it has been used in many applications. CA fibres for textile purposes showed market growth from the 1930s until the 1970s where demand then dropped away due to the increase in accessibility to other synthetic polymers such as polyesters [40]. At present, 95% of cigarette filters are made from cellulose triacetate (CTA) [40]. Mixed CEs such as cellulose acetate propionate (CAP) and cellulose acetate butyrate (CAB) are prominent additives in the coatings industry and are used for rheology control, metallic flake orientation and drying time modification, to name but a few [41]. Speciality applications in the pharmaceutical industry also exist, such as controlled drug release coatings [42].

1.5.3.1 Cellulose nitrate

In reviews published by Saunders [43] and Nikitin [28] the commercial chemistry of cellulose nitrates is discussed. Cellulose nitrates are generated by the esterification of cellulose with nitric acid in the presence of sulfuric acid and water. Ratios of sulfuric acid to nitric acid in the range 2.2:1 up to 2.7:1 generate the proposed reactive nitronium ion [31]. Careful control of the water present in the reaction is used to moderate the incorporation of the nitrate species. The end application of cellulose nitrate changes significantly with the DS as displayed in Table 1-1 [31].

Cellulose nitrate DS	Application
1.95	Moulding plastic (celluloid)
2.05-2.35	Lacquers
2.70	Explosives (gun cotton)

Table 1-1 Cellulose nitrate application with respect to DS.

Cellulose nitrates are inherently unstable, often highly flammable and in some cases explosive. Photographic film was exclusively made from cellulose nitrate but due its instability and propensity for combustion it was replaced by cellulose triacetate (CTA).

Of the three major commercial methods for derivatising cellulose that are discussed here, only one of them was deemed to be an appropriate strategy with regards to this research program. The process of regenerating cellulose simply reforms cellulose which retains the same poor solubility profile it had prior to being regenerated, thereby prohibiting further processing. Etherification of cellulose was considered, although the major drawback to this method was the accepted difficulty in producing a consistent product due to the variability of the cellulosic feed stock. The final and most promising derivatisation strategy was therefore esterification. As discussed, the formation of cellulose esters (CEs) is well documented in the literature and is a simple, effective way of modifying the cellulose polymer. In addition, the esterification process enables good control over the product obtained and was therefore chosen as the derivatisation method for this project.

1.6 Cellulose esters

There were several reasons why it was believed at the start of the project that CE chemistry would provide the level of control required to develop a novel cellulose derivative for a coatings application:

- Ready availability and low cost of anhydrides for use in the esterification reaction.
- A wide range of derivatives can be generated.
- The chemistry involved allows for full derivatisation of the free hydroxyls on the cellulose backbone.
- Control of polymer length (degree of polymerisation, DP) could permit tuning of the T_g, viscosity and solubility.
- A wide range of T_gs and mixed T_gs are observed for this class of compound (Section 1.8.2).
- The DS could be further tuned through hydrolysis which allows for the control of the solubility parameters (Section 1.7.3.2).
- Accepted manufacturing methodology.

A major aim for this project was developing a process which was readily scalable. It was therefore considered prudent to base any chemistry on existing commercial processes to provide synergy with industry, and a mechanism to fast track commercialisation. The extensive and well documented commercial production of CEs, and the points listed above, strongly suggested derivatisation of cellulose by esterification as the method of choice for this program of work.

1.7 Cellulose ester manufacture

Commercial chemical companies such as Eastman Kodak produce CEs on the multi-ton scale. Manufacture of CEs is limited to cellulose acetate (CA) and mixed CEs of cellulose acetate propionate (CAP), cellulose acetate butyrate (CAB) and cellulose acetate phthalate. As stated earlier, the commercial esterification chemistry has not changed since the sulfuric acid catalysed anhydride esterification of cellulose was first developed. The industrial process for CA production is discussed by Hummel [44] and Steinmeier [45] and involves first slurrying activated pre-treated cellulose (see Section 1.7.2 below) in the presence of the desired anhydride and catalytic sulfuric acid. This produces a viscous homogeneous solution on heating, which is then precipitated into water generating a CE as a hard white solid. There are alternative cellulose esterification methods which are discussed in Section 2, but commercial methods of manufacture will be the focus of this discussion.

1.7.1 Cellulosic raw material

De-lignified wood pulp consists of α-, β- and γ-cellulose; α-cellulose is defined as the material which is insoluble in a 17.5 wt% NaOH solution [46], while the β- and γ-cellulose forms are the short chain degraded cellulose and hemicellulose fractions which are soluble in the caustic solution [47]. Purified cellulose or highly pure unprocessed materials such as cotton linters and bacterial cellulose are almost entirely α-cellulose.

CEs are commercially produced using high purity cellulose sources [48, 49]. Cotton linters were commonly used until wood pulp processing techniques were developed to generate high purity α-cellulose. Cellulose esters

prepared from low quality, partially purified cellulose result in yellowing and false viscosities[3] during manufacture [45, 50] which can be attributed to xylan contamination [51]. Work has been carried out investigating the use of waste stream cellulose sources for cellulose ester production as a method of recycling and reducing product cost [52, 53].

Cotton linters are essentially a valuable by-product of cotton staple fibre production and are used as a raw material for cellulose production as discussed by Sczostak [54]. Ginning removes the staple fibres from the harvested cotton seed and the seed is further processed to remove the linters in a first and second cut before the seed is processed for oil and husks. The cotton linter fibre is short and thick in comparison to the cotton staple fibre. The final cotton linters are bleached and have an α-cellulose content of 99% [54]. Cotton linters account for 8.5 wt% of the total harvested cotton and are used for high quality paper and CE manufacture.

Wood is comprised of 40-47% α-cellulose, 25-35% hemicellulose and 16-31% lignin, the ranges quoted being due to variations in age and species of the wood used. In order to generate high purity α-cellulose pulp, also known as a dissolving pulp, mechanical or chemical processing is required [55]. The Kraft process developed by Dahl in 1884 [56] is the most commonly used commercial wood pulp processing technique, producing 73% of the 174.9 million tons of total wood pulp produced in 2006 [57]. The Kraft process as discussed by Smook [58] and Clayton [59] involves digesting the wood chips in a solution of sodium sulfide and sodium hydroxide, which breaks down and dissolves away lignin as well as degrading the hemicellulose into soluble fragments. This is followed by bleaching to increase whiteness and further remove any contaminants from the wood pulp. The final purified wood pulp contains between 15% and 20% hemicellulose. Pulp produced by the Kraft process is not

[3] The viscosity of a CE solution, where the CE has been produced from high grade dissolving pulp or cotton linters, can be assessed from its intrinsic viscosity. When wood pulp is used as the acetylation feed material, a higher than predicted viscosity is recorded, known as a false viscosity [44]. This affects the monitoring of the depolymerisation during the reaction which can result in the reaction time being unnecessarily extended and consequently a low molecular weight product. The high viscosity generated as a result of using low quality cellulose can also force additional reaction dilution to effect subsequent processing.

sufficiently refined for cellulose ester manufacture as the remaining hemicellulose component interferes with subsequent reactions and processing [49, 60]. High purity dissolving pulp is prepared using the pre-hydrolysis Kraft process [58, 61] where an initial acid hydrolysis step selectively hydrolyses the hemicellulose into water-soluble fragments. This step is then followed by the conventional Kraft process producing a product with an α-cellulose content of up to 98% [55].

1.7.2 Cellulose pre-treatment

The pre-treatment or pre-swelling of cellulose is an essential, well-known process to activate the cellulose to ensure even and complete esterification. Pre-swelling disrupts the inter- and intra-molecular hydrogen bonding promoting access of the reagents to the reactive hydroxyl sites. Fedale *et al.* [62] and El Seoud *et al.* [63] discuss the effect of aprotic and protic solvents on cellulose swelling and have developed a method for predicting solvent-cellulose interactions based on the solubility parameters of the solvents. The swelling and dissolution processes are controlled by the same solvent-polymer interactions, that is, both cases require the disruption of the strong hydrogen bonding network by the cellulose-solvent interactions. It has been proposed that the formation of solvent aggregates increase the inter-chain swelling. Water is a highly effective swelling agent, a feature attributed to its structure and ability to form a hydrogen bonding network [63].

The structural morphology of cellulose is critical to the degree of swelling observed. Mercerised cellulose swells more effectively than the native cellulose form; this is attributed to the change from crystalline polymorph I to II [63]. With the irreversible conversion from polymorph I to II there is an associated loss of a set of intra-molecular hydrogen bonds [63]. Mercerisation also increases fibre pore volume, as well as reducing crystallinity, producing a more disordered structure. All of these factors promote solvent access to the fibre and lead to solvent-induced swelling. Care needs to be taken so that the swollen cellulose fibres do not become excessively dry as this can cause hornification [64] which is an irreversible tightening of the fibril structure making solvent access to the hydrogen bonding network, and therefore dissolution, significantly more difficult.

Commercially, the cellulose feed stock is provided as pressed sheets, which are mechanically broken up by attrition or shredding, and then swollen in water. The water is removed by either mechanical or thermal drying methods, while maintaining a water content of between 4% and 15%. The pulp is then re-swollen by spraying or soaking the fibres in acetic acid [65, 66]. Acetylation of this material requires the addition of excess quantities of anhydride to react with the residual water still present in the treated pulp. An alternative method of water removal is by more rigorous solvent exchange where the water-swollen pulp is washed with glacial acetic acid to dehydrate the pulp [48, 67]. Small quantities of sulfuric acid are often introduced with the acetic acid to promote even esterification [68], where the sulfuric acid acts as a catalyst.

1.7.3 Cellulose esterification by the homogeneous method

Cellulose esterification on the industrial scale can be categorised into two processes, just like the cellulose ether production methods: a homogeneous or a heterogeneous process [28, 35]. The homogeneous reaction, in the context of cellulose esterification, refers to the reaction solution being homogeneous at the end of the reaction only. This can be can be further categorised into an acetic acid mediated or methylene chloride (DCM) mediated reaction [14, 69], both of which are commercially significant. The addition of solvents is not required as the reaction can be performed neat (anhydride only), although solvents can aid reaction efficiency and aid dissolution of the partially reacted products.

Cellulose esterification will be discussed with respect to generating CA; however, only small modifications to the process are needed to prepare the commercially significant mixed cellulose esters CAP and CAB. The "homogeneous process" remains heterogeneous until near the completion of the reaction when the cellulose material goes into solution as a high DS form of CA. During the course of the reaction, the cellulose peels into solution [70] as it is being esterified, resulting in a viscous homogeneous solution. The general reaction is similar for the acetic acid and DCM mediated processes. However, variations in reagent quantities and conditions for each CA production method are common [69] (Table 1-2).

In the acetic acid process, a mixture of acetic anhydride and acetic acid is cooled (−5°C) and charged concurrently with sulfuric acid catalyst (as a dilute solution in acetic acid) [69] to a slurry of cellulose pre-wetted with acetic acid [71]. The sulfuric acid solution is only added if it is not already present as part of the pre-treatment of the cellulose. The acetylation solution is cooled to counteract the initial exotherm generated by the reaction of the anhydride with residual water and to ensure the temperature does not exceed a pre-determined value causing excessive degradation of the cellulose. The reaction temperature is raised to between 30 °C and 70 °C over a 1-2 hour time period.

	Acetic acid process (kg)	**DCM process (kg)**
Cellulose (5-15% water)	3500	3500
Pre-treatment		
Glacial acetic acid	3500	1200
Acetylation		
Acetic anhydride	9500	10500
Sulfuric acid	250	35
Glacial acetic acid	24000	-
DCM	-	14000

Table 1-2 Typical reagent quantities for acetic acid and DCM mediated CA batch reactions [35].

The mechanism of sulfuric acid catalysed cellulose esterification is not completely understood, although sulfuric acid is the only catalyst that has gained commercial significance [45, 72] and can produce cellulose sulfate esters during the reaction. There are two proposed sulfuric acid catalysed cellulose esterification mechanisms discussed by Malm *et al.* [73, 74], Akim [75] and Nikitin [28]. Firstly, the reaction of sulfuric acid and acetic anhydride generates acetylsulfuric acid which has been proposed as the reactive species. Acetylsulfuric acid behaves as a mixed anhydride, acetylating cellulose and liberating sulfuric acid before the cycle repeats itself (Figure 1-8).

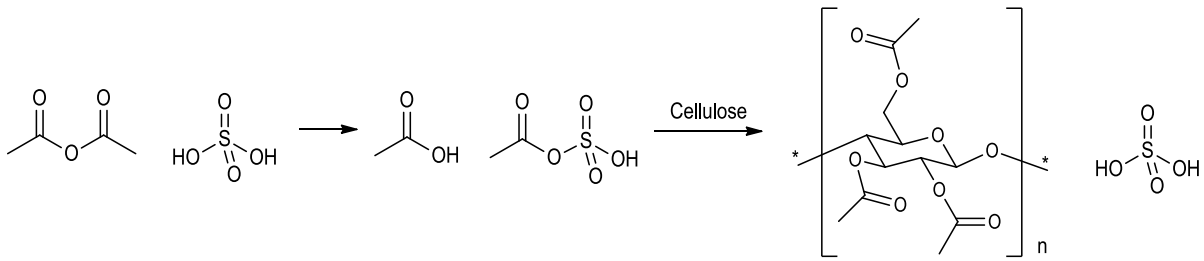

Figure 1-8 Cellulose acetylation with acetylsulfuric acid.

In the second proposed acetylation mechanism, sulfuric acid combines quickly and quantitatively with cellulose forming a cellulose sulfate ester. This then undergoes transesterification with acetic acid to form the product (Figure 1-9).

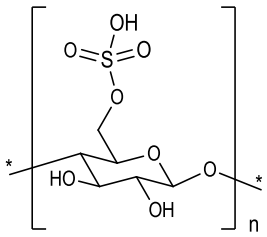

Figure 1-9 Cellulose sulfate ester.

In the methylene chloride mediated process, the DCM co-solvent serves two functions. Firstly, it is used to control the reaction temperature as the boiling point of DCM is 40 °C. The refluxing solvent removes heat energy from the reaction mixture, thereby maintaining a relatively constant reaction temperature. This temperature control method has been applied to large scale batch reactions where control of the reaction temperature is not otherwise possible. Secondly, CTA is readily soluble in DCM and a reaction with this co-solvent can generate both a per-esterified CA and a larger molecular weight product than the equivalent reagents without DCM present. In the absence of DCM (or another suitable solvent), but with the same molar proportion of acetic anhydride, the reaction gels and only shorter chain cellulose fragments can peel into the reaction media and undergo per-esterification [69]. The methylene chloride process uses approximately half the solvent content and 14% of the catalytic sulfuric acid in comparison to the acetic acid process (Table 1-2), most likely a function of the DCM being a more effective solvent for the CA product. A similar mechanism of temperature control can be achieved in the acetic acid process by utilising reduced pressure. Regulating the reaction pressure in turn

controls the reflux temperature of the acetic acid/acetic anhydride mixture and therefore the overall reaction temperature. Yamashita describes a method for a batch reactor taking advantage of this process [76].

CABs and CAPs are produced by the addition of butyric or propionic anhydride into the acetylation mixture with the acetic anhydride. The cellulose pre-treatment for these CEs may also involve addition of either butyric or propionic acid at the acetic acid activation stage depending on the DS required for either the butyrate or propionate groups.

1.7.3.1 Cellulose depolymerisation *via* acetolysis to alter DP

The cellulose degree of polymerisation (DP) is reduced during esterification as a consequence of acetolysis (depolymerisation). Acetolysis occurs in the presence of acetic acid and hydrolysis occurs in the presence of water. This process should not be confused with the hydrolysis step which involves the removal of unwanted ester functionality (see Section 1.7.3.2). The use of anhydrides generates an anhydrous reaction medium and therefore only acetolysis will occur during the reaction. In a homogeneous solution depolymerisation can be described as first order and the rate is dependent on the concentration of sulfuric acid and the reaction temperature [31]. The generally accepted mechanism describing acetolysis is shown in Figure 1-10 [48]. The process begins with the protonation of the glycosidic bridging oxygen atom, followed by cleavage of the glycosidic bond and formation of a carbonium ion on the glucose ring at the reducing end of the cellulose chain (A), and a free hydroxyl on the glucose at the non-reducing end (B). Subsequent nucleophilic attack by ROH on the carbonium ion completes the reaction mechanism.

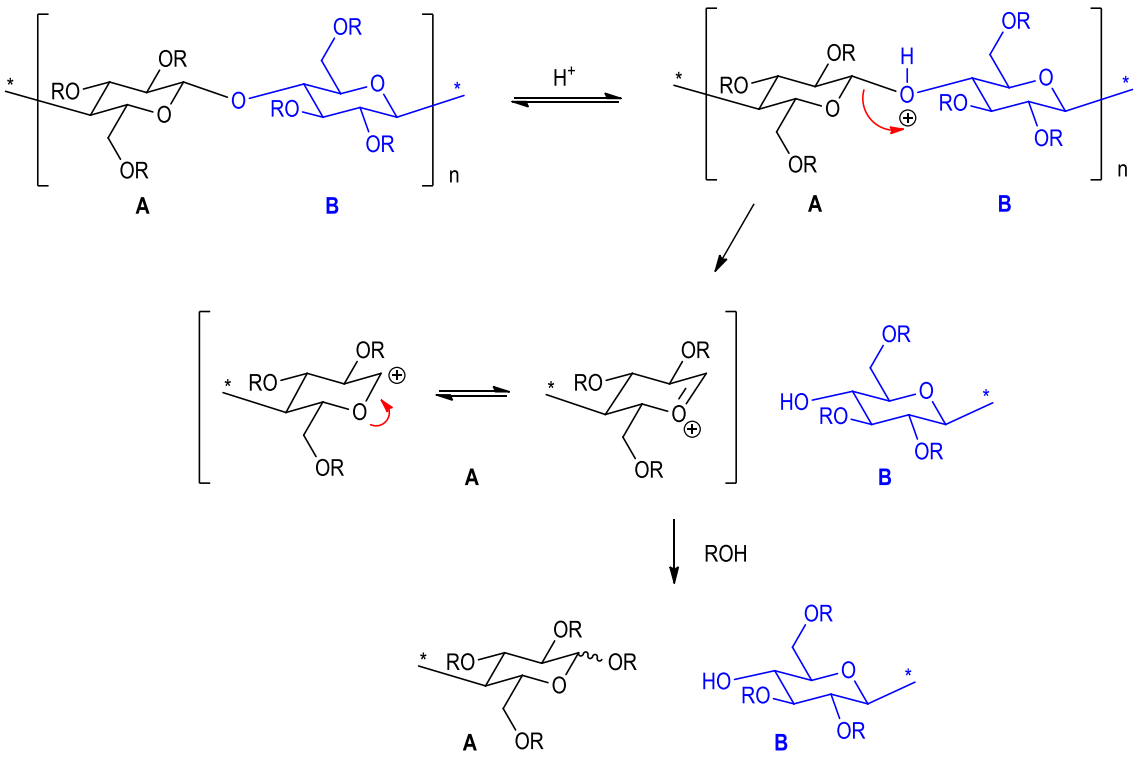

Figure 1-10 Acetolysis mechanism for CA, R= C(O)CH$_3$.

Depolymerisation of cellulose is an important concept, as the DP can have significant effects on the properties of the final CE product. The relative DP can be monitored during the reaction by viscosity measurement [28, 45]. If the desired viscosity and therefore the target DP has not been achieved, the reaction duration is increased resulting in further depolymerisation with a corresponding decrease in viscosity.

1.7.3.2 Hydrolysis step to alter the DS

Industrially, cellulose is reacted to generate a tri-ester material followed by a hydrolysis step to modify the DS to the desired level. Such hydrolysis is completed under acidic conditions where the ester carbonyl is protonated, followed by nucleophilic attack by water, overall ejecting the carboxylic acid and reforming the cellulose hydroxyl species [45], [77].

There are two hydrolysis processes used industrially to modify CTA; a sulfuric acid catalysed hydrolysis or, as it is known commercially, a catalyst-free hydrolysis which in effect uses acetic acid as the hydrolysing acid. These

processes are undertaken as a one-pot step directly after esterification. In the acid catalysed hydrolysis an aqueous acetic acid solution is dosed into the reaction solution to attain a water content of between 5% and 30%. This quenches residual free anhydride [69] and prevents precipitation of the CTA. Sulfuric acid (0.1-2.0%) [44, 78] is added to the reaction mixture and the solution is heated to 30-70 °C [71, 79] for up to 10 hours. For the catalyst-free hydrolysis process, between 4% and 25% of water is added to the reaction solution as an aqueous acetic acid solution, and the mixture heated to 90-150 °C [80] for 0.5-2.0 hours [44]. Hydrolysis of CEs can be completed in a continuous process, generally using the catalyst-free method and typically employing a static mixer to ensure that even hydrolysis occurs [80].

When hydrolysing CTA to obtain a DS-Ac of 1.6, the hydrolysing CTA shows decreased solubility in the reaction solution and consequently gels or solidifies [78]. Excess water can be added to further de-acetylate the CA [69], and it is possible to completely hydrolyse all of the ester groups to regenerate cellulose. Once the hydrolysis step is complete the reaction is quenched using a weak base.

The rate and degree of de-acetylation are modified by altering the temperature, acid catalyst concentration and water content of the reaction mixture. High water content has been reported to promote hydrolysis at position 6 of the AGU [81], however, it has also been shown that re-acetylation at this position with acetic acid can occur [82]. Higher concentrations of acetic acid will also result in increased re-acetylation while the CA is in solution, particularly at position 6.

As mentioned in Section 1.7.3, sulfate groups can attach to the cellulose AGU during esterification and these are rapidly hydrolysed in the initial stages of hydrolysis [74]. Such sulfate groups are reported to have a similar acidity to free sulfuric acid [68] and therefore it is crucial that the sulfate groups are removed or they can cause significant degradation in the downstream processing of the CEs produced [83].

1.7.3.3 Product purification

Once the esterification of cellulose is deemed to be complete the CE product is purified by precipitation and washing which removes any residual unbound acids present. The process relies on diffusion of the carboxylic acids out of the product into the washing liquor. The precipitate morphology impacts on a number of factors: bulk density, handling requirements, shipping costs, purification rate and formulation needs [44]. The main forms supplied to industry are:

- Powder, generated by the slow dilution of the reaction solution with a water or a water/acetic acid solution until the CE is no longer soluble and precipitates out of solution [44, 84].
- Flake, generated by the addition of the reaction solution to a water or water/acetic acid solution, the reverse of the powder process [35].
- Pellets or granules, which rely on the formation of a skin by the extrusion of a high viscosity CE dope solution (12 wt% in a 90:10 acetic acid:water solution) through an orifice plate where a series of rotating blades cut the stream into small pellets [85]. The residual unbound acids migrate from the interior of the pellet through the skin into the washing liquor by diffusion.

Generating pellets or granules is time consuming in comparison to purifying the flake morphology which, in contrast, is open and readily washable. The typical bulk CE density ranges between 0.3 and 0.7 kg/m^3 [42, 86], with pellets typically being at the higher end of that range. A key feature of the commercial CE precipitation process is minimising dilution of the residual acid and so the precipitation process uses the minimum amount of water to effect precipitation of the CE. This is to aid in the recovery of the acid in a cost-effective manner [85]. A final bleaching step, typically using sodium hypochlorite, chlorine or hydrogen peroxide [87] may also be used to remove colour and increase whiteness of the final product.

Figure 1-11 displays an overall generalised schematic for CE manufacture [88], a process which can be carried out using either a continuous or batch process.

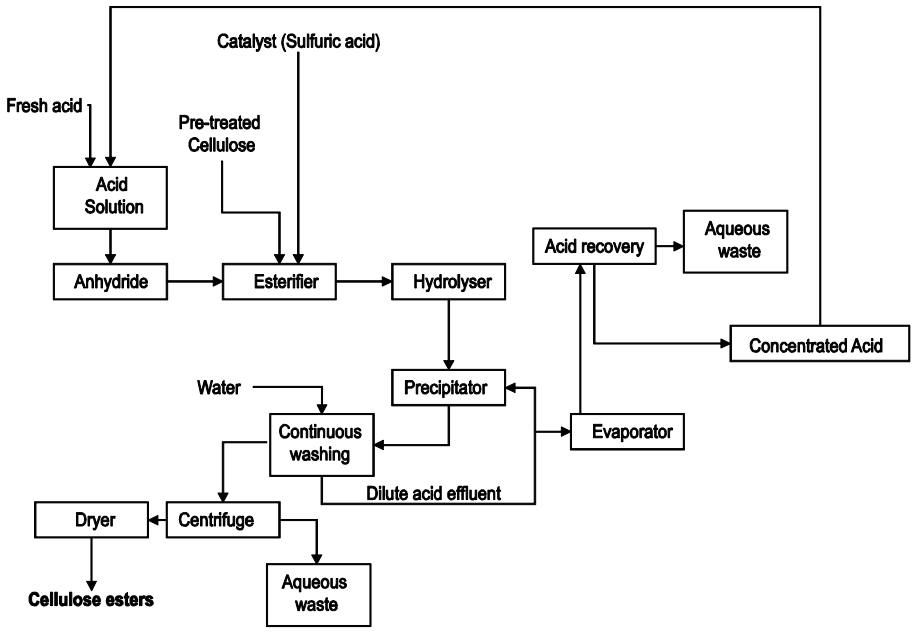

Figure 1-11 Cellulose ester manufacturing diagram.

1.7.4 Cellulose esterification by the heterogeneous method

The use of heterogeneous reactions has been limited to the preparation of fibrous CTA only [28, 89]. This reaction is a true two-phase system consisting of a cellulose phase (solid), which at no point in the reaction dissolves into the continuous phase (reaction medium). The reaction medium consists of a non-solvent, typically an aromatic hydrocarbon or carbon tetrachloride, and is loaded to a level that maintains the cellulose in a swollen, easily penetrable state while simultaneously prevents dissolution of the cellulose and the CTA product during the reaction [69]. As is typical for the esterification process, acetic anhydride is used as the acetylation reagent, with sulfuric [89] or perchloric [28] acid as catalyst. Pre-swollen cellulose is suspended [35] in a circulating 35:1 reaction medium to cellulose ratio. The reaction temperature is raised to 30 °C and the reaction is deemed to be complete when the sampled CTA fibres are soluble in a 9:1 DCM to methanol solution. The acid catalyst is then quenched with a weak base and the CTA fibres are collected by filtration.

The main advantages of the heterogeneous reaction system are:

- Production of a high molecular weight CTA due to limited acetolysis.

- Fast reaction work-up and purification. Precipitation is not required as cellulose dissolution does not occur and so the product can simply be isolated by filtration.
- Precise reaction temperature control. In a conventional homogeneous cellulose acetylation, as the cellulose is drawn into solution a viscous solution results which displays very poor thermal transfer characteristics.
- Efficient reagent and solvent recovery. Using fractional distillation, it is possible to separate out the reagents and recycle them. Additionally, there is no dilution of the reaction media, decreasing the cost of reagent recovery.

However, the main drawback to the heterogeneous reaction process is that it is not possible to modify the DS of the CA product using hydrolysis methods, restricting its application to generating fibrous CTA only. The heterogeneous process has not been used to commercially produce CTA fibres since the 1990s [45].

1.8 Cellulose ester properties

1.8.1 Solubility

The solubility profile of CEs can be altered by changing the substituent incorporated and varying the DS. This ability to vary the solubility profile is one of the key attributes of commercially produced CEs. Secondly, CTA is readily soluble in DCM and a reaction in this co-solvent can generate both a per-esterified CA and a larger molecular weight product than the equivalent reagents without DCM present. In the absence of DCM (or another suitable solvent) with the same molar proportion of acetic anhydride, the reaction gels and only shorter-chain cellulose fragments can peel into the reaction media and undergo per-esterification [88] (Table 1-3).

DS-Ac	Solvent used for CA solubilisation
3.0	Chloroform
2.0-2.5	Acetone
0.7-1.0	Water

Table 1-3 CA solubility with changing acetate incorporation (DS-Ac).

Mixed cellulose esters have increasingly broad solubility profiles with increasing aliphatic incorporation when the DS-Total is kept constant (Figure 1-12) [41, 90].

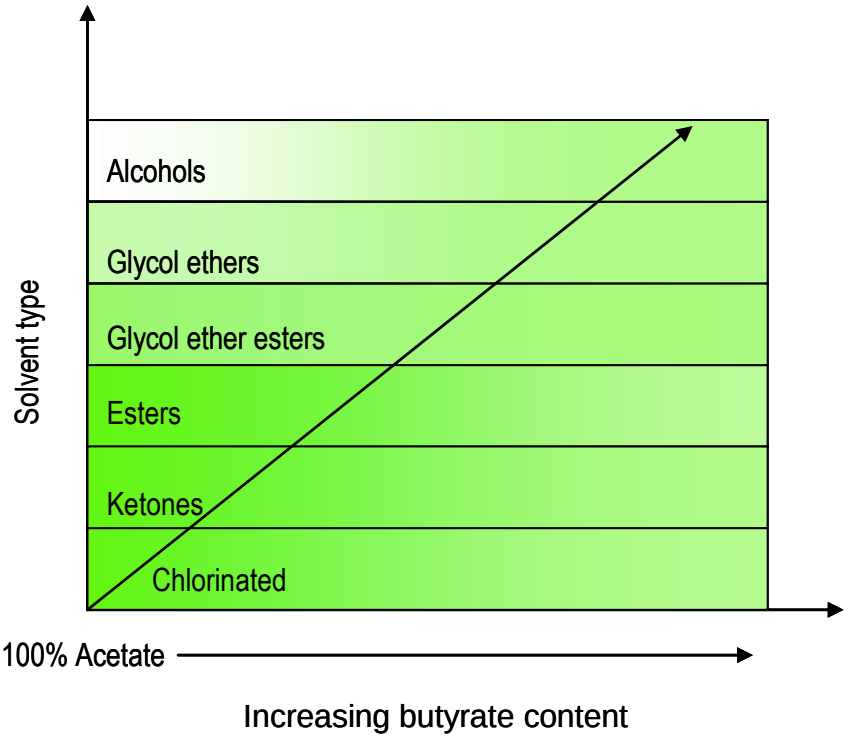

Figure 1-12 CAB solubility in various solvents with increasing butyrate content.

It is clear that modifying the cellulose structure with ester functionality alters the solubility parameters of the polymer, and permits tuning of its solubility characteristics. Solubility in hydrocarbons can be achieved by incorporating long aliphatic ester side chains, e.g. cellulose tricaproate [91], while incorporation of fluorinated groups eliminates the propensity of CEs to retain moisture [92].

1.8.2 Glass transition temperature (T_g) of CEs

As discussed earlier, T_g is the key attribute for determining the MFFT of a polymer dispersion. The T_g is a second order thermal transition where an amorphous polymer moves from a glassy to a rubber state and can be attributed to an increase in the polymer's free volume, permitting the molecules to move relative to one another [93].

The T_g of cellulose cannot be measured directly as the transition occurs after the onset of thermal decomposition at 220 °C [94]. To get around this issue, the T_g of cellulose can be approximated by recording successive measurements with increasingly hydrated cellulose. The water behaves as a plasticiser, reducing the T_g and thus, by extrapolation of the data, the T_g of the dry cellulose has been assigned with values ranging from 220-253 °C [94, 95].

Early publications used specific volume measurements to determine the T_g for CEs [96], but more recently thermal characterisation of CEs has been carried out by differential scanning calorimetry (DSC) and dynamic mechanical thermal analysis (DMTA). Both techniques have reported multiple transitions [97, 98]. A typical T_g range for a series of commonly produced commercial CEs is given in Table 1-4. It has been reported that aliphatic CE side chains can crystallise when > C_{11} forming a proposed hexagonal crystal lattice [97] and the observed melt temperature of the side chains (T_m) increases with side chain length. A melt range from –15-55 °C for esters with C_{12}-C_{20} chain lengths was observed and was attributed to increased crystal size [99] as the chain length increased. There was also an observed increase in the percentage of crystallinity with increasing chain length, increasing from 2.7%-6.7% from C_{14}-C_{18} [97].

Type	DS-Ac	DS-Prop	DS-But	DS-OH	T_g (°C)	Molecular weight (M_n g/mol)
Cellulose acetate						
CA 320S	1.8	-	-	1.2	180	38000
CA 398-3	2.4	-	-	0.6	180	30000
Cellulose acetate propionate						
CAP 504-0.2	0.1	2.1	-	0.8	159	15000
Cellulose acetate butyrate						
CAB 171-15	2.0	-	0.7	0.3	161	65000
CAB 321-0.1	1.3	-	1.4	0.3	127	12000
CAB 381-0.1	1.0	-	1.8	0.2	123	20000
CAB 381-2	1.0	-	1.8	0.2	133	40000
CAB 553-0.4	0.1	-	2.0	0.9	136	20000
CAB 500-5	0.3	-	2.5	0.2	96	57000

Table 1-4 Eastman Kodak CE properties.

DMTA has also been applied to the determination of T_g values where two values can be calculated: α and β. The α transition was assigned to the T_g which correlated well with DSC results obtained [97]. The β transition occurs at a lower temperature than the assigned T_g and has been attributed to either a chair to boat conformational change of the glucose pyranose ring [100, 101], or a transition of the aliphatic side chains [98]. Crépy *et al.* reported a second T_g by DSC and attributed it to a side chain transition not involved in the crystalline phase [97].

For a CE, the T_g is a function of the substituents, the DS and molecular weight as illustrated in Table 1-4. For a tri-substituted aliphatic CE, a T_g minimum, with respect to side chain length, is recorded for a side chain length of C_6 [99]. Increasing the ester chain length from acetate (C_2) to hexanoate (i.e. cellulose trihexanoate, CTH; C_6) increases the inter-molecular spacing, which increases the polymer's free volume and chain mobility. CEs tri-esterified with chains longer than C_6 have been reported to show an increase in the T_g [97] which is attributed to interactions of the side chains restricting chain rotation around the glucosidic bond [99]. However, data published by Garcia *et al.* [98, 102] for tri-substituted CEs with aliphatic chain lengths of C_8-C_{18} indicated that the T_g remains relatively constant across this range of esters.

Garcia *et al.* [98] have also shown a decrease in the T_g for a mono-substituted CE (DS 1) as the ester chain length increases from C_8 to C_{18} (220-150 °C) and a further decrease in the T_g for the same series prepared as the di-substituted CE (DS 2; T_g 189-109 °C, C_8-C_{18}). The overall T_g recorded for tri-substituted CEs (DS 3) was reduced even further (an average T_g of 65 °C), although it is interesting to note that this value did not vary significantly with changing chain length. The reduction in T_g, as the DS of the CE increased, was attributed to an increase in the free volume; however, it is also likely that the increased chain length restricts the hydrogen-bonding interactions of the residual hydroxyl groups, an effect which has been observed by Sealey *et al.* [92] and Glasser *et al.* [103]. Sealey reported that per-acetylation of all residual hydroxyl functionality for CEs gave an additional reduction in the T_g of 30 °C [99].

Cellulose mixed esters are usually based on acetate and one other longer chain ester group (> C_2), with commercially produced mixed esters restricted to propionate, butyrate or phthalate derivatives and are rarely per-

esterified [42]. To a point, the T_g of cellulose mixed esters decreases with increasing aliphatic chain length, as discussed above, and with increasing the DS of the aliphatic substituent. Glasser *et al.* [104] reported a T_g minimum for cellulose acetate hexanoate (CAH) with a DS-Hex of 2.95 and a DS-Ac of 0.05. It is possible that this particular level and ratio of substituents introduces the greatest level of disorder to the cellulose chain generating a maximum in the free volume for this class of molecule.

A correlation between a significant reduction of the DP and a reduction in the T_g has been reported in WO 2006/116367 A1 [48]. This is consistent with the polymer literature, which indicates that the T_g is only affected by molecular weight when considering relatively short-chain polymers [93]. The lowest T_g reported for a CE is for a trifluoroethoxy acetate derivative with a T_g of 41 °C [92].

1.9 Levulinic acid (LA)

The incorporation of levulinyl groups onto the cellulose backbone provides several points of difference from existing cellulose esters although there were a number of reasons that levulinic acid (LA) was chosen:

- LA is a renewable material derived from cellulosic biomass introducing a second aspect of renewability to this CE.
- It is a cost-effective raw material with a significant reduction in manufacturing costs being forecast [105].
- Incorporation of a ketone functionality gives a reactive moiety that may be used directly for subsequent derivatisation.
- The chain length of LA (C_5) was likely to produce a CE with a T_g near the minimum value based on current literature (see Section 1.8.2).

Levulinic acid (Figure 1-13) is a water-soluble γ-keto-carboxylic acid which has been developed into a renewably-derived platform chemical [106, 107]. It is a material from which many downstream chemicals are derived by taking advantage of its two reactive centres. Utilisation of LA has wide ranging applications from pharmaceuticals

to herbicides. The manufacture of renewable fuel extenders and additives such as methyltetrahydrofuran (MTHF) and ethyl levulinate are likely to see an increase in the production requirements of LA [108].

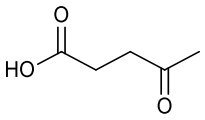

Figure 1-13 Levulinic acid (LA).

Rackemann and Doherty [107] and Kuster [109] discuss the conversion of carbohydrates to LA under acid catalysed conditions as illustrated in Figure 1-14. Glucose undergoes a series of dehydration steps forming the 5-hydroxmethylfurfural (HMF) intermediate, followed by a series of rehydration and dehydration steps to generate LA and formic acid. The theoretical yield of LA from glucose is 64.4 wt%, however, side reactions produce highly coloured soluble polymer species and insoluble humins reducing the effective yield. This process does not require refined feed stock material; lignocellulose can be used directly to generate LA. Both the cellulose and hemicellulose components are hydrolysed to their respective monosaccharides and all the hexose sugars then follow the glucose route to form LA. The pentose sugars can also produce LA through a furfural intermediate and the lignin is broken down into soluble species and removed as a by-product.

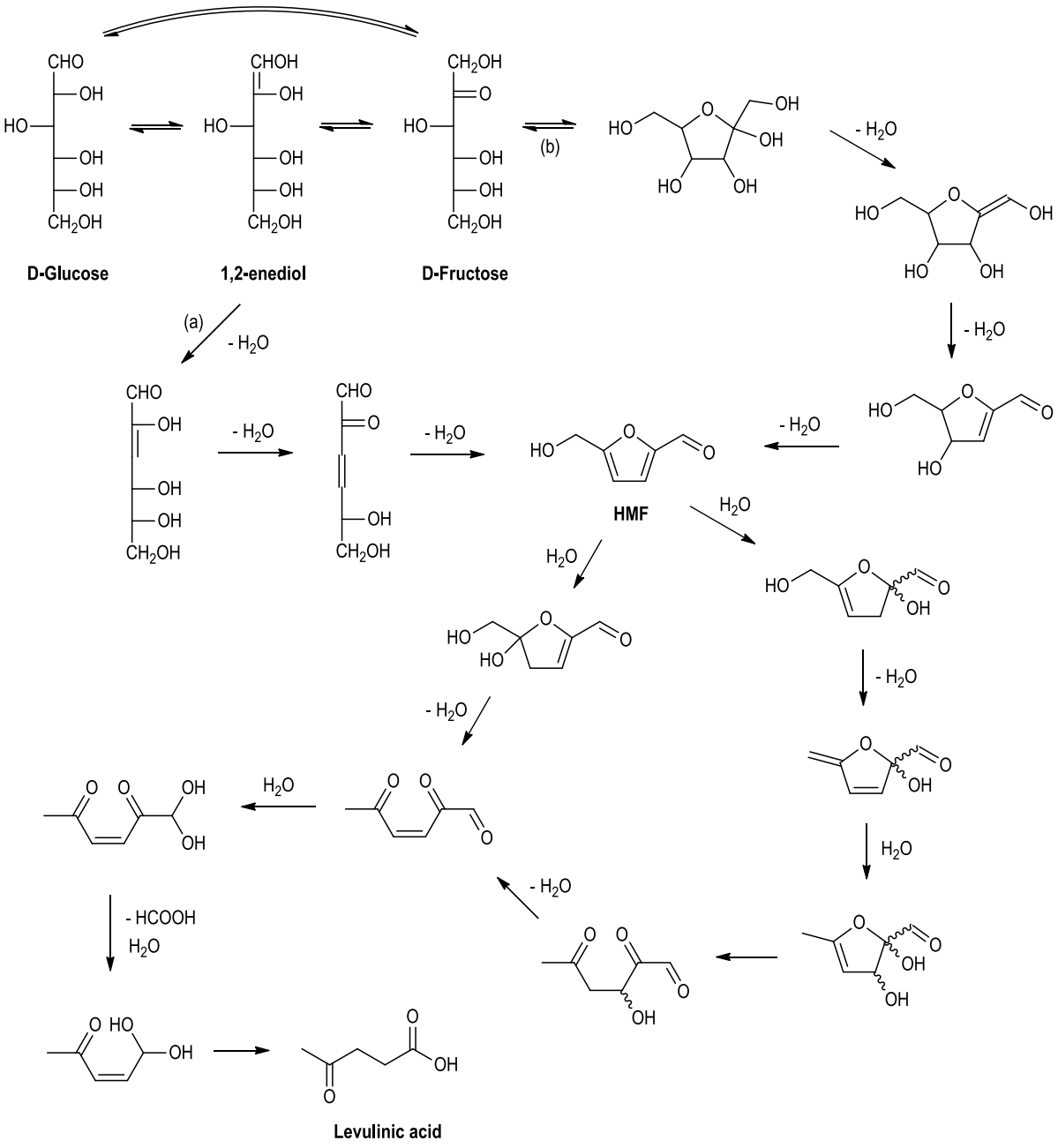

Figure 1-14 Reaction scheme for LA generated from glucose.

The Biofine process has been developed as a method to commercially produce LA from unrefined cellulosic sources using a continuous two reactor system [110, 111]. In the first stage, waste lignocellulose material feed stock is charged to a plug flow reactor and mixed with dilute catalytic sulfuric acid at 210-220 °C and 25 bar. In the short residence time of between 13 and 25 seconds, the cellulose is hydrolysed to hexose sugars and the HMF intermediate formed. During the second stage, HMF is transferred into a back mix reactor and heated at 190-200 °C at 14 bar for 20 minutes, generating a tarry material. Volatiles are then removed and LA is distilled

from the tarry residue to produce an initial crude batch of LA of 75% purity, that is further purified to 98% purity. Other methods for generating LA from carbohydrate biomass have been published, for example, Ghorpade and Hanna describe an LA production method using a twin-screw extruder using starch as the feed stock [112].

LA can be produced at 70-80% of the possible theoretical yield with the Biofine process by using effective reaction processing techniques and polymerisation inhibitors, thereby reducing side reactions. Biofine Incorporated currently operates a one ton per day pilot plant with plans to scale up to a 500 ton per day capability. This could bring the projected cost of LA down to USD$ 0.2 per kg [107]. Currently, high purity LA is produced from petrochemical sources, using maleic anhydride as the starting material at a cost of USD$ 11 per kg [113][4].

1.10 Chapter summary

The literature survey contained in this chapter provides a brief overview of the state-of-the-art in cellulose chemistry, and particularly in the field of cellulose esters. Although work in this area has been ongoing for more than a century, current processes have not been advanced over the past few decades, and very few new products have been commercialised. With regards to water-based paint binders, some research has been carried out to convert CEs into film forming materials. However, the water-dispersed CEs generated did not display the correct characteristics and consequently have not been commercialised for use in waterborne architectural coatings (discussed in Section 8). There is therefore scope for a new cellulose-based polymer to be developed which could potentially replace the currently used petroleum-derived polymer systems.

The aim of this research is to develop a novel levulinyl-modified cellulose ester, using existing processes and manufacturing techniques applicable to CE production. By employing current commercial manufacturing processes the commercialisation pathway for the introduction of new levulinyl-CE products is simplified. As a new side chain is being incorporated onto the cellulose backbone, a thorough investigation of the reaction

[4] Note that recent costings have the price of LA at NZD$ 8 per kg (Nuplex Industries).

chemistry involved is required to synthesise levulinyl-CEs in a reproducible manner and to generate a consistent product. As mentioned in the previous section, one of the main advantages of LA (other than its renewable nature) is its capability to be further modified *via* reaction of its ketone functionality. This derivatisation may be essential in the latter stages of the project in order to attain the correct dispersion characteristics and film forming properties for a water-based CE material, i.e. a low T_g, ready dispersion into water, and long-term stability.

Overall, the aim of this project was to develop a low VOC water-based levulinyl-CE coatings binder which could be formulated into a proof of concept, low-sheen interior architectural coating. If successful, it is the intention of our industry partners (Resene Paints Ltd) to commercialise this novel water-based binder derived from renewable sources, aiming the product at the environmentally aware consumer.

A summary of each chapter is given below:

- Chapter 2 – The synthesis of cellulose esters containing levulinyl functionality. Levulinyl cellulose esterification chemistry was investigated and compared to traditional chemistry used in the production of CEs.

- Chapter 3 – Cellulose ester characterisation. This chapter describes the characterisation methods developed for the investigation of the levulinyl-CE platform chemicals. Structural characterisation was completed and compared to CTA and mixed CEs.

- Chapter 4 – Reaction parameters. The reaction conditions for generating levulinyl-CEs were investigated with respect to product control and optimisation of the polymer synthesis. The levulinyl-CE properties examined were T_g, molecular weight and colouration. These three parameters control the film formation from a water-based dispersion, as well as the final dry film properties. Both external and internal plasticising was investigated as a method of reducing the T_g of the levulinyl-CE polymers.

- Chapter 5 – Miscellaneous reactions and characteristics of LAC. The use of alternative catalysts and reaction co-solvents, with a focus on improved production of the levulinyl-CE product, is discussed. The levulinyl acetyl cellulose (LAC) solubility characteristics in various solvents were also investigated to provide relevant information to aid dispersal of the final levulinyl-CE product.

- Chapter 6 – Scale-up production of LAC. A 1 kg LAC pilot plant experiment, demonstrating scaled production was performed, including reaction calorimetry.

- Chapter 7 – Cellulose ester carboxylation. The acetone process was utilised to generate a self-stabilised water-based dispersion. This method required the incorporation of ionisable groups onto the polymer backbone.

- Chapter 8 – Water-based levulinyl-CE dispersions. This chapter discusses the preparation of levulinyl-CE water-based dispersions using the acetone process.

- Chapter 9 – Conclusions and future work.

2 The synthesis of cellulose esters containing levulinyl functionality

2.1 Cellulose esterification chemistry

Cellulose esterification reactions can be separated into two categories; those employing an ionic liquid as a reaction solvent pre-dissolving the cellulose, and those using a "solvent-free" system. Using ionic liquids (including traditional cellulose dissolution systems in this definition [27]), esterification of cellulose with complex species is possible and high reaction yields can be obtained. The drawbacks to using ionic liquids are their high cost and toxicity [70], which for a commercial process would result in the need for additional recycling and recovery steps. A "solvent-free" reaction system implies no dissolution of the cellulose prior to reaction. In a further complication, reactions using a co-solvent such as DCM are considered to be "solvent-free" as dissolution of the cellulose starting material does not occur prior to reaction. In the "solvent-free" esterification process, the newly formed CE peels in to solution with the reagents acting as reaction solvents.

Cellulose esters are produced commercially using "solvent-free" reaction systems, heating activated (pre-treated) cellulose with acetic anhydride and catalytic amounts of sulfuric acid. Sulfuric acid is the only commercially significant catalyst [74] and was therefore the main catalyst utilised in this project (Section 5.1 addresses alternative catalysts) where all cellulose esterifications were completed "solvent-free".

For commercial applications, CEs are esterified with anhydrides of chain length up to C_4 (butyric). With increasing chain length there is an associated decrease in anhydride reactivity: acetic > propionic > butyric > isobutyric [72], attributed to steric effects. In addition to the increased work-up difficulties, anhydride reactivity limits the commercial incorporation of aliphatic acids beyond C_4 (butyric), i.e. CABs. However, aliphatic acid incorporation beyond the C_4 chain length is possible using anhydrides, and tri-substituted and mixed valerate CEs have been prepared using this method [114]. Although desirable properties were associated with cellulose valerates, it is possible that commercial success was not achieved due to the significantly higher cost of valeric anhydride compared to the shorter chain length anhydride reagents (discussed in Section 4.7).

Esterification of cellulose with even longer chain fatty acids beyond C_5 can be achieved using mixed anhydrides [70]. Combining acetic anhydride and a fatty acid forms an equilibrium of three reactive anhydride species (discussed in Section 2.5): acetic anhydride, the mixed anhydride and the fatty acid anhydride, of which the mixed and fatty acid anhydrides are capable of esterifying cellulose with the fatty acid moiety (Figure 2-1). Stearate (C_{18}) has been incorporated into a CE, albeit at a low DS (0.1), using the mixed anhydride reagent. Mixed anhydride chemistry provides an alternative route for incorporation of longer chain aliphatic acid groups on to cellulose without exclusively using expensive long chain anhydrides. The mixed anhydride method is likely to be readily scalable due to the chemistry being very similar to what is used commercially today. Commercially produced mixed CEs are generated *via* acid catalysis, where both short and long chain length anhydrides and acids are added to the reaction solution.

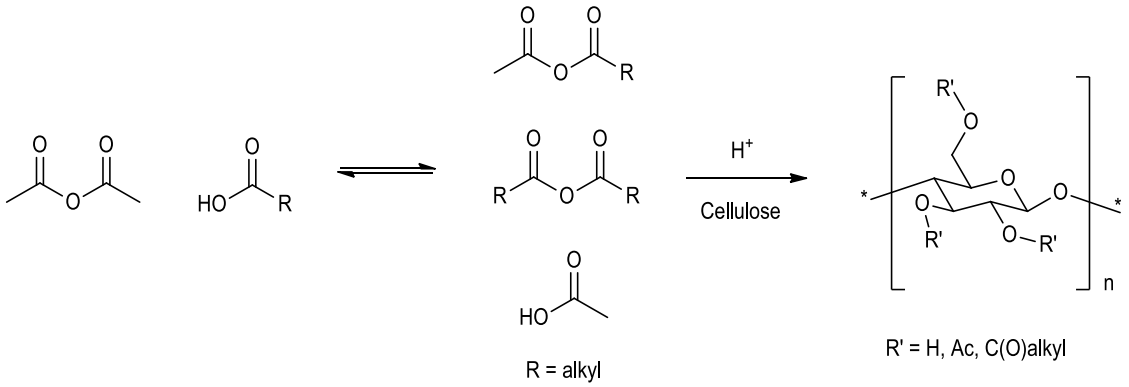

Figure 2-1 Reaction scheme for a mixed anhydride system.

The effective incorporation of aliphatic acids beyond the C_5-C_6 chain length has, until this point, required the use of different chemistry. Using a 9 wt% LiCl/DMAc ionic liquid solvent system a cellulose solution of up to 15% w/v [115] can be generated. Cellulose's strong inter- and intra-molecular hydrogen bonding is overcome by forming a Li(DMAc)Cl ion pair complex with the cellulose hydroxyl groups [31]. However, concentrations between 1 and 6% w/v are routinely employed in a laboratory setting for esterification reactions due to the rapid increase in solution viscosity [115]. A review published by Meng *et al.* [25], discussing the dissolution of cellulose in various ionic liquids, indicated that a 39 wt% cellulose solution was possible using cellulose with a low DP (DP 286) dissolved in 3-methyl-*N*-butyl-pyridinium chloride at 105 °C [116]. The solvated cellulose was then generally esterified with acid chlorides or anhydrides [117]. Tri-substitution of aliphatic ester groups up to C_{20} (eicosanoate) [99] onto

cellulose has been achieved in LiCl/DMAc using fatty acid chlorides. The pre-dissolution of cellulose using LiCl/DMAc is a powerful tool for incorporation of groups on to cellulose that would otherwise be unlikely; for example the preparation of cellulose[3,5-bis(3,5-bis(benzoyloxy)-benzoyloxy)benzoyloxy)benzoate] (Figure 2-2) although incorporation was low with a DS of 0.21 reported [118]. Currently, pre-dissolution of cellulose to generate CEs with single or multiple substituents is not employed commercially due to the relatively low solubility of cellulose, the time required to effect dissolution, the cost of the solvent, the difficulty in recovery of the CE and the fact that overall there is no significant advantage over the solvent-free process. However, commercial processes are limited in the chain length that can be incorporated at an effective level. Levulinic acid (LA) was therefore postulated as an intriguing target for cellulose esterification (see Section 1.9)

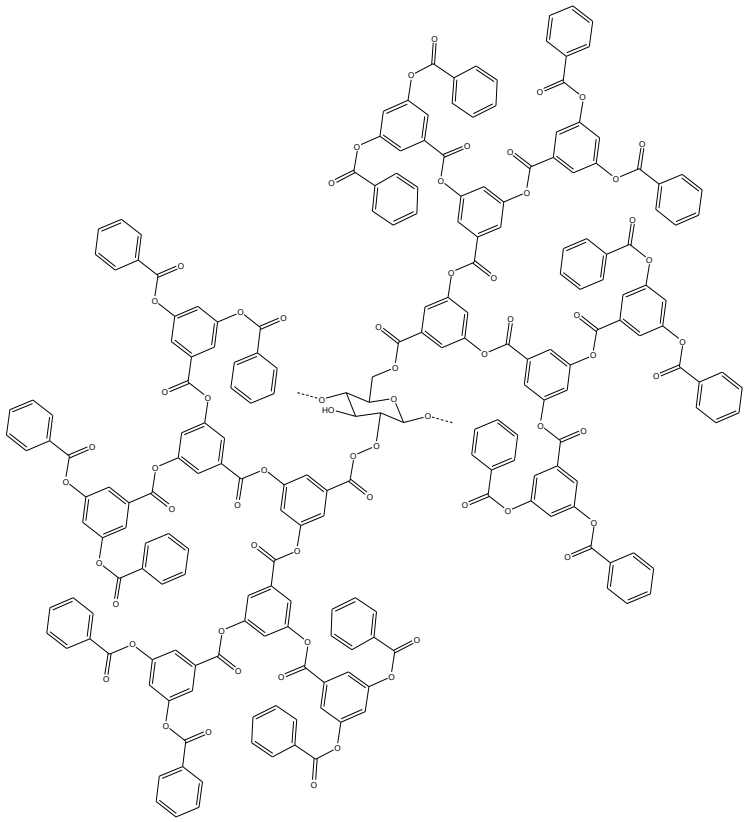

Figure 2-2 Cellulose[3,5-bis(3,5-bis(benzoyloxy)-benzoyloxy)benzoyloxy)benzoate].

There is little information reported regarding the esterification of cellulose with LA although the Vladimirova group reported the preparation of both cellulose levulinate and levulinyl acetyl cellulose (LAC) [119]. This is the only report of preparing a LAC using acetic anhydride but provided little supporting data of both the reaction

conditions and the chemistry involved. In addition, while the characterisation data implied that a high DS-Lev species was prepared, the nomenclature was obscure, and other key data were not reported.

Cellulose levulinate esters have also been prepared using a coupling reaction for use as wound healing dressings by Edwards *et al.* [120]. Although the DS of the final product is unclear, it was indicated in the report that a tri-substituted ester had been generated. A Japanese patent published by Nicca Chemical Company [121] reported the formation of cellulose levulinate using levulinyl chloride as the esterification agent. In both cases characterisation of the products was not provided and the limited methodology suggested that only a low DS was achieved.

2.2 Reactive species determination

For reproducible and predictable synthesis of a target compound, in this case a levulinated CE, control of the reaction chemistry is key. To achieve this, an understanding of the reactive species involved is critical. First principles would suggest that the reaction of LA and acetic anhydride with catalytic amounts of sulfuric acid would generate a mixture of anhydride species, Figure 2-1. In order to determine the reactive species involved in the esterification to produce LAC, a typical solution of reagents was prepared, but without cellulose. A mild exotherm was generated upon the addition of the sulfuric acid indicating that a vigorous reaction had occurred. Assessment of the ^{1}H NMR spectrum of the crude reaction mixture indicated a much more complex series of products than anticipated (Figure 2-3).

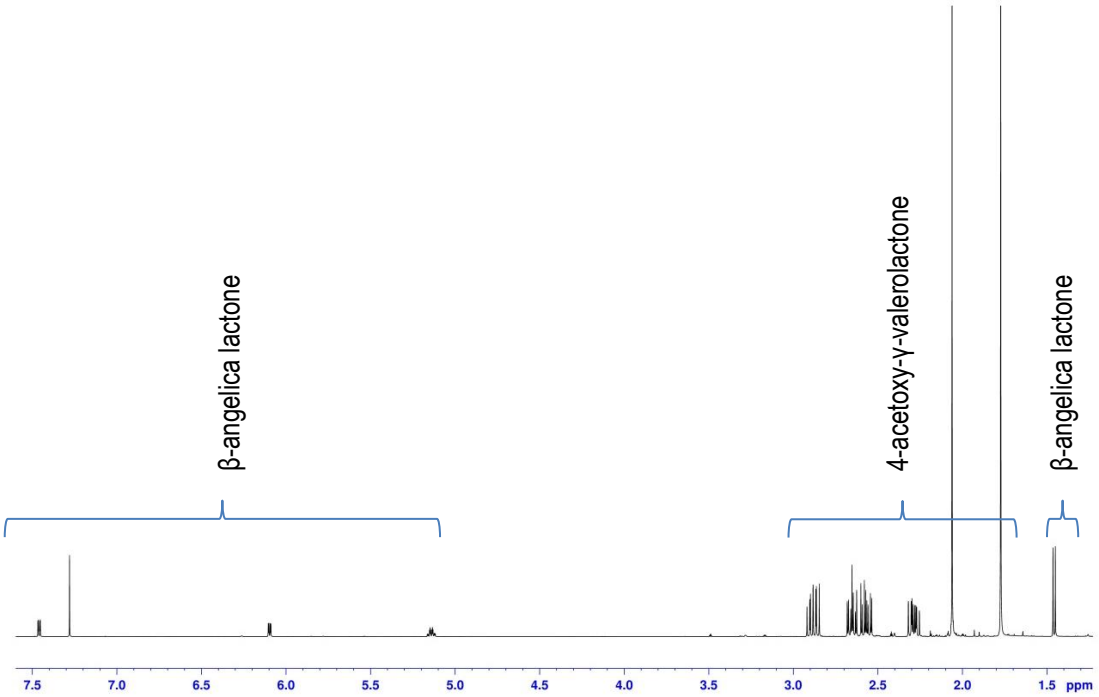

Figure 2-3 ^{1}H NMR of a cellulose-free reaction mixture showing 4-acetoxy-γ-valerolactone (1) and β-angelica lactone (3).

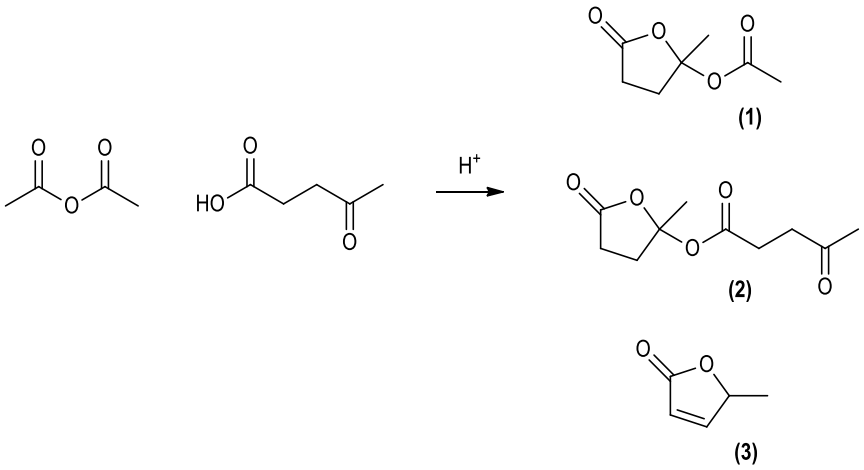

Figure 2-4 Major species isolated from the cellulose-free reaction solution: 4-acetoxy-γ-valerolactone (1), 4-levulinoyl-γ-valerolactone (2) and β-angelica lactone (3).

The reactive species were isolated by flash chromatography, analysed by NMR spectroscopy and identified as 4-acetoxy-γ-valerolactone **(1)**, 4-levulinoyl-γ-valerolactone **(2)** and a small amount of β-angelica lactone (β-AL) **(3)** (Figure 2-4). Acetic acid was also present due to the decomposition of acetic anhydride. Using butyric anhydride in place of acetic anhydride (i.e. for the preparation of levulinyl butyryl cellulose (LBC) and butyryl levulinyl acetyl

cellulose (BLAC)) generated 4-butyryloxy-γ-valerolactone **(4)** (Figure 2-5). When the LA/anhydride molar ratio is ≥ 1, all the available anhydride is expended. Therefore, the proportion of **(2)** in solution compared to **(1)** for LAC (**(2)** compared to **(4)** for LBC; **(2)** compared to **(1)** and **(4)** in the case of BLAC) is increased.

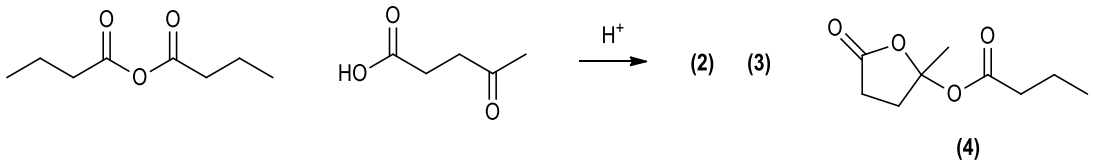

Figure 2-5 4-Butyryloxy-γ-valerolactone (4).

Mass spectral data for 4-acetoxy-γ-valerolactone **(1)** indicated the parent molecular ion to be $C_7H_{10}O_4Na$ (*m/z* 181.05, $M+Na^+$). The calculated degree of unsaturation was three, which was accounted for by the two ester groups and the lactone ring. Table 2-1 displays the NMR chemical shifts assigned to 4-acetoxy-γ-valerolactone. Notable chemical shifts were the quaternary ^{13}C signal at δ 108.4 ppm, assigned to the C-4 position, which is consistent with oxirane or dioxylane functional groups, and the C-5 methyl assigned to ^{1}H δ 1.77 ppm, which is more commonly attributed to an alkene methyl substitutuent. The structurally similar levulinyl and butyryl valerolactones were assigned in a similar fashion. Mass spectral data for 4-levulinoyl-γ-valerolactone **(2)** indicated a parent molecular ion of $C_{10}H_{14}O_5Na$ (*m/z* 237.07, $M+Na^+$), which gave a calculated degree of unsaturation of four. The extra degree of unsaturation was accounted for by the ketone group associated with the levulinyl ester, confirmed by NMR with a characteristic ^{13}C resonance observed at δ 206.5 ppm. Both the butyryl and levulinyl valerolactone species displayed the characteristic NMR signals at ^{1}H δ 1.77 ppm and approximately ^{13}C δ 108 ppm which were assigned to the lactone methyl resonances and the five membered ring quaternary carbon, respectively. All other signals observed were consistent with the butyryl and levulinyl ester functionality.

	γ-Valerolactone					
	4-Acetoxy (1)		4-Levulinoyl (2)		4-Butyryloxy (4)	
Position	^{1}H δ ppm	^{13}C δ ppm	^{1}H δ ppm	^{13}C δ ppm	^{1}H δ ppm	^{13}C δ ppm
1	-	175.4	-	175.6	-	175.4
2	2.61, 2.87	28.5	2.54, 2.87	28.7	2.57, 2.88	28.7
3	2.31, 2.61	32.7	2.26, 2.66	32.8	2.28, 2.64	32.9
4	-	108.4	-	108.9	-	108.6
5	1.77	26.1	1.77	26.2	1.77	26.3
1'	-	169.2	-	171.2	-	171.9
2'	2.06	21.6	2.55	28.6	2.25	36.7
3'	-	-	2.74	37.7	1.63	18.1
4'	-	-	-	206.5	0.95	13.5
5'	-	-	2.18	29.8	-	-

Table 2-1 Chemical shifts for 4-acetoxy, 4-levulinoyl and 4-butyryloxy-γ-valerolactone species.

There was no evidence of a mixed anhydride species being formed during the reaction of LA and an anhydride. Levulinic anhydride was synthesised by a DCC mediated coupling [122] for reference. NMR data obtained for levulinic anhydride and acetic anhydride showed the anhydride carbonyl ^{13}C shifts occur at δ 168.9 ppm and δ 168.4 ppm respectively, and resonances at these frequencies were not detected in the ^{13}C NMR spectra for the crude reaction mixture. A mixed anhydride of levulinate and acetate would have a very similar chemical shift for the anhydride carbonyl. NMR shifts for the lactone carbonyls of compounds **(1)** and **(2)** were assigned to ^{13}C δ 169.2 ppm and δ 171.2 ppm respectively. When using a LA/Ac_2O molar ratio of < 1, a ^{13}C NMR peak was detected, corresponding to acetic anhydride carbonyl (^{13}C δ 168.4 ppm). For a reaction having a molar excess of acetic anhydride there was no resonance at ^{13}C δ 205.8 ppm which could be assigned to the ketone group on LA, a signal, which would also be observed for compound **(2)**, but quantities of this compound would be negligible when using a molar ratio of LA/Ac_2O < 1. This indicated that the anhydride resonance seen corresponds with only unreacted reagent. Therefore, species **(1)** and **(2)** are likely to be responsible for the esterification of cellulose. Clearly when a LA/Ac_2O ratio of < 1 was used, acetic anhydride also acted as an esterifying agent.

Preparation of 4-acetoxy-γ-valerolactone has been reported by Rasmussen and Brattan [123], based on the work of Bredt [124] who first postulated the structure. Rasmussen and Brattan reacted levulinic acid and acetic anhydride and reported that they had produced 4-acetoxy-γ-valerolactone which was only characterised by IR [123]. No NMR data for any of the γ-valerolactone species discussed here has been located in the literature. Only one literature example was found for the use of 4-acetoxy-γ-valerolactone as an esterifying agent, where it was used in the preparation of levulinyl and acetyl amide species [125], [126]. Of note is the observation that levulinic anhydride spontaneously converts to **(2)** on extended standing, demonstrating that the cyclic species is the thermodynamically favoured form.

2.3 α-Angelica lactone

It is proposed that lactone species **(1)** and **(2)** are formed through an α-AL **(5)** intermediate. The formation of α-AL from LA is well known to occur under dehydrating conditions in the presence of an acid catalyst (Figure 2-6), as has been demonstrated in patent US2809203 [127]. Dehydrating reaction conditions due to the presence of acetic anhydride lead to the rapid formation of α-AL, a conclusion which was supported by conducting the reaction of LA, acetic anhydride and sulfuric acid under reduced pressure. The analysis of the recovered distillate contained α-AL with a proportion of acetic acid and acetic anhydride, both of which have a lower boiling points than α-AL. Dehydration of LA using acetic anhydride has previously been reported as an effective route to α-AL [128].

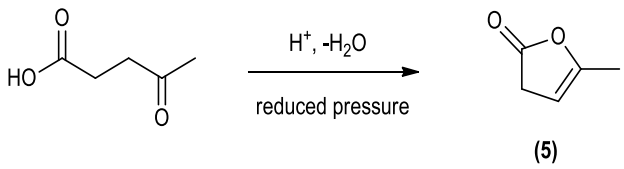

Figure 2-6 α-Angelica lactone formation.

The synthesis of lactones **(1)** and **(2)** from α-AL was further supported by experimental evidence. Heating α-AL with acetic acid and a catalyst (cH_2SO_4) exclusively formed 4-acetoxy-γ-valerolactone (Figure 2-7). Formation of LA, 4-levulinoyl-γ-valerolactone **(2)** and β-AL **(3)** was observed when α-AL was heated in toluene in the presence

of catalytic acid. It is likely that residual moisture hydrated a portion of the α-AL to LA which then further reacted with the remaining α-AL to form 4-levulinoyl-γ-valerolactone.

β-AL **(3)** has been previously reported as having greater thermodynamic stability than α-AL **(5)** [129] and therefore, heating α-AL should result in a transformation to β-AL. Under the reaction conditions used for synthesising LAC, the observation of β-AL in the reaction solution would suggest the prior formation of α-AL, although α-AL was not observed in the crude product mixture by NMR or during reaction product isolation. However, it was isolated by distilling directly from the reaction and was trapped as a neat solution.

These observations strongly support α-AL as a key, short-lived intermediate in the reaction media, which leads to the formation of β-AL and the lactone species **(1)** and **(2)**. The reactive nature of α-AL was further evidenced by the formation of a lactone derivative on cellulose where the hydroxyl AGU moiety acted as a nucleophile (see Section 2.6).

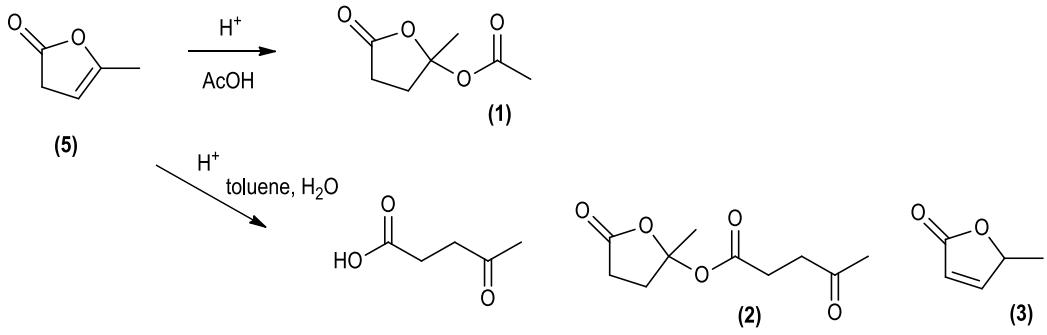

Figure 2-7 Reactive lactone formation from α-angelica lactone (5).

2.4 Reaction pathway

The reaction mechanism for cellulose esterification with lactones **(1)** and **(2)** was investigated using ethanol as a model compound. Reaction of ethanol with lactone **(1)** yields both ethyl acetate and ethyl levulinate, indicating that both the lactone and the activated ester can be an electrophilic site. Lactone **(2)** produced only ethyl

levulinate on treatment with ethanol. These model reactions demonstrated that lactones **(1)** and **(2)**, which are formed rapidly in solution upon catalyst addition to LA and acetic anhydride, are effective esterification reagents and likely to be responsible for the esterification of cellulose with this set of reagents.

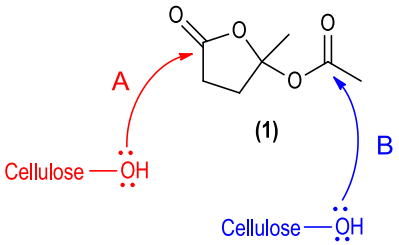

Figure 2-8 Possible lactone esterification mechanism. Pathway A, esterification utilising the lactone ring carbonyl; Pathway B, esterification through the activated ester carbonyl.

The reaction mechanism (Figure 2-8) is likely to proceed by protonation of either ester carbonyl, activating it towards nucleophilic attack, followed by reaction pathway A or B. Reaction at either carbonyl site would result in the concomitant opening of the lactone ring and ejection of the excess species. Pathway A would result in esterification of cellulose with levulinate and ejection of acetic acid. Conversely, pathway B would result in esterification with acetate and ejection of LA. Although it is possible for 4-hydroxy-γ-valerolactone **(6)** (Figure 2-9) to be ejected, this species was not detected in the reaction solution by NMR spectroscopic analysis (^{1}H or ^{13}C) and was not isolated by flash chromatography. Therefore, if compound **(6)** was formed, it is likely that the lactone ring reverts back to LA. This species has been mooted as a possible reactive intermediate but no evidence was found for its presence. In the literature Timokin *et al.* discuss the synthesis and isolation of compound **(6)** under aqueous conditions [129].

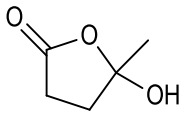

(6)

Figure 2-9 4-Hydroxy-γ-valerolactone.

In conclusion, the proposed reaction pathway for the formation of LAC (Figure 2-10) first entails the acid catalysed rapid dehydration of LA by a molar equivalent of acetic anhydride forming an α-AL intermediate.

Lactone species **(1)** and **(2)** quickly result from reaction of carboxylic acids with α-AL. Cellulose is likely esterified with these newly formed lactone species producing a mixed acetate and levulinate substituted cellulose polymer. It is expected that longer-chain aliphatic anhydrides (for example, valeric and hexanoic anhydrides) will provide the same dehydrating conditions as acetic anhydride and similar alkyl-ester lactone species.

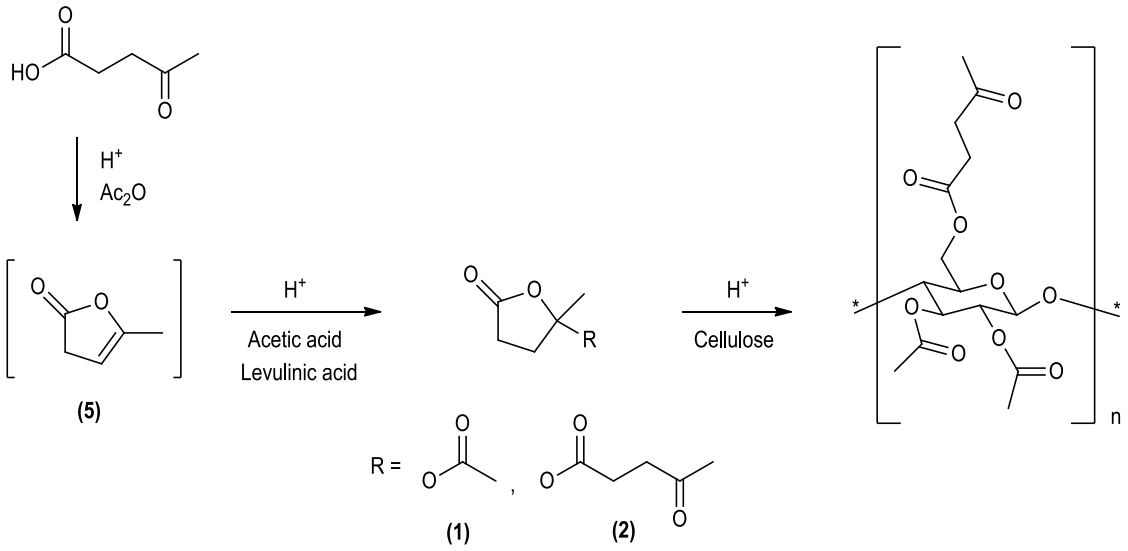

Figure 2-10 Cellulose esterification reaction overview using LA and acetic anhydride. The LAC ester substitution profile illustrated is only one of the permutations possible.

2.5 Levulinic acid vs. mixed anhydride chemistry

The proportion of the LA (C_5) incorporated into the levulinyl-CE was higher than expected in comparison to related aliphatic fatty acid analogues. This was likely to be a function of the different reaction mechanisms: the proposed levulinic lactone chemistry compared to the mixed anhydride chemistry. A comparison of the levels of levulinic, butyric, valeric and hexanoic acid incorporated onto cellulose clearly indicated that LA was incorporated to a higher extent under identical reaction conditions (Table 2-2). The acetic acid activated cellulose was reacted with equimolar proportions of acetic anhydride (3 equivalents per AGU hydroxyl) and one of the carboxylic acids in Table 2-2 (acid/acetic anhydride molar ratio of 1.33).

Acid	No. of carbons	DS
Levulinic	5	1.29
Butyric	4	0.74
Valeric	5	0.67
Hexanoic	6	0.56

Table 2-2 Mixed anhydride chemistry. Total DS of all samples ranged between 2.99 and 3.09.

Valeric acid (VA) and hexanoic acid (HA) were used as analogues for LA having similar chain length and molecular weight. Aliphatic acids show a trend of decreasing incorporation onto the cellulose backbone with increasing chain length from C_4-C_6 using mixed anhydride chemistry (Table 2-2). This effect is likely associated with the decreasing anhydride reactivity as a function of increasing chain length and also due to a combination of steric, electronic and solvation effects.

In comparison, levulinate incorporation into the cellulose backbone was 1.9 times and 2.3 times higher than VA and HA, respectively (Table 2-2). A possible rationale for the increased levulinate incorporation was postulated based on the reactive species present as the primary argument. Considering the lactone-based esterification chemistry, with a LA/Ac_2O molar ratio of ≥ 1, the equilibrium for lactone formation appeared to lie far to the right, since intermediates and anhydrides were not observed in solution (discussed in Section 2.2). Each of the possible lactone species in the reaction solution possess the capability to esterify with levulinyl, although species **(2)** can only esterify with levulinyl. An increase in acetic acid level in the reaction solution will alter the ratio of lactones **(1)** and **(2)** in solution, increasing the relative level of compound **(1)** but would not result in formation of acetic anhydride due to the reaction equilibrium lying to the right and favouring lactone formation. Therefore, esterification of cellulose in the presence of excess acetic acid using lactone esterification chemistry does not greatly affect the proportion of acetate incorporation. This is further discussed in Section 4.3.2.

When completing esterification with a mixed anhydride system there is an equilibrium between the reactive species, whereby an increase in acetic acid will favour formation of acetic anhydride (see Figure 2-11). Increasing the acetic anhydride content in solution will preferentially increase incorporation of acetyl groups onto cellulose over the longer acyl chain group, as acetyl is both more reactive and is present in a greater

stoichiometric amount. Levulinate esterification does not show the same level of sensitivity towards the presence of excess acetic acid due to the formation of the lactone species. Hence the effective reagents have always one functional moiety that can effect levulinate incorporation.

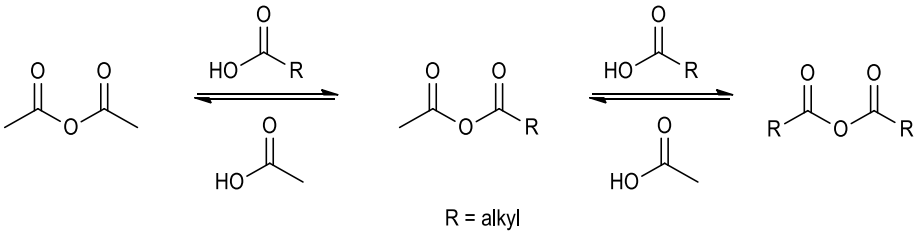

Figure 2-11 Mixed anhydride equilibrium.

In the commercial production of CABs with a high butyrate content, acetic acid present from the cellulose pre-swelling procedure must be exchanged with butyric acid. The same result can be achieved simply by the addition of more butyric acid or butyric anhydride to the reactor. Addition of butyric acid or anhydride offsets the additional acetic acid present and therefore results in greater incorporation of butyrate onto cellulose.

Interestingly, the mixed anhydride reaction was an order of magnitude faster in comparison to those completed using the lactone species based on the observed rate of cellulose solubilisation into the reaction solution. This could be due to two possible mechanisms. Firstly, that reaction between the anhydride and the cellulose was faster than between the lactones and cellulose, allowing partially esterified cellulose to be drawn into solution at a significantly higher rate. Secondly, the solvation power of the acid/anhydride solution could have a greater affinity for the partially reacted cellulose and therefore acts as a more effective solvent. These two factors working separately or in conjunction may be responsible for the increase in the relative rate of reaction.

2.6 Lactone functional group

Additional evidence for the active species completing the esterification of cellulose was provided by an unexpected moiety detected on the cellulose backbone. Preparation of LAC under mild conditions resulted in the inclusion of a γ-valerolactone substituent. Mild conditions are defined as reduced duration, temperature or

catalytic acid concentration compared to the standard reaction conditions (see Section 4.6). Synthesis of LAC under mild conditions gave a product containing unexpected broad NMR spectral features with a resonance centred at ^{1}H δ 1.65 ppm. Using a HSQC (Heteronuclear Single Quantum Correlation) experiment this showed that the aforementioned proton signals correlated to a ^{13}C resonance at δ 23.1 ppm. This indicated that the proton signals could not be attributed to water, as did the observation that this resonance did not diminish on exchange with D_2O. In addition, an unusual ^{13}C resonance was detected at δ 109.4 ppm that was not consistent with the characterisation of LAC.

To investigate these unexpected signals, a model reaction was completed substituting glucose for cellulose. This reaction generated a functionalised glucose product that also displayed these unexpected NMR signals. However, due to the complexity and apparent random nature of substituent placement on glucose, a discrete lactone containing compound could not be isolated, even after extensive chromatography. As an alternative, ethanol was chosen as the model reactant to simplify the system even further.

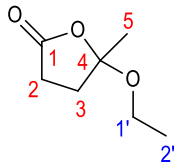

(7)

Figure 2-12 4-Ethoxy-γ-valerolactone (7).

Position	^{1}H δ ppm	^{13}C δ ppm
1	-	176.9
2	2.13, 2.28	34.8
3	2.53, 2.75	29.0
4	-	109.4
5	1.62	22.8
1'	3.64	58.6
2'	1.18	15.4

Figure 2-13 ^{1}H and ^{13}C NMR chemical shifts and positions related to 4-ethoxy-γ-valerolactone.

Reaction of ethanol with **(1)** in a 1:1 molar ratio generated **(7)** and ethyl acetate. NMR spectral data for **(7)** was assigned and confirmed using HMBC and HMQC spectroscopy and the ^{1}H and ^{13}C chemical shifts are detailed in Figure 2-13. The data confirmed an ethyl substituted lactone ring (Figure 2-12); a class of compound referred to in the literature as pseudo esters [130]. The NMR spectroscopic data obtained for compound **(7)** correlated well with the additional signals seen for the LAC prepared using mild conditions, confirming lactone inclusion onto the cellulose backbone (Figure 2-14).

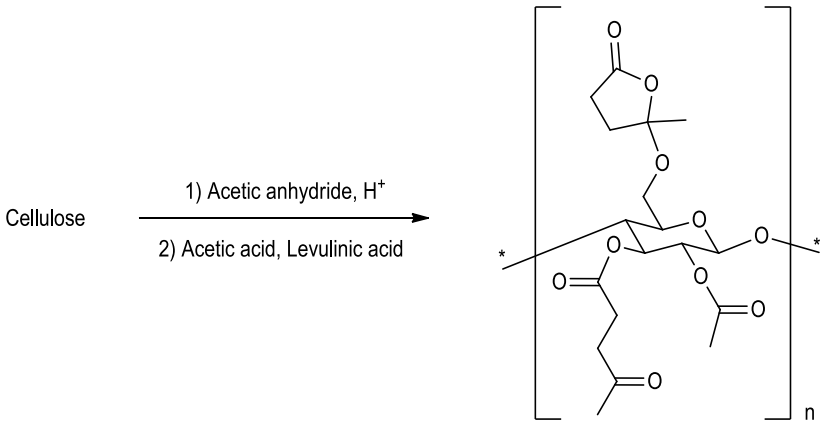

Figure 2-14 Lactone incorporation into LAC esters.

Compound **(7)** has been reported previously as the product of the reaction between α-AL and ethanol, but no supporting NMR spectroscopic data was published. Both ethyl levulinate and 4-ethoxy-γ-valerolactone have the same molecular mass, however, Shu and Lawrence showed that ethyl levulinate and 4-ethoxy-γ-valerolactone have different fragmentation patterns [131]. Unfortunately, this did not aid characterisation here due to a different ionisation method employed where only a strong parent ion signal and no significant fragmentation pattern was observed for these two compounds.

Having identified the lactone group as being responsible for the unexpected signals, it was possible to account for this group when calculating the DS for LAC products. Lactone ring resonances at ^{1}H δ 2.13, 2.28, 2.53 and 2.75 ppm overlapped with levulinyl and acetyl proton signals (see Section 3.5), which confounded the spectral data acquired and caused difficulties calculating the DS by ^{1}H NMR integration. The ^{1}H NMR spectrum for a cellulose ester that contained the lactone functional group was assessed using 2 dimensional proton-carbon correlation experiments (HSQC). For the lactone species, methylene protons overlapped with the region that the

levulinate methylenes occur (^{1}H δ 2.30-3.05 ppm) and with the acetate and levulinate methyl resonance (^{1}H δ 1.85-2.30 ppm). However, the DS for the lactone could be determined by integration of the methyl region that was distinct and not confounded with other proton resonances (^{1}H δ 1.42-1.71 ppm). With this value, a proportion of the integrated region for the levulinyl methylenes could be subtracted and the DS-Lev calculated (see Section 3.5). In a similar fashion, subtraction of the relevant value from the acetate and levulinate methyl region, as well as for the contribution from the levulinyl methylene species, permitted the DS-Ac to be calculated. The position of the NMR signals arising from the lactone species on the cellulose backbone was consistent with the resonances determined for the model compound **(7)**. This shows it is possible to account for the overlapping lactone protons when integrating a LAC-Lactone in order to determine an accurate DS. Lactone incorporation onto cellulose as discussed here was not observed with other levulinyl-CE species, as mild reaction conditions were not used to generate these compounds.

2.7 γ-Valerolactone removal

Removal of the undesired lactone functionality from LAC-Lactone compounds was completed by further heating in solvent with catalytic acid. When DMF was used as the solvent the acetate and levulinate incorporation remained constant (Figure 2-15), while the DS-Lactone was reduced from 0.24 to 0.13. There was also a corresponding decrease in the DS-Total. These findings were consistent with removal of the lactone species and hydroxyl regeneration.

The same reaction was carried out in acetic acid where complete removal of the lactone group was achieved and the DS-Lev values remained constant. An increase in acetate incorporation (DS-Ac 0.26) was noted, which was consistent with the amount of lactone removed (DS-Lac 0.24). There are two mechanisms proposed for the increased incorporation of acetate observed. Firstly, direct esterification with acetic acid has been reported, although an extensive reaction time of 500 hours was required to effect this on native cellulose which resulted in only low acetate incorporation [28]. This implies that under the reaction conditions used here direct esterification is unlikely. A second rationale for acetate incorporation was activation of the acetal oxygen on cellulose followed

by loss of the lactone ring, which concomitantly reformed α-AL (Figure 2-16). The regenerated α-AL then reacts with acetic acid to generate 4-acetoxy-γ-valerolactone **(1)**, and this newly-formed reactive lactone is able to re-acetylate cellulose in the proposed mechanism (Figure 2-16). It is possible that only acetylation occurs due to steric effects of the partially esterified cellulose preventing levulinylation.

DS	Pre-treament	Treatment in DMF	Treatment in AcOH
Acetate	1.67	1.67	1.93
Levulinate	0.83	0.83	0.85
Lactone	0.24	0.13	0.00
Total	**2.74**	**2.63**	**2.78**

Figure 2-15 DS changes with respect to solvent for removal of the lactone from LAC-Lactone.

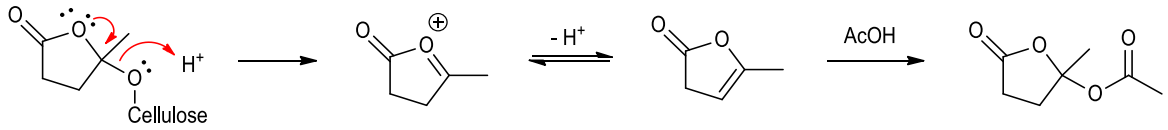

Figure 2-16 Proposed mechanism for removal of the lactone substituent and reactive lactone re-formation.

The observation of such lactone functionality provides further evidence that α-AL is an intermediate species in the formation of the "reactive lactones" discussed earlier in this chapter. It is possible that the free hydroxyls on cellulose are attacking α-AL directly, which results in the formation of LAC-Lactone. Under mild reaction conditions, this lactone substituent tolerated the reaction conditions without decomposition.

2.8 Reaction Colour

Esterification using LA generated coloured reactions and cellulose products, in direct contrast to the reaction using mixed anhydrides as reagents, which remained effectively colourless. This was exemplified by heating LA directly which generated a dark brown/red tar. Coloured compounds are likely to occur from side reactions due to the high temperatures and acidic esterification conditions used (colour mitigation is discussed in Section 4.5.4). Although it was not possible to separate and isolate discrete coloured compounds, a small amount of a mixture

of coloured compounds was isolated and NMR analysis indicated that there was significant alkene conjugation present, which is likely to result in colour. Kim *et al.,* using a related compound, demonstrated polymerisation of furfural alcohol and over time this coloured significantly due to the formation of conjugated alkene systems [132]. Angelica lactone polymerisation has also been shown to occur with the formation of a highly coloured material [133].

3 Cellulose ester characterisation

3.1 Introduction

Due to the importance and long history of CE manufacture, there is extensive literature devoted to the characterisation of this class of compound. Heinze *et al.* [134] and Lowman [135] have published detailed review articles which discuss many of the techniques used to characterise CEs. This chapter focuses on methodology pertinent to the novel levulinyl-CEs synthesised herein. The CE structure is characterised by the degree of substitution (DS) or level of ester incorporation, the ester type and the molecular weight. The level of ester incorporation for early CAs was characterised by determining the total combined acetyl content (total ester content) [136-138]. The ester groups were hydrolysed from the cellulose backbone and quantified by gravimetric analysis, or titration, and reported as a weight percentage. These traditional analysis methods are still suitable for determining total acetyl content; for example, ASTM method D817-96 [139] is still approved and describes a characterisation procedure based on hydrolysis of the ester groups and quantification of the cleaved acids by titration. Although these methods may seem crude today, and laborious when compared to modern techniques, accurate data can be obtained by experienced users. Total acetyl content as determined by hydrolysis is still relevant for CEs that contain one substituent, such as for CA.

Nuclear magnetic resonance (NMR) spectroscopy can be used to characterise the level and type of ester in a CE. Partial structural assignment of mixed CEs can thus be achieved using NMR analysis, where the overall DS of individual species can be determined by ^{1}H NMR spectroscopy. In addition, the substituent distribution between the three AGU reactive sites can be approximated using ^{13}C NMR spectroscopy. A number of CEs have been characterised by NMR spectroscopy, where both mono- and di-functionalised CE spectral resonances have been unequivocally assigned [134, 135, 140-142], showing that it is possible to account for, and resolve, the proton signals relating to both the ester and cellulose portions of the CE. Integration of the ^{1}H NMR spectrum provides the information necessary to calculate the DS: the integrated ratio of the cellulose region (assigned to the 7 AGU protons) to that of the ester substituent resonances gives the DS for the individual ester substituents (this is discussed in detail in Section 3.5). The DS information determined by ^{1}H NMR spectroscopy is however

limited to an average over the entire polymer. In the case of a CA that is not per-esterified, the AGU positions at C-2, C-3 and C-6 can either be a hydroxyl group or acetate, which results in eight possible AGU monomer units of varying substitution patterns. For a di-substituted CE (e.g. CAB or CAP) there are 27 possible monomer units. In general, a mono-substituted CE is not comprised of identical esterified AGU repeating units, thus the NMR spectra display broad peaks due to overlapping signals from the variously substituted monomer constituents in the polymer. The ^{1}H NMR spectrum displays significant peak broadening when moving from mono- to di-functionalised CEs, due to the increased number of monomer species present.

Several groups have investigated the substituent distribution at the C-2, C-3 and C-6 positions on the AGU using ^{13}C NMR spectroscopy and have assigned the ester carbonyl resonances [143-145]. The CE carbonyl resonance for acetate, propanoate or butyrate substituted CEs have been determined for substitution at the C-2, C-3 and C-6 positions (Table 3-1) and are located in the range ^{13}C δ 169-174 ppm. For mono- and di-functional CEs (provided the CE is comprised of acetate and one other substituent) it is possible to resolve and assign the resonances which can then be quantified to give a DS at each of the esterified AGU positions by integration and comparison of the relevant signal intensities. As mentioned above, acetate must be one of the substituents in the di-functionalised CE for this method to be applicable. For example, in the case of cellulose propanoate butyrate the ester carbonyl signals overlap and analysis of the individual ester distribution is not possible (Table 3-1).

Ester	AGU positioning	Carbonyl signals (^{13}C δ ppm)
Acetate	C-2	169.0
	C-3	169.5
	C-6	170.0
Propanoate	C-2	172.7
	C-3	173.1
	C-6	173.6
Butyrate	C-2	171.6
	C-3	172.1
	C-6	172.6

Table 3-1 ^{13}C NMR ester carbonyl shifts at positions C-2, C-3 and C-6 on the AGU.

When modifying a preformed polymer such as cellulose, there is no practical method for control over substituent positioning at each of the three reaction sites along the AGU backbone. While the lower steric hindrance of the primary alcohol at the C-6 position permits selective reaction at this site [146], acid-catalysed esterification is not site specific. The relative order of reactivity of the hydroxyls is C-6 > C-2 > C-3 [147, 148]. Gary *et al.* [149-151] and Mischink [152] demonstrated that using reductive cleavage and GC-MS (gas chromatography-mass spectrometer) analysis it was possible to quantify the individual monomer units which build up the CE backbone. The CA (DS 2.5) analysed showed an even distribution of acetate at the C-2, C-3 and C-6 positions, and it was noted that the most reactive C-6 position did not show complete acetylation. This finding was attributed to the CA having a DS of < 3 and therefore must have undergone a hydrolysis step during manufacture where hydrolysis occurred preferentially at the C-6 position [153]. Analysis of CAB and CAP samples, where a significant amount of both ester groups were present, showed that all 27 monomer species can be formed during the polymer's synthesis [149-151]. Clearly, the relative proportions of the 27 monomer units varied as the ratio of the ester substituents changed. A pivaloylysis[5] reaction was used by Redlich *et al.* [154] to generate monosaccharide and oligosaccharide units from CA, where only the β-1,4 glycosidic bond is cleaved. Complete conversion to the monosaccharide unit was only observed with a reaction time of > 200 hours. Preparative high-performance liquid chromatography (HPLC) was used to separate the monomeric and oligomeric species which were then fully characterised by NMR spectroscopy. Although only the tri-functionalised monomer units were characterised, this analysis of a CA (39.4 wt % acetyl) with a DS of 2.4 must have free hydroxyl sites and so a mixture of 8 monomer units would have been present. In theory characterisation of all species should have been possible.

Kamide *et al.* [155] investigated the monomer unit distribution of a CA using ^{13}C NMR spectroscopy. Integration of the 14 individual ester carbonyl signals that arise from the small chemical shift variations of the 8 different monomer units was completed. The signal resolution was poor, with significant peak overlap of the 14 signals, and in the published spectra it is clear that integration was difficult.

[5] Pivaloylysis is a mild method for efficient CE chain cleavage using pivalic anhydride, generating monomers and oligomeric units.

Analysis of the individual monomer units was not undertaken in this present study as the bulk polymer properties were the focus. Future work could include monomer analysis using the reductive cleavage/GC-MS technique.

3.2 Degree of substitution (DS)

Calculating the level of ester substitution is fundamental for the characterisation of CEs. The term "degree of substitution" (DS) is used for assigning ester incorporation onto cellulose and generally ranges from 0 to 3. Determination of the DS by ^{1}H NMR spectroscopy is a quick and accurate method of providing information such as functional group incorporation, and can also provide information on the degree of polymerisation (DP). However, it relies on the polymer being fully soluble in a compatible solvent and there being no overlap between the peaks of interest with those of the solvent used, neither of which is trivial.

For calculations of a hypothetical infinitely long cellulose polymer, the end groups of the polymer chain may be discounted and the total possible DS is therefore a maximum of 3. However, there can be significant chain cleavage (depolymerisation) that occurs during esterification, which results in the end groups contributing to the calculated DS. As chain length decreases, the relative proportion of end groups increases resulting in more reactive sites being available for esterification and therefore the DS values can exceed 3. For a CE with a DP of 200, the end groups make up 0.33% of the total reactive sites available, giving a possible DS of 3.01. A glucose unit (cellulose monomer; AGU) has five reactive sites, so in theory a fully depolymerised, fully substituted cellulose ester of this type would have a DS of 5. A DS below 3 indicates the presence of free hydroxyl groups on the cellulose chain. It should be noted that the DS determination is an average and in no way assigns the substituent positioning on the AGU.

3.3 CTA and CTLev characterisation

The structure of CA and the effect of ester substitution have been investigated using NMR spectroscopy by a number of groups [140, 145, 155, 156]. These studies have determined the structure of CAs and resulting

chemical shift changes observed due to the acetylation of cellulose. Cellulose trilevulinate (CTLev, Figure 3-2) was prepared to investigate the changes in the chemical shift patterns in comparison to CTA (Figure 3-1).

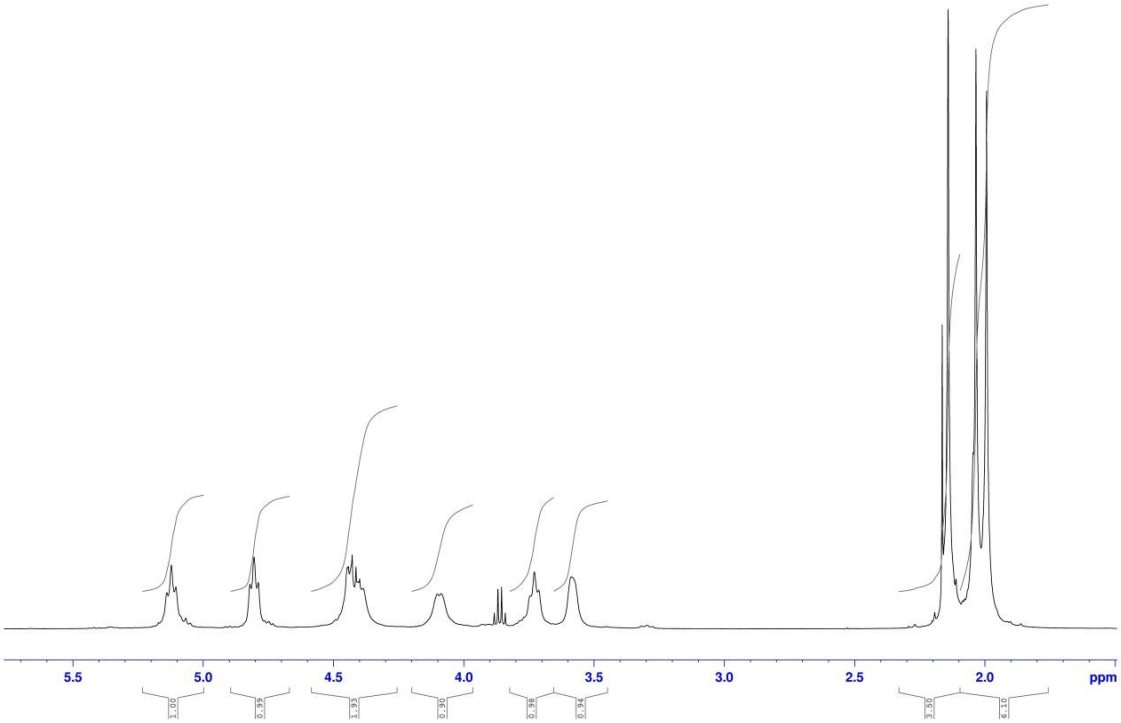

Figure 3-1 ^{1}H NMR of cellulose triacetate (CTA) with integrations showing the overlap of the ^{1}H signals for position 1 and position 6.

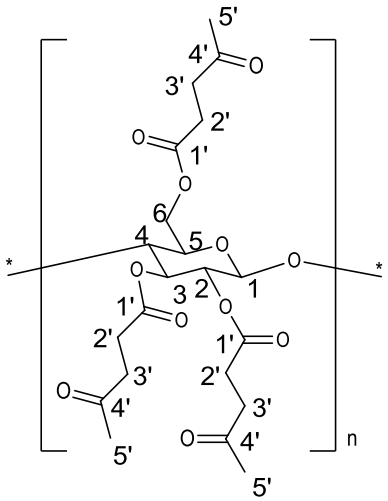

Figure 3-2 Cellulose trilevulinate (CTLev) representation and numbering.

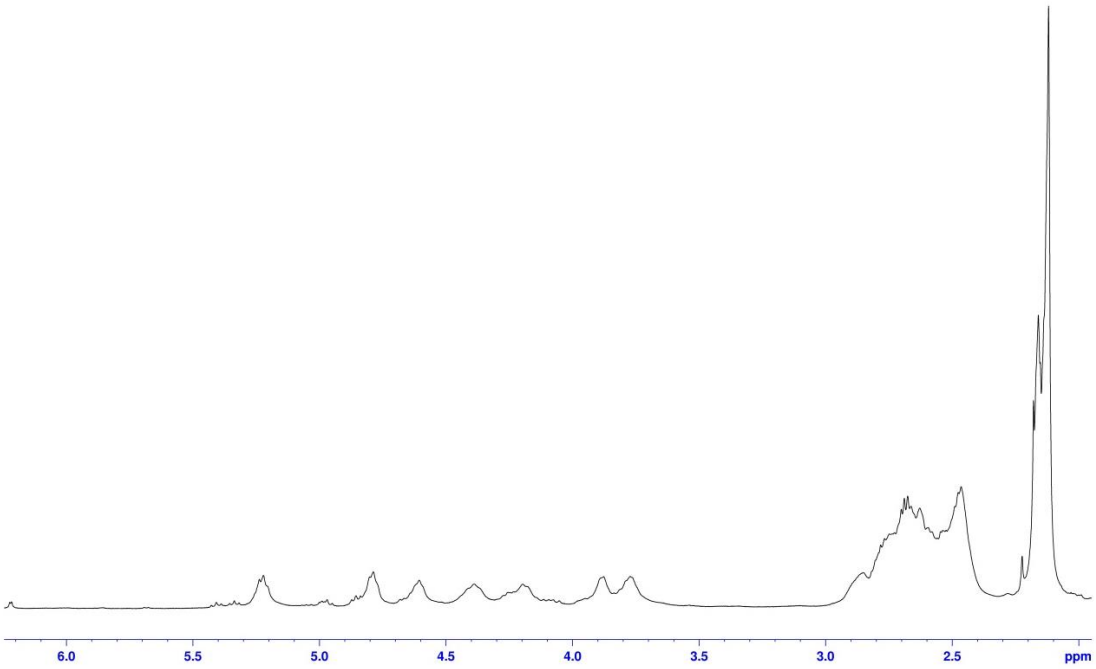

Figure 3-3 ^{1}H NMR of cellulose trilevulinate (CTLev).

To generate CTLev, the cellulose starting material was pre-swollen in water, steeped in acetic acid to displace the water, and this in turn was then displaced by LA. Following esterification, the DS was calculated by integration of the ^{1}H NMR spectrum for CTLev using the relevant signals attributed to the levulinyl methylene and methyl groups which gave comparable DS values of 3.04 and 3.03, respectively (Figure 3-3). That a very similar DS was calculated using the integration values of these two regions strongly suggested that little or no acetate had been incorporated. This was further evidenced by the lack of relevant ^{13}C NMR ester resonances relating to an acetate group. Based on the findings of Buchanan *et al.* [140] and Goux *et al.* [157], and combined with data obtained from 2D NMR experiments, the spectral assignment of CTLev was carried out (Table 3-2). The cellulose methine (C-1 to C-5) and methylene (C-6) ^{13}C NMR resonances for CTA and CTLev were comparable. Using the published CTA assignments and proton correlations from HSQC experiments, the ^{1}H NMR chemical shifts for CTLev were also assigned. For CTA one of the H-6 methylene (*b*) proton resonances (Table 3-2) overlapped with the H-1 resonance. These signals can be seen in Figure 3-1 at a chemical shift of ^{1}H δ 4.42 ppm, where the integration for this resonance equates to approximately two protons. In contrast, both of the CTLev H-6 proton signals could be distinguished as there was no overlap with the H-1 proton signal. Assignment

of the CTLev C-3 and C-5 ^{13}C NMR signals was possible through HSQC correlation with the clearly distinguished ^{1}H resonances at ^{1}H δ 5.23 ppm and 3.90 ppm, respectively.

	CTA		CTLev	
Position	**^{1}H δ ppm**	**^{13}C δ ppm**	**^{1}H δ ppm**	**^{13}C δ ppm**
1	4.42	100.4	4.61	100.5
2	4.79	71.7	4.79	71.4
3	5.07	72.5	5.23	72.3
4	3.71	76.0	3.78	76.0
5	3.53	72.7	3.90	72.5
6	*b* , 4.06	61.9	4.40, 4.21	62.5

Ester carbonyl	**CTA**	**CTLev**
Position	**^{13}C δ ppm**	**^{13}C δ ppm**
2	169.0	171.3
3	170.1	171.6
6	170.4	172.7

Table 3-2 Structural assignment of CTLev and comparison with CTA. The ^{1}H NMR signal at position 6 (*b*) of CTA was obscured by the ^{1}H signal at position 1.

Only two ketone resonances were recorded in the ^{13}C NMR spectra for the levulinyl γ-ketone: δ 206.7 ppm and δ 207.2 ppm. Integration of these two signals clearly indicated that the signal at ^{13}C δ 206.7 ppm accounted for two of the AGU esterification sites and the signal at δ 207.2 ppm accounted for one. Assignment of these resonances to the levulinyl groups attached at the C-2, C-3 or C-6 positions was not possible.

The CTLev ester carbonyl assignments for C-2, C-3 and C-6 were based on the literature assignments of propanoate [144] and butyrate [143] CE species. Propanoate and butyrate species substitution causes chemical shift changes in the ester ^{13}C NMR resonances for C-2, C-3 and C-6 in comparison to acetate, and levulinate appears to mirror that of the butyrate species (Table 3-1) consistent with the longer alky chain substitution. All ester variants displayed the same order for relative signal positioning in the ^{13}C NMR spectrum; the C-2 signal being the lowest ppm peak of the three, while the C-6 signal was the highest (Table 3-2).

3.4 LAC structural assignment

The ^{1}H and ^{13}C NMR spectra for a per-esterified CE such as CTA are relatively well defined. The substitution pattern on the AGU for a tri-substituted mono-functionalised cellulose ester does not vary, giving relatively sharp and defined resonances for tri-esters such as CTA and CTLev. For CTA the methine cellulose resonances can be readily resolved and $^{3}J_{HH}$ couplings calculated [140]. The CTLev resonances are not as clearly defined as CTA, most likely due to a series of sterically constrained conformations resulting from the longer ester chain present, generating different environments for the cellulosic methines.

When a second ester group is introduced onto the cellulose backbone, in what is anticipated to be a random distribution, 27 possible AGU substitution patterns result. This generates a complex ^{1}H NMR spectrum with significant peak overlap, and multiple resonances for each structural variation in the ^{13}C NMR spectrum. In comparison to the relatively well resolved peaks in the ^{1}H and ^{13}C NMR spectra of CTLev, incorporation of a second ester functionality (e.g. acetyl to generate LAC) results in significantly broader peaks due to the overlapping signals and numerous new chemical environments. Using the data obtained from the preparation of CTLev, and data collected for CTA (see Section 3.3), combined with 2D HSQC experiments on LAC, it was possible to determine a full spectral assignment for LAC (Table 3-3, Figure 3-4).

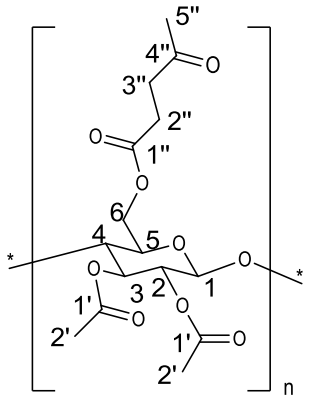

Figure 3-4 Substituent labelling for LAC.

	Acetate	Levulinate	Acetate/Levulinate
Position	^{1}H δ ppm	^{1}H δ ppm	^{13}C δ ppm
1	4.41	4.62	100.4
2	4.78	4.78	71.7
3	5.06	5.19	72.2
4	3.78	3.78	75.8
5	3.52	3.86	72.6
6	*b* , 4.07	4.37, 4.18	62.2

	Acetate	
Position	^{1}H δ ppm	^{13}C δ ppm
1'	-	173-168
2'	1.89-2.16	20.5

	Levulinate	
Position	^{1}H δ ppm	^{13}C δ ppm
1"	-	173-168
2"	2.31-2.71	27.6
3"	2.55-2.95	37.7
4"	-	207-205
5"	2.09-2.25	29.6

Table 3-3 Structural characterisation of LAC. The ^{1}H NMR signal for acetate at position 6 (*b*) was obscured by the ^{1}H signal at position 1.

Data obtained from 2D HSQC NMR experiments clearly showed a correlation between the broad ^{1}H NMR peaks in the cellulose region and the ^{13}C NMR signals which were previously assigned above to individual carbon positions in the AGU for both CTA and CTLev (Figure 3-5). Using the mono-substituted species as model compounds, and the fact that the carbon resonances do not differ greatly for a mixed ester compound, the LAC spectrum could be deconvoluted.

At the C-2, C-3 and C-6 positions of the AGU there was no significant difference in the relative proportion of acetate compared to levulinate incorporation for LAC. This was inferred qualitatively from the relative intensities of the cross peaks in the ^{1}H-^{13}C HSQC experiment. This lack of selectivity for esterification with acetate or

levulinate is proposed to generate a random substitution pattern on the polymer and is consistent with the results of Gray *et al.* [150].

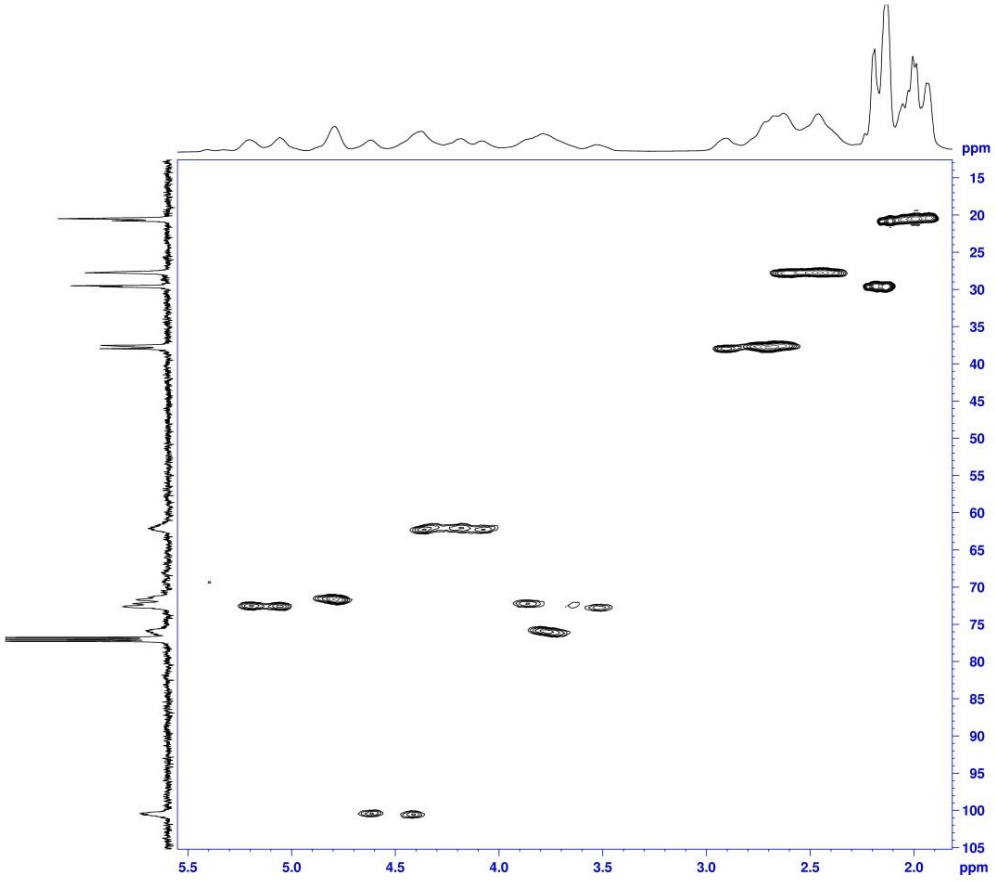

Figure 3-5 HSQC plot for LAC.

3.5 LAC degree of substitution calculation

The DS values (DS-Lev, DS-Ac and DS-Total) for LAC were determined using the ^{1}H NMR spectrum, assessing the ratio of the integrated areas of the ester functional groups to that of the cellulosic signals (methines and C-6 methylene, Figure 3-6). All of the ^{1}H NMR signals observed for LAC mixed esters were broad multiplets (Table 3-4). The cellulose region contains all of the proton resonances for the repeating glucose ring and was located in the region ^{1}H δ 3.30-5.50 ppm, with the two anomeric α and β end group resonances at ^{1}H δ 6.23 and 5.62 ppm, respectively. Assignment of the anomeric resonances was made by comparison with data for per-acetylated cellobiose [158]. The levulinyl methylene resonances in the ^{1}H NMR spectrum were observed in the region δ

2.30-3.05 ppm. The series of resonances at ^{1}H δ 1.85-2.30 ppm were assigned to the methyl groups of both acetate and levulinate.

LAC	^{1}H δ ppm
Cellulose	3.30-5.50
Levulinyl (methylene)	2.30-3.05
Methyl (acetyl and levulinyl)	1.85-2.30
Reducing end α	6.23
Reducing end β	5.62

Table 3-4 ^{1}H NMR signals for LAC.

Acetyl and levulinyl ^{13}C NMR methyl resonances were recorded at δ 20.5 and 29.6 ppm, respectively. Data from a HSQC experiment indicated that unambiguous proton assignment and deconvolution of the acetate and levulinate methyl resonances in the complex series of peaks between ^{1}H δ 1.85 and 2.30 ppm was not possible due to significant peak overlap (Figure 3-5) in the region ^{1}H δ 2.09 to 2.16 ppm.

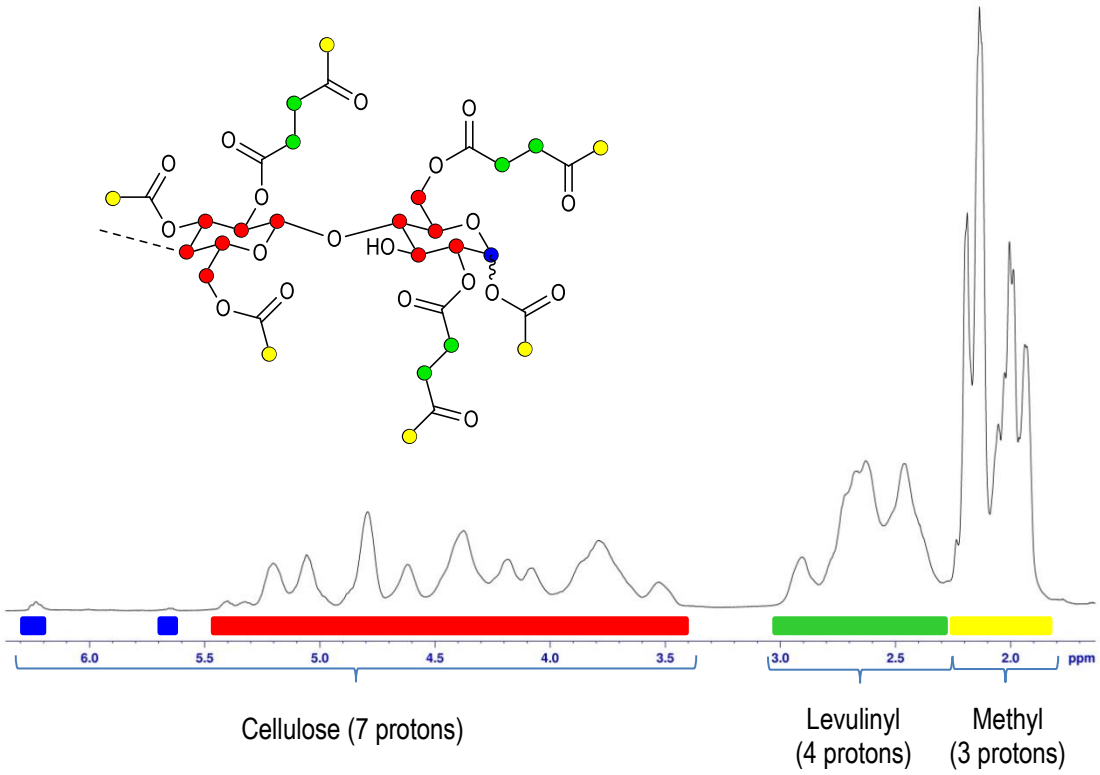

Figure 3-6 LAC ^{1}H NMR spectrum with integration regions colour coded to indicate structural components.

The ratio of the integrated area for the levulinyl methylene protons (4H), compared to the cellulosic methines (7H) permitted calculation of the DS-Lev (Figure 3-6). The DS-Total was calculated in a similar fashion by comparing the integration for all methyl resonances (3H) to that of the cellulose region. From the DS-Total and the DS-Lev values it was then possible to calculate the DS-Ac by simple subtraction of the DS-Lev from the DS-Total.

Quantification of the levulinate and acetate distribution between the C-2, C-3 and C-6 positions on the AGU was also possible by integration of the individual ^{13}C NMR ester carbonyl resonances (signal positions given in Table 3-5) as discussed in Section 6. This region of the spectrum could be resolved into two sets of three peaks which were used to determine the ester distribution (Figure 3-7). Using data reported here and literature values, it was possible to assign both acetate and levulinate ester carbonyl peaks to specific AGU positions (Table 3-5) [143, 144]. Although the LAC carbonyl region is not as well resolved as the literature examples, by using the information that was gathered and applying this to LAC it was possible to make an approximation of the levulinate and acetate distribution. This method was not particularly precise, therefore only LAC 500.1 was analysed using this method as a reference (see Section 6). The carbonyl resonances for CTLev were assigned to ^{13}C δ 171.3, 171.6 and 172.7 ppm, for positions C-2, C-3 and C-6 respectively. A minor discrepancy was noted in the ^{13}C NMR resonances of the acetate carbonyl peaks published in the literature [142, 143] in comparison to LAC, and for the levulinyl peaks in comparison to CTLev. This discrepancy could be attributed to the NMR spectroscopy experimental conditions used, but is more likely a function of the differing electronic environments experienced by the mixture of levulinate and acetate esters.

	Acetate	Acetate	Acetate	Levulinate
AGU position	W.J. Goux	Y. Tezuka	LAC 500.1	LAC 500.1
2	169.9	169.0	169.4	171.3
3	170.2	169.5	169.9	171.6
6	170.5	170.0	170.4	172.7

Table 3-5 Acetate and levulinate ^{13}C ester carbonyl resonances for AGU positions C-2, C-3 and C-6.

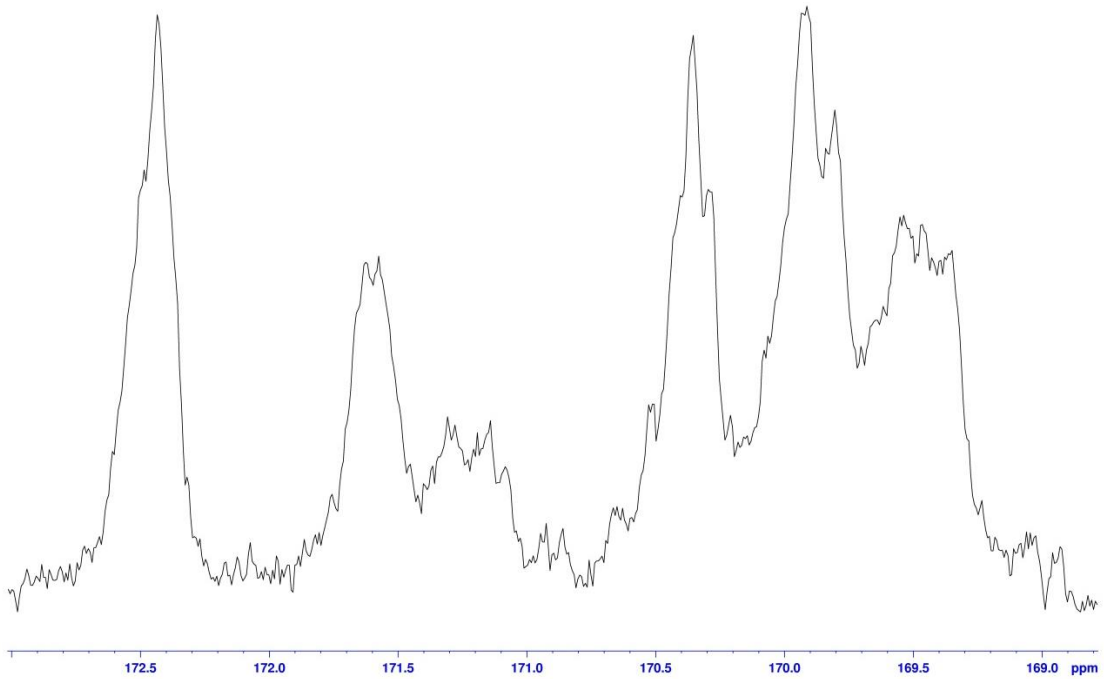

Figure 3-7 ^{13}C NMR spectrum of the carbonyl region of LAC 500.1.

3.6 NMR analysis and structural characterisation of levulinyl butyryl cellulose and related cellulose esters

This section describes CEs containing levulinate and one other linear aliphatic ester group (C_3-C_6), including isobutyrate. The ^{1}H NMR spectra for all of these mixed aliphatic levulinyl-CEs showed a series of broad multiplets which can be divided into defined regions. The cellulose methines were observed at ^{1}H δ 3.35-5.55 ppm. Levulinyl methylene signals were located between ^{1}H δ 2.04-3.06 ppm and overlapped with the alkyl ester C_3-C_6 α-methylene resonance (adjacent to the ester carbonyl) and the isobutyrate methine resonance. The C_3-C_6 aliphatic ester methyl resonances were observed as broad multiplets and were located in the range between ^{1}H δ 0.83-1.30 ppm (Table 3-6).

Ester group	Methyl resonance (^{1}H δ ppm)
Propanoate	0.96-1.23
Butyrate	0.76-1.06
Isobutyrate	0.98-1.30
Valerate	0.83-0.96
Hexanoate	0.83-0.96

Table 3-6 Methyl resonance for alkyl esters in mixed levulinyl-CEs.

The ^{1}H NMR spectra of levulinyl-CEs that contained valerate or hexanoate esters displayed two signals appearing as broad multiplets between ^{1}H δ 1.13 and 1.71 ppm, accounting for 4 or 6 protons, respectively. Levulinyl-CE species displayed a resonance of broad multiplets positioned in the range ^{1}H δ 1.38-1.80 ppm (2H) for the mixed ester with butyrate functionality.

The DS for mixed aliphatic (≥C_3) levulinyl-CE species was calculated in a similar fashion to LAC, where the ratio of the integrated levulinyl or aliphatic region, to the cellulose region, gave the corresponding ester's DS. For the calculation of the DS-Lev, the levulinate methylene, aliphatic α-methylene or isobutyrate methine proton resonances overlapped, and therefore the aliphatic α-methylene resonance (or the isobutyrate methine) must be subtracted from the levulinate contribution (Figure 3-8). Levulinyl butyryl cellulose (LBC) was characterised more fully as an example of this type of calculation for a mixed aliphatic levulinyl CE, as this was the material being progressed through the research program (discussed in Section 4.8). Key features of the characterisation methodology for other examples will be mentioned where relevant. The integrated regions used for the DS calculation of the LBC substituents are given in Table 3-7 and illustrated in Figure 3-8. The aliphatic methyl region was integrated for 3 protons (6 for the case of isobutyrate), which gave both the aliphatic ester DS and the information needed for subtraction of the 2 aliphatic protons (1 for isobutyrate) from the levulinyl region. These two aliphatic protons were subtracted from the levulinyl region, then the remaining peak area was integrated for 7 protons (two methylenes and a methyl resonance), and the ratio of this to the integrated cellulose region gave the DS-Lev. Substituent distribution could not be determined for these materials using the ester carbonyl resonances in the ^{13}C NMR spectra (discussed in Section 3.5) due to the C_3-C_6 alkyl ester carbonyl resonances overlapping with the levulinyl ester carbonyl resonance.

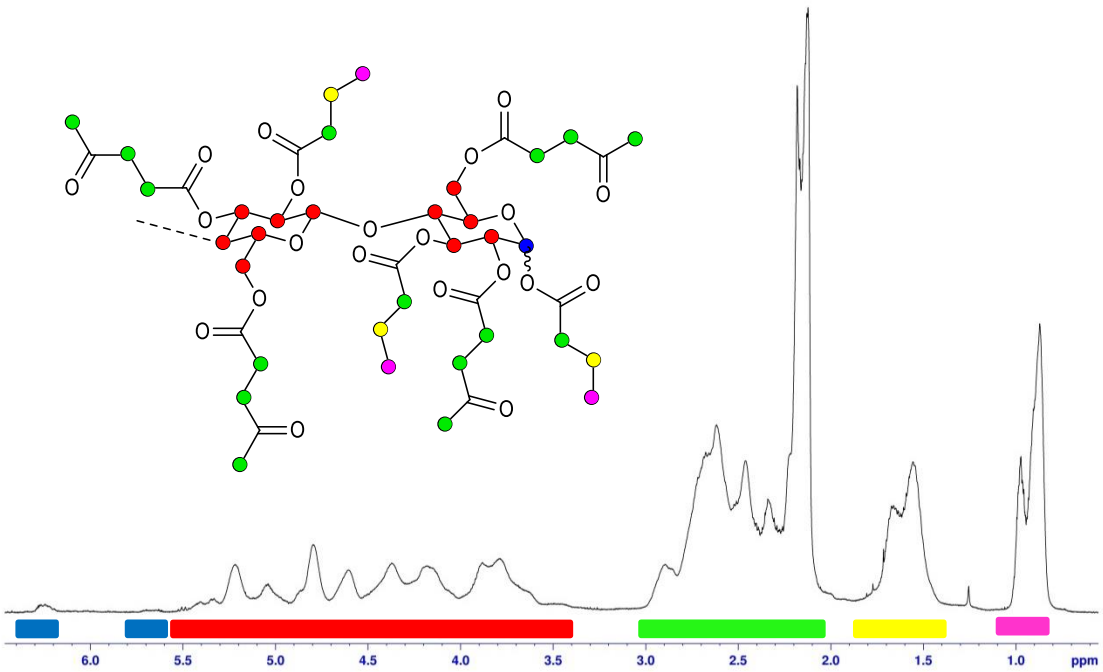

Figure 3-8 ^{1}H NMR spectrum of LBC.

LBC	^{1}H δ ppm
Cellulose	3.35-5.55
Levulinate	2.04-3.06
Butyrate (α-methylene)[a]	2.35
Butyrate (β-methylene)	1.38-1.80
Butyrate (methyl)	0.76-1.06
Reducing end α	6.23
Reducing end β	5.65

Table 3-7 ^{1}H NMR region resonances for LBC. [a] Due to the overlap of the butyrate α-methylene signal and the levulinate signals, the butyrate α-methylene signal position was assigned to the centre point of the resonance.

3.7 NMR analysis of butyryl levulinyl acetyl cellulose (BLAC)

The proton spectrum for BLAC was comparable to other mixed CEs showing discrete regions of broad multiplets (Table 3-8). BLAC contains a mixture of three ester substituents: butyrate, levulinate and acetate. As a consequence of signal overlap, full characterisation of BLAC by NMR spectroscopy and unequivocal determination of the DS for all three substituents could not be completed. However, it was possible to calculate the DS-But accurately from the NMR spectrum in a similar fashion to the LBC calculations; the ratio of the integrated butyrate methyl region to the cellulose region gave the DS-But. However, the DS-Ac and DS-Lev could not be calculated as separation and integration of the individual substituent signals was not possible. Nor was it possible to perform a subtraction due to the varied and unknown level of contribution for the differing substituent groups. The levulinyl region (^{1}H δ 1.80-3.06 ppm) was a complex set of broad overlapping multiplets containing the levulinate methylenes centred at ^{1}H δ 2.65 ppm, butyrate α-methylene (adjacent to the carbonyl) centred at ^{1}H δ 2.33 ppm and methyl resonances of levulinate and acetate centred at ^{1}H δ 2.17 and 2.00 ppm respectively. Analysis of HSQC experimental data showed that there was significant overlap of the levulinyl signals (methylene and methyl) and the butyryl α-methylene signal (adjacent to the carbonyl). The methyl signal for the levulinyl and acetyl groups also overlapped with the butyryl α-methylene signal, further confounding the data (Figure 3-9). Therefore, accurate separation and integration of the peaks relating to these three species which resonated in the region ^{1}H δ 1.80-3.06 ppm could not be achieved. Furthermore, assignment of the substituent distribution at the three positions on the AGU was not possible by ^{13}C NMR spectroscopy as the carbonyl resonances in the ^{13}C spectra for BLAC had broadened further, and again, the levulinyl and butyryl signals overlapped. In order to accurately determine the degree of substitution of the BLAC polymer, an alternative method was developed.

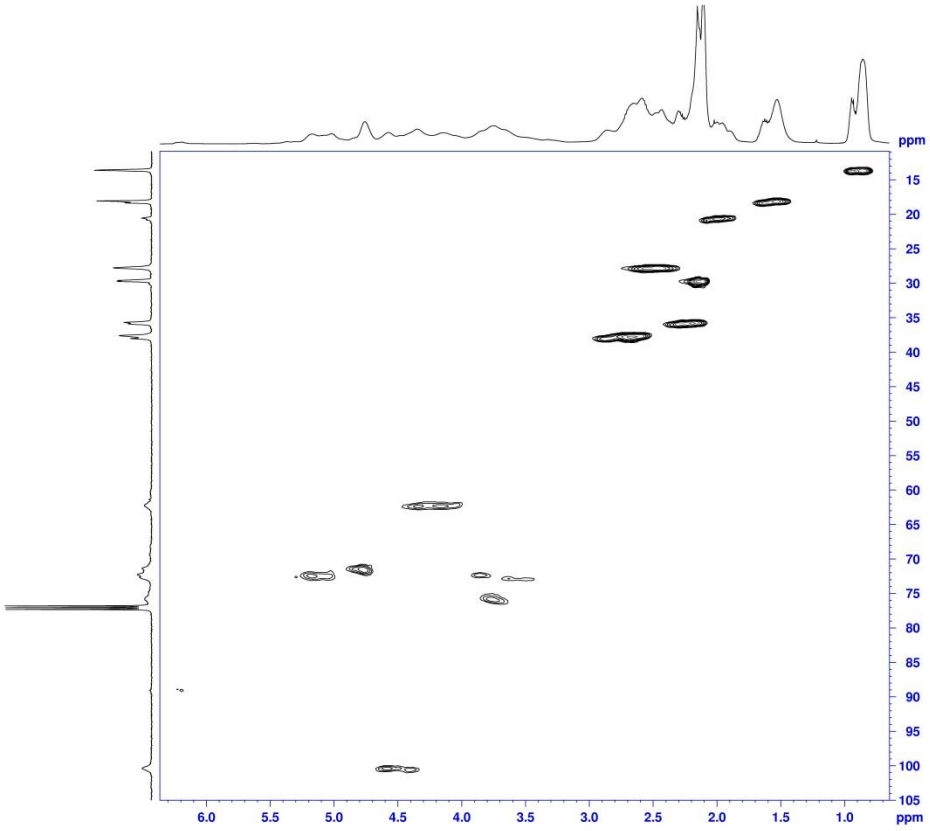

Figure 3-9 HSQC spectra of BLAC (CT-x429-1).

BLAC	^{1}H δ ppm
Cellulose	3.16-5.60
Levulinate	1.80-3.06
Acetate	1.81-2.13
Butyrate (α-methylene)[a]	2.33
Butyrate (β-methylene)	1.38-1.77
Butyrate (methyl)	0.76-1.06
Reducing end α	6.23
Reducing end β	5.65

Table 3-8 ^{1}H NMR spectral data for BLAC. [a] Due to the overlap of the butyrate α-methylene signal and the levulinate signals, the butyrate α-methylene signal position was given as the centre point of the resonance.

As an unexpected aside, it was possible to observe clear HSQC correlations for the α and β reducing end anomers was observed (see Table 3-9). This proton-carbon correlation had not been detected in previous NMR analyses.

End group	^{1}H δ ppm	^{13}C δ ppm
Reducing end α	6.23	88.9
Reducing end β	5.65	91.5

Table 3-9 NMR data for the α and β anomeric end group signals for BLAC.

3.8 Analysis by HPLC to determine the DS of CEs

Calculation of the DS of cellulose esters was attempted using a GC (gas chromatography)-based analytical method and was based on the reported methods of Tindall *et al.* and Sano *et al.* [159, 160]. This method involved hydrolysis of the CE and methylation of the liberated acids to the corresponding methyl esters. These were quantified against a set of standards with an internal standard present by GC.

Unfortunately, this method failed to provide suitable data for accurate LAC substituent analysis. Particular difficulties were encountered when attempting to quantify the levulinic acid ester derivative, a possible reason being that GC analysis requires high temperatures to volatilise the samples. Due to the reactive nature of the levulinic species it was speculated that degradation products formed at these high temperatures.

As a consequence of the unreliable nature of the method above, the focus turned to the development of a suitable HPLC-based technique. The first step in the development of the HPLC method was to ensure good separation of the species of interest with the specific chromatographic conditions used (Section 10.1.14). Analysis of a mixture of acetic, butyric and levulinic acids, where propionic acid was used as the internal standard, demonstrated these species were well separated with no peak overlap (Figure 3-10, elution times are given in Table 3-10; the acids were detected using a refractive index (RI) detector). Standards prepared for all

four acid species gave a linear response (R^2=0.99) over the tested range of 0.05 to 10 mg/mL, and relative response factors were determined.

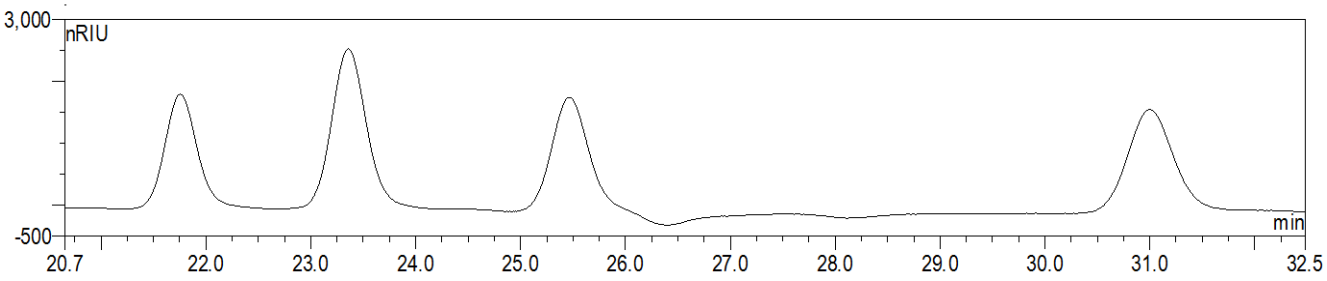

Figure 3-10 Chromatogram of acetic, propionic, butyric and levulinic acids at 0.5 mg/mL (RI detection).

Acid	Elution time (min)
Acetic	21.8
Propionic [a]	25.5
Butyric	31.0
Levulinic	23.4

Table 3-10 Carboxylic acid elution times using a Resex ROA column. [a] Internal standard.

3.8.1 Analysis of commercial CEs

Having successfully shown that the acids of interest could be well resolved by HPLC, a suitable method of cleaving these acids from the CE was investigated. Roxin *et al.* [161] demonstrated a simple ester hydrolysis method using cellulose acetate phthalate, and showed complete hydrolysis of the ester groups was achieved after two hours under basic conditions. The reaction was applied to a di-substituted CE sample (CAB 381-2) and the results indicated that a minimum reaction time of three hours was required to achieve complete hydrolysis (Table 3-11). The hydrolysis reaction was deemed complete after three hours as extending the reaction time did not increase the level of quantifiable carboxylic acids. A reaction time of three hours also showed that the standard deviation for the triplicate samples had reduced, further evidence of the reaction reaching a common end-point. Reaction times greater than three hours showed no reduction in hydrolysed acetic or butyric acid,

indicating that the hydrolysed acids were stable once cleaved, and did not decompose or distil from the reaction media.

Time (hours)	DS-Ac	DS-Ac (Stdev)	DS-But	DS-But (Stdev)
0.5	0.40	0.05	0.64	0.08
1	0.66	0.03	1.05	0.05
2	0.95	0.08	1.48	0.12
3	1.11	0.01	1.70	0.01
4	1.12	0.01	1.71	0.02
6	1.11	0.00	1.72	0.01

Table 3-11 Ester hydrolysis of CAB 381-2 with varied reaction time and the DS calculated by HPLC.

This method for calculating the DS of CEs was further tested using a commercially available Eastman CA and CAB in order to verify accuracy and detection limits. Comparison of literature data (^{1}H NMR and HPLC-derived values) indicated that this hydrolysis method provided a robust and accurate method for determining the DS of CEs (Table 3-12). The DS for CA320s could not be determined by NMR spectroscopy as no suitable solvent could be found. CA320s is insoluble in $CDCl_3$, the default NMR solvent for this project (the residual $CHCl_3$ signal at ^{1}H δ 7.26 ppm does not interfere with signals required for integration, refer to Section 10.1.1). All solvent systems that were found to be effective at solvating CA320s had residual solvent signals that overlapped with key signals (solvents tried: d_6-acetone, d_4-acetic acid, d_6-DMSO). A good correlation was observed between the reported literature value for the DS for CA320s and the HPLC results determined here. However, trace butyric acid was observed in the samples analysed by HPLC, which was not detected by NMR. One possible reason for this could be cross contamination of butyric acid (or anhydride) during the manufacture of CA320s, inadvertently incorporating butyryl functionality into the polymer structure. A second possibility for the trace butyrate reading for CA320s is cross contamination with CAB during the packaging process.

The DS results for CAB 381-2 obtained by NMR spectroscopy and HPLC analysis of the hydrolysed acids were very similar (Table 3-12). In comparison to literature values, the DS-But by both methods were 5% lower, while the calculated DS-Ac was 6% and 11% higher by NMR spectroscopy and the HPLC analysis method,

respectively. Batch variation during manufacture of CAB 381-2 could be responsible for the discrepancy in the literature compared to the DS calculated here.

Sample	DS	Literature	^{1}H NMR	HPLC
CA320s	DS-Ac	1.80	-	1.76
	DS-But	0.00	-	0.02
CAB 381-2	DS-Ac	1.00	1.06	1.11
	DS-But	1.80	1.71	1.72
CAB 553-0.4	DS-Ac	0.10	0.11	0.14
	DS-But	2.00	2.01	1.98

Table 3-12 Comparison of the literature DS values of commercial CEs with those measured by ^{1}H NMR spectroscopy and HPLC analysis of the hydrolysed acids.

Overall, the similarity of the values for the DS of the CEs as determined by NMR spectroscopy and by hydrolysis of the ester substituents, in addition to the close correlation of the data to literature values, gave good confidence in the characterisation of this class of compound.

3.8.2 Analysis of LAC ester constituents

The stability and reactivity of LA was tested in relation to the HPLC method discussed in this section. Two solutions of LA at different concentrations were subjected to the same conditions used for the hydrolysis of the CE. Over a 0.5-6.0 hour time course experiment, no loss of LA was observed (Table 3-13). At low concentrations of LA (A; 1.16 mg/mL) no variation in the concentration was observed, remaining constant at 1.15 ± 0.01 mg/mL over the time period monitored. At a higher concentration of LA (B; 5.19 mg/mL), a very small variation between samples was recorded. Overall, these results indicated that LA remained stable under the hydrolysis conditions employed with no side reactions taking place. Therefore, it should be possible to accurately quantify LA using the HPLC method described.

Time (hours)	A (LA mg/mL)	Stdev	B (LA mg/mL)	Stdev
0.5	1.15	0.01	5.19	0.01
1.0	1.15	0.01	5.20	0.02
2.0	1.15	0.01	5.18	0.01
4.0	1.15	0.01	5.18	0.01
6.0	1.15	0.01	5.17	0.01

Table 3-13 Stability testing of LA by HPLC at concentrations A, 1.16 mg/mL, and B, 5.19 mg/mL.

Time (hours)	DS-Ac	DS-Ac (Stdev)	DS-Lev	DS-Lev (Stdev)
0.5	1.88	0.02	1.04	0.01
1.0	1.83	0.02	1.00	0.01
2.0	1.84	0.14	1.00	0.08
3.0	1.81	0.06	0.98	0.03
4.0	1.83	0.05	0.99	0.03
6.0	1.85	0.03	1.01	0.02

Table 3-14 Ester hydrolysis of LAC 500.1 over time with the DS calculated by HPLC analysis.

Analysis of the DS of the LAC 500.1 polymer was completed and data obtained from HPLC analysis showed that the ester hydrolysis was complete after 30 minutes (Table 3-14). The increased rate of reaction in comparison to the commercial CEs tested could be attributed to LAC 500.1 being a smaller and more hydrophilic polymer making it more water labile with a greater level of solubility in the reaction medium than the more hydrophobic counterparts.

LAC 500.1	^{1}H NMR	HPLC
DS-Ac	1.89	1.85
DS-Lev	1.21	1.01

Table 3-15 Measurement of the DS of LAC 500.1 by two methods.

Unfortunately, the DS values for LAC 500.1 calculated by ^{1}H NMR spectroscopy and HPLC analysis of the hydrolysed acids were not in agreement (Table 3-15). It is unlikely that the discrepancies were caused by

incomplete hydrolysis or a side reaction of LA as previous data had demonstrated that LA was unaffected by the hydrolysis process. There are two possible explanations for the inconsistencies observed:

- Firstly, incomplete sample dissolution during NMR experiments. Over time the solutions prepared for NMR spectroscopic analysis of LAC in $CDCl_3$ became hazy, potentially due to the agglomeration of insoluble particles. NMR spectroscopy in solution only quantifies species which are soluble in the chosen solvent system, thus incomplete solubility would not deliver data representative of the entire sample. Differential solubility of CEs as a result of variation in the DS is discussed in Section 1.8.1. Chloroform is known to dissolve CEs with a DS of > 2.5 and the insoluble material is postulated to be the lower DS material (< 2.5) and therefore, the DS as determined by analysis of ^{1}H NMR spectra is likely to be overestimated.
- Secondly, the observed discrepancies could be attributed to line broadening in the NMR spectrum and peak overlap. Using a mixture of α and β per-levulinated cellobiose anomers (DS-Lev 7.89) as model compounds, the levulinyl methylene region was assigned to the region ^{1}H δ 2.40-3.00 ppm and the levulinyl methyl region to ^{1}H δ 2.11-2.24 ppm. In the case of LAC 500.1, these resonances broadened to ^{1}H δ 2.30-3.05 ppm (levulinyl methylene) and ^{1}H δ 1.89-2.30 ppm (levulinyl methyl), respectively, and the lower ppm range also includes the acetyl methyl resonance. This overlap at ^{1}H δ 2.30 ppm confounds the NMR results where a portion of the methyl resonances may be integrated as levulinyl methylene signals (see Section 3.5). For the calculations using ^{1}H NMR integrated values this also serves to over-approximate the levulinyl contribution.

3.8.3 Analysis of BLAC ester constituents

Calculation of the DS by hydrolysis of the cellulose ester and HPLC analysis of the resultant acids was completed on two BLAC species; both high levulinate content (DS-Lev >1; CT-x429-1) and low levulinate content (DS-Lev <1; CT-x311-2) compounds. A time course reaction series was completed for these two BLAC polymers to determine the minimum reaction time required.

High levulinate (DS-Lev >1, CT-x429-1)						
Time (hours)	**DS-Ac**	**DS-Ac (Stdev)**	**DS-But**	**DS-But (Stdev)**	**DS-Lev**	**DS-Lev (Stdev)**
0.2	0.38	0.06	0.93	0.14	1.11	0.17
0.3	0.44	0.02	1.05	0.04	1.24	0.04
0.5	0.43	0.01	1.03	0.03	1.20	0.03
1.0	0.43	0.01	1.01	0.03	1.16	0.03
2.0	0.42	0.02	1.01	0.04	1.15	0.05
3.0	0.43	0.00	0.99	0.00	1.14	0.01
4.0	0.44	0.01	1.02	0.02	1.14	0.02
6.0	0.45	0.01	1.03	0.02	1.16	0.02
Low levulinate (DS-Lev <1, CT-x311-2)						
Time (hours)	**DS-Ac**	**DS-Ac (Stdev)**	**DS-But**	**DS-But (Stdev)**	**DS-Lev**	**DS-Lev (Stdev)**
0.2	0.50	0.02	0.93	0.04	0.34	0.01
0.3	0.71	0.01	1.31	0.02	0.47	0.01
0.5	0.80	0.02	1.47	0.04	0.53	0.02
1.0	0.78	0.03	1.43	0.07	0.51	0.03
2.0	0.81	0.01	1.49	0.01	0.52	0.00
3.0	0.82	0.00	1.48	0.00	0.52	0.00
4.0	0.85	0.01	1.53	0.02	0.53	0.01
6.0	0.83	0.01	1.49	0.01	0.51	0.01

Table 3-16 Hydrolysis of BLAC esters with the DS calculated by HPLC analysis for compounds with high levulinate incorporation (DS-Lev >1; CT-x429-1) and low levulinate incorporation (DS-Lev <1; CT-x311-2).

The results indicated that for the high (CT-x429-1) and low (CT-x311-2) levulinate incorporated BLAC samples, reproducible HPLC data was recorded (Table 3-16). Both BLAC samples tested mirrored the results for LAC 500.1 where ester hydrolysis reached an end point after 30 minutes; no significant change in the levels of the hydrolysed acids was observed after this period. Although both BLAC samples tested only required 30 minutes

for complete hydrolysis to occur, all subsequent experiments used a reaction time of 3 hours to ensure complete hydrolysis - particularly for the larger polymers and very low level levulinyl containing CEs (both of which could display increased hydrolysis times).

Chromatography traces for all hydrolysis reaction products showed a series of impurity peaks likely relating to highly polar species or salts. However, these eluted before the acids of interest and did not affect quantification. A typical chromatogram showing the eluting acids is illustrated in Figure 3-11.

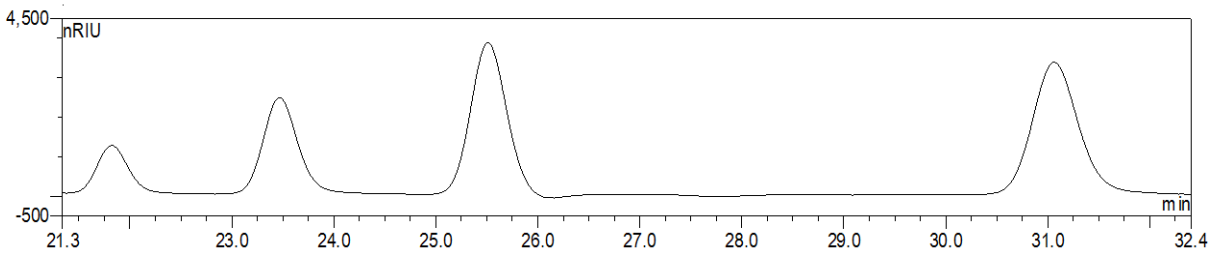

Figure 3-11 HPLC chromatogram of the hydrolysis products of a high levulinate content BLAC (CT-x311-2).

3.8.4 Errors and self-checks

Although the method developed for the quantification of the DS for CEs using HPLC analysis was a reliable and robust method, like most procedures, there are sources of error. Accurate sample weight is the most significant source of error for this procedure, as samples need to be carefully dried before weighing; any moisture present will significantly affect the results. Comparison of the HPLC results to data derived from NMR spectroscopy can be applied as a self-check for CE samples, but importantly, only when a fully chloroform-soluble polymer is being considered can the NMR data be directly correlated. In the case of BLAC it was only possible to obtain an accurate DS value for the butyryl substituent by NMR spectroscopy (for a fully chloroform-soluble BLAC) as this constituent had no overlapping peaks with the butyryl methyl resonance (Section 3.7). Therefore, only the DS-But of BLAC polymers could be compared by the two methods.

3.8.5 Summary

The method developed using HPLC analysis proved to be an accurate and robust method for quantifying ester groups hydrolysed from CEs irrespective of sample type and solubility characteristics. This permitted the precise calculation of the DS for a given sample. In the case of di-functionalised CEs (e.g. LAC and CAB), the substituent esters present were readily and accurately quantified by NMR spectroscopy so this method was preferentially applied in this case, mainly due to the ease and speed of sample measurements. The hydrolysis of CEs and subsequent HPLC analysis proved to be a valuable tool for quantifying tri-functionalised CEs, particularly in the case of BLAC which has a complex NMR spectrum.

3.9 Molecular weight of cellulose esters

Determination of the molecular weight of a polymer is fundamental to characterising and rationalising the physical parameters of such species and is usually reported as a number average molecular weight (M_n) and/or a weight average molecular weight (M_w). M_n is the mean weight of all of the polymer chains in the sample and skews the value towards low molecular weight species. The M_w measurement gives more weighting to higher molecular weight species and therefore skews the value towards higher molecular weight components. There are several techniques that can be used to determine M_n and M_w; Painter and Coleman [93] discuss a number of methods for quantifying M_n (end group or osmotic pressure analysis) and M_w (light scattering or ultracentrifugation). The ratio of M_w/M_n is defined as the polydispersity value and this is used to help describe the molecular weight distribution of a sample; a monodisperse sample has a polydispersity of 1 ($M_n=M_w$).

3.9.1 SEC

Size exclusion chromatography (SEC) is a technique used to separate individual polymer chains according to their hydrodynamic volume, from which the molecular weight (M_n and M_w) can be calculated by comparison to appropriate standards. The SEC technique is discussed by Yau [162]. When analysing a polymer sample using SEC, a dilute solution of the polymer is injected onto a column, or a series of columns, which are packed with

porous material. The time taken for a polymer to elute from the column system is dependent on the hydrodynamic volume for that polymer and determines the elution time (or solvent elution volume) for a particular polymer with a particular molecular weight. Smaller polymer chains have a corresponding smaller hydrodynamic volume and take a longer time to passage through the column and are eluted later than larger polymer chains. Therefore for SEC, elution of the individual polymer chains is from large to small, with time. The columns which are chosen have a working molecular weight range (the column exclusion limit), and outside of this range the column does not separate the polymer chains in a quantifiable fashion.

When a polymer sample is analysed by SEC, a peak is generated by the eluting polymer which contains the entire molecular weight distribution of the polymer sample. This peak is used to calculate M_n, M_w and M_p, where M_p is the molecular weight at the peak height maximum; the molecular weight of the most abundant species [163]. The columns are calibrated against a set of monodisperse standards, commonly polystyrene, by plotting the retention time (or eluted volume) against the standards. A calibration plot may be generated that permits calculation of M_n, M_w and M_p. Unless the polymer being investigated has the same chemical makeup and architecture as the polymer standards being used, the hydrodynamic volume will be different between samples and standards for a given molecular weight. Therefore, only a relative value based on the standards can be assigned. It is possible to calculate absolute molecular weight values using a universal calibration curve which is based on intrinsic viscosity, and this may be used to correct the molecular weight values [48, 93]. The universal calibration curve does not work for polymers with rigid backbones such as CEs [93], and therefore molecular weights determined by SEC are reported as relative to the standards used. In the technical literature that Eastman provides with their commercial CEs, molecular weight (M_n) is quoted as relative to polystyrene standards. All CE molecular weights analysed for this project are reported as M_p relative to polystyrene standards unless specifically stated otherwise. This approximation was chosen as the values determined were only used as a comparative tool to investigate trends between samples, and M_n, M_w and polydispersity analysis was not critical in assessing the effect of varying reaction conditions[6].

[6] Dr Jan Young Jon is acknowledged for his valuable discussions regarding the analysis of polymer molecular weight by SEC.

Software capable of calculating M_n, M_w and polydispersity was unavailable during the course of this project. However, full molecular weight analysis was completed, by hand, for a series of levulinyl-CEs and commercially prepared CEs, the results of which are given in Table 3-17 to show the relationship between M_n, M_w and M_p. The SEC peak that was generated for each sample was analysed by taking a height and relative molecular weight measurement at quarter minute intervals across the entire peak, from which M_n and M_w were calculated. The results showed that $M_n < M_p < M_w$ for all samples as expected [164], and that the M_n values that were calculated for the commercial CEs correlated well with the reported values (Table 3-18). The CEs analysed showed a wide molecular weight distribution with polydispersity values ranging between 3.1 and 5.7. It was expected that CEs would display a large molecular weight distribution as a function of the chemistry used where significant depolymerisation can occur to the cellulose backbone.

Cellulose ester	M_n (g/mol)	M_w (g/mol)	M_p (g/mol)	Polydispersity
Commercial samples				
CA 320s	35000	107000	70000	3.1
CA 398-3	29000	108000	77000	3.7
CAB 553-0.4	19000	109000	53000	5.7
BLAC samples				
CT-x429-1	6300	32000	15000	5.1
CT-RPa003K	8200	32000	17500	3.9

Table 3-17 Full molecular weight analysis of commercial CEs and BLAC species.

Cellulose ester	M_n (g/mol)
CA 320s	38000
CA 398-3	30000
CAB 553-0.4	20000

Table 3-18 Reported literature M_n values for commercial CEs (relative to polystyrene standards).

3.9.2 Levulinyl-CE SEC analysis

SEC analysis of levulinyl-CEs displayed an unexpected molecular weight distribution profile with three distinct regions (Table 3-19). Only one main peak was expected which would be consistent with analysis of commercial CEs. The molecular weight (M_p) was assigned to the major peak (primary region, 17.100 mins) which eluted last. The minor peaks (secondary molecular weight region, 8.675 and 12.117 mins) eluted first and were outside the column's calibrated range of $1.3x10^6$ g/mol. Should all three peaks be genuine levulinyl-CEs, that would imply that there were three distinct polymeric distributions where the minor peaks in the secondary molecular weight region represent polymers with molecular weights in excess of $30x10^6$ g/mol (extrapolating past the quantified range for the polystyrene standards and the exclusion limit of the column). This is difficult to explain considering the starting molecular weight (M_w) of cellulose is 490000 g/mol.

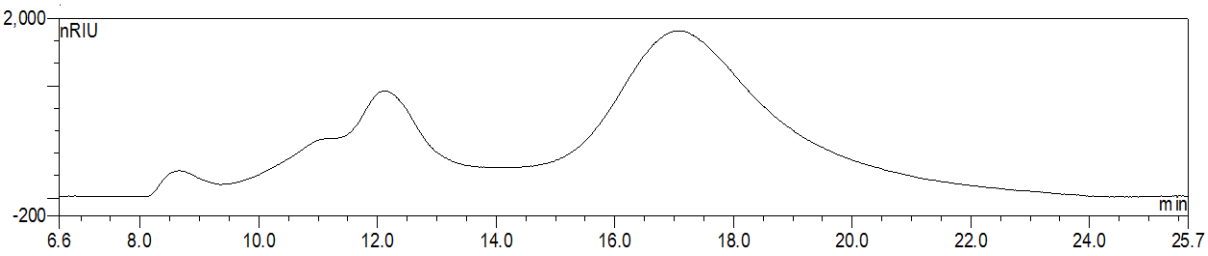

CT-x429-1	Retention time (min)	Peak %
Secondary region	8.675	2.6
	12.117	28.1
Primary region	17.100	69.3

Table 3-19 Retention time and peak area data for BLAC polymer CT-x429-1.

Characterisation of commercially manufactured CAs and CABs by SEC often displayed a small secondary molecular weight region, as a single peak, which correlated to < 6.5% of the total peak area (TPA) (Table 3-20). CAB analogues synthesised for this project also displayed a secondary molecular weight region as a single peak that correlated to < 2.0% TPA (Table 3-20, Figure 3-12). This indicated that the large proportion of the polymer represented by the secondary molecular weight region observed for levulinyl-CEs was not a function of the cellulose starting material.

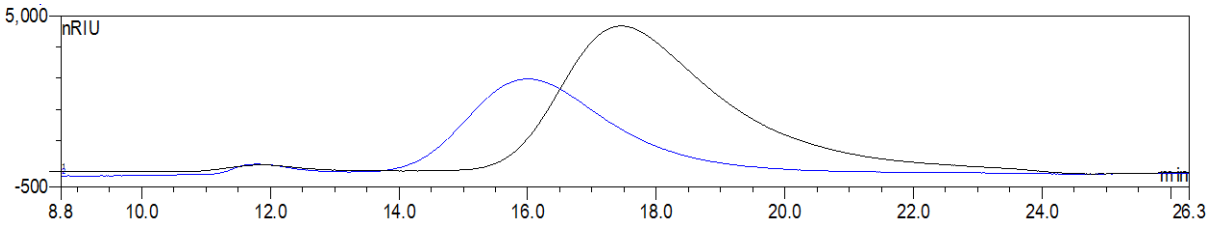

Figure 3-12 SEC chromatogram for CAB 553.04 (blue) and CAB (CT-RPa004a; black).

Sample	Retention time (min)	Peak area (%)
Commercial CAs and CAB		
CA 320s	11.458	6.1
	15.767	93.9
CA 398-3	11.283	4.8
	15.692	95.2
CAB 553-0.4	11.808	4.0
	15.992	96.0
Synthesised CABs		
CT-RPa004A	11.867	1.7
	17.475	98.3
CT-RPa004B	11.551	0.6
	17.408	99.4

Table 3-20 Retention times and peak areas for commercial CAs, CAB and synthesised CAB analogues (CT-RPa-004A and -004B).

With regards to this project, molecular weight analysis by SEC was being used as a comparative tool between samples for observing trends rather than obtaining an absolute value. Therefore, investigation into the chromatographic behaviour and compositions of these secondary molecular weight regions was not strictly relevant to the outcome of the project. However, reported here is a series of observations and possible rationales for the secondary molecular weight regions observed for the levulinyl-CE samples.

3.9.2.1 Solvent extraction

It was postulated that if the observed secondary molecular weight regions genuinely represented larger molecular weight species, then the larger molecules may display reduced solubility in certain solvents. Therefore, it may be possible to separate these polymeric species based on selective solubility. This theory was tested on a sample of BLAC (CT-x429-1, M_p 15000 g/mol) using three solvents with increasing solvent affinity for BLAC: toluene < methanol < methyl isobutyl ketone (MIBK) (Table 3-21). The toluene-soluble proportion of BLAC (28 wt%) had a molecular weight of 4200 g/mol and displayed a reduction in the secondary molecular weight region from a combined peak area of 30.7% to 1.5%. Conversely, the proportion of BLAC that was insoluble in MIBK (8%) showed an increase in the secondary molecular weight region to a combined peak area of 61.7%. NMR spectroscopy indicated that all extracted samples contained levulinate groups and had maintained the original relative proportion of functional groups. NMR spectroscopy also confirmed the SEC molecular weight results; the low molecular weight toluene-soluble BLAC showed a significant increase in the reducing end signal (α and β, Section 3.9.3). These experiments demonstrated it was possible to separate higher and lower molecular weight BLAC using differential solubility.

MIBK soluble (92%)		**Insoluble (8%)**	
Retention time (min)	**Peak area (%)**	**Retention time (min)**	**Peak area (%)**
8.733	1.0	9.603	27.1
12.583	20.5	12.717	34.6
17.550	78.6	17.150	38.3
Methanol soluble (62%)		**Insoluble (38%)**	
Retention time (min)	**Peak area (%)**	**Retention time (min)**	**Peak area (%)**
12.900	17.5	9.025	6.9
17.968	82.5	10.958	8.0
		12.142	22.2
		16.917	63.0
Toluene soluble (28%)		**Insoluble (72%)**	
Retention time (min)	**Peak area (%)**	**Retention time (min)**	**Peak area (%)**
11.800	1.5	8.858	3.4
18.492	98.5	12.808	28.3
		17.300	68.2

Table 3-21 Differential solvent extractions using MIBK, methanol and toluene.

Further evidence for the secondary molecular weight region being associated with a population of high molecular weight levulinyl-CEs (M_p > 100000 g/mol) was provided by studying a series of LAC polymers that had a range of molecular weights. This series of LAC polymers was generated by increasing the catalytic sulfuric acid concentration in the reaction media (discussed in Section 4.5.3) and a reduction in the combined peak areas of the secondary molecular weight region was found to correlate with a decrease in the molecular weight of the primary peak (Figure 3-13).

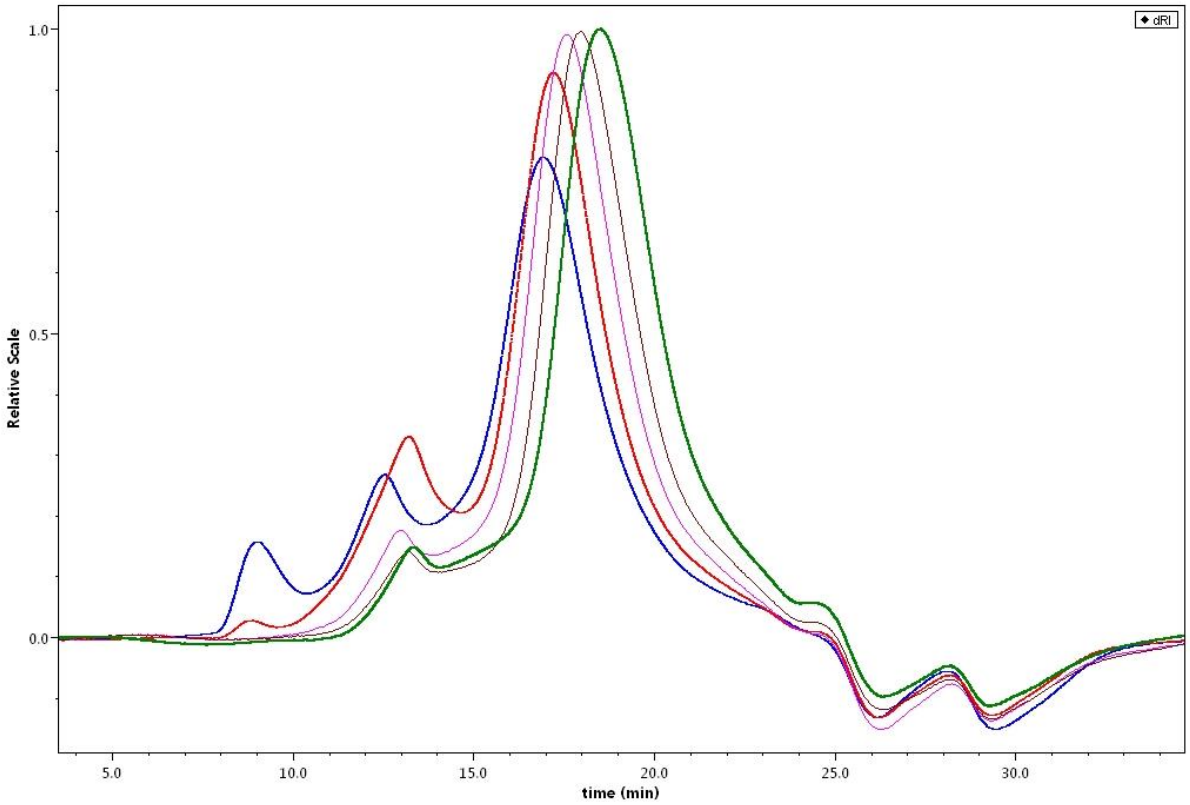

Figure 3-13 SEC chromatograms for LAC made with increasing sulfuric acid concentrations. Traces: blue (2.3 mmol/L), red (4.5 mmol/L), purple (9.1 mmol/L), brown (18.1 mmol/L), green (36.2 mmol/L).

3.9.2.2 Hydrazinolysis

The secondary molecular weight region was further investigated as a function of the levulinyl group, where selective removal of this group was completed using hydrazinolysis, commonly used in protecting group chemistry [165]. Characterisation of BLAC by NMR spectroscopy following a hydrazinolysis step was not

possible due to a significant reduction in the polymer's solubility meaning that a suitable solvent could not be found. To get around this problem, a proportion of the de-levulinated BLAC material was re-acetylated, using mild esterification conditions, and NMR analysis (of the now soluble polymer) indicated that the re-acetylated material was free of levulinate. Although the de-levulinated BLAC material had a different solubility profile, it was still soluble in DMAc permitting SEC analysis to be carried out. Analysis by SEC thus demonstrated that after levulinate removal, the de-levulinated BLAC sample showed a significant reduction in the secondary molecular weight region, to 7.5% (Table 3-22) from a combined peak area of 30.7% in the parent material. In contrast, analysis by SEC of the re-acetylated CE showed that the combined peak area of the secondary molecular weight region was now 10% (Table 3-22), consistent with that seen for commercial CABs.

Hydrazinolysis (A)	Retention time (min)	Peak area (%)
	8.475	1.0
	11.430	6.5
	17.367	92.4
Acetylation (B)	**Retention time (min)**	**Peak area (%)**
	8.508	1.4
	11.600	8.6
	17.308	90.0

Table 3-22 Peak areas from SEC analysis of BLAC (CT-x429-1) after hydrazinolysis only (A), and after hydrazinolysis and acetylation (B).

These results demonstrated that the levulinate group has a role in the material responsible for the secondary molecular weight region observed by SEC analysis. The BLAC used had a DS-Total of 2.64 and therefore unreacted hydroxyls (DS 0.36) were present in the polymer. While investigating CABs and CAs, Gray *et al.* [149, 150] (discussed in Section 3.1) showed that preparation of CEs does not yield a uniform polymer. Within the polymer structure it is possible to have all monomer unit variations present; for LAC 27 variations are possible, and for BLAC there are 64 possible combinations. Preparation of BLAC was anticipated to proceed in a similar fashion to CABs and CAs, generating a highly varied polymer backbone with respect to the ester substitution pattern. CE solubility has been well documented to vary with the substituents and the DS, which has been

discussed in previous sections. It was therefore possible that higher molecular weight levulinyl-CE species, dependent on the DS and substitution profile, display differing degrees of solubility in DMAc. Although still in solution, the solubilised structure, solvent sphere and therefore hydrodynamic volume could be significantly different between polymer chains with varying substitution profiles. These conformational changes would change the hydrodynamic volume of the polymer chains and consequently how long the polymer takes to passage through the SEC column.

Molecular polarity has also been shown to alter how polymers interact with SEC columns and can serve to increase the molecular weight of the polymer as calculated by SEC [162]. This effect was observed with CAB 553-0.4 after carboxylation using succinic anhydride. CAB 553-0.4 had a characteristic SEC trace showing a small secondary molecular weight region of < 4% (combined peak area of blue trace, Figure 3-14). Following carboxylation of CAB 553-0.4 (acid number 97.5 mg KOH/g), the SEC analysis displayed a molecular weight shift of almost the entire sample beyond the calibrated range of the column (Figure 3-14). Thus the polarity introduced by the ketone group on the levulinate group, in conjunction with certain CE substitution profiles, may increase the hydrodynamic volume of specific levulinyl-CE species and generate the secondary molecular weight regions that were recorded.

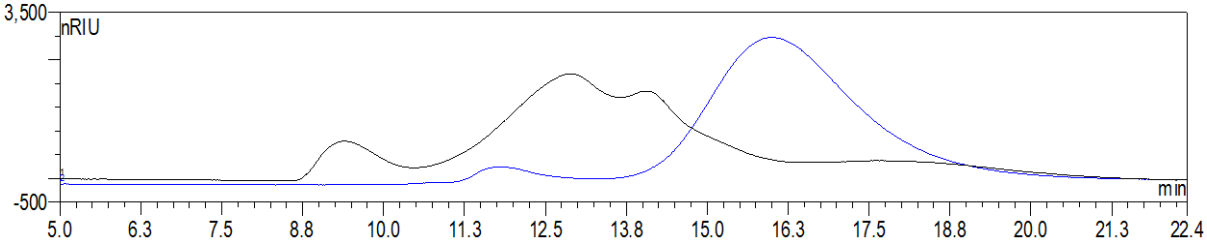

Figure 3-14 SEC chromatograms of CAB 553-0.4 (blue) and succinate modified CAB 553-0.4, acid number 97.5 mg KOH/g (CT-402-2, black).

3.9.3 Molecular weight determination by end group analysis

By determining the number of end groups relative to the number of monomer units, it is possible to calculate the M_n value for a polymer sample. End group analysis was completed using NMR spectroscopic data. The effect of increasing catalytic sulfuric acid concentration on a series of LAC polymers (discussed in Section 4.5.3) was investigated and a consistent reduction in molecular weight (M_p) was recorded by SEC analysis with increasing sulfuric acid concentration (Figure 3-15). The reducing end α and β anomer resonances were observed as discrete signals at ^{1}H δ 6.23 and 5.62 ppm, respectively. Integration of both of these peaks (one proton each) relative to the cellulose region (7 protons) gave an absolute DP value. The α:β anomeric ratio for the LAC produced with varying sulfuric acid concentration was unchanged at 3:1.

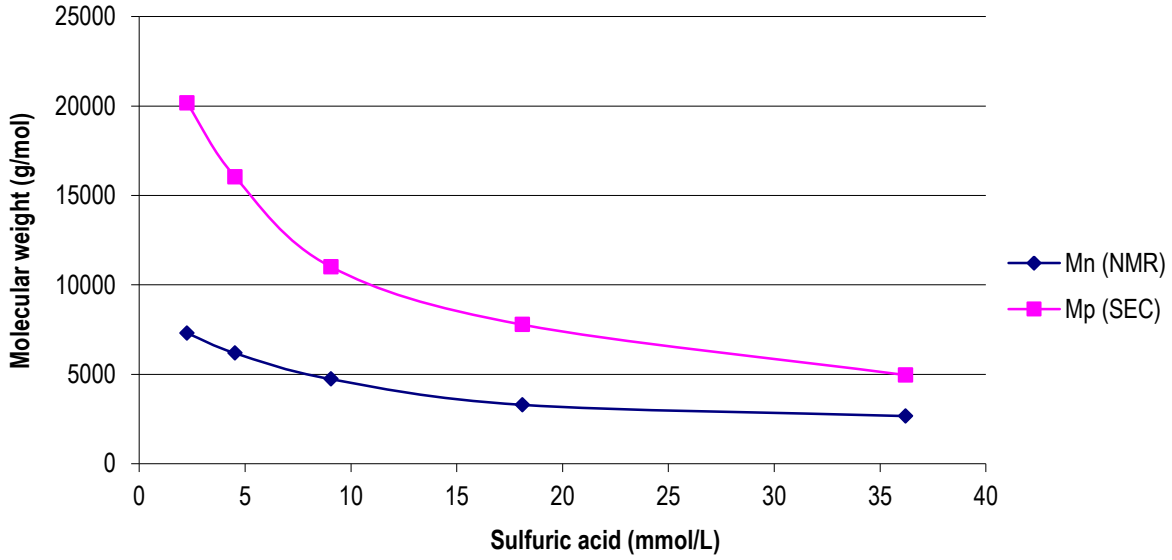

Figure 3-15 Determination of the molecular weight as a function of sulfuric acid concentration by SEC and end group analysis.

As expected, the M_n determined by assessment of the ^{1}H NMR spectrum, and M_p from SEC traces, followed a similar logarithmic trend. As shown earlier, CEs generated in this study can have a polydispersity of > 5 and M_n will only equal M_p in a monodisperse polymer.

End group analysis by ^{1}H NMR spectroscopy increases in accuracy as the DP decreases due to the increased concentration of end groups providing greater signal to noise and a more readily integrated signal for the key α and β anomer resonances. As the DP increases, the proportion of end group α and β anomer signals are reduced. The β signal, in particular, becomes increasingly difficult to integrate being the minor anomer. Individual proton resonances could not be accurately quantified unless they were greater than approximately 5% of the total signal in ^{1}H NMR spectrum. Therefore, with increasing DP, above a M_n of 7500 g/mol, it is not possible to accurately determine the proportion of end groups using NMR spectroscopy due to the relatively low concentration of the end group species. Overall, NMR spectroscopy provided a quick method for determining molecular weight (M_n) using end group analysis for low molecular weight samples.

4 Reaction parameters

4.1 Introduction

Consistently modifying cellulose, within a chosen parameter range, to form a target CE, requires tight control of the reaction parameters. When this material has the potential to be a commodity product, optimisation of the processing conditions is necessary to ensure the approach is cost-effective. This includes minimising reagent quantities while maintaining a pre-determined product specification. Other manufacturing processes such as reagent recycling also need to be considered before manufacture is undertaken. The development of the levulinyl-CEs herein was based on existing commercial manufacturing techniques (discussed in Section 1.7) with the goal of providing a synergy to current technology to aid with the commercialisation process.

The initial levulinyl-CE product specifications and targets for the principal proof of concept investigation included:

- The synthesis of a high yielding product.
- Gaining an understanding of the factors that influence the DS to control levulinate substitution between a DS of 0.1 and 2.5.
- Formation of a tri-substituted mixed levulinyl-CE (DS-Total in the range of 2.5-3.0).
- Low product colour to form a near colourless film when cast from solution.
- Attaining a molecular weight of > 10000 g/mol.
- Generating a polymer with a T_g of ≤ 25 °C.
- Maintaining full chloroform and acetone solubility; chloroform solubility was required for NMR spectroscopic characterisation while acetone solubility was envisioned as a requirement for readily creating a water-based polymer dispersion (Section 8).

The outcome of the results discussed in this section formed the basis of the standard reaction conditions used for subsequent investigations and finalisation of the lead levulinyl-CE. This lead compound was a butyryl levulinyl acetyl cellulose (BLAC) compound which was taken through to the dispersion stage of the project.

4.2 Anhydride requirements in LAC synthesis

The proportion of anhydride used (equivalents per hydroxyl or Eq|OH) for levulinyl-CE preparation was calculated based on the molar equivalents of anhydride per AGU hydroxyl group (the AGU contains 3 available hydroxyl groups). Theoretically, a stoichiometric equivalent (1 Eq|OH) of acetic anhydride would be required for complete esterification of cellulose, forming CTA. The amount of anhydride required was optimised for the synthesis of LAC by minimising the Eq|OH of anhydride used while maintaining high yields and meeting product specifications. Using 3 Eq|OH of anhydride a maximum yield of 85% (based on the calculated theoretical yield) was obtained, and further anhydride additions did not increase the LAC yield (Table 4-1). The LAC products generated from reactions using between 2 and 6 Eq|OH of anhydride displayed complete solubility in acetone and chloroform. Conversely, samples produced with less than 2 Eq|OH of anhydride displayed a high degree of insolubility in acetone, indicative of an incomplete reaction. By using 2 Eq|OH of anhydride it was possible to produce a fully soluble LAC product that meets the criteria which has been established for production of a paint binder system. However, 3 Eq|OH of acetic anhydride will be used in the "standard reaction conditions" ensuring high product yield and complete reaction.

Acetic anhydride Eq|OH	LAC yield %
1.2	28
1.5	55
2.0	74
3.0	85
6.0	80

Table 4-1 LAC yield with respect to equivalents of acetic anhydride used per AGU hydroxyl (Eq|OH).

Two possible rationales were postulated for the excess anhydride required in order to drive the reaction to completion:

- Firstly, it is possible that complete cellulose dehydration with glacial acetic acid did not occur during pre-swelling which introduced water into the reaction media. This water will then react with the reactive intermediates forming their constituent acids. As indicated in the literature, commercial CE production

requires a small excess of anhydride for complete reaction to occur (1.4 Eq|OH); this excess anhydride removes any residual water present in the reaction media [69].

- Secondly, it is possible that the excess reagents required for complete reaction to occur were a function of the proposed LA reaction chemistry. As noted in Section 2.5, the lactone esterification appears to progress an order of magnitude slower than the equivalent mixed anhydride reaction. Due to this observed decrease in lactone reactivity (compared to anhydrides as reagents), it is possible that an excess of reagents were required to drive the reaction to completion in a timely fashion and without extensive acid-catalysed depolymerisation.

For the optimised conditions (3-6 Eq|OH) a yield of close to 100% was not achieved as a function of both the reaction chemistry and the material processing techniques employed. There were two possible contributing factors for the sub-optimal yields recorded for the preparation of a LAC:

- Vaca-Garcia and Borredon reported increased polymer degradation with increasing reaction temperature and catalyst concentration [70]. It is therefore likely that the reduced yield recorded was a function of CE degradation during the esterification process. It was proposed that cleavage of the glycosidic linkage was likely occurring through an acetolysis process forming oligomeric species. Below a critical DP these small species are water-soluble and will not precipitate [70], and are then washed out resulting in a reduced yield. In the case of the LAC synthesis here, it was not possible to isolate the individual degradation compounds.
- Work-up procedures required several extensive batch washing and filtration steps, and regularly required a re-precipitation step to further purify the material. This extensive processing resulted in small sample losses at each stage. Every effort was made to keep processing losses to a minimum to maintain accurate yield data.

4.3 Proportion of levulinyl species incorporated into a mixed CE

From consideration of first principles, it was initially thought that a mixed anhydride effected the esterification of cellulose to generate a levulinyl-CE. Based on this assumption, the incorporation of acetate and levulinate would have been a function of the molar ratio of LA/Acetate, where acetate in this case accounts for acetic acid (1 equivalent) and acetic anhydride (2 equivalents). This was consistent with reported values for traditional mixed CEs [88]. However, due to the unique esterification chemistry occurring using LA, it was noted that the LA/Acetate ratio was not the sole factor determining the substituent DS (Figure 4-1). Unexpectedly, the DS for LAC (both acetate and levulinate) was found to be a function of two different esterification reagent ratios:

- The ratio of LA to acetic anhydride (LA/Ac_2O) which primarily controls substituent incorporation in the mixed LAC ester (discussed in the following Section).
- A secondary, but equally important parameter was the ratio of LA to total acetate (acetic anhydride and acetic acid, LA/Acetate). The LA/Acetate ratio was a function of excess acetic acid introduced into the reaction media which had a subtle effect on substituent incorporation (discussed in Section 4.3.2)

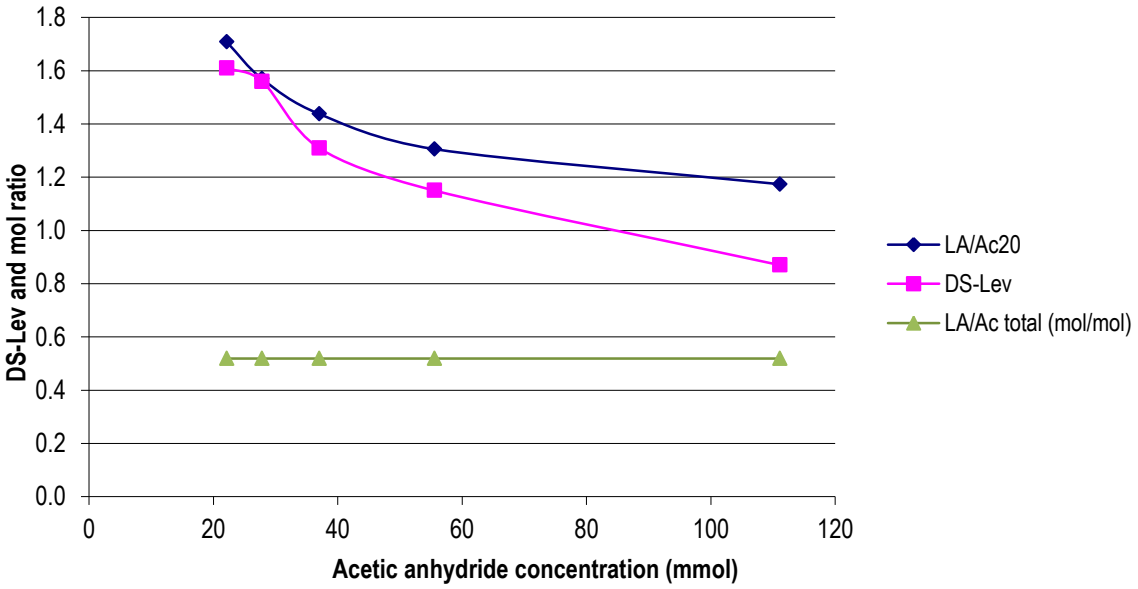

Figure 4-1 Incorporation of levulinate with respect to reagent ratios.

4.3.1 LAC synthesis: Effect of changes to the molar ratio of LA to acetic anhydride

This section discusses the effect of varying the molar ratio of LA/Ac_2O when generating a levulinyl-CE. A predictable increase in DS-Lev was shown to occur with an increasing LA/Ac_2O ratio (Figure 4-2). Three zones were evident across the LA/Ac_2O range tested. Zone 1 occurred when the LA/Ac_2O ratio was < 0.6, where there were two competing esterification mechanisms based on the proposed reaction chemistry for levulinyl esterification. The first mechanism is the conventional anhydride esterification, and the second is esterification *via* the lactone pathway. It is expected (and observed in Section 2.5) that the reaction using acetic anhydride is faster than that utilising activated lactones, which would result in a disproportionate increase in the DS-Ac, as seen when DS-Lev is < 0.6. Zone 2 was located between a LA/Ac_2O ratio of 0.6 and 1.6, indicating a greatly increased rate of levulinate incorporation, likely due to lactone-derived esterification becoming the dominant process. In zone 3, where the LA/Ac_2O ratio was > 1.6, the rate of levulinate incorporation slowed and the DS-Lev began to plateau as steric effects begin to play an ever increasing role, favouring acetate incorporation. For ratios of LA/Ac_2O > 2, only a minor increase in the DS-Lev is anticipated based on results from a later series of reactions (see Section 4.8, Figure 4-7).

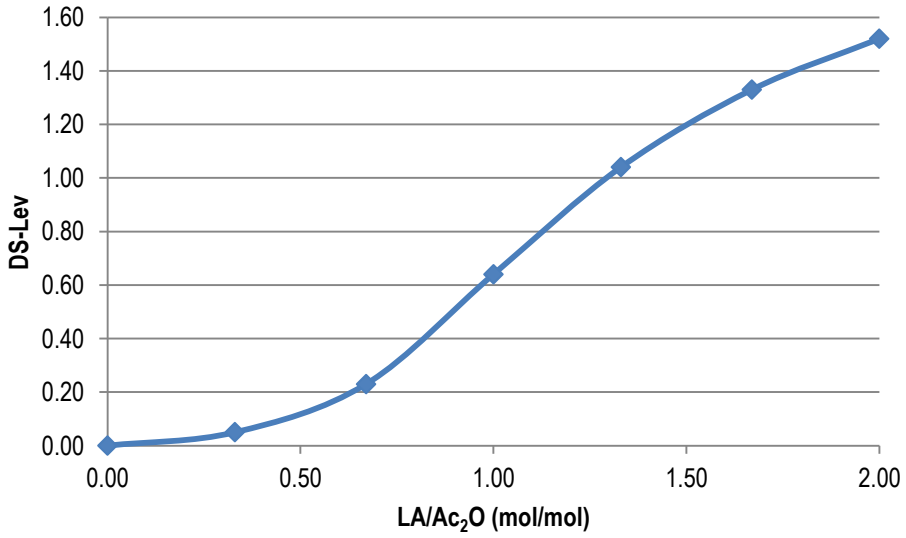

Figure 4-2 Levulinate incorporation with respect to LA/Ac_2O ratio.

Substituent incorporation, as a function of the LA/Ac_2O molar ratio, was tested using two experimental methodologies. The first methodology involved maintaining a constant 3 Eq|OH of anhydride, and the second was centred around maintaining a constant reaction volume. The findings were consistent between both reaction series, with respect to substituent incorporation trends (Table 4-2, Table 4-3). The absolute DS values differ between the two data sets due to batch to batch variation in the activated cellulose. The activated cellulose used in the constant volume reaction series contained 126 wt% more acetic acid than the activated cellulose used in the constant anhydride reaction series. The effect of residual acetic acid is discussed in Section 4.3.2.

Samples prepared with a LA/Ac_2O molar ratio of 0.33 and 0.67, using a constant proportion of acetic anhydride in the reaction were not fully esterified (DS-Total < 3), and contained free unreacted hydroxyl groups (Table 4-2). The reaction solutions for these samples became highly viscous during the reaction suggesting that the newly formed CEs were not fully compatible with the reaction solution (i.e. showed decreased solubility). As stated earlier, the reagent mixture (consisting of a mixture of free acids, lactones and anhydrides) acts as the solvent for the reaction, so the significantly increased viscosity seen implies that the CEs generated were not dissolving fully in the reaction reagents. Consequently, the increased solution viscosity most likely resulted in inefficient reaction conditions, poor mixing, and in particular, poor thermal transfer, all of which contributed to incomplete esterification. This effect was exacerbated by the reduced reaction volume of these samples. In the series of reactions using a constant volume for the reaction, samples prepared with a LA/Ac_2O ratio of 0.33 and 0.67 also displayed gelling, but to a lesser extent, as the excess reagents behaved as diluents thinning the reaction solution. All samples prepared in the series with a constant volume of reactants were fully esterified (Table 4-3).

Reaction volume (mL)	LA/Ac_2O	DS-Lev	DS-Ac	DS-Total
8.6	0.33	0.10	2.75	2.85
10.5	0.67	0.49	2.48	2.97
12.4	1.00	0.88	2.17	3.05
14.3	1.33	1.29	1.75	3.04
16.2	1.67	1.45	1.60	3.05
18.1	2.00	1.70	1.35	3.05

Table 4-2 Constant anhydride content (3 Eq|OH) reaction series.

Eq|OH Ac_2O	LA/Ac_2O	DS-Lev	DS-Ac	DS-Total
8.41	0.33	0.05	2.99	3.04
6.64	0.67	0.23	2.82	3.05
5.59	1.00	0.64	2.42	3.05
4.68	1.33	1.04	2.02	3.06
4.08	1.67	1.33	1.75	3.08
3.61	2.00	1.52	1.56	3.08

Table 4-3 Constant volume reaction series.

CEs containing a high proportion of acetate substitution, in particular CTA, are known to form highly viscous reaction solutions, a feature attributed to the poor solubility of CA in the reaction mixture [35, 69]. It was therefore possible that the high acetate content of the LAC polymers generated was a contributing factor to the poor solubility displayed in the reaction media. With increasing levels of levulinate incorporation LAC becomes increasingly soluble in the reaction solution.

Importantly, it was shown that levulinate and acetate can be introduced on to the CE in a predictable fashion.

4.3.2 LAC synthesis: Effect of changes to the molar ratio of LA to total acetate

The key function of acetic acid in the manufacture of CEs is primarily to dehydrate the water-swollen cellulose pulp, although, in the reaction mixture, it may also be considered a reactive solvent. Acetic acid is introduced to the reaction mixture from the pre-treatment of cellulose, but is also liberated from the reaction of acetic anhydride with a hydroxyl nucleophile. Additionally, in commercial processes acetic acid has been introduced to the reaction as a diluent to aid mixing efficiency.

The primary factor shown to control the relative proportion of substituents of a LAC was the ratio of LA/Ac_2O. However, the effect of excess acetic acid on the relative substituent incorporation was also investigated as a function of the LA/Acetate ratio. Incrementally increasing the acetic acid content while maintaining a LA/Ac_2O ratio of 1.21 indicated, as expected, that acetic acid was behaving as a reactive solvent and not only a diluent. The acetic acid content was increased in the reaction media from 17.1 mol% to a maximum of 56.4 mol% of the

initial reaction solution. A corresponding decrease of the DS-Lev from 1.00 to 0.62 was recorded, with an equal and opposite increase in acetate incorporation (Figure 4-3).

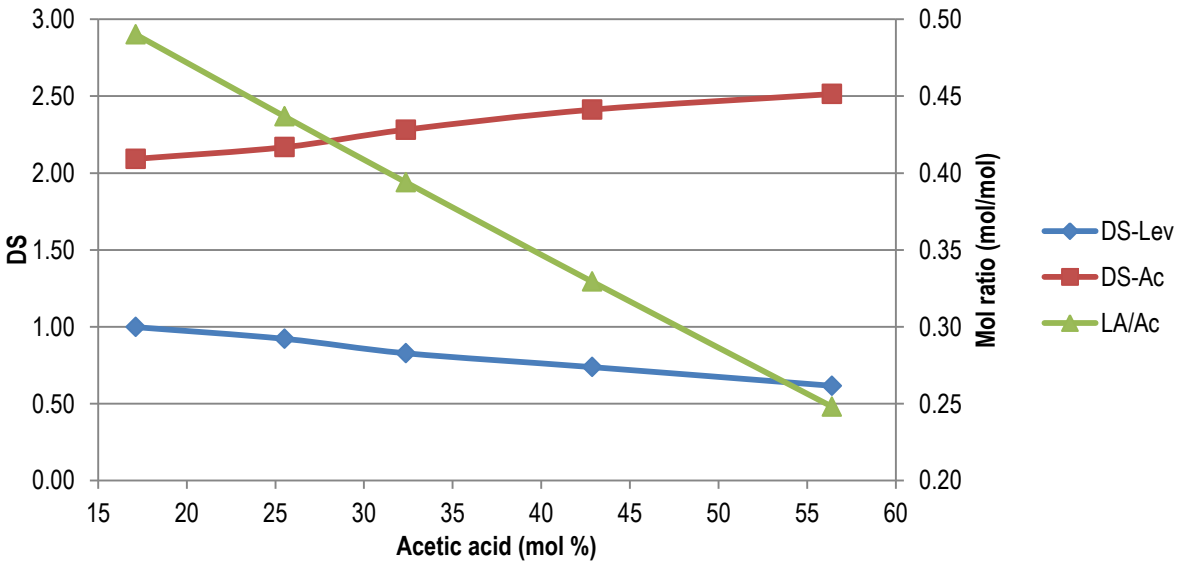

Figure 4-3 Effect of acetic acid content on LAC substituents; LA/Ac_2O molar ratio kept constant at 1.21.

The effect of acetic acid on substituent incorporation was not as dramatic as one might expect. If the reaction was solely dependent on the LA/Ac_2O ratio, it would be expected that addition of acetic acid would have no effect. Conversely, if the reaction was solely dependent on the LA/Acetate ratio (which has previously been shown not to be the case) the effect of acetic acid addition would be far more pronounced. In a conventional reaction using mixed anhydrides, consisting of acetic anhydride and one other aliphatic acid, the reactive species are in equilibrium and increasing the acetic acid content would result in a proportional increase in acetate substitution based on the aliphatic acid/acetate ratio. Therefore, the reduced effect of excess acetic acid on substituent incorporation was proposed to be a function of the esterification chemistry using lactones derived from LA (covered in Section 2).

When considering an esterification process using a LA/Ac_2O ratio of > 1, all the anhydride is expended forming both lactone species **(1)** and **(2)** through the proposed α-AL intermediate (Figure 4-4). The generation of α-AL is a non-reversible step due to the dehydrating reaction conditions. There were no species found in the reaction solution that were capable of esterifying with acetate only. Each lactone species is capable of levulinyl addition

via reaction pathway A (Section 2.4), whereas pathway B can introduce either an acetyl or levulinyl functionality from reaction with lactone **(1)** or **(2)** respectively.

Increased incorporation of acetate into a LAC was recorded with increased acetic acid concentration; likely a function of an increased concentration of **(1)** generated during the formation of the reactive lactone species, rather than the acetate carbonyl in **(1)** being a significantly more attractive centre (electronically and sterically) compared to the lactone ring carbonyl. This rationale is supported by consideration of the crystal structure for **(1)** which indicated that the approach to the acetate carbonyl is sterically hindered by the nearby quaternary centre.

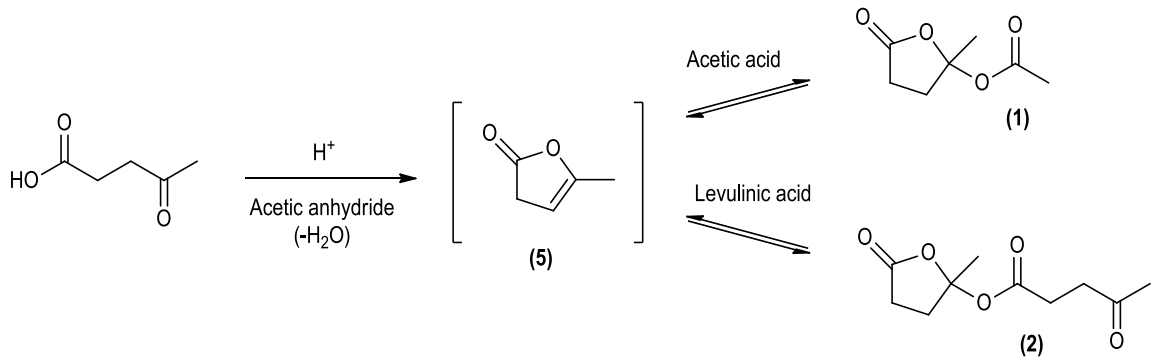

Figure 4-4 Lactone equilibrium.

This work illustrated that levulinate and acetate incorporation is primarily controlled by the molar ratio of LA/Ac_2O, and that the LA/Acetate ratio plays a minor, but important role, in affecting the substituent incorporation in the formation of LAC. This indicated that minor formulation adjustments will be required to produce LAC within a given parameter range, with particular focus on the quantity of excess acetic acid present in the activated cellulose starting material.

4.4 Transesterification of CE

A set of experiments were completed to ascertain whether acid-catalysed transesterification was occurring using the activated lactones produced from the reaction of LA and Ac_2O. Two commercial CAs (CA 320S and CA 398-3) and a laboratory produced CTA were used for these experiments (Table 4-4), with the LA/Ac_2O ratio fixed at

1.67. It was proposed that if the ester groups were highly labile and transesterification occurred, such a ratio would generate a similar substituent incorporation ratio to what was observed for a standard esterification reaction starting with activated cellulose (DS-Lev 1.45 and DS-Ac 1.60 based on Section 4.3.1).

CA source	DS-Ac	DS-OH
SH-x11-1	2.92	0.08
CA 320S	1.74	1.26
CA 398-3	2.56	0.44

Table 4-4 CAs used in the transesterification reactions.

Following treatment of the CAs in the LA-Ac_2O reaction solution, it was observed that both of the CAs and the CTA were fully capped with a mixture of levulinyl and acetyl groups (Table 4-5). A significant amount of depolymerisation had occurred during the reaction, indicated by the DS-Total being > 3. The level of incorporated levulinyl and acetyl groups was consistent with capping of the free hydroxyl groups and those produced by depolymerisation. This indicated that transesterification was not occurring under the esterification reaction conditions employed here.

CA source	DS-Lev	DS-Ac	DS-Total
SH-x11-1	0.18	2.95	3.13
CA 320S	0.73	2.45	3.18
CA 398-3	0.41	2.72	3.13

Table 4-5 Cellulose ester composition post-reaction.

4.5 Reaction conditions

There were four main reaction variables to consider in the formation of LAC:

- The starting reagent ratios which determine the DS (discussed above).
- Reaction duration.
- Reaction temperature (°C).
- Catalytic acid concentration.

The aim was to determine a set of reaction parameters that optimised the desired characteristics in the synthesised LAC, such as T_g and molecular weight, while undesirable traits such as polymer colour were minimised. Three sets of reactions were designed and completed to test the effect of the last three variables (reaction time, temperature and catalytic acid concentration) on the characteristics of the LAC product. All the reactions used a common work-up procedure.

It was noted that when using mild reaction conditions (standard reaction conditions are defined in Section 4.6) for each parameter tested, incorporation of a third substituent was observed; a lactone species. Characterisation and discussion of the lactone groups' origin is discussed in Section 2.6. Inclusion of this group was undesirable, and in part led to the development of the standard reaction conditions designed to prevent the incorporation of this lactone species and generate a per-esterified, di-functionalised CE only.

4.5.1 Reaction duration

A series of reactions were completed varying the reaction duration from 15-120 minutes while maintaining a constant reaction temperature (120 °C), LA/Ac_2O molar ratio (1.66), and sulfuric acid concentration (9.1 mmol/L). An increase in levulinyl and acetyl incorporation was observed from a reaction time of 15 minutes up to a reaction time of 90 minutes, where a steady state was observed (DS-Lev of 1.83, DS-Ac of 1.16, no lactone incorporation, Table 4-6). It was expected that had the reaction continued beyond 120 minutes, further

depolymerisation would have occurred and a concurrent increase in the DS of both substituents would result. A reaction duration of 15 and 20 minutes generated materials that were not completely chloroform- or acetone-soluble and were thus considered not fully reacted.

Time (min)	DS-Ac	DS-Lev	DS-Lac	DS-Total
15	1.42	0.96	0.29	2.67
20	1.49	1.01	0.22	2.72
30	1.65	1.01	0.18	2.84
60	1.76	1.13	0.05	2.94
90	1.83	1.16	0.00	2.99
120	1.83	1.18	0.00	3.01

Table 4-6 LAC substitution with increasing reaction time.

4.5.2 Reaction temperature

In the next series, the reaction temperature was increased from 90-140 °C in 10 °C increments while maintaining a consistent reaction time (2 hours), LA/Ac_2O molar ratio (1.20) and sulfuric acid concentration (9.1 mmol/L). At the lower reaction temperatures (up to 110 °C) lactone incorporation was observed (Table 4-7). With increasing reaction temperature there was a corresponding increase in substituent incorporation, although significant depolymerisation was observed when using reaction temperatures of > 120 °C. Beyond a DS-Total of 3, incorporation of acetyl was favoured over levulinyl, most likely due to steric effects (Table 4-7). All samples generated from this series were chloroform and acetone soluble.

Temperature (°C)	DS-Ac	DS-Lev	DS-Lac	DS-Total
90	1.50	0.76	0.56	2.82
100	1.64	0.77	0.41	2.82
110	2.02	0.92	0.10	3.04
120	2.11	0.95	0.00	3.06
130	2.14	0.97	0.00	3.11
140	2.22	0.96	0.00	3.18

Table 4-7 LAC substitution with increasing reaction temperature.

4.5.3 Sulfuric acid concentration

The sulfuric acid concentration was increased incrementally between 2.3 mmol/L and 36.2 mmol/L, with the other three reaction parameters remaining constant: time (2 hours), temperature (120 °C) and LA/Ac_2O molar ratio (1.20). This resulted in a steady increase in the DS-Total as shown in Table 4-8. The ratio of the substituents incorporated onto the CE (DS-Ac/DS-Lev) increased to a maximum of 2.0 at a catalyst concentration of 9.1 mmol/L, then remained constant. Incorporation of the lactone species was noted for sulfuric acid concentrations of ≤ 4.5 mmol/L. With the exception of the sample generated using a sulfuric acid concentration of 2.3 mmol/L, all samples were fully soluble in the test solvents.

H_2SO_4 concentration (mmol/L)	DS-Ac	DS-Lev	DS-Lac	DS-Total	DS-Ac/DS-Lev
2.3	1.82	0.77	0.30	2.89	1.7
4.5	1.95	0.87	0.16	2.98	1.9
9.1	2.05	1.01	0.00	3.06	2.0
18.1	2.06	1.05	0.00	3.11	2.0
36.2	2.18	1.12	0.00	3.30	2.0

Table 4-8 LAC substitution with increasing sulfuric acid concentration. Substituent ratio (DS-Ac/DS-Lev ratio) includes lactone as levulinate.

4.5.4 Reaction colour

As discussed in Section 2.8, preliminary reactions to synthesise a levulinyl-CE generated highly coloured reaction solutions and polymer products. Even after extensive re-purification complete removal of colour from the polymer was not possible. Various processing methods were trialled in an attempt to generate a low colour polymer. These were:

- Precipitation of the cooled reaction solution into the organic anti-solvent ethanol, based on methods used by Vaca-Garcia and Borredon [70]. This strategy resulted in further complications, most notably the production of ethyl levulinate, due to the esterification of ethanol with the reactive species present. The ethyl levulinate became entrained in the polymer and was then difficult to remove. There was also

an associated loss in yield using ethanol which was attributed to increased solubility of the levulinyl-CE in the work-up solution, particularly for the lower molecular weight polymer material.

- Soxhlet extraction of levulinyl-CEs in either ethanol or methanol. The LAC polymer was highly soluble in both of these solvent systems (hot), but resulted in extraction of both the polymer and the related coloured material.
- Multiple re-precipitations from an 8% acetone solution into 11.5 volumes of water.
- Repeated and extended overnight washings followed by suspension of the precipitated polymer in water.
- Variations to the standard work-up procedure (see Section 10.2.1) which included:
  - Increasing the precipitation volume to a maximum of 25 volumes of water.
  - Modifying the dilution procedure prior to precipitation.
  - Addition of precipitation co-solvents such as acetone and acetic acid up to 18% v/v.
  - Increasing the temperature of the anti-solvent to 40 °C.

Unfortunately none of the purification processes attempted above resulted in reduced product colour in comparison to the standard work-up procedure (described in Section 10.2.1).

The colouration of the levulinyl-CE was, however, best improved by modifying the reaction conditions to limit the initial colour formation. Polymer colour intensity (Abs) was measured as the integrated absorbance of a 1% w/v polymer solution in acetone over the range of 400-600 nm. This type of measurement was observed to give a more consistent representation of actual polymer colour intensity than using a single wavelength extinction coefficient (ε) measurement. Quantification of colour, or colour intensity, can be difficult; Kim *et al.* [132] used a simple visual representation as a method of comparing the degree of colouration for related compounds. Colour measurements were categorised as lightly coloured (< 25 Abs), mildly coloured (25-70 Abs) and highly coloured (> 70 Abs). Thus categorisation of the colour intensity can be seen in Figure 4-5 by directly comparing the reaction solutions: tubes 1-3 are lightly coloured (1 and 2 are milky due to the presence of insoluble material), tubes 4 and 5 are mildly coloured, and tube 6 is highly coloured. No evidence was found that indicated whether the coloured material was chemically bound to the levulinyl-CE structure, although it was proposed that the

colouration observed was a function of a small amount of highly coloured material that was entrained with the CE polymer.

Figure 4-5 Series showing reaction colour.

There was no correlation between the entrained colour and increasing levulinate incorporation (Lev/Ac_2O reaction series, see Section 4.3), with all samples being in the range of 62 ± 8 Abs (mildly coloured). All reaction conditions investigated displayed a similar trend of increased polymer colour with increasingly aggressive reaction conditions. By altering three fundamental reaction parameters (duration, temperature and catalytic acid concentration) it was possible to significantly vary the colour intensity of the final polymer (Table 4-9). There were several reaction condition combinations which produced lightly coloured LAC esters; reaction times of ≤ 30 minutes, reaction temperatures of < 100 °C, and sulfuric acid concentrations of ≤ 2.3 mmol/L. However, as discussed in previous sections, all of these conditions resulted in the inclusion of the lactone functionality in the product, and often incomplete polymer solubility.

Temperature (°C)	Colour (Abs)	Time (mins)	Colour (Abs)	H_2SO_4 concentration (mmol/L)	Colour (Abs)
90	18.5	15	12.7	2.3	23.8
100	25.6	20	15.5	4.5	49.4
110	44.9	30	20.8	9.1	76.4
120	73.4	60	37.4	18.1	142.8
130	120.0	90	48.8	36.2	175.9
140	131.3	120	71.3		

Table 4-9 Colour intensity measurements with respect to temperature, time, and sulfuric acid concentration.

4.5.5 Molecular weight and glass transition temperature (T_g) of LAC

With regard to polymers, T_g and molecular weight are closely related parameters; low molecular weight polymers require less thermal energy for chain rotation to occur, thereby reducing T_g. In the patented work of Shelton *et al.* [48], the dependence of T_g on molecular weight for CEs was demonstrated using a number of small molecular weight CABs. The balance of these two parameters was important as reducing the T_g at the expense of molecular weight can result in a loss of mechanical properties which, in the context of a coatings application, will ultimately result in poor quality films. For LAC, increasing the levulinyl incorporation was concomitant with a decrease in molecular weight (Table 4-10), an observation which was postulated to be a function of levulinyl-CE solubility in the reaction solution. With increasing levulinate incorporation, the newly formed CE was increasingly soluble in the reaction media resulting in a greater level of acetolysis experienced by the polymer, reducing the molecular weight. It is important to note that all of the reaction conditions remained constant (temperature, time, stirring, catalyst concentration, reaction scale) while investigating the molecular weight dependence of LAC as a result of changing the LA/Ac_2O molar ratio.

CTA was synthesised (LA/Ac_2O 0.00, Table 4-10) for reference by the reaction of Ac_2O and catalytic I_2 completed neat at 100 °C over 10 minutes [166]. The CTA was recovered by precipitation from water followed by extensive water washing to remove residual reagents and reaction by-products. Characterisation by NMR demonstrated a per-esterified polymer had been generated. Longer reaction times led to significant depolymerisation as evidenced by complexity in the NMR spectra and a different set of solubility parameters.

LA/Ac_2O	Molecular weight (M_p g/mol)	T_g (°C)
0.00	52000	185
0.33	36000	160
0.67	12000	124
1.00	11000	115
1.33	9400	105
1.67	8500	101
2.00	7100	95

Table 4-10 Molecular weight and T_g for LAC products.

Three other key reaction variables were investigated for their effect on the properties of LAC: temperature, time and sulfuric acid concentration. With increasingly aggressive reaction conditions and increased reaction duration, a consistent incremental decrease in molecular weight for LAC was observed (Table 4-11, Table 4-12 and Table 4-13). The observed molecular weight range for all the LAC samples generated was 5000-27000 g/mol. Reaction times between 15-30 minutes all showed comparable molecular weight values (Table 4-12) although the shortest reaction times (15 and 20 minutes) did not produce LAC esters that were fully soluble in chloroform, acetone or DMAc. Analysis by HPLC-SEC is only capable of characterising polymers that are soluble in the chosen eluent (DMAc) and therefore only the soluble fraction of the samples could be characterised; the insoluble high molecular weight material could not be analysed. This resulted in a plateau effect for reaction products produced with reaction times over the 15-30 minute range. A reaction time of 30 minutes gave the first fully soluble sample and was the first representative data point in this reaction series.

Temperature (°C)	Molecular weight (M_p g/mol)
90	25000
100	27000
110	20000
120	15000
130	13000
140	9000

Table 4-11 Molecular weight for LAC with variation of the reaction temperature.

Time (min)	Molecular weight (M_p g/mol)
15	23000
20	22000
30	23000
60	16000
90	14000
120	13000

Table 4-12 Molecular weight for LAC with variation of the reaction duration.

H_2SO_4 concentration (mmol/L)	Molecular weight (M_p g/mol)
2.3	20000
4.5	16000
9.1	11000
18.1	8000
36.2	5000

Table 4-13 Molecular weight for LAC with variation of the sulfuric acid catalyst concentration.

The two factors known to decrease the T_g for LAC are molecular weight and the amount of levulinyl incorporation. However, based on the known reaction chemistry it was not possible to determine which parameter was having the greatest effect on the T_g. There was a decrease in T_g observed with increasing levulinyl content and a concurrent decrease in molecular weight (Table 4-2 and Table 4-10). Samples with low levulinate levels, e.g. DS-Lev 0.1 (LA/Ac_2O 0.33), gave a molecular weight of 36000 g/mol and had a corresponding T_g of 160 °C, which was consistent with CABs with low butyrate content [42]. A total decrease in T_g of 90 °C was recorded from CTA (185 °C; see Table 4-10) as a function of both molecular weight and levulinate incorporation.

The reaction series where sulfuric acid concentration was incrementally increased (Table 4-8) provides a series of LAC polymers that vary in substituent composition only slightly (ratio of DS-Ac/DS-Lev = 1.7-2.0), but demonstrate a large variability in molecular weight and T_g. Plotting T_g as a function of molecular weight for this series generated Figure 4-6 and demonstrates the significant decrease in T_g as the molecular weight decreases.

This plot (Figure 4-6) also permitted the comparison of other LAC polymers that had a significantly different ratio of levulinate to acetate substitution. By using the products generated from the LAC series that investigated the effect of catalytic sulfuric acid concentration (Section 4.5.3), it was possible to generate Table 4-14. In entry 1, a polymer with a molecular weight of 12000 g/mol and DS Lev of 0.49 is compared to the polymer series graphed in Figure 4-6. This material has lower levulinate incorporation (DS-Lev difference = −0.51) and a T_g of 6 °C higher. Similarly, at the other end of the spectrum, a polymer of molecular weight 7100 g/mol and DS-Lev of 0.70

units higher has a T_g 11 °C lower than the equivalent species graphed in Figure 4-6. Therefore, this clearly demonstrates that molecular weight and levulinate incorporation have a significant effect on the T_g of the LAC polymers. This data also serves to provide a framework for prediction of the glass transition temperature for a given LAC polymer based on substitution and molecular weight data. It is relevant to note that the LAC thermal properties (T_g) were in a similar range to the commercially produced CABs [42].

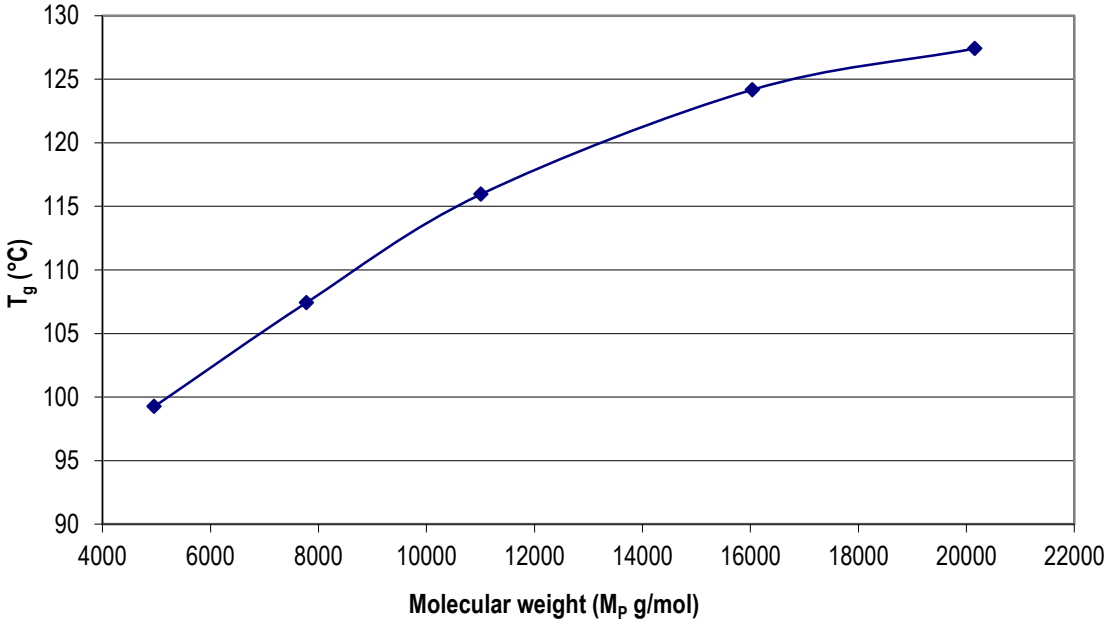

Figure 4-6 T_g with respect to molecular weight for LAC, with comparable DS-Ac/DS-Lev substitution ratio.

MW (g/mol)	Δ DS-Lev (nominal value of DS-Lev 1.00)	Δ T_g (°C)
12000	-0.51	6
11000	-0.10	1
9400	0.29	-7
8500	0.45	-10
7100	0.70	-11

Table 4-14 T_g difference with respect to DS-Lev and varying molecular weight; nominal DS-Lev value of 1.

4.6 Summary of LAC production

Preparation of LAC can be achieved with control of the substituents incorporated by manipulating the LA/Ac_2O ratio and, to a lesser extent, the LA/Acetate ratio. It was not possible to generate a LAC polymer which had all three properties required; a low T_g and a high molecular weight, whilst also having minimal colour. Reductions in T_g could be achieved by either elevating the level of levulinate incorporated, or lowering the molecular weight of the product. Unfortunately, reduction of the molecular weight was achieved at the expense of increased product colour. Standard conditions gave the best balance of properties, and these conditions were a reaction temperature of 120 °C over two hours with a sulfuric acid concentration of 9.1 mmol/L and an anhydride content of 3 Eq|OH. Other factors considered in defining these parameters were the absence of the undesired lactone group, the DS-Total of the product, and its solubility. These standard reaction conditions permit access to a per-esterified LAC polymer with good solubility in chloroform and acetone.

4.7 Longer chain mixed levulinyl-CEs

In order to derive CEs with a low T_g, one approach first mooted was the incorporation of longer chain alkyl esters. Commercially produced mixed CEs and longer alkyl-chain (> C_4) containing CEs detailed in the literature are primarily based on acetate with a second ester component [42, 102, 104]. A range of mixed aliphatic (from C_3-C_6 including isobutyric) levulinyl-CEs were therefore prepared and investigated. The “standard reaction conditions” were used, except that acetic anhydride was replaced with a series of aliphatic anhydrides of chain length C_3-C_6, including isobutyric anhydride. All mixed aliphatic levulinyl-CE reactions used cellulose pre-swollen with LA to ensure only a di-functionalised CE was generated. Section 3.6 discussed the DS analysis of mixed aliphatic levulinyl-CEs.

The proportion of the aliphatic ester groups’ incorporation compared to levulinate decreased as the chain length increased (Table 4-15), when a constant LA/Anhydride ratio of 1.33 (mol/mol) was used. This indicated that esterification *via* the exocyclic carbonyl (pathway B, see Section 2.4) was progressively less favoured with

increasing anhydride chain length. This effect is likely to be a function of both the steric hindrance caused by the progressively increasing size of the aliphatic moieties restricting access to the cellulose reactive sites, and also the electronic effects of the increasing chain length reducing the reactivity of the carbonyl. Both of these mechanisms reduce the reactivity of the aliphatic group and were exemplified by the significantly lower incorporation of isobutyrate compared to butyrate (Table 4-15).

Group attached	DS-Group	DS-Lev	DS-Total
Acetate	1.49	1.56	3.05
Propionate	1.23	1.84	3.07
Butyrate	1.13	1.80	2.93
Isobutyrate	0.59	2.45	3.04
Valerate	1.10	2.03	3.13
Hexanoate	0.91	2.04	2.95

Table 4-15 Levulinyl-CE aliphatic ester incorporation.

With respect to the T_g of the mixed levulinyl-CEs prepared here, it was found that incorporation of the longer aliphatic chain lengths resulted in a reduced T_g (Table 4-16). There are three contributing factors to the aliphatic levulinyl-CEs T_g: levulinate content (or the ratio of levulinate to aliphatic group), molecular weight and aliphatic chain length. The effect of the first two factors has previously been demonstrated in Section 4.5.5. With regard to the aliphatic chain length it should be noted that each polymer species was not optimised for a T_g minima with respect to substituent incorporation. The data in Table 4-16 shows no clear molecular weight trend with increasing aliphatic chain length and, due to the similar DP, this was not expected to have a dominant effect on the T_g (except when comparing acetate and propionate groups which showed a molecular weight difference in the polymers analysed of 3400 g/mol). The molecular weights of all the other aliphatic samples varied by a maximum of only 2200 g/mol. Based on Section 4.5.5 (T_g variation of LAC with respect to molecular weight, Figure 4-6), it was expected that the molecular weight variation recorded for the samples in Table 4-16 (except acetate and propionate substitution) would correlate to a T_g variation in the range of 1-4 °C.

A clear reduction in the T_g was recorded with incorporation of increasing aliphatic chain length, with a minimum T_g of 45 °C at C_5 (valerate). Hexanoate displayed a T_g of 54 °C, an increase compared to valerate, which could be attributed to interaction of the side chains restricting the polymers movement. This rationale has been previously postulated by Sealey *et al.* [99] and Crepy *et al.* [97] in reference to long chain fatty acid CE derivatives.

Group attached	T_g (°C)	Molecular weight (M_p g/mol)
Acetate	104	11000
Propionate	76	7600
Butyrate	64	9100
Isobutyrate	61	8800
Valerate	45	8500
Hexanoate	54	9800

Table 4-16 Aliphatic levulinyl-CE T_g and MW data.

At the outset of this project, a T_g of ≤ 25 °C was specified for the final levulinyl-CE product. Although a T_g of 25 °C was not attained here, the most promising candidate for use in a water-based paint formulation would be levulinyl valeryl cellulose (LVC). However, considerations around material processing and cost must be taken into account when choosing optimal candidates to take forward. The cost of valeric anhydride is 11.1 times greater than acetic anhydride, whereas butyric anhydride is only 1.6 times greater (Table 4-17), which is likely a function of commercial demand. Therefore, the use of valeric anhydride represents a significant increase in manufacturing cost and would likely make the process cost-prohibitive for a commodity product. Another important consideration was material processing, and in particular, work-up procedures. It becomes increasingly difficult to precipitate the CE without entraining by-products due to decreased water solubility of the residual acid present (Table 4-18). Purification of LVC required additional steps involving several solvent/water washes and re-precipitations to remove the entrained valeric acid from the CE which dramatically increased processing time. Consideration of the material cost and subsequent processing led to the decision to take levulinyl butyryl cellulose (LBC) on to the next development stage of the project. This material displayed a T_g advantage of 40 °C below that for LAC, while butyrate incorporation aligns with industry produced CEs (CABs) which will be beneficial when moving through the commercialisation stages of this project.

Anhydride used	Relative cost for 1 kg
Acetic	1.0
Propionic	1.6
Butyric	1.6
Isobutyric	1.8
Valeric	11.1
Isovaleric	11.8
Hexanoic	10.1

Table 4-17 Relative pricing for alkyl anhydrides (Sigma-Aldrich, NZD).

Acid	Solubility in water (g/L)
Acetic	soluble
Propionic	soluble
Butyric	50
Isobutyric	40
Hexanoic	11

Table 4-18 Alkyl acid solubility in water.

4.8 Optimisation of T_g and molecular weight for LBC

As discussed in the introduction (Section 1.8.2), Glasser *et al.* reported a T_g minima for the di-functionalised cellulose acetate hexanoate (CAH), with an acetate and hexanoate DS of 0.05 and 2.95, respectively [104]. This corresponded to a T_g for CAH which was 8 °C lower than cellulose trihexanoate (CTH). LBC prepared in Section 4.7 (Table 4-16) displayed a T_g of 64 °C which is significantly lower than either of the two parent tri-esters: CTLev has a T_g of 71 °C and cellulose tributyrate (CTB) has a T_g of 80 °C (Table 4-19). The T_g of LBC was optimised by mapping substituent incorporation with respect to T_g.

Notably, many of the same reaction traits that were observed for LAC were also observed for LBC, for example, poor solubility was observed for CEs that had low levulinate incorporation (DS-Lev of < 0.5). During the reaction

to generate a low DS-Lev LBC a free-flowing solution was not formed, but rather a high viscosity reaction gel was observed.

Predictable control of substituent incorporation into LBC was possible by varying the molar ratio of LA/But_2O (Figure 4-7). It was expected that if excess butyric acid was present, the ratio of LA/Butyrate would also be a contributing factor for substituent control, similar to the effect of varying the ratio of LA/Acetate for LAC. However, as all reactions completed for this series used cellulose pre-swollen with LA, this facet was not addressed. The same levulinate incorporation behaviour displayed for LAC was also observed for levulinate incorporation in LBC (Figure 4-7). Zone 1 (where the ratio of LA/But_2O is < 0.6) displayed little levulinate incorporation due to an excess of anhydride being present. Zone 2 (where the ratio of LA/But_2O was between 0.6 and 1.6) displayed significant incorporation of levulinate, followed by zone 3 (where the ratio of LA/But_2O is > 1.6) where there was no significant addition of levulinate compared to zone 2. Again, this reduced incorporation of levulinate at a high ratio of LA/But_2O was likely due to steric hindrance of the reacting levulinate group having restricted access to the free hydroxyl groups on the partly esterified cellulose chain. This reaction series was restricted to a LA/But_2O ratio of ≤ 3, as any significant excess of reagents at this point would make commercial processing unlikely, unless an efficient reprocessing and recycling method was in place.

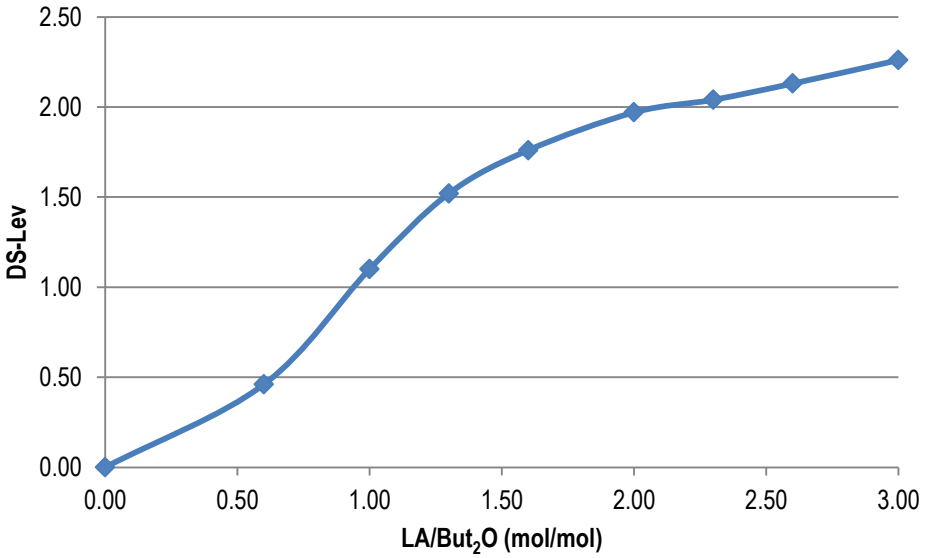

Figure 4-7 Levulinate incorporation for LBC varying the LA/But_2O ratio.

The series of LBC polymers synthesised displayed a much tighter molecular weight range in comparison to the LAC series although for reactions that displayed gelling, high molecular weights were recorded due to a reduced degree of depolymerisation (Table 4-19). A LA/But_2O ratio of 0.6 formed a clear homogeneous gel, similar to that observed for LAC samples produced with a low LA/Ac_2O molar ratio. Clearly, with no LA present (DS-Lev of 0) the CTB species was produced using traditional anhydride chemistry. An overall trend of decreasing molecular weight for the LBC with an increasing LA/But_2O ratio was observed, a feature again assigned to increased product solubility due to the increased levulinate incorporation. In addition, this results in the polymer being dissolved in the reaction media for a longer time period leading to increased chain cleavage.

A steady decline in the T_g was observed progressing from CTB (DS-Lev of 0, T_g of 80 °C) to high DS-Lev LBC polymers (DS-Lev of 2.26, T_g of 60 °C), a function of both molecular weight reduction and increased levulinate incorporation. The dominant effect is likely to be the increase to the DS-Lev, as the variation in molecular weight was relatively small (Table 4-19). It is not possible to say if 60 °C for LBC with a DS-Lev of 2.26 is a global T_g minimum for LBC, as a complete series up to a DS-Lev of 3 was not produced. However, it is clear that at some point between a DS-Lev of 2.26 and 3.00 the T_g begins to increase as CTLev demonstrated a T_g of 71°C (Section 3.3). The minimum T_g obtained for LAC was 95 °C (Table 4-10), while the minimum for LBC was 60 °C, a reduction of 35 °C. However, a T_g of 60 °C was still 35 °C too high compared to the target of 25 °C, meaning that further T_g reductions were necessary in order for LBC to be a film forming, water-based dispersion candidate.

LA/But_2O	T_g (°C)	Molecular weight (M_p g/mol)
0.0	80	16500
0.6	78	22700
1.0	71	12900
1.3	66	11400
1.6	64	11000
2.0	63	10200
2.3	62	10200
2.6	60	9800
3.0	60	9800

Table 4-19 T_g and molecular weight for LBC with respect to the molar ratio of LA/But_2O.

4.8.1 Effect of plasticising LBC

Incorporating plasticisers is a common technique for lowering the T_g, either as an external or internal plasticiser. An external plasticiser is a small polymer-miscible compound which promotes chain flexibility but does not form a chemical bond to the polymer substrate; commonly polymer-compatible high boiling liquid. In contrast, an internal plasticiser introduces a secondary low T_g monomer or chemical structure onto the polymer backbone which is chemically bound to the structure. Both internal and external plasticiser methods were trialled on a LBC with a levulinate DS of 1.52, a butyrate DS of 1.47 and a T_g of 66 °C.

4.8.1.1 External plasticiser

Commonly used in the coatings industry as an additive and plasticiser, sucrose acetate isobutyrate (SAIB), was the external plasticiser of choice for this project as it has a high renewable component and thus fitted with the project theme of renewable polymers. SAIB is also known to be highly compatible with CAs and CABs. Eastman SAIB-90EA was used for this project and had a DS-IsoBut of 6 and DS-Ac of 2.

The T_g of LBC (DS-Lev 1.52, DS-But 1.47) was incrementally lowered with increasing SAIB addition between 0 and 40 wt% (Figure 4-8). The initial project target T_g of 25 °C was exceeded using 40 wt% of SAIB where a T_g of 21 °C was recorded, accounting for a 68% reduction in T_g over the LBC starting material. Extrapolation of the data indicated that 34.1 wt% of SAIB would be required for the trialled LBC to reach the targeted T_g of 25 °C. These results indicated that SAIB was compatible with LBCs and the target T_g can be achieved using moderate SAIB loadings.

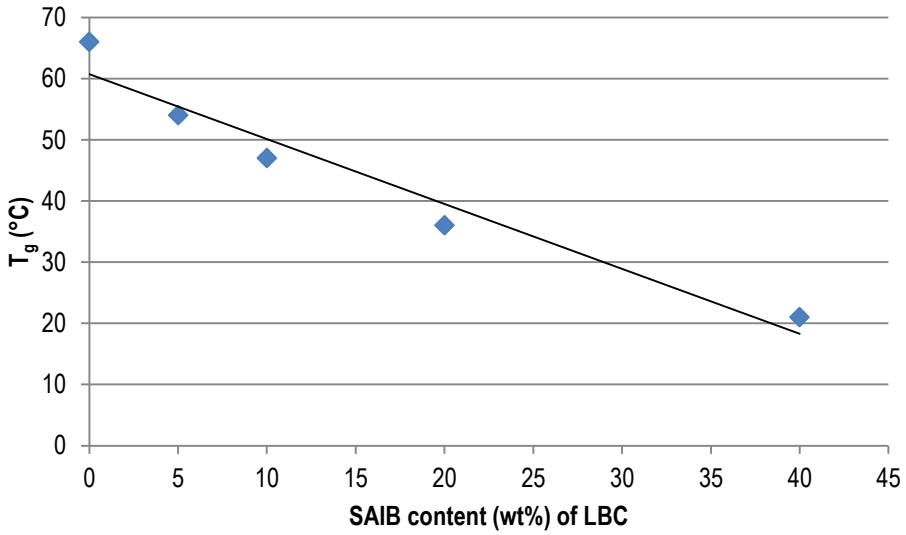

Figure 4-8 Effect of SAIB on the T_g for LBC (DS-Lev 1.52, DS-Ac 1.47, T_g 66 °C).

4.8.1.2 Internal plasticiser

Internal plasticising was performed using an oxime link which utilised the free levulinyl ketone group, as discussed in Section 7.4. A short PEG chain consisting of three PEG units terminating with an alkoxy amine **(8)** was chosen as the internal plasticiser (Figure 4-9). The T_g of LBC (DS-Lev 1.52, DS-But 1.47) was reduced almost linearly with respect to PEG incorporation, as shown in Figure 4-10. The oxime linked PEG was incorporated up to a maximum of 23.9 wt%, which resulted in a T_g of 8 ºC for the modified LBC, correlating to a reduction of 58 ºC (88%) from the starting LBC. Unlike SAIB which can be indefinitely loaded, PEG incorporation was limited to the DS-Lev and, in this case, a maximum PEG incorporation of 58.7 wt% was theoretically possible. Extrapolation of data obtained for this particular LBC (DS-Lev 1.52, DS-But 1.47) modified with PEG groups indicated that to achieve the target T_g of 25 °C, 15.2 wt% of PEG would be required.

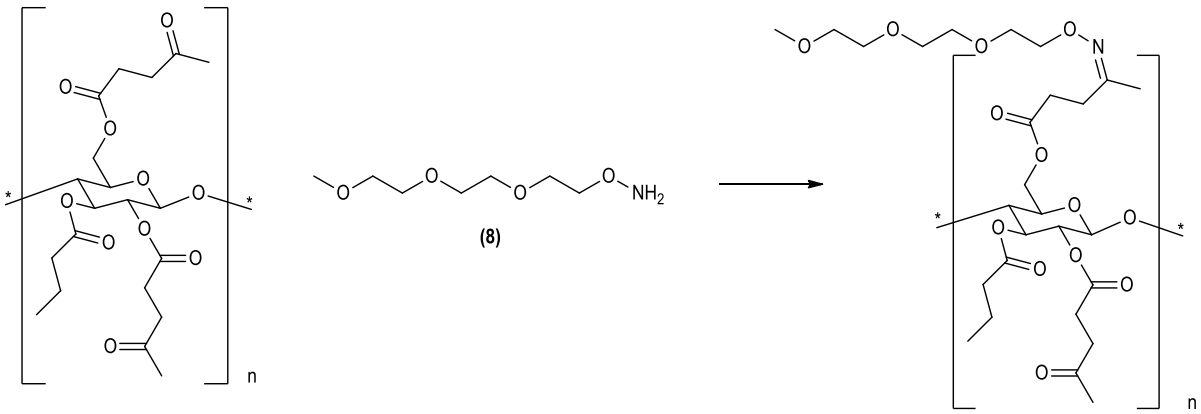

Figure 4-9 PEG modified LBC.

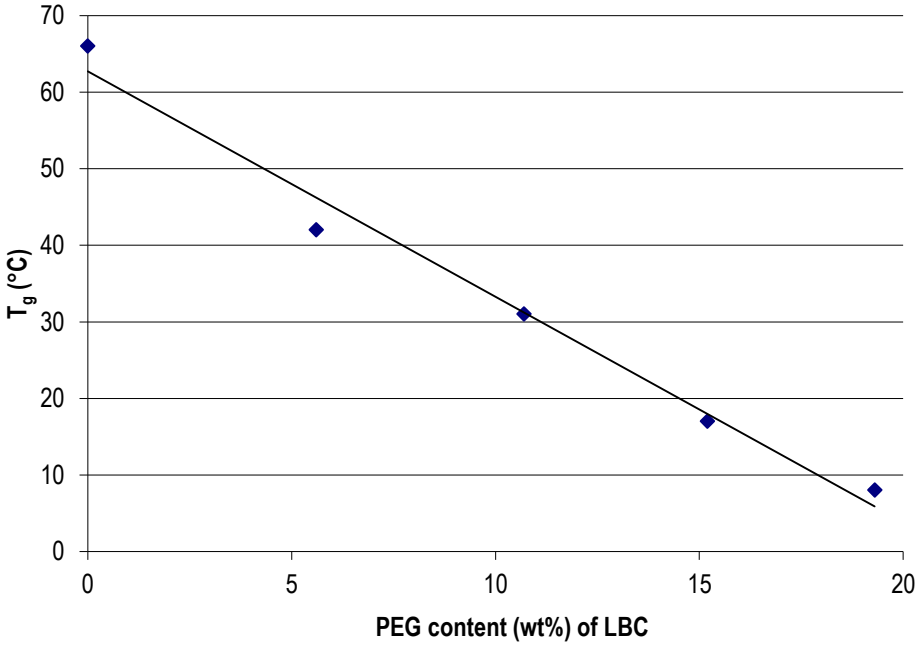

Figure 4-10 Effect of internal plasticisation with PEG-oxime on LBC (DS-Lev 1.52, DS-Ac 1.47, T_g 66 °C).

On a wt% basis the use of a PEG alkoxy amine as an internal plasticiser was shown to be more effective than the SAIB external plasticiser. In order to achieve the target T_g of 25 °C, 18.9 wt% less PEG alkoxy amine plasticiser was needed for a LBC with a DS-Lev of 1.52 and DS-But of 1.47. This could be attributed to the PEG being covalently bound to the polymer structure as well as being highly hydrophilic and having a secondary hydro-plasticising effect due to the attraction of water to the PEG-modified polymer. It is expected that PEG incorporation into the levulinyl-CE backbone will increase the water sensitivity of the product since glycols are common humectants. This serves to compound the water susceptibility of this class of polymer as both the low

molecular weight chains and high levulinyl incorporation have demonstrated higher water solubility than the equivalent commercial alkyl species (CA, CAB). This would reduce the polymer's effectiveness as an architectural coating in certain applications, especially in high humidity areas such as bathrooms and kitchens.

Modification of the T_g for LBC demonstrated the utility of the levulinyl-CE moiety. Through a non-destructive secondary oxime modification step, a significant change to the T_g was effected highlighting the ease of modification of the levulinyl-CE polymer's behaviour and characteristics. It is anticipated that the compatibility and effectiveness of both SAIB and PEG plasticisers will translate to all levulinyl-CEs. However, SAIB will only be an effective plasticiser as long as it is compatible with the specific levulinyl-CE; any variation in substituent and degree of incorporation will affect the solubility parameters and will likely impact on SAIB's compatibility. Plasticising with oxime linked PEG groups should not suffer from compatibility issues due to the PEG being covalently bound to the levulinyl-CEs.

4.9 Butyryl levulinyl acetyl cellulose (BLAC)

Processing time and raw material cost savings can be made by removing the pre-swelling solvent exchange from acetic acid to butyric acid (or LA). Performing the preparation of LBC with acetic acid present would incorporate acetate functionality and form a tri-functionalised CE. Such tri-functionalised CEs appear to be unique compounds with no evidence of their production reported in the literature.

4.9.1 Optimisation of T_g and molecular weight for BLAC

The T_g and molecular weight properties of BLAC were characterised with respect to substituent incorporation. BLAC reactions were completed by both varying the LA/But_2O molar ratio with a fixed acetic acid content, and varying the acetic acid content with a fixed LA/But_2O ratio. The previously optimised "standard reaction conditions" were used when completing these reactions. Unexpectedly, reactions undertaken to form a BLAC with a low levulinyl content did not display the characteristic gelling which was observed in the synthesis of both LAC and LBC samples. It is possible that the mixture of lactones **(1)**, **(2)** and **(4)** provided better solubility characteristics for synthesising a low levulinyl content BLAC. This proved particularly advantageous when producing low levulinyl content BLAC materials for the dispersion of the polymer into an aqueous phase.

Levulinate incorporation, consistent with that observed in the preparation of LAC and LBC, was primarily a function of the LA/Anhydride molar ratio. Again a significant increase in the level of levulinate incorporated onto the polymer was observed when the LA/But_2O ratio was between 0.3 and 1.6. The proportion of levulinate incorporated onto the polymer was reduced when a LA/But_2O ratio of > 1.6 was used (Figure 4-11). Since BLAC was a more complex species than LBC, it was hoped that incorporation of the third substituent (acetate) would increase the degree of disorder in the polymer and would yield reduced T_gs in comparison to LBC. However, this was not observed, as can be seen in Table 4-20. The T_g minimum for BLAC with respect to a changing LA/But_2O ratio was observed over the range 1.3-2.0, however, the true T_g minimum (62 °C) was suspected to be at a LA/But_2O ratio of 1.3. This point also corresponds to the highest molecular weight of the three samples with the lowest T_g and it was likely that the reduced molecular weight of the other two samples (LA/But_2O 1.6 and 2.0) would artificially reduce the T_g. An unexpected advantage that BLAC displayed over LBC was that the minimum T_g polymer of this series was produced using a LA/But_2O ratio of 1.3, in comparison to 2.6 which was required for LBC. This was a highly advantageous outcome as it represented a significant cost saving as only half the quantity of LA is required to produce a low T_g levulinyl-based CE (BLAC).

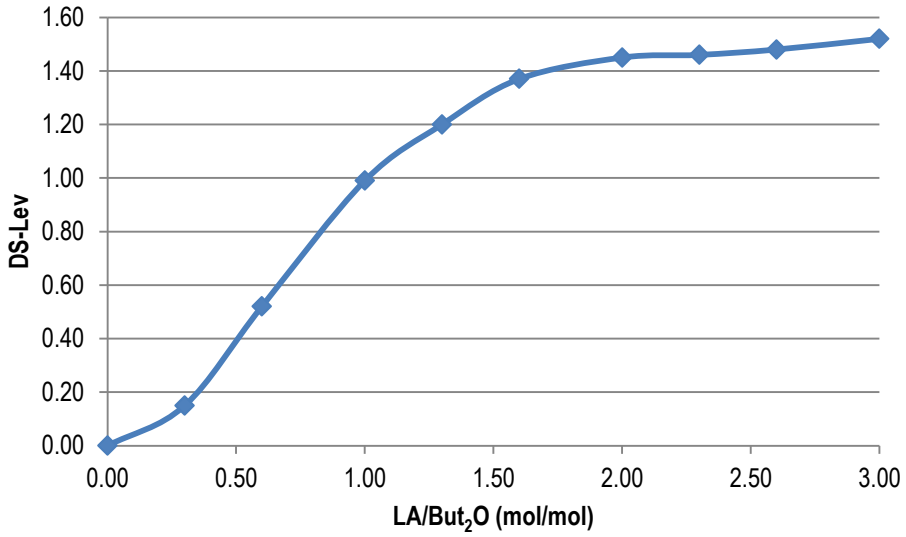

Figure 4-11 Levulinate incorporation in BLAC.

LA/But$_2$O	T_g (°C)	Molecular weight (M_p g/mol)	Insoluble material (%)
0.0	89	17000	0.9
0.6	78	11000	0.8
1.0	76	9000	5.0
1.3	62	8200	2.0
1.6	63	7100	6.4
2.0	62	6800	8.2
2.3	65	6600	15.4
2.6	66	6600	18.6
3.0	66	5600	28.3

Table 4-20 Molecular weight, T_g and % of insoluble material with respect to LA/But$_2$O ratio for a series of BLACs.

Increasing the acetic acid content in the reaction media, while using a fixed LA/But$_2$O molar ratio showed, as expected, a concomitant increase in the DS-Ac (Table 4-21) and resulted in a corresponding increase in T_g for the BLAC species generated (Table 4-21). The acetate substitution most likely produced a more ordered structure allowing the cellulose chains to pack closer together, restricting chain movement, which resulted in an increase in T_g. The molecular weight remained relatively constant (8600 ± 400 g/mol) and was therefore not considered to be a contributing factor to the changes in T_g observed for these materials.

Acetic acid (mol%)	DS-Lev	DS-But	DS-Ac	DS-Total	Molecular weight (M_p g/mol)	T_g (°C)
23.7	1.19	0.86	0.35	2.40	8900	76
28.5	1.16	0.87	0.46	2.49	8600	80
32.6	1.14	0.84	0.57	2.54	8200	82
39.6	1.04	0.77	0.76	2.57	8800	86

Table 4-21 BLAC DS, molecular weight and T_g with varying acetic acid content.

An unexpected feature of the BLAC polymers generated in this series was the observed decrease in acetone solubility with the corresponding increase in the LA/But_2O molar ratio used (Table 4-20). This insolubility is likely to be a function of two processes. Firstly, it was proposed that **(2)** is likely to display reduced reactivity in comparison to **(4)**, and in particular to **(1)**, and generate a polymer with a low DS-Lev. When using LA/But_2O molar ratios of > 2 there will be a corresponding increase in the concentration of **(2)** in solution. Secondly, the reactions generating LAC, LBC and BLAC have all been performed using wood pulp which contained hemicellulose. Hemicellulose is reported in the literature to create hemicellulose-cellulose agglomerates [60] which are likely to display reduced reactivity. Therefore, it is possible that the combination of high concentrations of **(2)** in the reaction media, coupled with the reduced reactivity of the hemicellulose-cellulose aggregates, has reduced the level of reaction achieved in the two hour time frame, resulting in a less acetone-soluble polymer. The percentage of insoluble BLAC material was determined by removing all of the acetone-soluble material by an exhaustive extraction process (see Experimental, Section 10.2.32). Assessment of the DS by HPLC analysis of the hydrolysed substituents of the insoluble BLAC residues indicated the level of esterification was low, and the reactions had not progressed far enough to yield a product that was sufficiently esterified to produce an acetone-soluble polymer (Table 4-22).

BLAC fraction	DS-Lev	DS-But	DS-Ac	DS-Total
Soluble	0.53	1.54	0.83	2.90
Insoluble	0.44	0.09	0.11	0.64

Table 4-22 HPLC analysis of acetone portioned fractions of BLAC.

4.9.2 BLAC generated from α-cellulose

Partial product insolubility was not a trait that was acceptable for this project as the product specifications required the final levulinyl-CE to be fully soluble in chloroform and acetone. Solubility in chloroform was a requirement so that NMR analysis could be carried out on the materials synthesised. Acetone solubility was a fundamental requirement for the water dispersion process, and removal of any insoluble material from the bulk polymer would be an unfeasible process due to the excess costs involved for a low value commodity product.

Wood pulp is not used for commercially produced CEs due to the insolubility of the hemicellulose aggregates [60, 167] and the negative effects they can have on the finished product [45]. Therefore, commercially, α-cellulose (dissolving pulp) is used [49] and is known to be the most reactive form of cellulose. With regards to this project the initial specifications called for low grade wood pulp to be used. However, based on the BLAC work which derived the lead candidate, to produce an aqueous dispersion it was clear that a more uniformly reactive form of cellulose was required and the change to dissolving pulp was made.

The α-cellulose used in this project was prepared from Kinleith BKT bleached wood pulp (81.2% α-cellulose and 18.8% hemicellulose) using method four described by Ritter [168]. This process involves removing the hemicellulose by steeping the wood pulp in sodium hydroxide (5.3 mol/L), which preferentially breaks down the hemicellulose and dissolves it away from the α-cellulose. After following the procedure described by Ritter, the resulting α-cellulose dissolving pulp was thoroughly washed with water, re-filtered and the standard pre-swelling procedure applied. Three large lab-scale BLAC synthesis reactions were carried out with LA/But_2O ratios of 0.5, 1.3 and 1.6 (material data given in Table 4-23), using dissolving pulp, to generate BLAC samples which contained less than 0.5% insoluble material. The BLAC materials produced in these reactions were those used for subsequent dispersion experiments.

There were several notable features of the BLAC synthesis reactions using dissolving pulp, the first being the speed of cellulose dissolution. The dissolving pulp dissolved within 30 minutes, in contrast to the > 90 minutes needed for solvating wood pulp. Secondly, the dissolving pulp reaction solution was clear and free of the

commonly observed insoluble spears. The BLAC polymers prepared with dissolving pulp displayed a DS that was consistent with the soluble fractions prepared using wood pulp. Thirdly, shortened reaction times were possible which resulted in minimisation of product colour (with no evidence of incorporation of the lactone species) and also allowed a higher molecular weight product to be obtained. As expected, due to the increased molecular weight there was a corresponding increase in T_g. Comparing the BLAC material produced with a LA/But_2O ratio of 1.3 from wood pulp (Table 4-20), and the related reaction using dissolving pulp (Table 4-23), an increase in molecular weight from 8200 to 15000 g/mol respectively was observed. These materials had comparable substituent incorporation and the T_g increased from 62 °C to 78 °C.

LA/But_2O	DS-Lev	DS-But	DS-Ac	DS-Total	Molecular weight (g/mol)	T_g (°C)
0.5	0.35	2.23	0.34	2.92	17500	88
1.3	1.16	1.03	0.45	2.64	15000	78
1.6	1.45	0.86	0.33	2.64	12000	89

Table 4-23 DS, molecular weight and T_g of BLAC generated from dissolving pulp.

4.10 Summary

LAC, LBC and BLAC polymers were all successfully prepared and shown to display predictable substituent incorporation values dependent on the LA/Anhydride and LA/Acetate ratio (or LA/Butyrate etc.). Of the three levulinyl-based CEs generated, BLAC was considered to be the most viable lead compound as it fulfilled all target product specifications, with the exception of T_g, although a minimum T_g of 62 °C was recorded for BLAC. The work investigated with the LBC materials clearly demonstrated that the target T_g of 25 °C could be obtained with the use of either an internal or external plasticiser. In addition, the required solubility profile of the CE was achieved by using α-cellulose (dissolving pulp) as the starting material for the synthesis of BLAC.

5 Miscellaneous reactions and characteristics of LAC

5.1 Alternative reaction catalysts

Early CE publications investigating the acetylation mechanism and the role of the acid catalyst focused on perchloric and sulfuric acid catalysts [68, 75]. As discussed in Section 1.7.3, sulfuric acid is a combining acid, forming a sulfate ester with cellulose which, if not removed, can lead to CE degradation during downstream processing. The use of so-called non-combining acid catalysts has been investigated as a way of minimising CE degradation during product processing [169, 170].

Hydrochloric, phosphoric and sulfonic acids have all been described as alternative reaction catalysts for the production of CEs. Acid catalyst mixtures, namely sulfuric and phosphoric, have also been investigated with respect to CE production [169]. Commercial CE reactors are commonly constructed from stainless steel and since hydrochloric and perchloric acids corrode stainless steel, this has limited the commercial use of these two acids. Perchloric acid is also explosive when brought into contact with readily oxidisable materials [170]. As demonstrated by Wininger, sulfonic acids were used to catalyse the esterification of cellulose [170] where a catalyst loading of between 0.3 % and 3.0 % by weight of cellulose was used to generate a variety of CEs. Methane sulfonic acid (MSA) has also been used as an effective acid catalyst where a loading of 1 % by weight of cellulose has been reported to give a cellulose acetylation rate equal to using a 10 % by weight of cellulose sulfuric acid catalyst loading [171]. Touey has reported the use of sulfonated phenolic ion-exchange resins as catalysts in the preparation of CEs with a variety of anhydrides [172] where the phenolic resins contained between 0.5 and 1.2 sulfonate groups per aromatic centre. One advantage of this solid phase catalysis technology was the efficient recovery and recycling of the catalyst from the reaction media; the phenolic ionic exchange resins are insoluble in the reaction solution and could therefore be recovered by filtration.

There have been several alternative catalytic systems reported in the literature that promote the esterification of cellulose. Biswas *et al.* reported that cellulose was converted to CTA at room temperature following a 24 hour reaction using acetic anhydride and catalytic quantities of iodine [166] (14 wt% based on cellulose), generating

CTA with a molecular weight of 57000 g/mol. In our laboratory CTA was readily prepared using acetic anhydride at 100 °C with catalytic iodine (5 wt% per AGU) in 10 minutes. Strong acid salts have also been reported as catalysts for CE preparation; ammonium sulfamate was reported by Takahashi [173] and zinc chlorides were reported by Malm *et al.* [174]. Zinc chloride loadings of up to 100% by weight of cellulose were required to effect cellulose esterification, generating a cellulose butyrate with a DS of 2.32. Yan *et al.* developed a solvent-free cellulose acetylation system based on solid phase super acid catalysts [175]. The reactions were carried out in a ball mill with cellulose, acetic anhydride and a SO_4^{2-}/ZrO_2 solid phase super acid catalyst, generating CA in 7.5 hours with a DS-Ac of 1.8.

With regards to the preparation of LAC several alternative Brönsted acids catalysts were investigated to determine whether an advantage could be gained over sulfuric acid (Table 5-1). The catalyst loading remained constant for all the experiments and was chosen based on successful LAC reactions using sulfuric acid. The exception to this was para-toluene sulfonic acid (pTSA), where the catalyst loading was increased by 50% (experimental details are discussed in Section 10.2.37). Under the conditions employed here, only MSA and pTSA were effective catalysts for generating LAC, with both reactions complete within 2 hours and products with a high DS produced (Table 5-1). The reaction catalysed by MSA generated LAC with a DS-Total of 2.84 in comparison to the pTSA catalysed reaction, which resulted in a LAC product with a DS-Total of 3.14. This indicated that significant cellulose depolymerisation had occurred during the pTSA catalysed reaction which was likely a function of the increased concentration of pTSA used to generate LAC.

Reactions catalysed with TFA, HCl and phosphoric acid were allowed to proceed for a further 18 hours to investigate whether esterification would proceed. At the end of this time period the cellulose was still not dissolved which indicated incomplete reaction. It is likely that a suitable LAC could have been generated using TFA, HCl or phosphoric acid as catalysts by increasing the proportion of catalyst or altering the reaction conditions.

The results showed that sulfonic acid catalysts successfully generated LACs using the same reaction conditions that are applied to sulfuric acid catalysed LAC reactions. There was no obvious advantage to be gained from using sulfonic acids MSA or pTSA in place of sulfuric acid, so sulfuric acid was standardised as the reaction catalyst.

Acid catalyst	Cellulose dissolution	DS-Lev	DS-Ac	DS-Total
TFA	✗	-	-	-
HCl	✗	-	-	-
Phosphoric	✗	-	-	-
MSA	✓	1.41	1.43	2.84
pTSA	✓	1.68	1.46	3.14

Table 5-1 Alternative acid catalysts to effect cellulose esterification.

5.2 LAC solubility

The solubility of LAC 500.1 (the preparation of this material is discussed in Section 6) was investigated and assessed based on Hanson solubility parameters. Hanson solubility parameters are used commercially by our industry partner and were therefore chosen for use in this project (over the also commonly used Hildebrand solubility descriptions). The goal was to generate a set of Hanson solubility parameters for LAC 500.1, information which would then be used for investigating co-solvents to aid cellulose dissolution during esterification (see Section 5.3) and to aid in the levulinyl-CE water dispersal process (see Section 8). Hanson solubility parameters are widely used as a description of a polymer's solubility characteristics, and can be used in a predictive sense for assessing alternative solvent systems for dissolution of a polymer [176].

Solutions of LAC were prepared (10% w/v) at room temperature and the solubility was determined by visual inspection. LAC 500.1 was soluble in a range of solvents (Table 5-2) and so by plotting the Hanson solubility values of these solvents on a ternary plot, a centroid that approximates the Hanson solubility parameters for LAC should be calculable. However, no clear region on such a plot could be defined and therefore a discrete set of Hanson solubility parameters for LAC 500.1 could not be assigned. The range of solvents that dissolve LAC

were comparable to those used to dissolve CABs with a similar level of substituent incorporation (e.g. CAB 321-0.1). The LAC 500.1 polymer displayed good solubility in keto solvents: acetone, MEK, MIBK and cyclohexanone, which was likely a result of the keto functionality present in the levulinyl moiety. This served to aid formulation in subsequent processing.

Solvent	LAC solubility	Solvent	LAC solubility
Acetic acid	S	Dipropylene n-butyl glycol ether	I
Acetic anhydride	S	Ethanol	I
Acetone	S	Ethyl acetate	S
Amyl alcohol	I	Ethyl cellosolve	S
Butyl acetate	G	Isopropyl alcohol	I
Butyl cellosolve	I	Methanol	I
Butyl lactate	G	Methyl ethyl ketone	S
Chloroform	S	Methyl isobutyl ketone	S
Cyclohexanone	S	Methylene chloride	S
Dibasic ester	S	N-Methyl-2-pyrrolidone	S
Diacetone alcohol	S	Propylene n-butyl glycol ether	I
Dimethylacetamide	S	Pyridine	S
Dimethylformamide	S	Texanol	I
Dimethylsulfoxide	S	Toluene	G
Dioxane	S	Water	I

Table 5-2 Solubility profile (10% w/v) for LAC (DS-Lev 1.21, DS-Ac 1.88, DS-Total 3.09); I=Insoluble, S=Soluble, G= gel or semi-soluble.

5.3 Reaction co-solvents

The methylene chloride (DCM) process (or the Dormagen process) uses DCM as a reaction co-solvent [45] (discussed in Section 1.7.3). DCM is the only known CE acetylation co-solvent used in commercial processes. Both Saka *et al.* [60, 177] and Shashidhara *et al.* [178] published work on the esterification of low-grade cellulose in the presence of a co-solvent. The preparation of CTA from a low-grade cellulose source (α-cellulose content 79-94%) resulted in the generation of insoluble agglomerates comprised of esterified hemicellulose residues and CTA [60]. In particular, the addition of nitro containing or chlorinated solvents was shown to reduce the amount of

insoluble residue recovered after esterification. This was attributed to the solvent reducing the interaction of esterified hemicellulose residue with the CTA. Interestingly, when dichloroacetic acid was used as a co-solvent, chlorine was incorporated into the polymer structure [60], most likely through a reaction utilising a mixed anhydride.

Reaction co-solvents, both chlorinated and non-chlorinated, were investigated with respect to the formation of LAC. Based on the literature it was expected that chlorinated solvents, in particular DCM, would be effective co-solvents. However, chlorinated solvents are toxic and can be carcinogenic, therefore a series of non-chlorinated solvents were also trialled. A second aspect of moving away from chlorinated co-solvents was water solubility. For efficient CE purification, the chlorinated co-solvent must be completely removed from the reaction media by distillation before precipitation of the CE into water. Use of a water-soluble co-solvent would remove the need for an additional solvent removal step before CE purification. The solvents chosen for this body of work were selected according to the solubility data that was previously collected for LAC 500.1. The following reactions were completed based on the rationale that solvating power of the reaction co-solvent would draw the partially esterified cellulose into the reaction solution earlier and at an increased rate, giving a more even esterification. This was based on the premise that the cellulose peels into the reaction solution [70].

The same reaction conditions were used for all experiments utilising co-solvents and the reaction temperature was maintained at the reflux temperature of DCM. Previous experiments using a DCM co-solvent required an overnight reaction, a function of reduced reaction temperature, and therefore the reaction duration for these experiments was 18 hours. Under these conditions the esterification of cellulose to produce LAC did not proceed when using non-chlorinated co-solvents. Complete dissolution of cellulose was not achieved and characterisation of the cellulosic material recovered showed very little esterification had occurred. This indicated that the non-chlorinated co-solvents did not enhance the reaction, but instead appeared to have an inhibitory effect. It is not yet understood why the non-chlorinated reaction solvents did not provide an effective esterification media.

Solvent	δ_D	δ_P	δ_H
Acetone	15.5	10.4	7.0
Chloroform	17.8	3.1	5.7
Dimethylformamide	17.4	13.7	11.3
Dimethylsulfoxide	18.4	16.4	10.2
Dioxane	19.0	1.8	7.4
Ethyl acetate	15.8	5.3	7.2
Ethylene dichloride	19.0	7.4	4.1
Methyl isobutyl ketone	15.3	6.1	4.1
Methylene chloride	18.2	6.3	6.1
N-Methyl-2-pyrrolidone	18.0	12.3	7.2
Tetrahydrofuran	16.8	5.7	8.0

Table 5-3 Hansen solubility parameters of the co-solvents trialled [179, 180].

The use of chlorinated co-solvents resulted in clear homogeneous reaction solutions and required reduced reaction temperatures to generate a LAC product which displayed greatly reduced colour by visual examination (estimated to be < 20 abs). However, as a result of the particularly mild reaction conditions employed, a significant increase in the level of the lactone group described in Section 2.6 was evident and consequently the use of reaction co-solvents was abandoned even though their use did demonstrate desirable features in the synthesis of levulinyl-CEs (e.g. colour reduction). The three chlorinated co-solvents used for this investigation had boiling points ranging from 40 °C - 84 °C (Table 5-4) and this feature could be used to vary the reaction temperature in an effort to minimise the incorporation of the lactone species, while maintaining a high molecular weight product with low colour. These preliminary reactions indicated that the inclusion of chlorinated solvents is a promising avenue and further exploration of this aspect is proposed.

Chlorinated solvents	b.p. (°C)
Chloroform	60.5 - 61.5
Ethylene dichloride	82.0 - 84.0
Methylene chloride	39.8 - 40.0

Table 5-4 Chlorinated co-solvent boiling points.

6 Scale-up production of LAC

At the outset of this project, several key criteria were specified, one of which being that the chemistry used should be readily scalable to pilot plant scale manufacture. A scaled-up synthesis of the LAC polymer was therefore undertaken. The issues identified in this process were anticipated to be comparable to the batch manufacture of a BLAC polymer.

6.1 Reaction calorimetry

During the lab-scale synthesis of the levulinyl-CEs, exotherms were routinely observed at the start of the reaction upon mixing the reagents prior to the addition of cellulose. Due to the obvious safety concerns of exothermic reactions in large scale processes, reaction calorimetry was undertaken on this initial exotherm[7]. Investigating the reaction calorimetry for the entire process was not possible with the equipment available, as upon addition of cellulose to the reagent solution a dense slurry formed making accurate data collection impossible.

With the initial addition of small quantities of acetic anhydride to the stirring mixture of levulinic acid and sulfuric acid, an immediate draw of power on the cooling circuit of the calorimeter was observed, attributed to the anhydride reacting with residual water (Figure 6-1). Once this energy demand had levelled off, a rapid dose-limited exotherm was evolved proportional to the addition of acetic anhydride (8 g/min). The maximum specific power observed during this reaction period was 70 W/L (35 W for this 0.5 L calorimetry monitoring reaction) associated with the formation of lactone species **(1)** and **(2)**. Therefore, from the data obtained here, it was possible to calculate the expected power output of the 8 L pilot scale LAC reaction to be 560 W. This was a critical calculation as it was essential that the power output did not exceed the 5 kW cooling capacity of the large scale reaction vessel.

[7] The assistance of Dr Graham Caygill is gratefully acknowledged in completing the reaction calorimetry experiments.

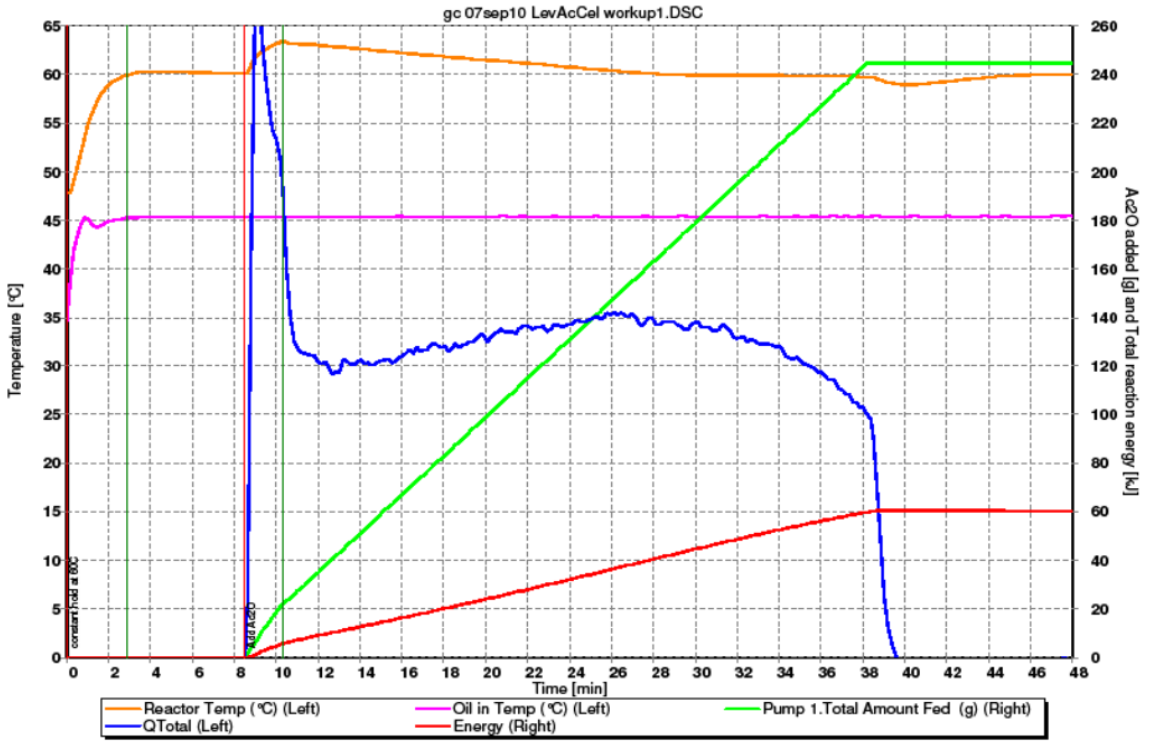

Figure 6-1 LAC reaction calorimetry.

The total reaction energy observed during the reaction calorimetry measurement was 60 kJ for the 2.39 mol of acetic anhydride used (the limiting reagent). Thus the reaction enthalpy was determined to be 25.1 kJ/mol and the adiabatic temperature rise was calculated to be 58 K.

6.2 Scale-up batch of LAC

Having investigated the reaction calorimetry for the esterification process, a demonstration LAC synthesis scale-up batch using 0.5 kg of cellulose (bleached wood pulp) was manufactured (designated LAC 500.1) using the GlycoSyn 75 L pilot plant reactor [8]. It was proposed that the starting temperature for the scaled-up reaction should be 60 °C such that the exotherm(s) observed would not drive the reaction temperature above 120 °C. In addition, this starting temperature ensured that the LA was liquid (m.p. 35 °C). Purification of this large scale reaction yielded 900 g of LAC product (80 % of the theoretical yield) and characterisation of this material is detailed in Table 6-1. Prior to beginning the LAC scaled-up batch, a target was set to determine if the same level

[8] The assistance of Jeremy Jones is gratefully acknowledged in the synthesis of the large scale LAC 500.1 batch.

of reaction control could be achieved on large scale in comparison to lab-scale reactions; this target was a DS-Lev of 1.20. As can be seen from Table 6-1 the calculated DS-Lev for LAC 500.1 was 1.21, indicating that the pilot scale LAC production was consistent with lab-scale reactions.

As discussed in Chapter 3, the location of the acetate and levulinate esters on the AGU was determined by ^{13}C NMR spectroscopy for LAC 500.1. Levulinate incorporation was highest at position C-6, with a DS-Lev of 0.53. Interestingly, the levulinate incorporation did not follow the expected trend for positional reactivity (C-6 > C-2 > C-3). Position C-3 was expected to display the lowest degree of levulinate incorporation, although in this case, position C-3 had an associated DS-Lev of 0.40, the second highest. But, the combined total DS of position C-3 for both levulinate and acetate was 1.18. A possible explanation for this unexpected result would be that the end group carbonyl ester signals in the ^{13}C NMR spectrum for both acetate and levulinate may be overlapping the C-3 position signals, artificially increasing the DS-Lev at this position.

LAC 500.1	
Molecular weight (M_p g/mol)	8900
T_g (°C)	103
DS-Lev	1.21
Position C-2	0.25
Position C-3	0.40
Position C-6	0.53
DS-Ac	1.89
Position C-2	0.63
Position C-3	0.78
Position C-6	0.49
DS-Total	3.10

Table 6-1 LAC 500.1 characterisation.

The following aspects were identified as most critical with respect to scale-up:

- Pre-treatment of cellulose is required to activate the cellulose in order for complete reaction to occur, specifically for the case when using low-grade cellulose sources. Large volumes of both water (20 L/kg

of cellulose) and glacial acetic acid (20 L/kg of cellulose) were used to process the cellulose pulp. Warm water handling does not pose any significant risk, but the glacial acetic used to dehydrate the swollen wood pulp poses a significant risk to the operator at scale.

- The work-up of LAC 500.1 generated large waste volumes associated with several washing steps to increase product purity (900 g of product generated 160 L of waste). However, it should be possible to recover a high proportion of the reagents through recycling.
- Precipitation morphology was unpredictable with formation of micron-range fines that blocked filters, a significant and unpredictable problem that created delays in processing. Predictable particle morphology is a must to produce a readily filterable product. Alternatively, centrifuging techniques could be used to separate the precipitate from the washing liquor thus removing the need for filtration.
- An extended reaction time of 3 hours was used for the preparation of LAC 500.1 as a precaution due to the anticipated reduced rate of thermal transfer slowing the rate of reaction at this scale. Samples were taken at 30 minute intervals during the reaction which indicated that the LAC 500.1 reaction was complete between 1.5 and 2 hours. This was consistent with laboratory scale reactions and indicated that extended reaction times were not required. It is likely that this was a function of the highly efficient stirring that was available in the 75 L reactor compared to the lab scale where magnetic fleas or overhead stirrers with a limited paddle size (due to the round bottom flask's dimensions) were used.

A comparison of the relative cost, based on reagents required, was completed comparing LAC 500.1, BLAC (used for dispersion work, Section 8.5) and a comparable CAB with high butyrate substitution. The formulation for the CAB was taken from the Kodak Eastman's patent WO 2006/116367A1, example 1 [48]. It is expected that the cellulose pre-treatment and work-up would remain largely unchanged between CE types with respect to the cost of materials. The cost comparison indicated that to date the relative production cost (based on materials only) of LAC and BLAC would be 2.65 and 1.75 times greater than a comparable CAB, respectively (Table 6-2). The increased anhydride content required to complete levulinyl-CE reactions was the main factor responsible for

the increased costs. Feedback was obtained from communication with the Dow Chemical Company who indicated several points to be addressed before levulinyl-CEs would become a commercial possibility:

- Reducing the reagent excess required to produce levulinyl-CEs, ultimately leading to a lower product cost.
- Recycling of LA and other reagents.
- Product colour.

LAC 500.1	Quantity (g)	Cost ($)	BLAC (RPa003K)	Quantity (g)	Cost ($)	CAB (HS-CAB-38)	Quantity (g)	Cost ($)
Cellulose	100.0	3.42	Cellulose	100.0	3.42	Cellulose	100.0	3.42
Acetic anhydride	568.0	26.51	Butyric anhydride	878.0	27.57	Acetic anhydride	121.0	5.65
Levulinic acid	898.0	35.92	Levulinic acid	309.0	12.36	Butyric anhydride	282.0	8.85
Sulfuric acid	1.3	0.04	Sulfuric acid	1.3	0.04	Butyric acid	182.0	6.73
						Sulfuric acid	4.3	0.15
Total	**1567.3**	**65.89**		**1288.3**	**43.39**		**689.3**	**24.80**

Table 6-2 Cost comparison of LAC 500.1, BLAC and CAB 100 g reactions (Sigma Aldrich, NZD).

In summary, the esterification chemistry employed to synthesis a LAC polymer was shown to be highly reproducible at scale. The tuneable incorporation of LA by esterification translated well from the laboratory scale to a pre-production pilot scale, indicating that the technology would scale to even larger commercial quantities. Based on the current technology an estimate of production cost was 1.75-2.65 times greater than a high butyrate substituted CAB.

7 Cellulose ester carboxylation

Incorporation of free carboxylic acid groups (carboxylation) onto the levulinyl-CE backbone was a key step in the development of this material into a water-based coating. The decision to use the acetone process as the method for producing aqueous levulinyl-CE dispersions (Section 8.1.3) meant that readily ionisable groups were required to be covalently bound to the polymer structure in order to form a self-stabilised aqueous polymer dispersion. One of the most common ways to do this is to incorporate carboxylic acid functionality along the polymer chain. Allen and Cuculo published a review regarding carboxylated cellulose derivatives and discussed many of the possible carboxylation methods [181]. The two most common commercially produced carboxylated cellulose derivatives are carboxy methyl cellulose (CMC) generated using an etherification process, and cellulose acetate phthalate produced by esterification of CA with phthalic anhydride. Three methods for producing a carboxylated levulinyl-CE were investigated:

- Levulinyl esterification of CMC.
- Secondary esterification of levulinyl-CEs with cyclic anhydrides.
- Incorporation of carboxyl functionality through the levulinyl ketone using alkoxyamines.

7.1 Acid number characterisation

The carboxylated CE derivatives developed during this project were characterised using two methods: NMR spectroscopy was used to confirm structural incorporation of the carboxylated species onto the CE chains and the level of incorporation was quantified by determining the acid number [182]. The acid number is an absolute measure of the free carboxylic acid groups per gram of material and was quantified by dissolving the carboxylated CE in a pyridine:acetone:water solution and titrating this solution against a KOH solution at room temperature. An acid-base titration curve was generated by monitoring the pH and the acid number was recorded as the inflection midpoint, reported in mg KOH/g.

7.2 Modification of carboxy methyl cellulose

CMCs are prepared by cellulose etherification following the Williamson ether synthesis [183] using chloroacetic acid and sodium hydroxide (Figure 7-1), typically generating the sodium salt of the carboxyl methyl cellulose, with a carboxy methyl DS of between 0.4 and 1.5 [183]. The commercial applications of CMCs range from the food to the oil industry, and in the coatings field they are used as rheology modifiers.

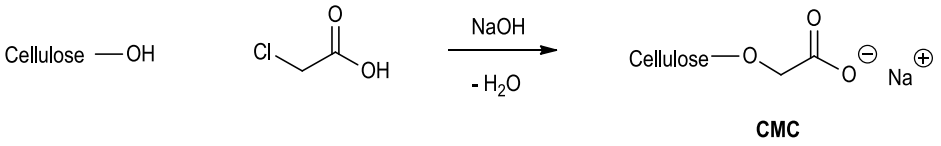

Figure 7-1 Williamson etherification of cellulose to generate CMC.

There have been a number of publications that discuss the generation of carboxy methyl cellulose esters (CMCEs) by the esterification of CMCs. Before esterification can take place, the CMC sodium salt must be protonated to form the free acid of CMC. To do this, the fibrous CMC powder is slurried in a weak sulfuric acid solution (2-10%) to generate the re-protonated form. This is then followed by solvent exchange with glacial acetic acid to remove the excess water, and then the protonated CMC can be esterified using conventional CE esterification chemistry to generate a CMCE. The Eastman chemical company has commercially produced CMCEs (CMCAB 641-0.2. and CMCAB 641-0.5), however, these products now appear to be discontinued. CMCEs have been discussed as a possible replacement for the standard organic solvent-soluble CEs for use in low VOC coatings [184].

Of the literature and commercial methods reviewed for the preparation of carboxylated-CEs, CMC ester modification to generate a carboxylated levulinyl-CE was the favoured technique. CMCs are a commercially available product with a relatively low cost of USD$ 0.60 per kg and are available in a range of carboxylation levels which make them a viable starting material for modification. However, when the esterification procedures that are described in the patent literature [182],[185] were used to produce a levulinyl-CMCE using the CMC at hand, generation of the desired product was unsuccessful. Formation of the CMC free acid proved to be difficult with the material used; instead of forming a slurry, the CMC was soluble in the aqueous sulfuric acid solution and

despite numerous attempts, a water-free, protonated CMC could be not produced. The water-soluble protonated CMC was, however, readily precipitated as a gel using ethanol, although subsequent solvent exchange failed to remove all of the residual water and ethanol from the swollen CMC gel. Esterification of the solvent-laden polymer with a vast excess of reagents did not generate the desired product and at this point, the focus of the project was shifted to developing alternative methods for generating a carboxylated levulinyl-CE.

7.3 Carboxylation using cyclic anhydrides

Generating a carboxylated CE from cellulose using a cyclic anhydride is a two-step procedure; a conventional CE is first generated and purified (with a proportion of free hydroxyl groups retained), then a secondary esterification takes place with a cyclic anhydride capping the remaining hydroxyl groups and generating a carboxylated-CE. Esterification with cyclic anhydride species occurs under base catalysed conditions where, upon reaction with cellulose, the cyclic anhydride ring opens resulting in a pendent carboxylic acid group as the sodium salt (Figure 7-2). Cyclic anhydride modified CAs have an increased solubility range [181] and in some cases are water-soluble as the acid salt [186]. The change in solubility properties between the free acid and its salt form is used for the basis of enteric coatings [187]. Commercially, this class of CE is limited to cellulose acetate phthalate, produced by both Eastman and Aquacoat as a coatings material in pharmaceutical applications.

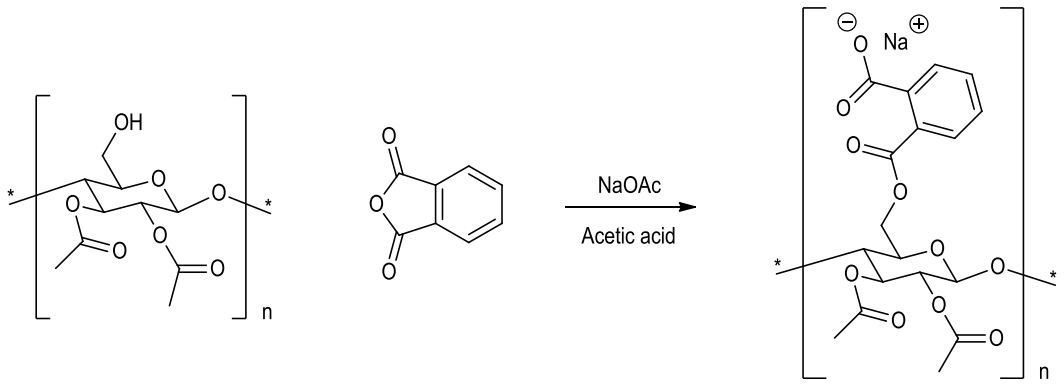

Figure 7-2 Synthesis of cellulose acetate phthalate.

Using commercially available CAB 553.04 as a model compound, both CAB phthalate and succinate were prepared using standard literature methods [186]. Phthalate and succinate were incorporated to an acid number

of 73 and 98 mg KOH/g respectively. The experimental outcomes of the reactions and the characterisation of the materials obtained, and their ability to form a stable dispersion, are discussed in the following chapter (see Section 8.4).

Using the same procedure, BLAC phthalate was also prepared. The starting BLAC material had a DS-Total of 2.64 and a DS-Lev of 1.45, thus a proportion of the levulinyl groups were selectively removed (59.2%) using hydrazinolysis to generate suitable free hydroxyl sites for phthalate incorporation (resulting in a DS-OH of 1.21). A BLAC phthalate was generated with an acid number of 104 mg KOH/g.

The generation of both CMCEs and cyclic anhydride modified CEs as methods for producing carboxylated CEs has two main drawbacks. The first being that both methods are two step processes; a modified cellulose polymer is generated and purified and this is then taken forward into a secondary modification step using a different set of reaction conditions, before being purified again. The use of a two-step process is undesirable as it increases production time and final material cost. The second drawback is the limited control of the acid number which could impact both the properties and the dispersion of the final product. The oxime carboxylation method (see below) was thus specifically designed for the levulinyl-CEs used in this project to overcome these problems.

7.4 Carboxylation via oximes

A novel method for carboxylating CEs, specifically targeting levulinyl-CEs was developed. By utilising the available ketone group on the levulinyl substituent an oxime link can be formed by reaction with an alkoxy amine. The technology is not limited to carboxylation; it is a general method for secondary modification of levulinyl-CEs and was used to incorporate short chain PEG groups into LBC as a method of internal plasticising, as discussed in Section 4.8.1.2.

An oxime is formed by the condensation reaction of the levulinyl ketone and the primary amine of the alkoxy amine [188]. The reaction proceeds through a carbinolamine intermediate and results in the formation of both E and Z isomers (Figure 7-3).

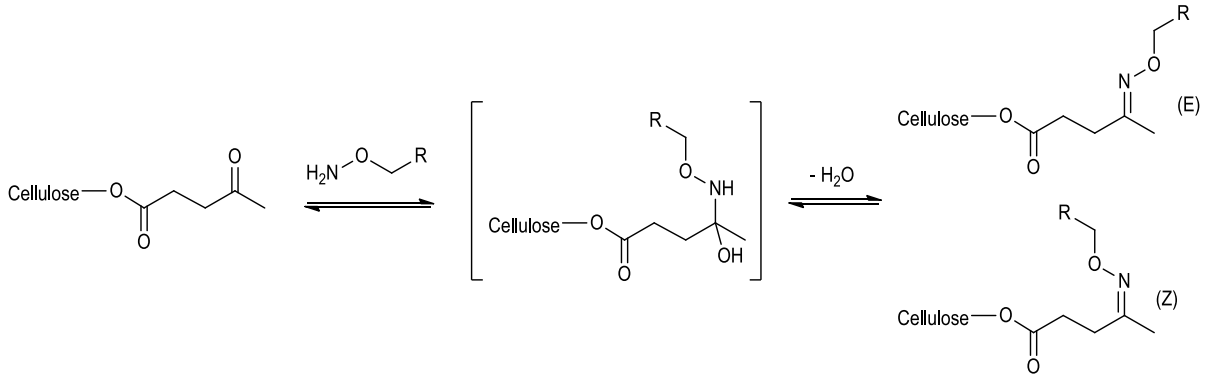

Figure 7-3 Oxime linking reaction.

Oxime linking allows for the modification of levulinyl-CEs under very mild conditions. The levulinyl-CE and alkoxy amine species are dissolved in an appropriate solvent and allowed to stir for two hours at room temperature, at which point the modified levulinyl-CE can then be recovered by solvent evaporation or precipitation. Carboxylation of the levulinyl-CEs for this project was performed using the *O*-(carboxymethyl)hydroxyl amine species **(9)** (Figure 7-4). It was recognised that **(9)** was an expensive reagent (NZD$ 1095 per 25 g, Sigma Aldrich) and it is unlikely that this would be acceptable for the long-term production of a commodity product.

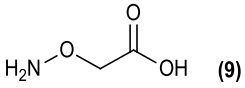

(9)

Figure 7-4 Alkoxy amine species (9)

To aid the NMR spectroscopic characterisation of the carboxylated levulinyl-CEs developed, a model levulinyl ketoxime compound **(10)** was synthesised by the reaction of isobutyryl levulinate and alkoxy amine **(9)** (Figure 7-5). The ^{1}H and ^{13}C NMR spectra for compound **(10)** were unambiguously assigned using HSQC spectroscopic data. On formation of the oxime linkage, the levulinyl ketone resonance (^{13}C δ 206.5 ppm) was lost and resonances appeared at ^{13}C δ 158.3 and 159.1 ppm (C-4; E and Z isomers respectively) consistent with formation of an oxime. The ratio of E:Z isomers was observed to be 3:1 which was assigned based on the

relative intensities for the levulinyl methyl resonances (C-5; ^{1}H δ 1.92 ppm for E, 1.90 ppm for Z) and literature data [189]. The resonance used as confirmation of incorporation of the alkoxy amine onto the BLAC structure was the C-6 methylene resonance at ^{1}H δ 4.59 ppm; this is consistent with the data reported by Liu *et al.* [190].

Position	^{1}H δ ppm	^{13}C δ ppm
1	-	172.8
2 E	2.54	30.3
2 Z	2.67	25.1
3 E	2.54	30.9
3 Z	2.61	30.1
4 E	-	158.3
4 Z	-	159.1
5 E	1.92	14.9
5 Z	1.90	19.7
6	4.59	69.7
7 E	-	175.1
7 Z	-	174.9
1'	3.86	70.7
2'	1.92	27.8
3'	0.93	19.0

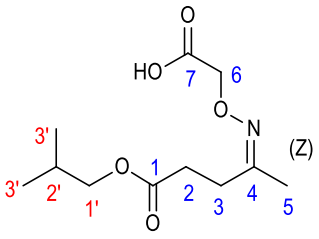

Figure 7-5 Compound (10) structure and NMR data.

NMR characterisation of BLAC modified by reaction with compound **(9)** displayed the characteristic ^{1}H NMR resonance at δ 4.56 ppm. ^{13}C NMR resonances were also observed at δ 69.8 ppm and approximately δ 173 ppm, corresponding to the alkoxy methylene group and the carboxylic acid resonance respectively. The oxime functionality was observed as a broad series of peaks centred at ^{13}C δ 158.0 ppm, with a corresponding reduction in the levulinyl ketone resonance. The ketone signal did not disappear entirely as not all of the levulinyl groups were capped. Characterisation of the carboxylated levulinyl-CEs by acid number showed that the incorporation of compound **(9)** was nearly quantitative, allowing very accurate control over the acid number for modification of levulinyl-CEs. The solvent chosen for the reaction was important, both for polymer and reagent solubility, however, use of the wrong solvent system resulted in side reactions. The reaction of BLAC with compound **(9)** was carried out in a 1:1 methanol:chloroform solution and unexpectedly resulted in the complete methylation of the carboxylic acid groups resulting in an acid number of 3 mg KOH/g. Incorporation of the oxime

species was confirmed by the characteristic resonance at ^{1}H δ 4.56 ppm (Figure 7-6) and the methylation was evidenced by a ^{1}H and ^{13}C NMR resonance at δ 3.74 ppm and δ 51.8 ppm respectively, as confirmed by HSQC.

Incorporation of carboxyl functionality onto BLAC resulted in an increase in the T_g (Table 7-1). With an acid number of 63 mg KOH/g, the T_g increased 14 °C from the parent BLAC material up to 92 °C. Allen and Cuculo discussed the affinity of cellulose derivatives functionalised with carboxylic acid groups towards hydrogen bonding and forming network structures [181]. It is therefore likely that the carboxylic acid groups were forming an associated network structure as a function of hydrogen bonding between the polymer chains, resulting in an increase in the T_g. This was further evidenced by methylation of the free carboxylic acid groups, removing the carboxylic acid hydrogen bond donor sites. The T_g of the carboxylated and methylated BLAC material was reduced to 72 °C, 20 °C lower than the carboxylated BLAC and 6 °C lower than the parent BLAC material. It is likely that the 6 °C reduction recorded for the methylated BLAC material in comparison to the parent BLAC, was a function of the methylated carboxyl species increased side-chain length, increasing the intermolecular distance between chains.

CT-x429-1	T_g (°C)
Parent material	78
Carboxylated (acid number 63)	92
Carboxylated and methylated	72

Table 7-1 T_g comparison of the parent BLAC material to the corresponding carboxylated species, and the carboxylated and methylated species.

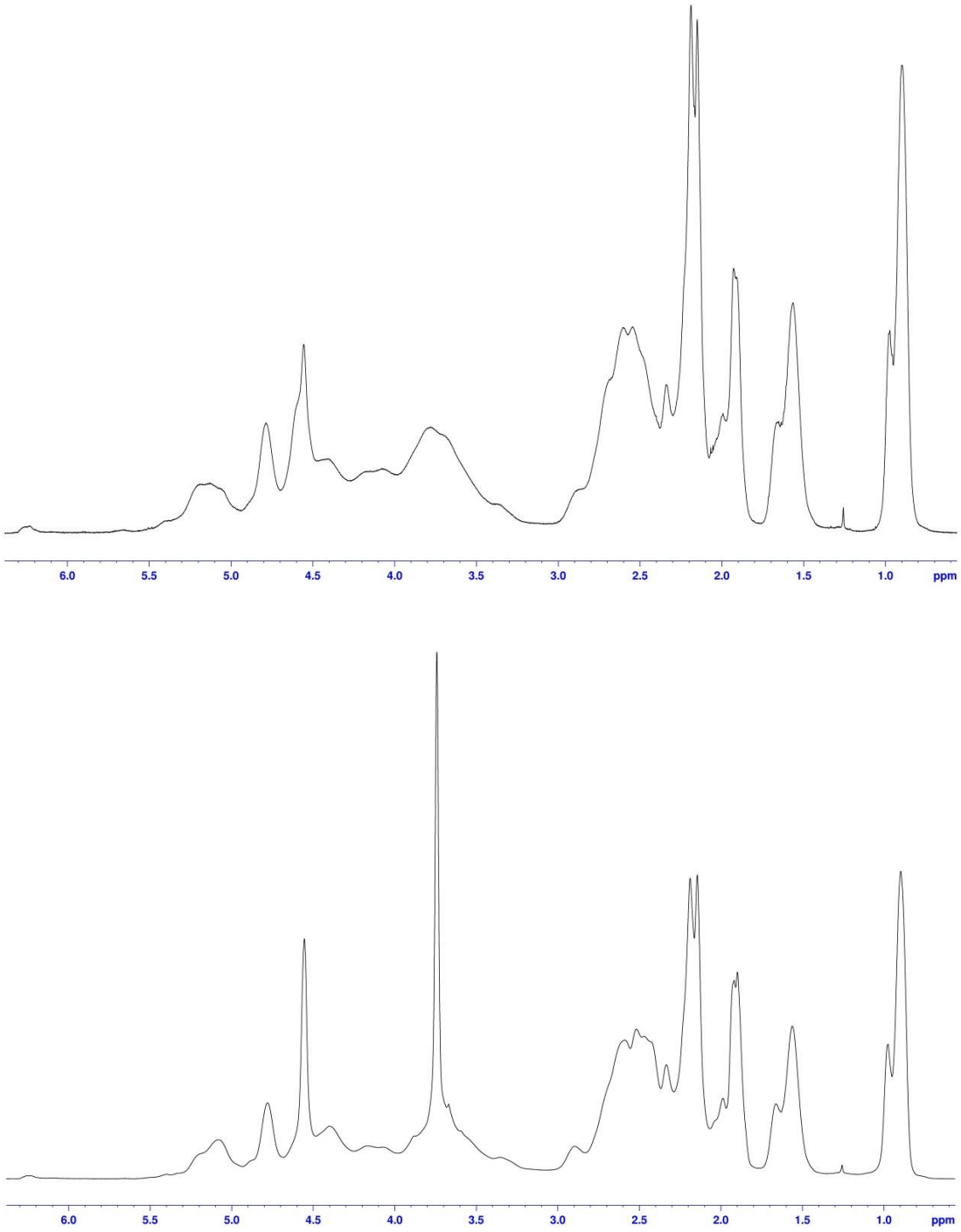

Figure 7-6 ^{1}H NMR spectra of carboxylated BLAC (top) and a carboxylated and methylated BLAC (bottom).

An important feature of carboxylation with the oxime linking technology was the ability to produce a CE with an accurate acid number as the oxime linkage forms near quantitatively. However, due to the high cost of the alkoxy amine reagent, an alternative, cheaper reagent would be required should this strategy be progressed. In

contrast, both CMCE and cyclic anhydride modified CEs are less precise in their acid incorporation. Generation of a levulinyl-CMCE would be a more cost-effective method and should be further investigated using different raw material sources.

One considerable advantage of the oxime carboxylation technology, specifically relating to polymer dispersal using the acetone process, was the reduction in the total number of processing steps required to a pseudo one-step process. Using an appropriate solvent system for both carboxylation and dispersal removes the need for a purification and second dissolution step which is required for the synthesis of CMCEs and cyclic anhydride modified CEs. This reduces both production time and costs. However, for this project, acetone was chosen as the dispersal solvent and, as the oxime reaction cannot be completed in acetone (as a function of the free ketone), an extra purification and dissolution step was required. Future work would involve screening suitable dispersion solvents that the oxime reaction could be carried out in.

8 Water-based levulinyl-CE dispersions

8.1 CE water-based dispersion techniques

The last step to develop a water-based levulinyl-CE binder was to produce a stable water-based dispersion, from which a uniform coherent film could be cast at room temperature. The main challenge faced when producing a CE dispersion, or latex, is the dispersal of a preformed polymer to generate a stable colloid. Unlike conventional acrylic waterborne paint binders which are *in situ* emulsion polymerised to produce a stabilised, high-molecular weight polymer dispersion (discussed in Section 1.3.1), CEs are preformed polymers and have to be dispersed as such. There are several methods for forming water-based nanoparticle dispersions of preformed polymers [191, 192], although only the methods relevant to CE dispersions are discussed here:

- Spontaneous emulsification.
- Preformed polymer emulsification and solvent extraction by vacuum distillation.
- The acetone process.

8.1.1 The ouzo effect

The ouzo effect is a term used to describe the spontaneous formation of a stable emulsion of nano droplets (the dispersed phase) by precipitation from a ternary system [193]. The mechanism is based on a narrow metastable region existing between the spinodal and binodal boundaries; the ouzo region. To generate a stable emulsion or dispersion of nano-sized droplets or particles giving rise to the ouzo effect, low solute concentrations and high precipitation dilutions are required. This precipitation mechanism is a facile, low-energy method of producing a stable dispersion of nanoparticles. It can be used to generate nanoparticle dispersions of preformed polymers including CEs. These are generated by adding an anti-solvent (commonly water) to a dilute polymer solution in a miscible solvent. A spontaneous precipitate results forming a nano dispersion with a narrow particle size distribution (PSD) [194]. This methodology does not require specialised equipment or stabilisation media, however, these can be employed. There are several different methods that promote polymer insolubility and nano precipitation based on the ouzo effect [191], all utilising the same general principles described above:

- Salting out - the addition of a saturated electrolyte solution to the polymer solution to effect a nano precipitation.
- Nano precipitation - a dilute polymer solution is prepared in a water-miscible, low boiling point solvent (e.g. acetone, THF or ethanol) and an anti-solvent (usually water) is added directly to the polymer solution which results in precipitation.
- Dialysis - a dilute polymer solution is prepared using a high boiling point, water-miscible solvent (e.g. DMAc, DMF or DMSO) and then dialysed with an anti-solvent, resulting in nano precipitation.
- Supercritical fluid technology - dissolution of the polymer in a supercritical fluid (e.g. CO_2), followed by expansion of the supercritical fluid into water results in the formation of a nano dispersion.

Nano dispersions of CEs have been prepared by a number of groups using both nano precipitation and dialysis technology to generate an average particle size typically in the range of 60-400 nm [195-197]. Depending on the CE and the conditions used to generate the nanoparticles, the morphology ranged from spherical to bean shaped [195, 196].

Spontaneous emulsification described by the ouzo effect is dependent on the polymer solution concentration and viscosity. Heinze *et al.* [195] plotted a concentration versus reduced viscosity [relative viscosity/polymer concentration] curve showing an inflection point assigned as the critical overlapping concentration. This point described the maximum polymer concentration where a uniform (narrow particle size distribution) nano dispersion can be produced. The major drawback of this technology is the low polymer solution concentration required to generate nanoparticles, which results in dispersions that have a low percentage of polymer in the final dispersion (i.e. low solids content). Although using such techniques that display the ouzo effect can generate a nanoparticle polymer dispersion efficiently, this process was unsuitable for preparing a polymer dispersion for an architectural coatings application due to the low final solids/polymer content of the dispersions.

8.1.2 Preformed polymer emulsification

The earliest cited literature reference for a water-based CE system was in a 1965 Eastman Kodak patent that described the use of water-based CAB emulsions as wood lacquers and filler binder as an alternative to nitro cellulose lacquers and linseed oil-based fillers [198]. The CAB was emulsified generating a stable O/W emulsion where the dispersing solvent (immiscible in water) was not removed, resulting in an emulsion containing up to 46 wt% VOC. It was reported that when the CAB emulsion was applied to a wooden substrate, a coherent film was formed upon drying.

More recently, CE dispersions have been prepared by emulsification and subsequent removal of the organic solvent to yield low VOC dispersions. The generation of a low VOC CE dispersion by this method involves dissolution of the CE in a water-immiscible volatile solvent with surfactants [199] or colloidal stabilisers [200], which are used to stabilise the emulsion once formed. A crude emulsion (large particle size) is generated and then passed through a high energy homogeniser, commonly a microfluidiser, reducing the particle size and narrowing the PSD. Vaithiyalingam *et al.* demonstrated that a constant average droplet size of 300 nm and a PSD of 216-401 nm [200] was achieved after five passes through a microfluidiser. Vacuum distillation was then used to remove the volatile solvent, leaving an aqueous dispersion with a solids content of up to 18.1 wt% [201]. Quintanar-Guerrero demonstrated that it is possible to produce a latex with a solids content of > 30% w/v without the use of a homogeniser, employing partly water-soluble solvents and using conventional high-speed stirrers [202]. Water dispersed CEs generated using this technique have been investigated for use in pharmaceutical and automotive coatings applications. Aquacoat CPD is a commercially available CE dispersion used for pharmaceutical coatings based on CA phthalate, with a solids content of 30 wt% [203]. Quintanar-Guerrero indicated that commercial CE dispersions such as Aquacoat are produced using an emulsion-solvent stripping process similar to what has been discussed here [202].

A patent published by PPG teaches a method for preparing water-based CAB dispersions using emulsification and solvent removal. These dispersions were exemplified for use as a low-bake acrylic automotive refinishing additive for metal flake orientation, although the CE dispersions were not exemplified as a primary coating

system [201]. In addition to automotive coatings applications, both CA and CAB latexes have been used as pharmaceutical coatings for controlled drug release [199, 200]. It was suggested that an advantage of using water-based CE dispersions as pharmaceutical coatings was the reduced risk of ingesting toxic organic solvents or monomer residues, which may be present from alternative polymeric systems. However, high plasticiser loadings were required (up to 160 wt% of the CA) to form a coherent continuous film from the CE dispersions [199].

8.1.3 The acetone process

The acetone process was developed as a method for generating a self-stabilised water-based polyurethane (PU) dispersion. The conventional emulsion polymerisation techniques could not be used to generate PU dispersions, as the PU chemistry uses isocyanate monomers, which react rapidly with water, and therefore the acetone process was developed as a method to disperse preformed PU*s*.

In the acetone process the PU is polymerised in the presence of acetone, which acts as a non-reactive diluent. A key feature of the acetone process is the modification of the PU backbone with a series of ionisable groups creating an ionomer [192, 204]. A water-based dispersion is then generated using the PU ionomer. The ionic groups self-stabilise the dispersed polymer particles and therefore surfactants and other stabilising media are not required.

The mechanism for generating a polymer dispersion using the acetone process is complex. Dieterich describes the mechanism of the PU acetone process and its associated characteristics, represented in Figure 8-1 [192, 205]. Firstly, the acetone solvated PU ionomer is activated by the addition of a counter-ion. Because of this charge incorporation the ionic centres may now self-associate, effectively increasing the molecular weight of the PU species in solution. The slow addition of water (anti-solvent) to the acetone-based polymer solution results in several observable changes that can be attributed to the changing solubility parameters of the continuous phase. An initial sharp decline in viscosity is observed, attributed to water reducing the ionic interaction between the

polymer chains, resulting in an optically clear solution. Further water additions induce a second rise in viscosity, associated with the initial stages of polymer collapse as polymer-polymer interactions become favoured. The continued addition of water decreases the solubility of the polymer in the continuous phase, resulting in precipitation. As the polymer-polymer interactions become increasingly more favoured over the polymer-solvent interactions, this ultimately results in polymer collapse [206] and precipitation generating a cloudy dispersion of marked lower viscosity. During this process the hydrophilic ionic groups migrate to the surface of the polymer particle while the hydrophobic polymer core collapses inwards. Strong inter-particle repulsive forces are induced by the migration of the ionic centres to the particle surface, where a diffuse electrical double layer of ionic centres and counter ions has been formed. The charged surface of the polymer particles prevents particle interactions and generates a stable dispersion.

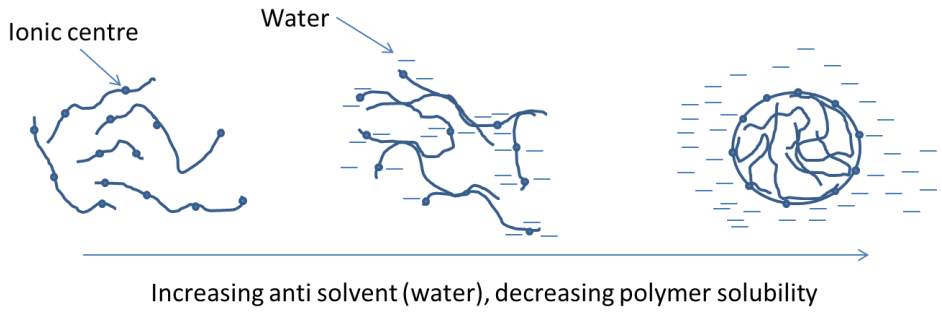

Figure 8-1 Graphical representation for the nano dispersion and precipitation of a polymer.

During the precipitation process, the particle size increases until the particles reach their critical charge density stabilising them towards further growth. Zhang *et al.* reported that for a high molecular weight polymer there is no barrier to nucleation, and particle growth follows a model of initial nucleation followed by aggregation to grow particle size [207]. However, particle aggregation can occur between two smaller particles that have not yet reached the critical size and size to charge ratio. A second mechanism of particle growth can occur between a charge stabilised particle and a unimer (single collapsed polymer chain). Here the repulsive forces are significantly reduced and aggregation can occur. The combination of smaller non-stabilised particles leads to a larger PSD. The average particle size of a polyurethane dispersion can range from 10-5000 nm [192] but more commonly from 40-200 nm [208]. Two of the advantages the acetone process has, in comparison to emulsifying a preformed polymer are, firstly, the solvents used are relatively non-toxic compared to the chlorinated solvents

commonly used to emulsify polymers. Secondly, the incorporation of self-stabilising ionic centres limits the overall complexity of the formulation by reducing the need for compatible surfactants and other stabilising media. In addition, only simple dispersing equipment is needed.

Only one example using the acetone process to form a cellulose ester dispersion has been reported [209]. The process used a carboxylated CAB with an acid number of 60 mg KOH/g, dissolved in a polar water-soluble solvent, with the addition of a coupling solvent. An aqueous amine solution (neutralising 20% of the carboxylic acid functionality) was added under mild agitation and heating, and the solvent then distilled under reduced pressure. This generated a nano dispersion with a solids content of 20 wt%. The CAB dispersions were exemplified for use in a water-based automotive coating as an additive to enhance flow and levelling properties, as well as metal flake orientation, but were not described as a potential resin coating in their own right. Overall it was believed that the acetone process would provide an ideal mechanism to generate levulinyl-CE dispersions.

8.2 Criteria for the water-based dispersion of BLAC

The formulation of a water-based CE into an architectural coating, with the CE as the main binding agent, is a novel process. The target of this project was to develop a water-based levulinyl-CE dispersion that could be formulated and used in an interior architectural coating where the levulinyl-CE dispersion forms the primary binder component of the coating. The target dispersion criteria were:

- Dispersion particle size of < 500 nm.
- VOC of < 50 g/L (primarily aiming for the dispersion to have 0% VOC).
- Solids content of > 25 wt%.
- Dispersion stability of > 4 weeks at room temperature.
- A dispersion which coalesces at room temperature.
- A dispersion which accepts a mill base and can be formulated into a low-sheen paint.

8.3 Dow dispersing technology

As a direct result of collaboration with our industry partners an exciting opportunity arose to trial the Dow chemical company's proprietary BLUEWAVE[9] water dispersion technology. The BLUEWAVE technology is commercially sensitive and therefore detailed information about the equipment and processing was not disclosed. The BLUEWAVE process is known to be based on direct water dispersion of a polymer from the melt phase and has been shown to produce excellent results in generating water dispersions of hydrophobic polymers such as polystyrene.

Two levulinyl-CE samples were sent to Dow for dispersion; these samples were LAC 500.1 (discussed in Section 6) and LAC 500.1 which had been modified with PEG groups using the oxime chemistry discussed in Section 7.4. A sample of the lead dispersion produced by Dow was returned, but unfortunately it was unclear which LAC 500.1 sample had been used to generate the dispersion. Also, no dispersion formulations or methods were divulged due to the sensitive nature of the technology. It was immediately evident that during the dispersal process using the BLUEWAVE technology, significant degradation of the levulinyl-CE had occurred. The LAC dispersion had a strong acetic acid aroma indicating hydrolysis of the ester groups had occurred, and the polymer had coloured significantly which was also an indication of significant degradation. The BLUEWAVE technology is a high temperature process and this would have likely caused the observed ester hydrolysis and polymer degradation. A portion of the LAC was purified from the material dispersed by the Dow BLUEWAVE technology by distillation of the continuous phase. The polymer that was recovered was insoluble in a wide range of solvents, indicating significant alteration to the parent structure. The insolubility, strong aroma of acetic acid and visibly blackened solution all pointed to significant degradation of the levulinyl-CE.

[9] Due to the collaboration with Resene Paints Ltd, the opportunity arose to engage with their industry contacts and trial the BLUEWAVE technology that would have been otherwise unavailable. The author acknowledges Dr Mark Glenny and Mr Colin Gooch for their contribution with this collaboration.

The properties of the dispersion generated by Dow using their BLUEWAVE technology are given in Table 8-1. Particle size analysis of the dispersion indicated a bi-modal distribution with an average particle size of 3.8 µm and a PSD range of 335 nm-62.63 µm (Figure 8-2). Of the measured sample, 80.6% was larger than 1 µm and this accounted for the sedimentation that was observed when the sample was allowed to stand for an extended period of time. The solids content was 6.71 wt% and a coherent film could not be cast directly from the dispersion. The morphology of the dispersed LAC particles was imaged using microscopy, where an elongated particle shape was observed (Figure 8-3). It was likely that when the molten polymer was introduced into the water phase there was insufficient time for a spherical polymer droplet to form before solidifying.

Based on the results of the sample that was returned from Dow, the BLUEWAVE technology was unsuccessful and did not produce a water-based levulinyl-CE dispersion to meet the criteria set out for this project. Unfortunately, further levulinyl-CE dispersion trials using the BLUEWAVE technology were not possible, and the former therefore the acetone process became the primary focus of the project.

Dow dispersion	
Polymer	LAC 500.1
PSD (µm)	3.819 ± 0.496
Solids content (wt%)	6.71
Stability at RT	> 4 weeks
Film casting	No

Table 8-1 Dow BLUEWAVE dispersion.

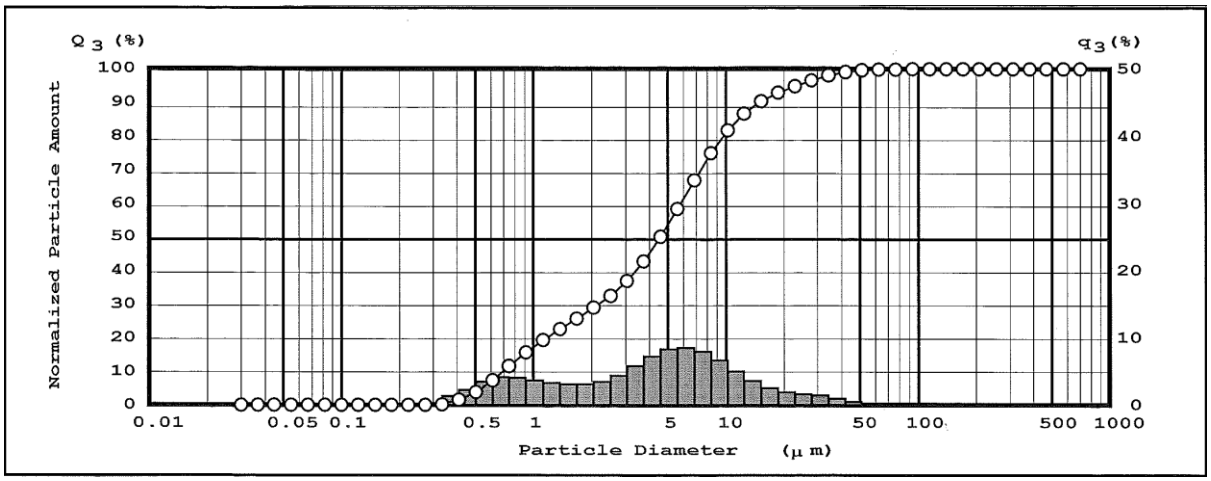

Figure 8-2 Particle size distribution for a LAC dispersion generated by the Dow BLUEWAVE dispersion.

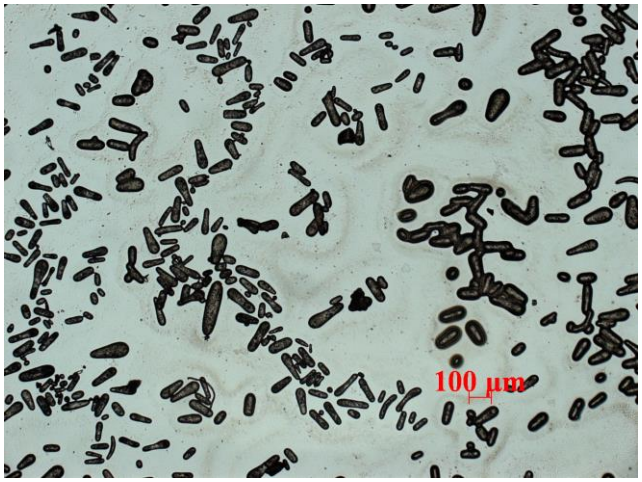

Figure 8-3 Micrograph of Dow BLUEWAVE dispersion.

8.4 Evaluation of CAB analogues

Eastman patent US2005/0203278 A1 [209] discusses the generation of waterborne CAB nano dispersions based on the PU acetone process. The patent describes the use of a variety of water-soluble solvents to generate CE dispersions, with ketone solvents favoured in the examples disclosed. One of the examples (Example 7) details a method for the generation of a water-based CAB dispersion using acetone as the dispersing solvent; an example thought to be most relevant to the project and therefore was replicated to evaluate the method.

The carboxylated CAB used in example 7 (CMCAB 641-0.5) was no longer commercially available, nor was the data sheet detailing this CAB's properties (DS, MW, T_g). The patent referred to an Eastman company report No. GN-431A from February 2003, but Eastman Limited would not release this document when contacted. Based on available literature data [182, 184], the CMCAB 641-0.5 material was likely to be an esterified carboxyl methyl cellulose (CMC) with an acid number of 60 mg KOH/g. Therefore, a similar carboxylated CAB analogue was synthesised and used to test this dispersion procedure.

A commercially available CAB (CAB 553-0.4, Table 8-2) was chosen as an appropriate analogue for two reasons. Firstly, there were sufficient free hydroxyl groups (DS-OH 0.9) to introduce sufficient carboxyl

functionality, that is, to give an acid number of between 10 and 150 mg KOH/g. Secondly, based on a series of experiments it was postulated that a high butyrate content would provide a level of hydrophobic character necessary for dispersion stability.

CAB 553-0.4	
DS-But	2.0
DS-Ac	0.1
DS-Total	2.1
T_g (°C)	136
Molecular weight (M_n g/mol)	20000

Table 8-2 CAB 553-0.4 commercial specifications.

Following the carboxylation method of Malm *et al.* [186], phthalate and succinate derivatives of CAB 553-0.4 were prepared separately by reaction with the appropriate cyclic anhydride. The maximum theoretical acid number that could be achieved using CAB 553.-0.4 was 114.8 and 127.3 mg KOH/g for the phthalate and succinate analogues, respectively. These values fall within the range specified in the patent as suitable for the dispersion of CABs. Incorporation of the phthalate moiety was evidenced by the signals at ^{1}H δ 7.39-8.05 ppm and ^{13}C δ 131.0 ppm attributed to the aromatic portion of the molecule. For the CAB derivative substituted with succinate functionality the incorporation of this functional group was evidenced by signals at ^{1}H δ 2.00-3.05 ppm and ^{13}C δ 28.6 ppm. These resonances did overlap with spectral data for the acetate methyl and butyrate α-methylene (δ 1.85-2.40 ppm), however, an HSQC experiment clearly identified the additional correlating signals of ^{1}H δ 2.00-3.05 ppm and ^{13}C δ 28.6 ppm that were new to the polymer structure compared to the parent CAB starting material.

The introduction of this third substituent on the cellulose backbone was additionally evidenced by a marked broadening of the proton and carbon resonances compared to the CAB starting material. This is consistent with the increased diversity of potential anhydroglucose monomers; each AGU can now be hydroxy, acetate, butyrate or succinate/phthalate modified (27 possible combinations for a non per-esterified CAB, and 64 possible combinations for the succinate or phthalate modified CAB). Molecular weight characterisation by SEC was not possible due to an observed shift in elution time which was postulated to be a function of the polarity of the

cellulose polymer (discussed in Section 3.9.2.2). The succinate and phthalate modified CAB 553-0.4 were calculated to have acid numbers of 97.5 and 72.7 mg KOH/g respectively. The difference in acid numbers recorded for these two carboxylated CABs was due to the differing level of incorporation; a result of the succinate being a smaller less sterically hindered molecule, in comparison to the bulkier more rigid phthalate group, and was therefore incorporated to a greater extent.

A dispersion was generated with the succinate derivative of CAB 553-0.4 following the procedure given in example 7 in patent US2005/0203278 A1 [209]. Similarly, a second dispersion using the CAB 553-0.4 phthalate derivative was generated following the same literature procedure. The dispersion process in both cases used acetone as the water-miscible dispersing solvent and propylene glycol n-butyl ether (PnB) as the coupling solvent. Table 8-3 compares data for the two dispersions to the reported literature values. For a comparable solids loading a similar PSD was recorded for the succinate derivative, however, the phthalate moiety produced a significantly larger PSD. It is interesting that this change to the PSD showed an inverse relationship to the acid number for the synthetic derivatives here. It is difficult to comment on the literate values, but it is likely this is a different parent CAB to what was used here. Neither the succinate or phthalate CAB dispersions produced a coherent film when casting the water dispersions on to a glass plate, but instead generated clear, colourless, highly brittle, cracked films (shown in Figure 8-4). Based on the results here, it seems very unlikely that the CAB dispersion reported in this key literature would be film forming. This is possibly why the only exemplification of this technology was as a water-based automotive re-finishing additive.

	Acid number (mg KOH/g)	PSD (nm)	Solids (wt%)
Example 7	60.0	131	19.8
CAB succinate	97.5	199 ± 248	21.6
CAB phthalate	72.7	483 ± 176	21.2

Table 8-3 Comparison of dispersion properties from patent US2005/0203278 A1 and synthesised CAB succinate and phthalate.

Figure 8-4 Films cast from CAB succinate and phthalate dispersions.

SEM images of the two dispersions prepared here demonstrated that the particle shape was roughly spherical, as expected, and a representative image is shown in Figure 8-5. Particle size dimensions obtained from the SEM also confirms the PSD data obtained from the laser light scatterer. In summary, it was possible to replicate the example method (7) of patent US2005/0203278 A1 [209], and using the synthetic derivatives manufactured in this work, satisfactory dispersions could be generated. The use of this methodology with acetone as the water-miscible dispersing solvent was utilised throughout the rest of this investigation.

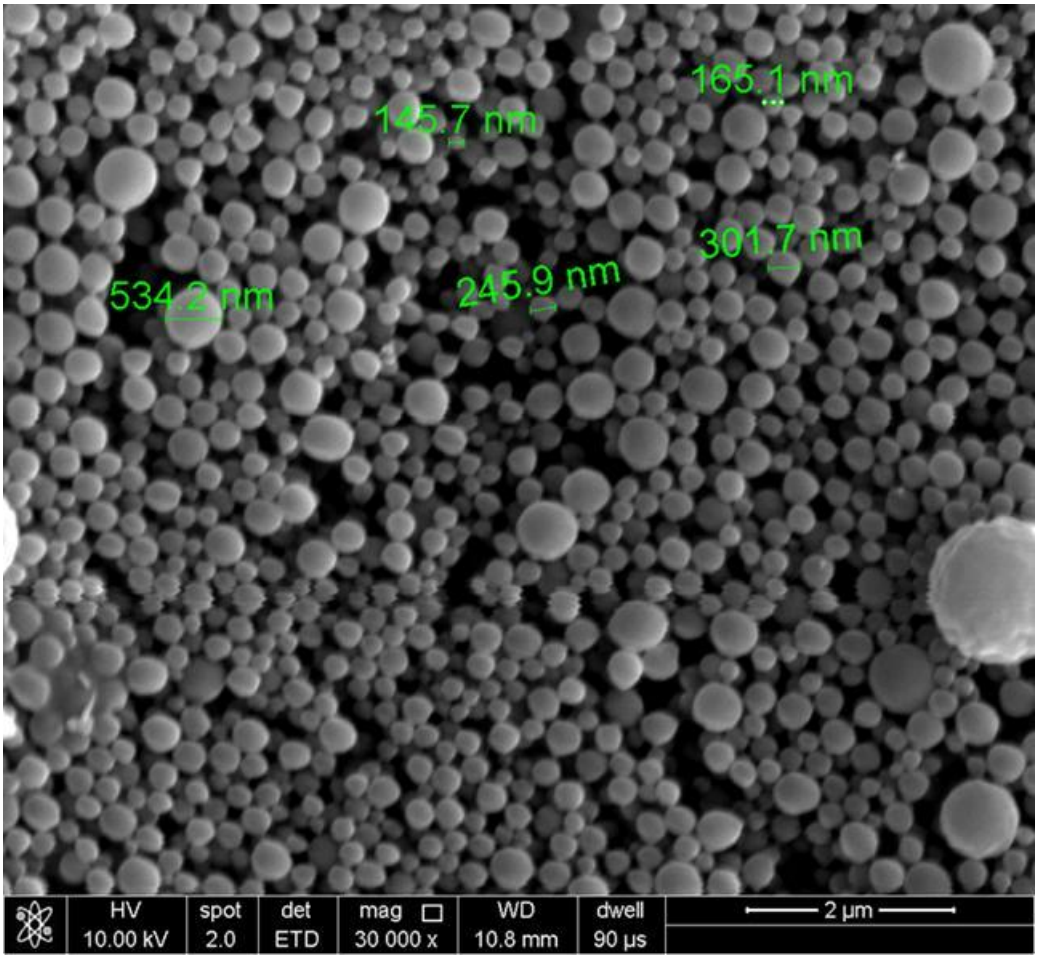

Figure 8-5 SEM micrograph of the particles recovered from a dispersion of CAB 553-0.4 phthalate.

8.5 Dispersions of carboxylated BLAC by the acetone process

Experimental work was completed using BLAC (Table 8-4), however, in several dispersion examples, LAC was used and will be indicated when relevant. Low and high levulinyl content BLACs (DS-Lev 0.35 and DS-Lev 1.24 respectively) were produced for the dispersion work, and these polymers were carboxylated using *O*-(carboxylmethyl)hydroxyl amine. The DS-Lev 0.35 BLAC was carboxylated to an acid number of 32 mg KOH/g while the DS-Lev 1.24 material was carboxylated to an acid number of 100 mg KOH/g and 63 mg KOH/g.

DS-Lev	DS-But	DS-Ac	DS-Total	T_g (°C)	Molecular weight (M_p g/mol)	Acid number (mg KOH/g)
0.35	2.23	0.34	2.92	88	17500	32
1.24	1.05	0.44	2.73	78	15000	100 and 63

Table 8-4 Carboxylated BLAC specifications.

8.5.1 Dispersion methodology with varying acid number

This section details how it was determined that for carboxylated BLAC with different acid numbers, a change to the dispersion method was required to effect a stable dispersion of suitable PSD. BLAC samples were modified to contain low (32 mg KOH/g), medium (63 mg KOH/g) and high (100 mg KOH/g) acid numbers (Table 8-4) as the examples for dispersion experiments. The initial methodology was based on what was learnt from replicating example 7 of patent US2005/0203278 A1 [209]. For all BLAC samples, an anionic self-stabilised polymer was dispersed into an aqueous continuous phase using acetone as the water-miscible solvent. Coupling solvents were not used in the BLAC dispersion formulations.

It became evident that when using BLAC samples with different acid numbers, a change in the dispersion methodology was required. Listed below are the three dispersion methods used and processing observations relating to each of the carboxylated BLAC species (high, medium and low acid number). All crude dispersions

were concentrated using reduced pressure to generate solvent free or low VOC water-based levulinyl-CE dispersions.

- A 16.1 wt% solution of BLAC with an acid number of 100 mg KOH/g was prepared in acetone. An amine was added to neutralise 28% of the carboxyl functionality, which caused an increase in the solution viscosity. The organic solution was maintained at 30 °C with gentle stirring and water was then added dropwise at the rate of 21 mL/min. The initial addition of water caused a reduction in the viscosity of the solution, although with further additions of water, an increase in viscosity was noted. With further additions of water the solution became cloudy and a rapid decrease in viscosity with concomitant precipitation into a two phase system occurred. These subtle changes are consistent with the behaviour described for generating a PU dispersion [192]. This methodology generated a carboxylated BLAC dispersion with an average particle size of 670 ± 140 nm.
- A 16.1 wt% solution of BLAC with an acid number of 63 mg KOH/g was prepared in acetone. An amine was added to neutralise 44% of the carboxyl functionality, and an associated increase in solution viscosity was observed. The organic solution was then added dropwise to vigorously stirred water, resulting in rapid polymer precipitation. A milky dispersion with a characteristic blue tinge was generated indicating that a dispersion of nano particles had been generated. This methodology generated a carboxylated BLAC dispersion with an average particle size of 420 ± 170 nm.
- An 18 wt% solution of BLAC with an acid number of 32 mg KOH/g was prepared in acetone and 57% of the carboxyl functionality was neutralised with an amine. Again there was an associated increase in polymer solution viscosity, but also partial polymer insolubility in the organic phase was noted. The addition of 3% water to the polymer acetone solution caused a decrease in viscosity and re-dissolved the polymer, reforming a homogeneous solution. An equal volume of the BLAC acetone solution and water was then brought together at a T-mixer (see Section 10.1.15, Figure 10-5) interface from separate streams using a constant flow rate of 5 mL/s. The resulting precipitate was collected in a round bottom flask from the outlet. This method of dispersing a carboxylated BLAC generated a dispersion with an average particle size of 180 ± 420 nm.

For the carboxylated BLAC materials used here, a lower acid number necessitated an increasingly rapid method of precipitation in order to produce a nano particle dispersion. This was attributed to the need to limit the particle growth phase as the acid number is reduced; particle growth is controlled by the charge density of the diffuse electrical double layer surrounding each polymer particle, and once a particle has reached a critical size the surface charge density stabilises the particle against aggregation (see Section 8.1.3). In addition, it is also likely that particle aggregation is a function of the changing solubility parameters of the continuous phase. While the continuous phase will still partly solubilise the polymer, the particles will be in a softened "sticky" state. This will likely promote aggregation of particles which have not reached the critical charge stabilising density. Rapidly changing the solubility parameters of the continuous phase will limit the duration of the growth phase. Reducing this growth phase to less than the time needed for particle aggregation to occur, by changing the solubility parameters of the continuous phase, rapidly freezes particle growth and particle size becomes growth limited.

Based on the argument postulated above it is possible to rationalise why a different mixing protocol was required for the three different carboxylated BLAC materials. In the conventional acetone process, water is slowly added to the acetone-polymer solution. This process generates a slow change in the continuous phase's composition from a 100% acetone to a 1:1 acetone:water solution which in turn effects a slow change in the solubility of the polymer in solution. As a result this gives a long growth phase, prolonging polymer solubility which promotes particle aggregation. Therefore, dispersions of carboxylated BLAC produced using the conventional acetone process methodology required an increased charge density (provided by an acid number of 100 mg KOH/g) to stabilise the nanoparticle dispersion and limit aggregation. Using this addition methodology with a carboxylated BLAC with an acid number of less than 100 mg KOH/g, the charge density was not great enough to stabilise the nanoparticles during the extended growth phase and resulted in large aggregates of > 1 μm.

For the dispersions generated from carboxylated BLAC with an acid number of 63 mg KOH/g, a shortened growth phase was achieved by the reverse addition of the organic acetone-polymer solution into the water phase (anti-solvent). The acetone-polymer solution was added dropwise to the anti-solvent slowly producing a 1:1 acetone:water solution. Every drop of polymer solution added to the anti-solvent resulted in rapid BLAC

precipitation, thereby limiting the growth phase. Addition of the BLAC solution to the anti-solvent permits the acetone to rapidly disperse into the water and away from the precipitating particle, thereby freezing particle growth. As a function of the reduced growth phase, less charge density was required to stabilise the nanoparticles until the continuous phase no longer promoted particle aggregation. For a carboxylated BLAC with an acid number of less than 63 mg KOH/g, insufficient charge density was present to stabilise the particle through the growth period and aggregation occurred. Although the period for the growth phase was reduced, the limiting factor for this process relied on the diffusion of acetone into water. Without an effective method of mixing, the localised transport of acetone away from the precipitating carboxylated BLAC particle to the bulk continuous phase was not rapid enough to prevent particle aggregation.

To produce a nanoparticle dispersion of carboxylated BLAC with an acid number of 32 mg KOH/g, following the argument above, rapid mixing was required at the point where the acetone-polymer solution and anti-solvent were brought together, and therefore a high flow rate T-mixer was employed. This method further reduced the length of time that particle growth could occur by introducing rapid mixing of the polymer solution and anti-solvent, thereby very rapidly generating a continuous phase where the polymer particle was insoluble, and freezing particle growth. The high mixing rate induced at the mixing head facilitated transportation of the acetone away from the precipitating particle into the bulk continuous phase. This method of rapid precipitation further reduced the particle growth phase in comparison to the reverse addition acetone process (discussed above) and less charge density was therefore required to stabilise the polymer nanoparticles during this time. In effect, shortening the growth phase by increasing the rate of precipitation means less charge density was required for particle stabilisation.

Whereas utilising the literature methods (US2005/0203278 A1 example 7) was applicable for carboxyl-functionalised CABs, this method did not translate directly to the BLAC derivatives carboxylated with *O*-(carboxylmethyl)hydroxyl amine. Dispersion of these carboxylated BLAC species, following this literature method, often resulted in particle aggregation and average particle sizes of > 1 μm. Carboxylated BLAC required 66% more carboxyl functionality (acid number 100 mg KOH/g) than the CAB example (acid number 60 mg KOH/g)

given in the patent literature [209] to form a nano dispersion. This is possibly a function of the hydrophilicity of the polar keto groups which are present in the levulinyl-CE. The more hydrophobic the polymer is, the faster polymer collapse and precipitation will occur with the addition of water. It is therefore possible that due to the water affinity of the carboxylated BLAC species, the precipitation process was slower with an extended particle growth phase which required greater surface charge density to maintain a stable dispersed particle.

Once a nanoparticle levulinyl-CE dispersion has been generated, the dispersion must remain stable for an extended period of time to be viable as a water-based coating. Stability testing was carried out on the BLAC dispersions generated here by measuring the particle size distribution at the beginning and the end of a four week period, and also by visually monitoring the dispersion over this time. As illustrated in Table 8-5, an increase in the dispersion stability was observed with decreasing acid number. Dispersions produced with acid numbers of 100 and 63 mg KOH/g failed the four week test, where the mechanism of destabilisation for these samples was by gelation and syneresis (discussed further in Section 8.9). PSD measurements showed that for the dispersion produced using carboxylated BLAC with an acid number of 32 mg KOH/g, the average particle size had increased by 41 nm, but still remained within the desired limit (< 500 nm). The poor long-term stability of the carboxylated BLAC dispersions that had been generated with acid numbers of 63 and 100 mg KOH/g was attributed to the increased carboxylic acid content, where increased water affinity led to an increased rate of gelation.

Acid number (mg KOH/g)	PSD (nm)	PSD after 4 weeks at RT (nm)
32	117 ± 279	158 ± 233
63	695 ± 372	Gelled
100	669 ± 140	Gelled

Table 8-5 Behaviour of carboxylated BLAC dispersions on storage.

For the remainder of the project the carboxylated BLAC material with an acid number of 32 mg KOH/g was progressed using the acetone process and the T-mixer to generate the carboxylated BLAC dispersions. This material and dispersion technique had achieved two of the desired criteria: particle size and stability for 4 weeks at room temperature. A further benefit of reducing the acid number required to formulate a BLAC dispersion was

cost. The *O*-(carboxymethyl)hydroxyl amine reagent used to carboxylate the BLAC species cost NZD$ 1095 for 25g (Sigma Aldrich) and so reducing the required acid number from 63 to 32 mg KOH/g for a carboxylated BLAC resulted in a cost saving of NZD$1357.80/kg.

8.5.2 Particle morphology

The particle morphology of the carboxylated BLAC dispersion was investigated using SEM. Dispersions were diluted 1000x and the particles were isolated on filter paper with a 200 nm pore size. The isolated particles from the dispersions generated using the conventional acetone process (acid number 100 mg KOH/g) and the reverse addition method (acid number 63 mg KOH/g) were an irregular spherical shape (Figure 8-6), similar to the particles recovered from the dispersion generated from CAB phthalate and CAB succinate. It was therefore anticipated that the dispersions produced using the T-mixer apparatus would also have an irregular spherical morphology. Unexpectedly, however, the particles isolated from the dispersion generated using the T-mixer (32 mg KOH/g) had an elongated fibrous morphology with an average aspect ratio of 10 (Figure 8-7).

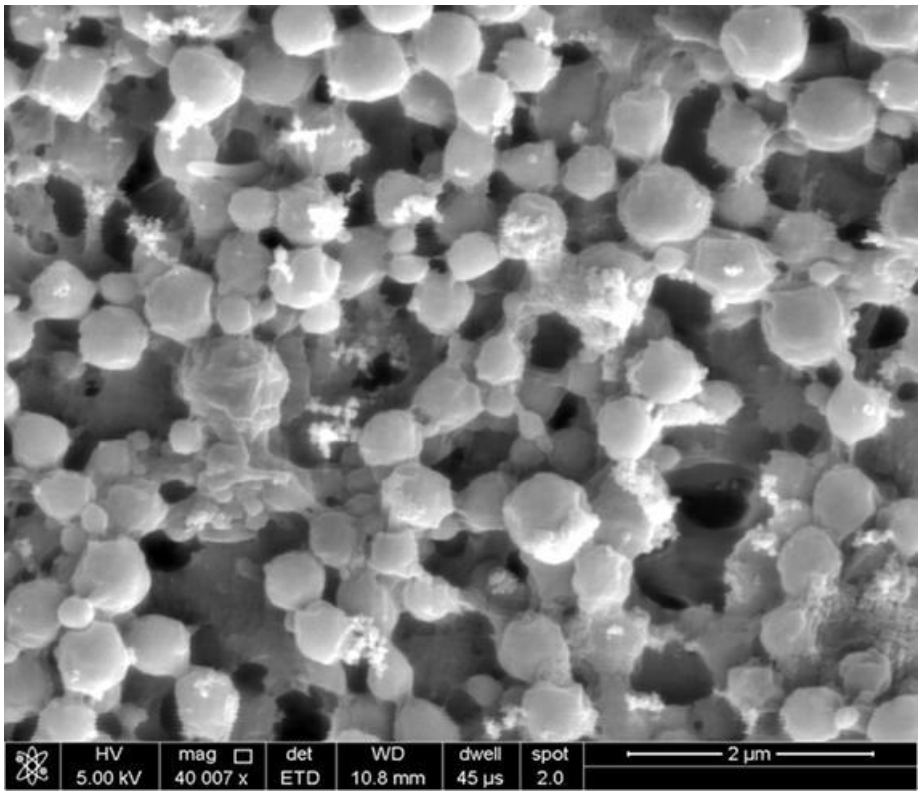

Figure 8-6 SEM micrograph of BLAC dispersion (acid number 100 mg KOH/g).

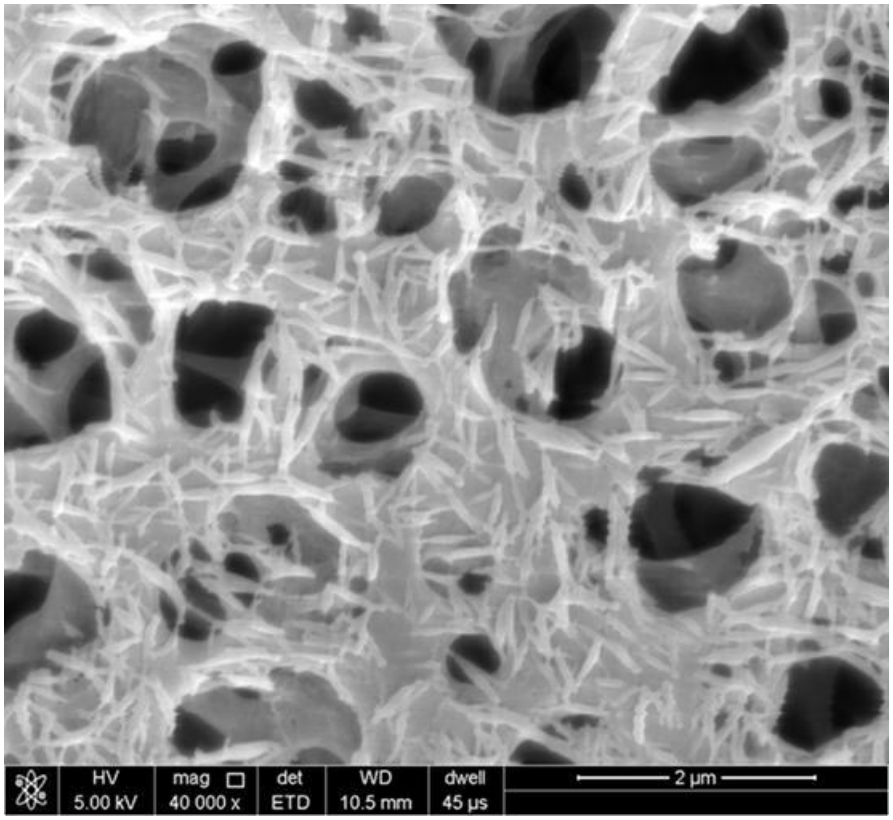

Figure 8-7 SEM micrograph of carboxylayed BLAC dispersion particles isolated from a T-mixer dispersion (acid number 32 mg KOH/g).

The particle morphology is a result of the rapid dispersion processes used. As described earlier, during precipitation the polymer transitions through a series of conformational changes and, as the precipitated particles grow, they adopt a low-energy spherical morphology. Once sufficient anti-solvent has been added to the continuous phase the particle morphology freezes due to the polymer no longer having an affinity towards the continuous phase.

Dispersions produced with the T-mixer method undergo very rapid mixing. As the polymer solution and anti-solvent are brought together in a 1:1 ratio at the T-mixer head interface, the polymer rapidly precipitates. The particle will only experience a fleeting transitional precipitation state where the polymer is still softened by the continuous phase as the acetone diffuses into the water. During this time it is likely the polymer particle was being extruded through the T-mixer outlet in its softened state, elongating the particle, creating a noticeably fibrous morphology. It was postulated that shortly after this process had occurred, the acetone diffused away

from the localised continuous phase surrounding the particle and the continuous phase then no longer had any affinity for the particle, freezing its morphology. Therefore, the fibrous particle morphology that was observed for dispersions generated using the T-mixer method was likely to be a result of the short lived precipitation transition state and the forces that were exerted on the polymer particle during precipitation. In contrast, substantially reduced forces were acting upon the polymer produced using the conventional acetone process and the reverse addition method. Therefore, during precipitation the softened particles were able to conform to a low-energy, roughly-spherical state.

8.6 Level of carboxyl neutralisation for dispersion generation

The effect of neutralising the carboxylated BLAC and how it influences the dispersions generated was evaluated. All of the dispersions prepared in this series used the carboxylated BLAC material with an acid number of 32 mg KOH/g, an amine (triethylamine, TEA) to neutralise the carboxylic groups and the T-mixer method with a constant ram pressure (6 bar). The amount of amine used was increased incrementally in order to study the effect the level of neutralisation had on the PSD. A clear trend was observed where the particle size decreased for the dispersed polymer and the PSD narrowed with increased neutralisation (Table 8-6). A nano dispersion of carboxylated BLAC was produced with 53% neutralisation of the carboxyl functionality which reduced the average particle size to 120 nm and narrowed the PSD to ± 200 nm (1 standard deviation).

Percentage carboxyl neutralisation (%)	PSD (nm)
21	5300 ± 700
32	2600 ± 600
42	1700 ± 700
53	520 ± 500
58	120 ± 200
64	N/A

Table 8-6 Dispersions of carboxylated BLAC with varying percentage of carboxyl neutralisation.

The trend in the average particle size observed for the dispersions, with respect to level of neutralisation, was consistent with literature for PU dispersions [210]. When using the acetone process the average particle size of a PU dispersion incrementally reduces as the neutralisation of the ionisable groups increases [211]. The carboxylated BLAC (32 mg KOH/g) did not form dispersions beyond 58% neutralisation as increasing the neutralisation beyond this point resulted in the carboxylated BLAC material showing increased solubility in the acetone-water continuous phase and resulted in a high viscosity solution. Even after acetone distillation the solution did not decrease in viscosity and therefore a dispersion had not formed. These results demonstrated that a carboxyl neutralisation level of 58% was suitable to generate a carboxylated BLAC (32 mg KOH/g) within the specified average particle size limit of 500 nm, and was progressed forward through the project as the standard level of neutralisation for the carboxylated BLAC dispersions.

8.7 T-mixer mixing rate

The effect of the mixing rate generated by the T-mixer (see Section 10.1.15, Figure 10-5) on PSD was investigated. The flow rate of the polymer solution and anti-solvent through the T-mixer, and therefore the mixing rate, could be increased by increasing the pneumatic ram air pressure. The maximum ram pressure that the 6 mL Luer lock syringe would tolerate before failure occurred was 6 bar with the solutions used here. While the percentage neutralisation of carboxylated BLAC was maintained at 58%, increasing the ram pressure from 2 to 4 bar displayed a steady decrease in average particle size down to 76 ± 257 nm (Figure 8-8). Increasing the ram air pressure beyond 4 bar did not further reduce the average particle size.

Increasing the mixing rate of the polymer solution and anti-solvent reduced the average precipitated particle size by minimising aggregation. Rapid solvent exchange reduced the time available for particle aggregation during the particle growth phase. It was postulated that an increased rate of mixing (beyond 4 bar) under the experimental conditions used did not further reduce the average particle size of the dispersion due to the solvent exchange becoming diffusion limited. Solvent diffusion therefore became the limiting factor for solvent mixing,

and therefore controlled the rate of polymer precipitation, the duration of the growth phase where particle aggregation occurred, and particle size.

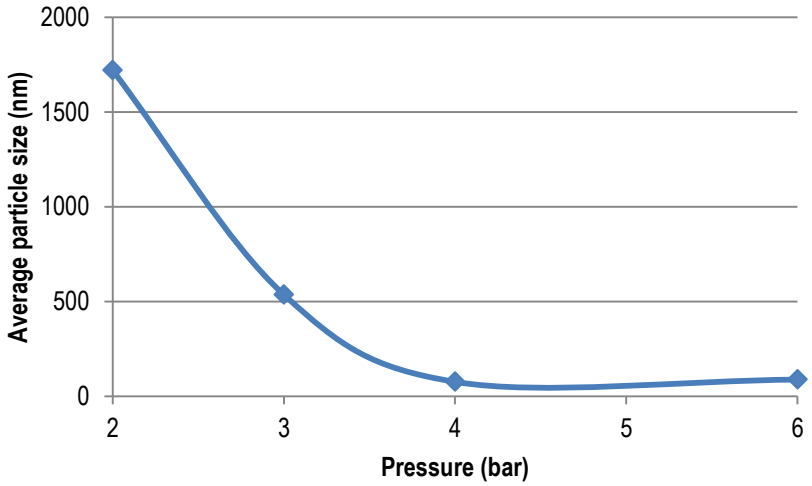

Figure 8-8 Dispersion particle size with increasing ram air pressure.

8.8 Solvent distillation

The final step in the process is removal of the organic solvent, creating an aqueous dispersion, and generating a concentrated polymer formulation with a high solids content. Acetone has a boiling point of 56 °C and does not form an azeotrope with water, so should preferentially be distilled away from the aqueous phase. This distillation process removes the acetone (generating the low VOC formulation), and increases the solids loading by removal of the organic phase and a small portion of the aqueous phase.

Acetone was distilled under reduced pressure from the dispersion of carboxylated BLAC that comprised 15.8% w/v solids and 47.8% v/v acetone in water with 0.3% v/v TEA, as prepared in Section 10.2.55. A series of experiments were completed where the distillation temperature was increased incrementally between 20 °C and 50 °C, while the duration (2 hours) and vacuum profile remained constant. Distillation under reduced pressure caused the dispersion to bump and foam, therefore the minimum pressure was restricted to 100 mbar to control these effects. Distillation of PU dispersions, performed at elevated temperatures over extended periods, has been shown by Nothnagel *et al.* to result in particle coagulation [208]. The level of coagulation increased with

increasing temperature and duration of the distillation process and, as a result, the average particle size increased. It was anticipated that the carboxylated BLAC dispersions would demonstrate similar behaviour, however, the average particle size increased between 80 and 90% across all temperature ranges (Table 8-7). Therefore, it does not appear that distillation temperature over the time frame used was a causative factor in particle growth. The comparable particle growth for all of the formulations used, would suggest that residual aggregation of particles and unimers was occurring. It was postulated that there was a portion of soluble carboxylated BLAC material (likely low molecular weight chains) in the mixed acetone-water continuous phase which became insoluble during removal of the acetone, and these unimers aggregated with the larger stabilised particles. Zhang *et al.* has reported that the barrier to aggregation of unimers and charge stabilised particles is very low in comparison to that for two charge stabilised particles [207].

Distillation temperature (°C)	PSD pre-distillation (nm)	PSD post-distillation (nm)
20	100 ± 300	190 ± 400
30	100 ± 300	180 ± 400
40	100 ± 300	180 ± 200
50	100 ± 300	180 ± 300

Table 8-7 Change in carboxylated BLAC dispersion PSD after a 2 hour distillation.

8.8.1 Solids content of carboxylated BLAC dispersion

To generate a carboxylated BLAC dispersion with the target solids content of > 25 wt%, the dispersion had to be concentrated by the removal of acetone, and also water. The effect of distillation temperature on the solids content of the dispersion was investigated, while keeping the pressure profile and process duration constant. As expected, the solids content increased steadily with increasing distillation temperature (Figure 8-9), where a solids content of 25.7 wt% was achieved after distillation at 50 °C for 2 hours. In an attempt to increase the polymer solids content further, distillation was carried out at 50 °C for an extended time period of 2.5 hours using a reduced pressure profile (minimum pressure 80 mbar) which resulted in a solids content of 29.2 wt%. A rapid

increase in the dispersion's viscosity was observed as the solids content increased from 19 to 29.2 wt% and, at 29.2 wt%, the dispersion resembled a thick cream. The viscosity of a dispersion increases rapidly when a critical volume fraction is reached. At this point the particles become crowded and particle interactions restrict movement. Schneider *et al.* produced polymer dispersions with a multimodal particle distribution where the critical volume fraction exceeded 0.65 [9]. The onset of this effect for the carboxylated BLAC dispersion was observed for a relatively low polymer volume fraction (0.26; 29.2 wt% dispersion) based on a polymer density of 1.2 g/mL (CAB-381-2) [86]. However, it is possible that due to the hydrophilic nature of the polymer there was an increased hydration sphere associated with the carboxylated BLAC particles which therefore artificially increased the volume fraction of polymer in the dispersion. This resulted in a reduction in the wt% of dispersed polymer that could be achieved before the critical volume fraction was reached and an exponential increase in viscosity was observed beyond a solids content of 25 wt%.

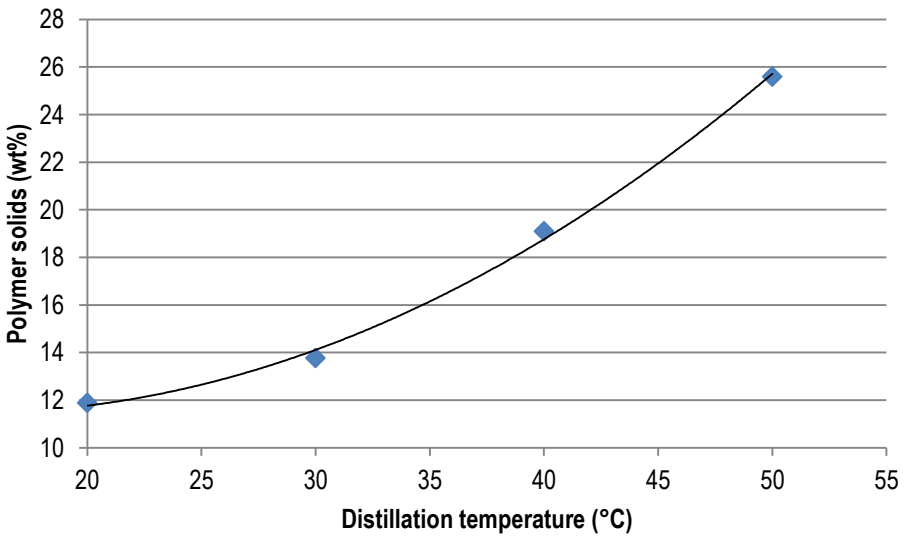

Figure 8-9 Carboxylated BLAC dispersion solids (wt%) with increasing distillation temperature for a two hour process.

8.8.2 Increasing the percentage solids in a carboxylated BLAC dispersion

The use of a more concentrated polymer solution in the dispersion process would minimise the distillation time required to produce a dispersion of a required solids loading. A set of experiments were therefore completed to assess the effect of varying the concentration of the polymer solution in the T-mixing dispersion process. One of the limitations of the dispersion apparatus was that only a 1:1 ratio of water to organic polymer solution could be fed into the mixing head. Therefore, increasing the concentration of the polymer solution for a given polymer loading would reduce the polymer solution volume, and therefore the volume of anti-solvent required. Carboxylated BLAC nano dispersions were produced using polymer concentrations of up to 21.3 wt% in acetone. There were no appreciable differences in the PSD of the dispersion produced when varying solution concentration, however, increasing the polymer concentration beyond 21.3% revealed another limitation of the dispersion equipment: the plastic syringes began to fail due to the increased polymer solution viscosity which was a consequence of increased concentration. Increasing the solution viscosity increased the loads generated at the syringe plunger, which was a function of maintaining the mixer outlet orifice diameter and flow rate. This issue could potentially have been resolved by heating the polymer solution to reduce the viscosity thereby allowing highly concentrated solutions to be used in dispersion production using this T-mixer methodology. However, this laboratory scale equipment could not be readily adapted to this proposed strategy in a controlled, reproducible fashion.

Future development of the T-mixer methodology would involve a re-design of the dispersion apparatus used. An improved device would have an independent dual-feed system to control the ratio of the anti-solvent to polymer solutions and would also permit temperature control of the two solutions. At scale, where the T-mixer would be pump-driven and the polymer and anti-solvent solutions would be independently controlled, such permeations would be feasible. The limitations of the current dispersion apparatus were borne out of the need to disperse small quantities of material due to the limited amount of levulinyl-CE polymer available.

8.8.3 VOC content of carboxylated BLAC dispersions

Production of a low VOC coating was one of the criteria for the renewable coatings program. There were two compounds used in the dispersal of the carboxylated BLAC that are classed as VOCs (boiling point of < 250 °C or a vapour pressure of > 0.1 mm Hg at 25 °C [2]): TEA and acetone, although interestingly, acetone has received VOC exempt status in the United States [212]. For this project, the ECNZ VOC guidelines were used as the standard to align with as our industry collaborators use these standards in their commercial products. The specification detailed for interior architectural coatings was a VOC content of 50 g/L in paint. It was known that additives classed as VOCs could be used in the mill base to aid in pigment dispersion and therefore a VOC free dispersion was targeted. This left room for VOC classed additives to be added to the mill base or resin binder if required.

A GC method based on ASTM D6886-03 [213] was developed to quantify the amount of residual acetone which was determined against a set of standard solutions. It was found that the level of acetone present was reduced with increasing distillation temperature (Table 8-8) and, at 40 °C, no residual acetone was detected and so the dispersion could be considered VOC free. TEA meets the VOC criteria specified by ECNZ, however, TEA would have reacted with the free carboxylic acid groups to form a salt or complex which would have a significantly increased boiling point. The dispersion process was also investigated substituting TEA with a number of commercial amines, all of which successfully produced nano dispersions (see Section 8.10). Ideally, TEA would be substituted for an alternative amine which is not classed as a VOC, such as triethanolamine (b.p. 335 °C).

Distillation temperature (°C)	VOC (%)
20	4.79
30	0.03
40	0.00
50	0.00

Table 8-8 VOC content of carboxylated BLAC dispersions produced with increasing distillation temperature.

8.9 Dispersion stability

Four different carboxylated BLAC dispersions of varying polymer concentration were assessed for stability over a four week period at room temperature. Monitoring consisted of particle size measurements at the beginning and end of the four week period to determine the extent of particle growth or aggregation, as well as visually monitoring physical characteristics for signs of destabilisation such as gelation. The samples tested displayed no physical signs of destabilising over the test period. However, the PSD measurements showed that all samples displayed a uniform increase in particle size, except for the carboxylated BLAC dispersion sample with a solids content of 19.1 wt% (Table 8-9), although they all remained well within the specification limit given (< 500 nm). These results indicated that the stability of the dispersion was not dependant on concentration, over the range tested.

Following the initial stability trials, the dispersions were visually monitored and remained stable for a further 1-2 months. The only observed mechanism of destabilisation was gelation followed by syneresis. This was observed as a rapid increase in viscosity, followed by the formation of a rigid gel structure, and then contraction of the gel, expelling the continuous phase. These characteristics are consistent with that reported in the literature [214]. It is possible that the hydrophilic polymer was swelling with the incorporation of water which would serve to decrease the charge density on the surface of the particle. The particles could then coagulate, forming a network conferring a rigid gel structure. In addition, this could be a product of hydrogen bonding through the available ketone and carboxylic acid sites on the polymer chain, and any water molecules present, forming a bridge structure. It is likely that with the addition of a compatible surfactant system, or colloidal stabilisers such as PVA, there would be an improvement in dispersion stability.

Polymer solids (wt%)	PSD (nm)	PSD after 4 weeks at RT (nm)	Δ PSD (%)
11.9	190 ± 400	210 ± 400	10.5
13.8	180 ± 400	200 ± 400	11.1
19.1	180 ± 200	170 ± 300	-5.5
25.6	180 ± 300	200 ± 300	11.1

Table 8-9 PSD analysis of carboxylated BLAC dispersions after 4 weeks.

8.10 Neutralisation using commercial amines

A variety of amines commonly used in the coatings industry were trialled to assess their compatibility with the carboxylated BLAC dispersions, and whether they conferred any advantages to the dispersion technology being utilised. Hydroxylated amines are commonly used in paint formulations to maintain compatibility between mill bases and resin dispersions; they are used in mill bases as a counter ion and to aid pigment dispersion [215]. The conditions used to generate the carboxylated BLAC dispersions were unchanged when assessing the different amines. It was observed that the PSD varied depending on the amine used, however, all samples remained below the 500 nm average particle size specification limit (Table 8-10). It is likely that the particle size variation observed was due to a lack of optimisation of the proportion of DMEA, AMP-95 and ammonia used. With respect to particle morphology, no differences between the dispersions were seen as a direct result of amine choice. All samples passed the four week room temperature stability trial, with only the ammonia sample showing significant evidence of particle aggregation (Table 8-10). This sample displayed the formation of a bi-modal particle distribution where the second distribution was centred at 917 nm (Figure 8-10), likely due to evaporation from the dispersion.

Amine	PSD (nm)	PSD after 4 weeks at RT (nm)
DMEA	120 ± 280	160 ± 230
AMP-95	250 ± 130	220 ± 230
Aqueous ammonia (28%)	240 ± 210	350 ± 210

Table 8-10 PSD of carboxylated BLAC dispersions neutralised with commercial amines, and their PSD following the four week stability trial.

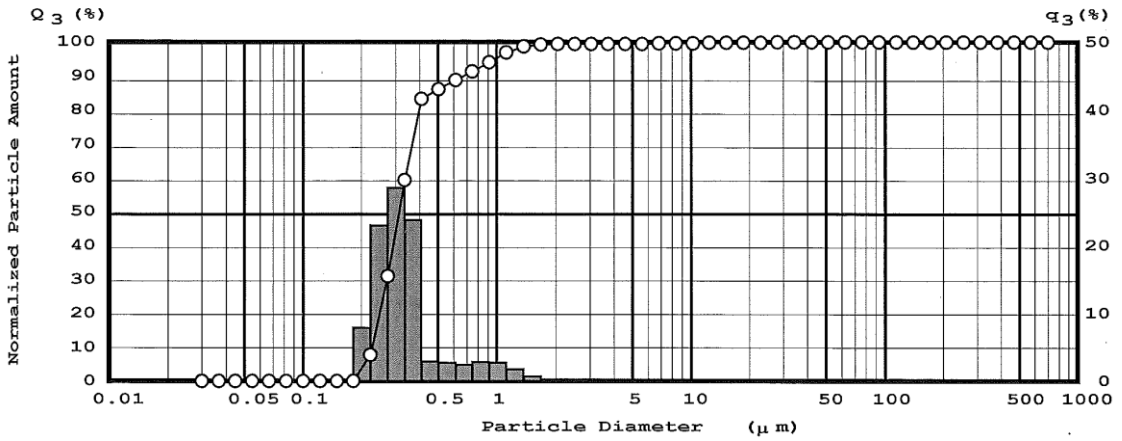

Figure 8-10 PSD of a carboxylated BLAC dispersion neutralised with ammonia after 4 weeks.

8.11 Film formation of a water-based dispersion of carboxylated BLAC

One of the key project targets was to form a continuous, coherent levulinyl-CE film from a water-based dispersion, the mechanism of which was discussed in Section 1.3.2. Briefly, film formation is a process of polymer particle coalescence due to the forces that result from the evaporation of the continuous phase resulting in a homogeneous film. The film formation properties of the carboxylated BLAC dispersion were investigated by applying the dispersion to a glass surface, which was allowed to dry at room temperature. All unmodified carboxylated BLAC dispersions resulted in a hard, brittle, transparent, light-yellow, highly-cracked film; examples of which are shown in Figure 8-11. This indicated that coalescence had occurred during drying, since otherwise a powdery residue would have remained. Particle coalescence of the carboxylated BLAC particles was further evidenced by SEM images taken of a carboxylated BLAC dispersion that had been diluted 1000x and allowed to air dry on filter paper (200 nm pore size) at room temperature. In an area of concentrated particle deposits, it was clearly seen that the particles had fused together to form a coherent mass (Figure 8-12). The elongated fibrous particle shape observed was not expected to alter the mechanism of film formation.

Figure 8-11 Unplasticised films cast from a water dispersion of carboxylated BLAC.

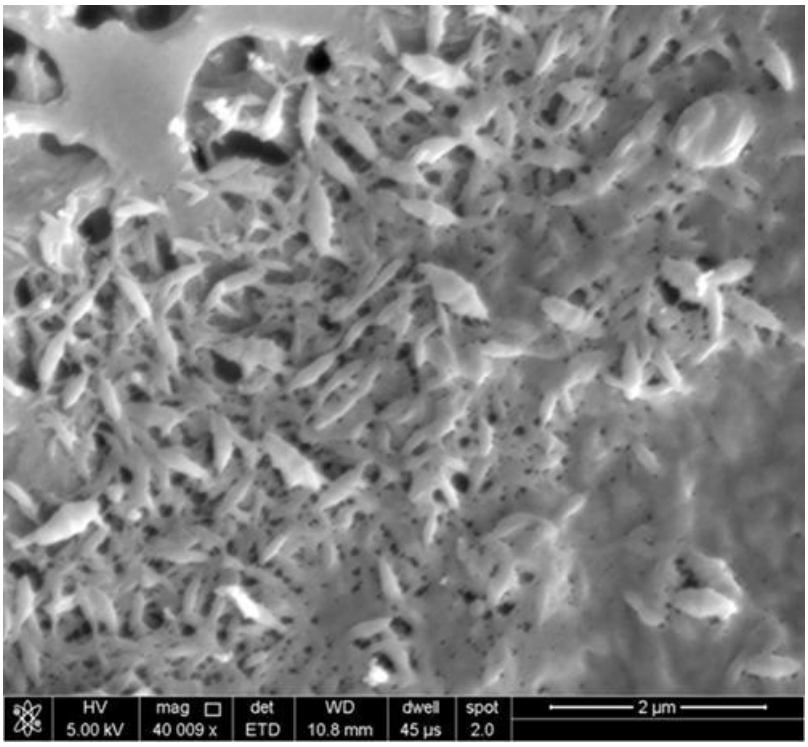

Figure 8-12 SEM micrograph of unplasticised carboxylated BLAC dispersion particles forming a coherent mass.

Film formation of the unplasticised carboxylated BLAC polymer dispersions was unexpected. It is generally accepted that the polymer T_g and the dispersion MFFT are closely associated [5] and therefore the dispersed carboxylated BLAC (T_g 88 °C) was an unlikely candidate for film formation at room temperature. A possible explanation for the unexpected film formation could be as a result of hydro-plasticisation. The carboxylated BLAC

polymer used was a hydrophilic polymer chain with a variety of polar functional groups. It is therefore possible that an association between the aqueous continuous phase and the polar groups on the polymer chain existed, allowing the water to behave as a plasticiser. This would lower the T_g and soften the particle sufficiently for coalescence to occur well below what the T_g would suggest was feasible. However, during the drying process, evaporation of water returned carboxylated BLAC to its unplasticised state forming a hard, brittle film. Cracking of the polymer film occurred due to dimensional changes of the film and stress build-up during the drying process since the hard carboxylated BLAC film is neither tough nor plastic enough to cope with the induced stress. The drying characteristics of the unmodified BLAC dispersion were observed as a horizontal drying front with the crack propagation front following closely behind (Figure 8-13). Crack propagation was attributed to the capillary forces that are associated with drying, which cause polymer deformation and cracking [216]. The cracks occurred at even intervals which is consistent with the literature [216].

Figure 8-13 Sample of a carboxylated BLAC dispersion drying, showing drying and cracking fronts.

8.11.1 Coalescing solvents

To alleviate the stress build-up in the film during drying, a number of coalescing solvents and plasticisers were investigated to address film cracking. High boiling point coalescing solvents were chosen as their evaporation is slower than water, allowing the film to remain plastic, and therefore relieving the stress build-up induced on drying. The coalescing solvents should then slowly diffuse out of the film resulting in a hard continuous film. Initially, the coalescing solvents were added to the polymer dispersion, and the addition range was between 3.3 and 20.0 wt% of the polymer. Films were cast from the dispersions and allowed to dry for 24 hours at room temperature before being assessed for film cracking. The results for crack mitigation with respect to the coalescing solvents trialled is given in Table 8-11.

	Amount of solvent present (wt%)					
Solvent	**20.0**	**13.3**	**8.9**	**5.6**	**4.4**	**3.3**
Butyl cellosolve acetate	1	2	4	-	-	-
Butyl levulinate	1	1	1	3	-	5
Cellusolve	-	-	-	-	-	-
Diacetone alcohol	1	3	4	5	-	-
Dibasic ester	-	-	-	-	-	-
Diethylene glycol	1	2	3	-	4	-
Ethyl levulinate	1	1	1	5	-	5
Propylene n-butyl glycol ether	5	-	-	-	-	-

Table 8-11 Carboxylated BLAC film crack mitigation with respect to plasticiser/coalescing solvent and content (wt%). Crack scale is rated 1-5; 1 = no cracking, 2 = limited fine crazing, 3 = fine crazing with some heavy cracking, 4 = heavy cracking, 5 = heavy cracking and material flaking. Formulations represented by a (-) were not prepared.

Propylene glycol n-butyl ether (PnB) is a commonly used coalescing additive, but showed no evidence of crack mitigation for the cast carboxylated BLAC film at the incorporation level used. Carboxylated BLAC was insoluble in PnB, and to be an effective coalescing solvent, the polymer must display some affinity towards the solvent chosen. Dibasic ester and Cellusolve both showed good affinity towards carboxylated BLAC, however, these solvents immediately destabilised the dispersion causing coagulation. Ethyl and butyl levulinate both showed excellent crack mitigation with relatively low solvent additions (8.9 wt% of BLAC) and the cast films were crack-

free 24 hours after drying. Additionally, butyl levulinate showed good levulinyl-CE compatibility and is not classed as a VOC (boiling point of 252 °C, Sigma Aldrich). Butyl levulinate was an ideal coalescing solvent, as it is produced partly from a renewable source and has previously been described as an effective plasticiser [217]. However, carboxylated BLAC dispersions modified with levulinyl esters (either post addition or co-dispersed) did display an accelerated dispersion destabilisation compared to those without a coalescing solvent. A rapid gelation onset was observed within two days and a rigid gel structure had formed. All of the cast films that displayed no cracking after 24 hours, were monitored for a further four weeks at room temperature, and unfortunately all of the films failed within this aging period. It was apparent that either residual stress in the film or stress build-up during diffusion was causing the hard polymer film to crack. Based on the results obtained here this method of crack mitigation was not going to be effective.

8.11.2 Dispersions of carboxylated BLAC plasticised with SAIB

The incorporation of a plasticiser was investigated in an attempt to mitigate film cracking. SAIB was previously shown to be an effective plasticiser for LBC (discussed in Section 4.8.1.1) and it was expected that these results would translate well to carboxylated BLAC samples. Incorporation of the SAIB plasticiser was projected to soften the polymer film, permitting film deformation to occur while drying, ultimately resulting in a continuous polymer coating. The effect of SAIB addition on BLAC dispersions and on film formation was thus investigated.

SAIB is a non-volatile material with a molecular weight of 832-856 g/mol [218] and, unlike the volatile coalescing solvents, will remain in the film and should prevent cracking even over an extended period of time. The solubility reported for SAIB in water was 0.1 wt% [218] and therefore the SAIB (already pre-dissolved in ethyl acetate) was co-dissolved with the polymer in acetone and dispersed in the usual fashion. Due to the low water solubility of the SAIB plasticiser, it was expected that the SAIB would remain intimately dissolved within the polymer particle.

SAIB (wt%)	PSD (nm)	PSD after 4 weeks at RT (nm)
5	120 ± 290	Gelled
10	110 ± 300	314 ± 97
20	70 ± 250	110 ± 310
40	90 ± 280	100 ± 280
50	110 ± 290	90 ± 90
60	90 ± 280	80 ± 300
80	80 ± 270	120 ± 340
100	110 ± 210	100 ± 190

Table 8-12 PSD of carboxylated BLAC co-dispersed with SAIB following distillation and after four weeks at room temperature.

A lower T_g polymer was anticipated to display a greater propensity for particle aggregation, especially during the distillation of acetone, where the additional facet of heating the dispersion was introduced. However, there was no evidence that the plasticised dispersion was behaving in a manner different to the unplasticised dispersed polymer (Table 8-9 and Table 8-12). Dispersions of carboxylated BLAC modified with SAIB were within the project specified average particle size of 500 nm and displayed a similar PSD to the unplasticised dispersions. The T_gs for carboxylated BLAC were not measured directly, but a similar T_g lowering effect to un-carboxylated BLAC was anticipated, and so plasticisation with SAIB was based on the results for the un-carboxylated BLAC (Table 8-13).

BLAC	
SAIB (wt%)	T_g (°C)
0	88
10	70
20	59
40	41
80	18

Table 8-13 Comparison of the T_g of BLAC with increasing SAIB content.

The stability of the SAIB modified carboxylated BLAC dispersions was monitored over a four week period (Table 8-12). Destabilisation was observed for the material containing SAIB at 5 and 20 wt%. Gelation was observed with 5 wt% addition of SAIB, at 10 wt% of SAIB the average particle size increased by 2.85 times, and with

20 wt% the average particle size had also increased over the four week period. However, for the majority of samples beyond a SAIB level of 20 wt%, the effect of SAIB on particle stabilisation was negligible and the information gathered remained consistent with the unplasticised dispersions. It was unclear why low level SAIB incorporation was destabilising the carboxylated BLAC dispersions.

With regard to the particle morphology, an unexpected change was observed with increasing SAIB content: the dispersed polymer particles changed from an elongated fibrous morphology to increasingly irregular spheres (Figure 8-14 and Figure 8-15). Dispersions made with 80 and 100 wt% SAIB were not scanned by SEM, however, it was expected that the morphology trend would be to increasingly spherical particles. The gradual change in particle morphology with increasing SAIB content was likely to be a function of the decreasing T_g. The softened polymer would essentially have a longer transitional window where the particle may deform to a lower energy spherical state, before being trapped in a physical form once fully precipitated from the continuous phase.

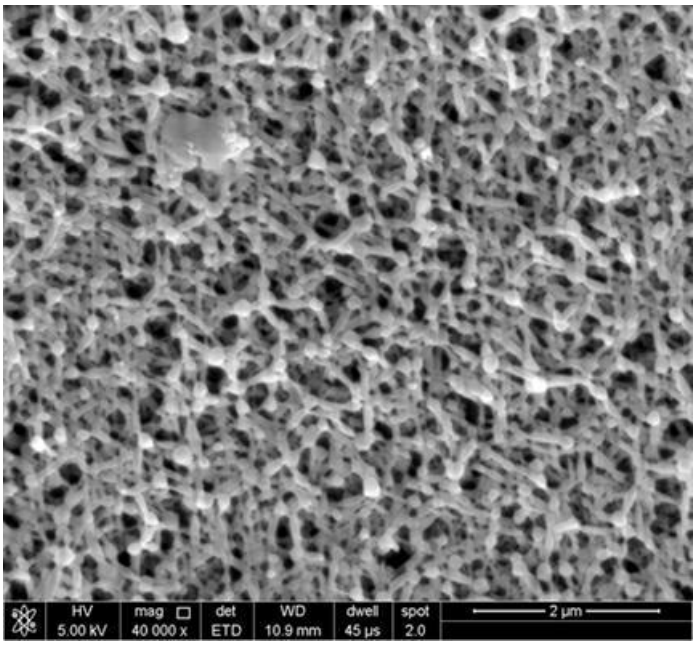

Figure 8-14 SEM micrograph of a carboxylated BLAC dispersion plasticised with 20 wt% SAIB.

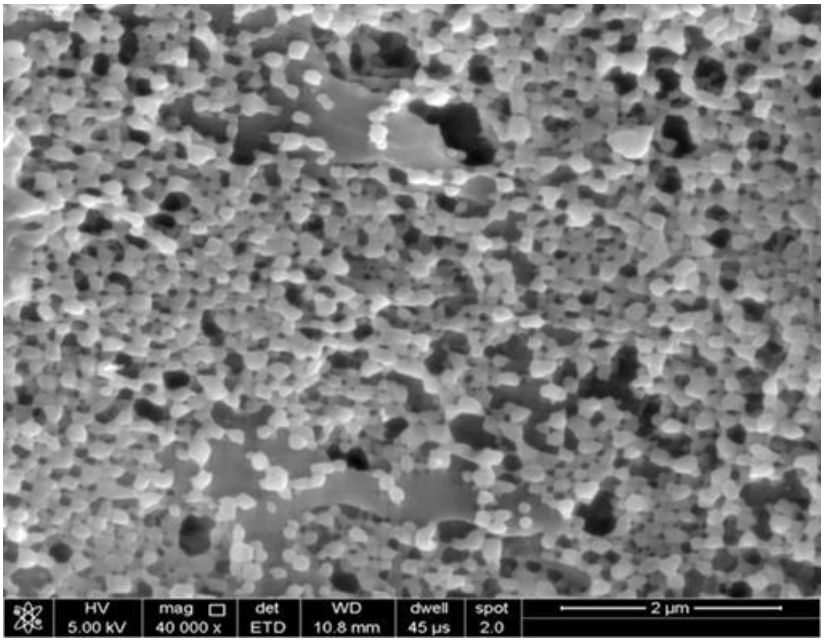

Figure 8-15 SEM micrograph of a carboxylated BLAC dispersion plasticised with 40 wt% SAIB.

When SAIB was incorporated to a level of 60 wt% of the polymer, a crack-free film was formed initially but with time, cracking was observed. The BLAC sample with an 80 wt% SAIB loading displayed a T_g of 18 °C which was low enough to allow the film to remain plastic, permitting crack-free film deformation to occur during drying. The dispersion of carboxylated BLAC formulated with > 80 wt% of SAIB did not demonstrate film cracking as it cured, and a crack-free film was maintained for > 4 weeks (Table 8-14).

SAIB (wt%)	Crack value	Crack value after 4 weeks
5	5	5
10	5	5
20	5	5
40	5	5
50	3	3
60	1	2
80	1	1
100	1	1

Table 8-14 Crack evaluation of films cast from carboxylated BLAC plasticised with SAIB. Crack scale is rated 1-5; 1 = no cracking, 2 = limited fine crazing, 3 = fine crazing with some heavy cracking, 4 = heavy cracking, 5 = heavy cracking and material flaking.

An observation worthy of reporting was that addition of SAIB at > 20 wt% to the formulation had an additional positive outcome with respect to dispersion processing. It was noted that while concentrating the polymer dispersions by distillation, the addition of SAIB greatly reduced bumping and foaming. It is unclear why this occurred, however, this does aid in dispersion processing allowing further reduced pressures to be used which can result in either decreased distillation temperatures or distillation times. Furthermore, the addition of non-volatile SAIB to the dispersion increased the solids content, so dispersions modified with SAIB were reported both as total solids and as polymer solids.

8.11.3 Dispersions of PEG-modified carboxylated BLAC

A dispersion of carboxylated BLAC modified with PEG groups was prepared using the conventional acetone process methodology. A continuous film was cast from the dispersion at room temperature which showed no signs of cracking over a 6 month aging period (Figure 8-16). The high level of PEG incorporated resulted in the film remaining tacky once dry. It is expected that the PEG incorporation will increase the polymer film's susceptibility to water, which could result in the tackiness noted, or alternatively, this feature could be a function of the low T_g of the CE. Unfortunately, no dispersion data was collected for this material relating to PSD and VOC content. Any future work undertaken would include developing dispersions of PEG-modified carboxylated levulinyl-CEs as the next stage for waterborne film forming levulinyl-CEs.

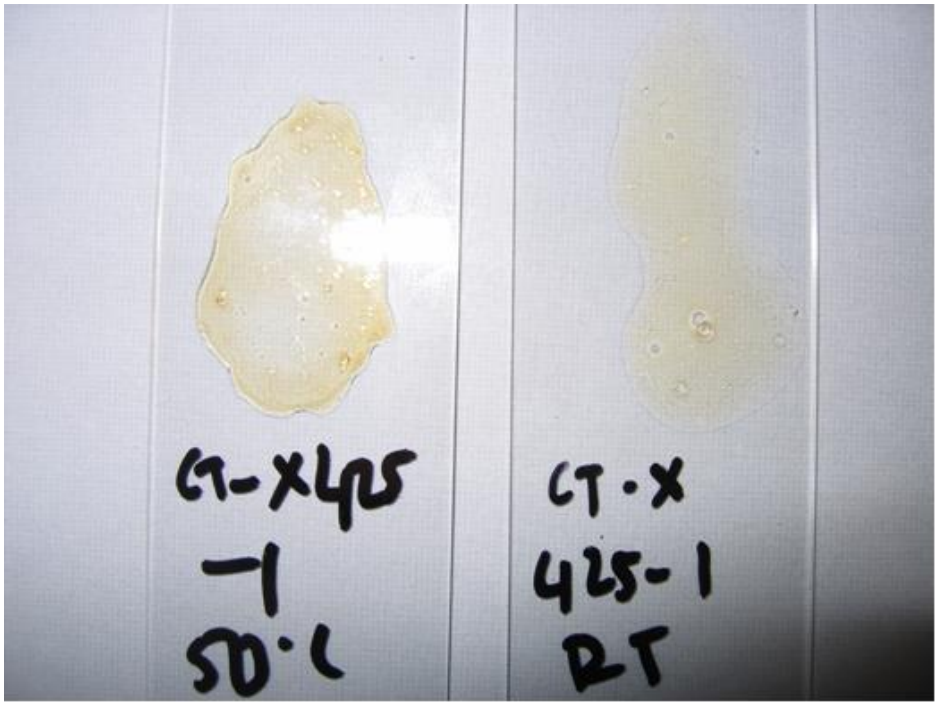

Figure 8-16 Films cast at 50 °C (left) and room temperature (right) from a water-based dispersion of BLAC modified with both PEG and carboxyl groups.

8.12 Low-sheen paint formulation (with a carboxylated BLAC binder)

The final step of the project was to formulate an interior architectural coating from the optimised carboxylated BLAC dispersion. The mill base[10] and resin loading were specified by Resene based on the known requirements for a low-performance, low-sheen interior paint [215]. The carboxylated BLAC dispersion is detailed in Table 8-15, where the total solids were 47.0 wt% (26.1 wt% BLAC and 20.9 wt% SAIB) and the VOC content was 0%. The coating was formulated with a mill base to a resin solids loading ratio of 1.4:1 (by weight) to give the coating the correct TiO_2 content of 250 g/L (Table 8-16).

[10] The low-sheen mill base was formulated and provided by Resene.

BLAC dispersion	Wt%
BLAC	26.1
SAIB	20.9
TEA	0.9
Water	52.1
Total	**100.0**

Table 8-15 Carboxylated BLAC dispersion specifications for the final paint formulation.

BLAC dispersion, 26.1 wt% resin solids (wt%)	74.1
Mill base	25.9
Polyacrylic acid dispersant, ammonium salt (0.8% actives)	
Polypropylene glycol (4.6%)	
Polymeric surfactant (0.8%)	
Titanium dioxide (76% mass)	
Water	
Defoamer (silicone based)	
AMP-95 (amine)	
Fungicide/algicide package for in-can and dry film preservation	
Total	**100.0**

Table 8-16 Low-sheen interior coating formulation using carboxylated BLAC.

Interior architectural coatings must contain less than 75 g/L of VOCs to comply with the ECNZ specifications (2009) for a low VOC interior architectural coating [2]. This has recently been reduced to 50 g/L for paints and undercoats to be used in most interior applications [1]. The final carboxylated BLAC dispersion coating formulation had a VOC content of 12 g/L, which is significantly under the required volatile component levels. In addition, the entire VOC content of the film was associated with the mill base. Propylene glycol (b.p. 188 °C) was added at 4.6 wt% to aid pigment dispersion and so optimising the mill base formulation through reducing the propylene glycol content would lower the VOC of the paint further.

The paint formulation was assessed by application of a 100 µm thick film, using a draw down bar on an opacity card. Following aging for 1-2 months it was clear that the BLAC dispersion had accepted the basic mill base and

formed a coherent film that was compatible with the pigment used (Figure 8-17 and Figure 8-18). Thus the initial paint formulation tests were successful and proof of concept had been achieved.

The paint films were then given to the project's industry collaborator for preliminary assessment where basic tests of film adhesion, flexibility, toughness and water susceptibility were conducted. The reported results described the water-based carboxylated BLAC coating as giving a low-sheen appearance and having appropriate film toughness, adhesion and flexibility. As expected, the films were susceptible to water, however, for the initial target of a low-grade ceiling paint, moisture interaction is limited. Further work using cross-linkers, such as adipic acid dihydrazide could alleviate or altogether reduce the water susceptibility issues.

Figure 8-17 Carboxylated BLAC-based paint film image (white).

Figure 8-18 Carboxylated BLAC-based paint film image (grey).

8.13 Summary

A water-based dispersion based on a carboxyl-modified BLAC polymer was generated that met all of the specified targets given for this project. The dispersion was stable over a four week period when generated with a carboxylated BLAC species with an acid number of 32 mg KOH/g. A modified acetone process was developed using a high-energy T-mixer to create the conditions necessary to form a nano dispersion with this material. A high flow rate syringe pump delivered a 1:1 feed of a carboxylated BLAC (acid number 32 mg KOH/g) solution and an anti-solvent into a T-mixing head to create the necessary mixing rate to reduce particle aggregation during the precipitation process, generating a nanoparticle dispersion. The average dispersion particle size could be modified by changing either the flow rate or the level of carboxyl neutralisation. Optimisation of these parameters produced nano-dispersions with a PSD of 180 ± 200 nm in a reproducible fashion. The flexibility of the process was demonstrated by producing dispersions with different amines commonly used in the coatings industry. A polymer solids content of > 25 wt% was achieved in the dispersion although a polymer solids content as high as 29.2 wt% was possible. However, beyond 20 wt% a rapid increase in viscosity was observed and this was attributed to an increased hydrodynamic volume related to the polymer's hydrophilic character. Casting of a coherent crack-free film from the water-based dispersion required plasticising with 80 wt% SAIB based on

polymer weight. A low-sheen interior decorative coating was formulated with a levulinyl-CE using a SAIB plasticised carboxylated BLAC water-based dispersion as the binder component. This successfully generated a paint formulation as a proof of concept, cellulose-derived, architectural coating.

9 Conclusions and future work

A proof of concept levulinyl-CE water dispersed binder was formulated and successfully demonstrated as a low-performance interior architectural coating. A continuation of this project would extend the development of the levulinyl-CE class with a view to further the binder's performance, in particular:

- Investigation and quantification of the monomer units by development of the reductive cleavage technique of R. Grey *et al.* discussed in Section 4.
- Further investigation into reducing the levulinyl-CE product colouration resulting from the reaction. It was proposed that the colour was a function of polymeric species forming due to side reactions, so optimising the reaction conditions would be desirable (e.g. replacing the acid catalyst, see below).
- Investigation into the long-term dispersion stability of the product. The dispersion destabilisation occurred by gelation and was attributed to BLAC's hydrophilicity. Therefore, decreasing the hydrophilicity of the materials may increase long-term dispersion stability. It may also be possible to increase the dispersion resin solids content by decreasing the levulinyl-CE hydrophilicity. It was postulated that the rapid increase in dispersion viscosity observed at relatively low wt% resin solids was associated with a large hydrodynamic volume, a function of the polymer's hydrophilicity.
- Investigate the reaction conditions to increase the molecular weight of the levulinyl-CEs generated, targeting > 50000 g/mol. Replacement of the sulfuric acid catalyst may also be used as a method to increase molecular weight. Recent work in the laboratory using metal triflates has shown them to be effective catalysts for levulinyl-CE generation. Alternatively, changes to the solvation of cellulose may be feasible, for example by using ionic liquids (Section 2.1). Alternatively, a different reagent such as an acid chloride may assist the reaction process. It is conjectured that high molecular weight levulinyl-CE water-based dispersions could have increased long-term dispersion stability.
- Incorporation of fluorinated groups into CEs has been shown to increase the hydrophobicity of the polymer to the point where moisture is no longer retained. Incorporation of these groups into the levulinyl-CE ester may have positive effects for both the dispersion and for the final film, reducing water sensitivity.

- Further investigation of the oxime linking technology, particularly with regards to incorporation of secondary groups and their effect on the T_g. Introducing crosslinking into the dry film using industry technologies such as adipic acid dihydrazide should also be explored.
- The BLAC polymer was not dispersed using the Dow BLUEWAVE process. With the knowledge gained to date with respect to temperature, polymer stability and hydrophobicity, it may be possible to disperse this material directly.
- It is essential that reagent recycling is investigated in order to reduce costs and environmental impact. Initial work would be aligned with current commercial recycling protocol and would most likely involve reagent recovery by distillation of the waste streams. Currently the optimised process does not use a co-solvent, which is desirable, however, the introduction of environmentally benign solvents to aid in heat transfer and reaction work-up should be assessed. In particular, if ionic liquids could be utilised to increase the rate of cellulose dissolution and subsequently be recovered, this could provide a significant enhancement in overall economics. As part of the ongoing research in the laboratory, a series of experiments have been proposed that aim to reduce reagent requirements by the use of high-shear processing equipment, the use of microwave energy, and semi-continuous processing.
- Reaction work-up volumes and overall waste production need to be addressed. Whilst recycling of reagents, distillation and recovery of the acids produced in the process, and re-use of aqueous streams from the work-up processes are all good economic targets, the complete utilisation of the reaction products in the final formulation would be advantageous. A proposed improved work-up would involve the addition of a chemical (or chemicals) following cellulose esterification which would react with all of the excess reagents, generating materials which would then contribute to the plasticisation, dispersion and ultimately film forming processes of the final CE. This could potentially be achieved if the current excess of reagents could be reduced, and suitable reaction chemistry involving the additional chemical (or chemicals) could be developed which was compatible with subsequent processes.
- It would be desirable to complete a pilot plant scale, low-sheen decorative paint production run to test the dispersion techniques and to produce a large optimised paint batch for film testing.

10 Experimental

10.1 Methods

10.1.1 NMR

NMR spectra were recorded using a Bruker Avance III 500 MHz spectrometer. The sample (15 mg) was dissolved in $CDCl_3$ unless otherwise specified (0.7 mL) and recorded in a 5 mm O.D. NMR tube. The spectra were collected at 25 °C. ^{1}H NMR spectra were referenced to the $CDCl_3$ solvent peak at δ 7.26 ppm, while the ^{13}C spectra were referenced to δ 77.08 ppm. NMR data was processed using Bruker Topspin 2.1 software.

10.1.2 Mass spectroscopy

Positive ion high resolution mass spectroscopy was completed using a Waters Q-TOF Premier™ Tandem Mass Spectrometer with a Waters 2795 HPLC

10.1.3 DSC

Differential scanning calorimetry was completed on a Mettler Toledo DSC1 STAR^{e} System with a GC200 gas controller using an auto-sampler and operating under a constant flow of nitrogen (30.0 mL/min). Samples were weighed (0.5-15 mg) into aluminium crucibles (40 µL, P/N ME-26763), the lid punctured and the crucible crimp-sealed. Analysis in comparison to a blank crucible was completed using a 7-stage temperature method: -30 to 180 °C; 180 to -30 °C; hold 10 minutes; -30 to 180 °C; 180 to -30 °C; hold 10 minutes; -30 to 180 °C; all ramp rates of 10 °C/min. For all samples the first heating run was used as an annealing period to remove residual solvent or water from the sample. After this initial annealing period and cool down, the second and third heating runs produced reproducible heat-flow curves and showed no sample decomposition. Spectra were also collected with a ramp rate of 5 °C/min and, apart from a slight variation (1-3 °C) in the calculated T_g attributed to hysteresis effects, very similar data was recorded. The T_g was assigned electronically and also by assessment of

the second-order inflection points of the DSC heat-flow to temperature plot with the centroid of the inflection points taken as the T_g.

10.1.4 CE relative colour measurement

Relative colour measurements were completed using a Jasco V-530 UV/Vis spectrophotometer. The CE samples were prepared as a 1% w /v solution in acetone. Measurements were taken using a quartz cell with a 10 mm path length. The wavelength range scanned was 200-900 nm with a scan speed of 400 nm/min. The relative colour measurement was calculated by the integration of the absorbance (Abs) between 400-600 nm.

10.1.5 Resin solids content

Resin solids content was determined following the ASTM method D2369-10 [219]. In brief, a representative sample of the dispersion was accurately weighed (1.0 g ± 0.1 mg) into a watch glass (weighed and dried). The sample was dried in an oven at 115 °C for 1 hour and then allowed to cool in a desiccator to RT and the sample weight was recorded to the nearest 0.1 mg. Samples were run in duplicate and an average was recorded.

10.1.6 VOC content – by GC

VOC content of dispersed CE aqueous systems were measured following the ASTM method D6886 – 03 [213]. Measurement conditions: Agilent Technologies GC 6890N equipped with a flame ionisation detector (hydrogen carrier gas, constant flow rate of 1 mL/min, using a split ratio of 100:1) was loaded with a J and W Scientific HP-5 column (length 30 m, I.D. 0.32 mm, film thickness 0.25 μm) with an inlet temperature of 260 °C and a detector temperature of 270 °C. The oven temperature was held at 40 °C for 2 minutes then ramped at 10 °C/min up to 200 °C. The sample injection volume was 2 μL.

Standard solutions of acetone and propan-1-ol (internal standard) were prepared in THF (HPLC grade) with concentrations ranging from 0.1 mg/mL to 35 mg/mL. A plot of concentration versus area gave a R^2 value of

greater than 0.995 (Figure 10-1). The samples were prepared by weighing out approximately 0.5 g (± 0.05 g) of the dispersion, 0.5 mL of internal standard stock solution (4 mg/mL propanol in THF) was added to the sample, followed by dilution with THF (up to 2 mL). The sample was sealed and thoroughly mixed for 5 minutes then centrifuged at 14000g for 3 minutes. An aliquot was removed, tested immediately and quantified against the standard curve.

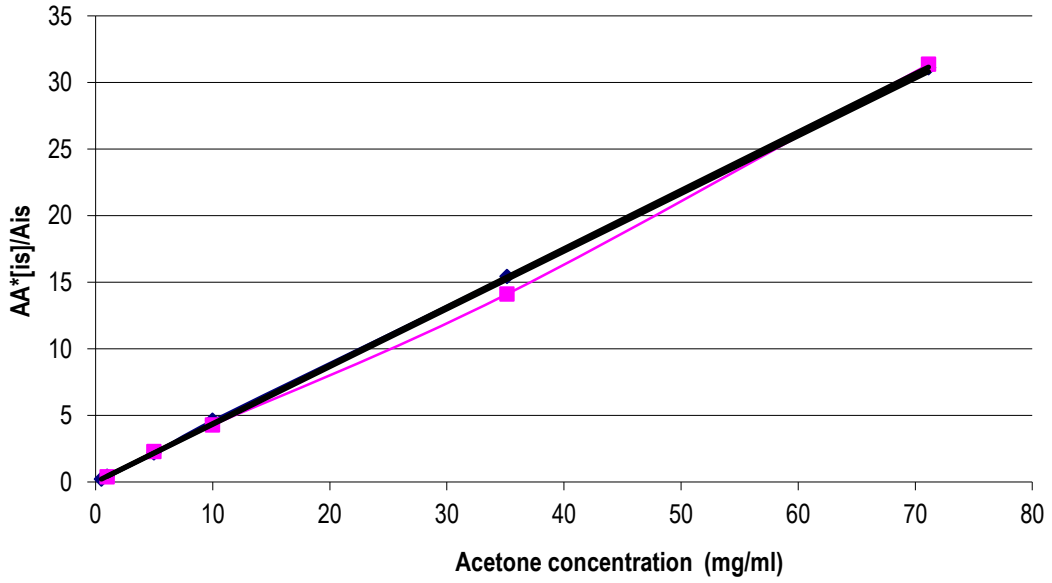

Figure 10-1 Acetone standard curve.

10.1.7 Film formation and film cracking

Film cracking was assessed by visual observation and evaluated based on the ASTM method D7306 – 07 rating system [220]. Films were cast from the CE dispersion by applying a uniform 0.5 mm thick layer to a glass substrate. The samples were dried at RT and 50 °C. Crack ranking was recorded immediately after drying, then at 7 and 28 days. The crack ranking system used for cast films was as follows:

Ranking system 1 – 5:

1 – No cracking.

2 – Limited fine crazing.

3 – Fine crazing with some heavy cracking.

4 – Heavy cracking.

5 – Heavy cracking and material flaking.

10.1.8 Acid number

US patent 5792856 [184] described a method for acid number determination and was carried out as follows. Dried carboxylated-CE (0.5-1.0 g) was dissolved in pyridine (50 mL) and acetone (40 mL). Once a homogenous solution had formed, DI water (20 mL) was added with continued stirring. The solution was titrated against a KOH solution (0.1 mol/L) and the pH monitored using an Eutech instruments pH510 meter with glass electrode (ECFG7451901B). The endpoint was assigned as the midpoint of the inflection. Samples were run in duplicate and an average of the two values was taken. Blanks were run concurrently with the samples, titrating the pyridine (50 mL), acetone (40 mL) and water (20 mL) solution. The acid number was calculated (Equation 10-1) giving a value in mg KOH/g

E_{Point} – Titration end point (mL)

Blank – Blank titration end point (mL)

$$\text{Acid number (mg KOH/g sample)} = \frac{(E_{Point} - \text{Blank}) * \text{NaOH (N)} * 56.1}{\text{Sample weight (g)}}$$

Equation 10-1 Acid number calculation.

10.1.9 Particle size

Dispersion particle size analysis was completed using a Shimadzu SALD-2001 laser diffraction particle size analyser, with a minimum measurable particle size of 30 nm. DI water was used as the dispersion medium, with a pump and stirrer speed of 6. The CE dispersion was mixed thoroughly to re-disperse any settled particles to

ensure a representative sample. The dispersion was added dropwise to the stirring and pumping water until an absorbance of 0.07 was recorded. The sample was left to stir and pump for 2 minutes until the reading had stabilised. The particle size was calculated using the Shimadzu software (SALD-2001-WEA2: V1.00) by volume using a refractive index of 1.45-0.10i. Samples were run in duplicate and an average value was recorded. The particle size distribution (PSD) was reported as the average particle size ± the particle size range (1 standard deviation).

10.1.10 Stability trial

Dispersion stability was monitored over a 4 week period at RT. Initial PSD measurements were taken soon after distillation had been completed. Dispersions were visually monitored for signs of destabilisation over 4 weeks and a test failure was recorded if destabilisation occurred before the end of the 4 week test period. A second PSD measurement was taken after 4 weeks and examined for signs of particle growth or aggregation. A pass was recorded if the average particle size remained < 500 nm.

10.1.11 SEM analysis

Dispersions prepared for particle size and morphology analysis by SEM were diluted 1:1000 in DI water then filtered through a Sartorius cellulose acetate filter, pore size 200 nm. Samples were air dried for 3 days before being prepared for SEM analysis. The samples were coated in silver and images were taken using a FEI Nova NanoSEM 450.

10.1.12 Molecular weight analysis (SEC)

Measurement conditions: An Agilient Technologies 1260 HPLC equipped with an RI and UV detector was operated with TSKgel SuperHM-L and TSKgel Super HM-H columns inline and a TSKgel SuperH-H guard column. The calibration curve reported for the columns was in the molecular weight operating range of 100 – $5x10^6$ g/mol, with a reported exclusion limit of $4x10^8$ g/mol. An isocratic solvent system (DMAc, HPLC grade) was

used with a flow rate of 0.25 mL/min and column temperature of 60 °C. The RI detector was operated at 40 °C with a step size of 0.5 s and wavelength measurements were taken at 210, 254, 450, 475 and 550 nm by the UV detector. Sample injection size was 5 µL with an analyte concentration of 10 mg/mL.

The SEC samples were prepared by CE dissolution in DMAc (10 mg/mL) and then were centrifuged at 14000 g for 5 minutes, to remove any insoluble material. An aliquot was removed being careful not to disturb any sediment and the sample was dispensed into a HPLC vial for testing. CE molecular weight analysis was completed by comparison to monodisperse polystyrene standards. The standards (TSKgel standards A-500 through F-128; Table 10-1) were injected and the retention volume plotted against the published M_w values. The plot of retention volume versus log M_w can be approximated by a third order polynomial of R^2 value greater than 0.998 (Figure 10-2). Comparison of the retention volume for the peak maxima for the cellulose ester derivatives permitted calculation of the molecular weight.

TSKgel standards	Molecular weight (M_w, g/mol)
A-500	590
A-1000	1000
A-2500	2500
A-5000	6200
F-1	9500
F-2	15000
F-4	37000
F-10	99000
F-20	190000
F-40	400000
F-80	710000
F-128	1100000

Table 10-1 Nominal molecular weight for TSK-gel polystyrene standards used.

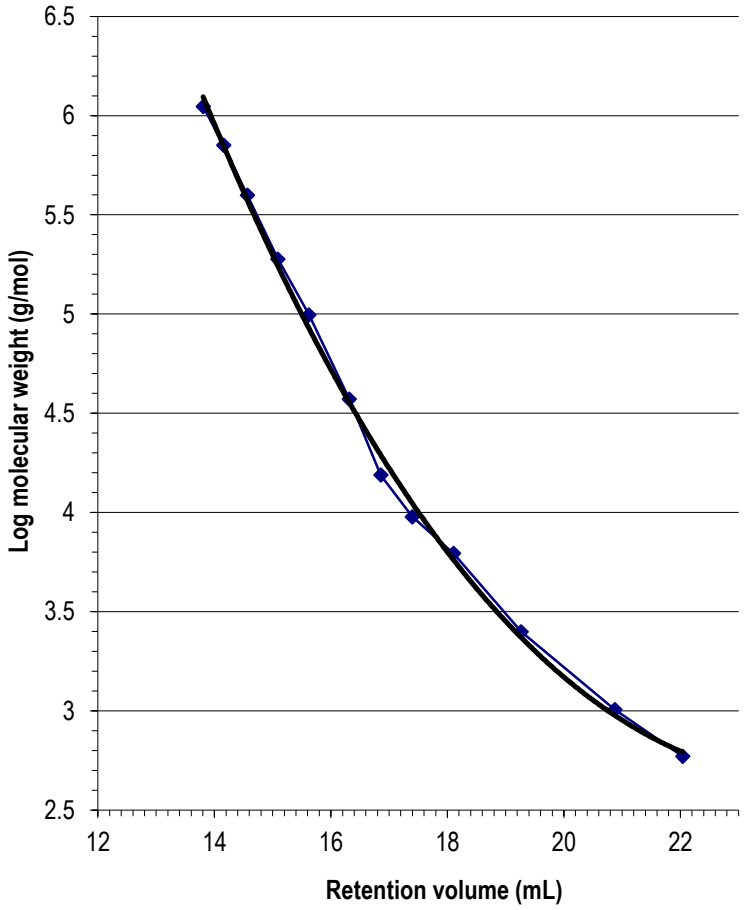

Figure 10-2 Polystyrene standards.

10.1.13 Degree of substitution, GC method

Measurement conditions: Agilent Technologies GC 6890N equipped with a flame ionisation detector (hydrogen carrier gas, constant flow rate of 1 mL/min, using a split ratio of 80:1) was loaded with a SGE solgel wax column (length 30 m, I.D. 0.32 mm, film thickness 0.25 µm) with an inlet temperature of 100 °C and a detector temperature of 200 °C. The oven temperature was ramped at 5 °C/min to 200 °C. The sample injection volume was 1 µL.

Standard solutions of LA, butyric acid and acetic acid with concentrations of between 10 mg/mL and 100 mg/mL with 5 evenly spaced steps were prepared. A plot of concentration vs peak area gave a R^2 value greater than

0.995 for each acid (Figure 10-3). The CE was dried and weighed into a 25 mL flask and dissolved in acetone (3 mL). A hexanediol internal standard was added from a stock solution (1 mL, 35 mg/mL) and then 1 mL of a 5 mol/L NaOH/MeOH solution was added then mixed for 1 minutes. Water (5 mL) was added and mixed for 1 minute. The sample was then washed into a volumetric flask (25 mL) with water and acidified with concentrated phosphoric acid (0.7 mL). The solution was then made up to 25 mL with water and a 2 mL sample was then removed and filtered through a 0.45 µm PTFE filter.

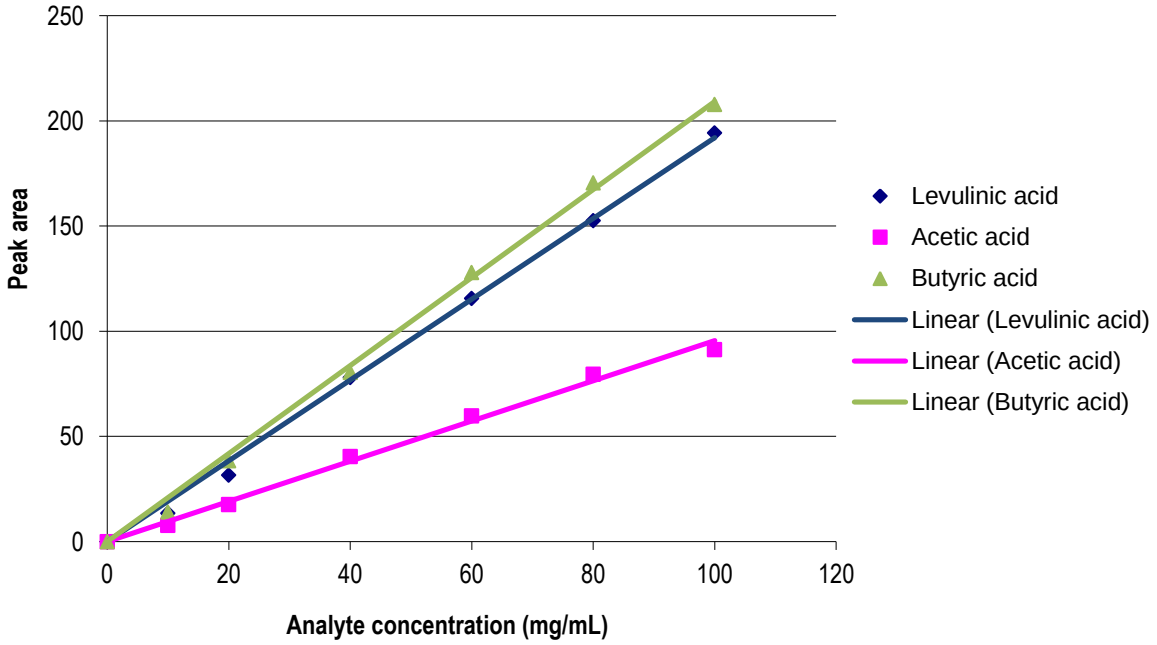

Figure 10-3 Carboxylic acid standard curves.

10.1.14 Degree of substitution, HPLC method

Measurement conditions: An Agilient Technologies 1260 HPLC was loaded with a Rezex ROA organic acid column. Samples were run isocratically in 5 mmol/L H_2SO_4 in high purity water at 0.5 mL/min with a column temperature of 60 °C. The RI detector cell was operated at 40 °C with a step size of 0.5 s and the UV detector monitored wavelengths at 210, 254, 450, 475 and 550 nm. Sample injection size was 10 µL.

Standard solutions of levulinic, butyric, acetic and propionic acid (internal standard), with concentrations of between 0.05 mg/mL to 20 mg/mL at 8 evenly spaced steps, were prepared. A plot of concentration versus peak area gave an R^2 value greater than 0.995 for each acid (Figure 10-4). The CE sample was dried and weighed (20 mg ± 0.1 mg) into a sealable 7 mL test tube. An internal standard stock solution (500 µL propionic acid at 10 mg/mL) and NaOH solution (2 mL, 2 N) were added to the CE sample. The tube was sealed and heated to 105 °C and mixed every 45 minutes over a period of 3 hours then allowed to cool to RT. Once cool the turbid solution was acidified with sulfuric acid (3 mL, 1 mol/L), re-sealed and thoroughly mixed, then left to stand for 5 minutes. The sample was then centrifuged at 4000 g at 10 °C for 5 minutes before a 2 mL aliquot of the supernatant was taken and centrifuged at 14000 g for 10 minutes. The carboxylic acid content analysis was calculated using the relative response factor (Table 10-2) generated from the standard solutions with respect to the internal standard.

Acid	Relative response factor
Acetic	1.239
Butyric	0.867
Levulinic	0.767

Table 10-2 Carboxylic acid relative response factors with respect to propionic acid.

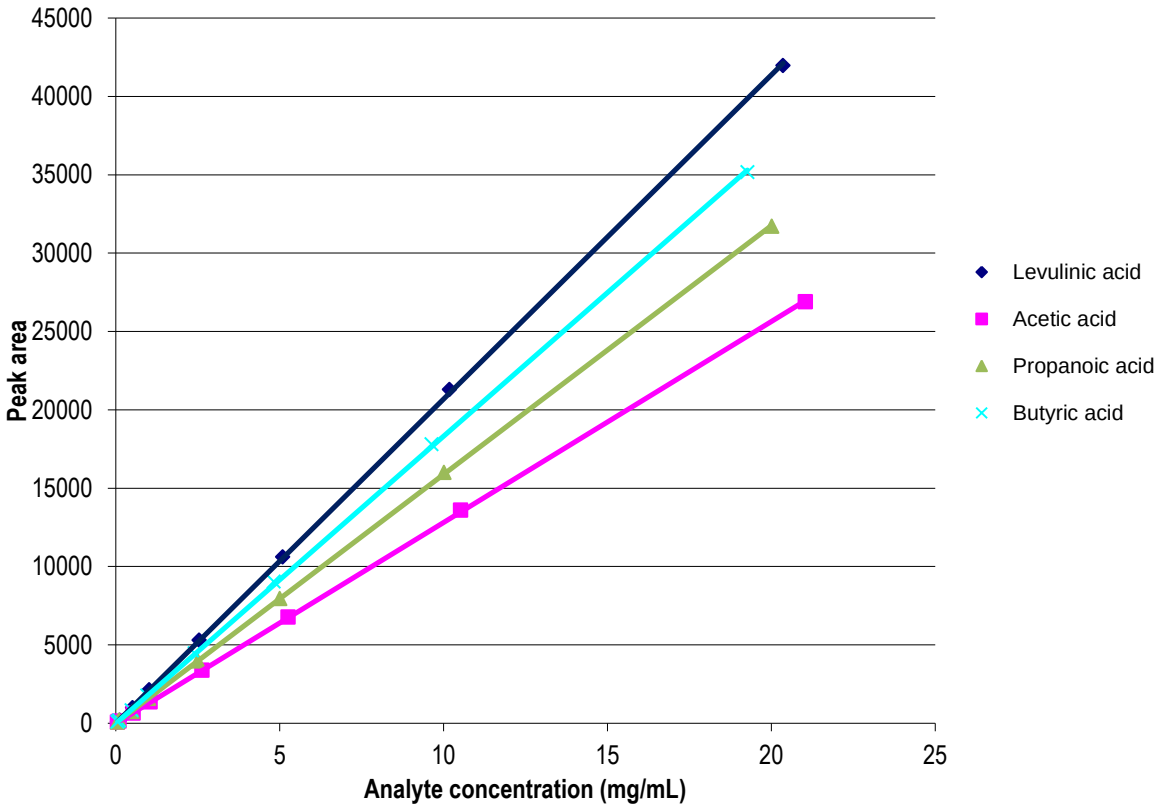

Figure 10-4 Carboxylic acid standard curves.

10.1.15 T-Mixer

The pneumatic T-mixer (Figure 10-5) was designed to disperse up to 2 g of levulinyl-CE. The mixer used a Norgren pneumatic actuator (RT-57232/m/80) which simultaneously depressed two syringes (3, 6 or 12 mL) at a constant rate. The T-mixer had two 1/16" I.D. inlets, mixing cavity and outlet. Stainless steel tubing and luer lock connectors were used to connect the syringes to the mixer. The actuator was rated to 10 bar, while the maximum line pressure that was available was 7 bar. Pressure was controlled using a regulator.

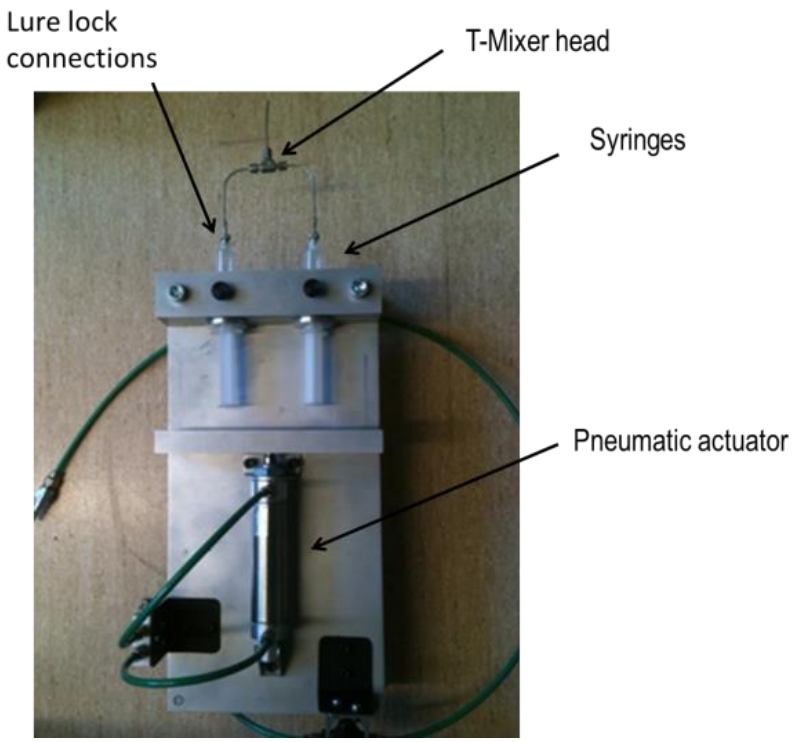

Figure 10-5 Pneumatic T-mixer.

10.2 Experimental

Reactions and compounds which are used in multiple steps and procedures have been designated their original lab book code as a means to distinguish them. The experimental data follows the order as presented in the results and discussion.

10.2.1 Standard levulinyl-CE preparation

Wood pulp (cellulose) pre-swelling was completed as follows: shredded wood pulp (BTK, Kinleith pinus bleached) was stirred in 60 °C water at a 1:20 w:v (g/mL) ratio for 3 hours. The cellulose was press filtered using a Teflon membrane, then re-suspended in 60 °C water (1:20 w:v) and stirred for 3 hours. The cellulose was press filtered being careful to remove as much water as possible without drying the cellulose. The water-swollen cellulose was slurried in glacial acetic acid (1:15 w:v) for 3 hours and then press filtered. The acetic acid-wet

cellulose was re-suspended in glacial acetic acid (1:15 w:v) and slurried for 3 hours. The cellulose was press filtered giving a weight of 2.5-3.5 g of acetic acid-wet cellulose per gram of dry cellulose.

The standard levulinyl-CE preparation was completed as follows: An aliphatic anhydride (3 Eq|OH), LA and concentrated sulfuric acid (9.1 mmol/L) were charged to a reaction vessel, generating an exotherm. The pre-swollen cellulose was charged to the reaction vessel generating a slurry which was heated to 120 °C with stirring for 2 hours forming a clear orange/brown solution.

The standard reaction work-up was completed as follows: the reaction was cooled to RT, then diluted 2:1 with a magnesium acetate dope solution (5% magnesium acetate in 1:1 acetic acid: water solution), generating the doped reaction solution. The reaction dope was then poured slowly into vigorously stirring water (11.5 volumes of the total dope solution) precipitating the levulinyl-CE, and was stirred for 2 hours. The precipitate was collected by filtration using a PTFE membrane (200 µm mesh size), followed by a water plug wash (1 volume). The precipitate was re-suspended in water (5.5 volumes) and stirred for 3 hours. The precipitate was collected by filtration using a PTFE membrane (200 µm mesh size), followed by a water plug wash (1 volume). The precipitate was re-suspended in water (5.5 volumes) and stirred for 3 hours before being collected by filtration using a PTFE membrane (200 µm mesh size). The precipitate was dried on the filter bed for 2 hours and then placed in a 50 °C oven for 18 hours.

The acetone re-precipitation was completed as a contingency strategy if the levulinyl-CE was still contaminated with reaction species (e.g. lactones, LA). The dried levulinyl-CE was dissolved in acetone (9% w/v solution) and poured slowly into vigorously stirring water (11.5 volumes) precipitating the levulinyl CE before stirring for 2 hours. The precipitate was collected by filtration using a PTFE membrane (200 µm mesh size), followed by a water plug wash (1 volume). The precipitate was re-suspended in water (5.5 volumes) and stirred for 3 hours. The precipitate is collected by filtration using a PTFE membrane (200 µm mesh size), followed by a water plug wash (1 volume). This process was repeated once more. The precipitate was allowed to dry on the filter bed for 2 hours and then dried in a 50 °C oven for 18 hours.

10.2.2 Valerolactones

LA (5.24 g, 45.1 mmol), acetic anhydride (3.46 g, 33.9 mmol) and concentrated sulfuric acid (12.9 mg, 129 μmol) were charged to a 50 mL round bottom flask. The solution was heated to 120 °C for 10 minutes with stirring. The reaction solution was allowed to cool to RT, then quenched with a 5 wt% $Mg(OAc)_2$ solution in acetic acid:water (1:1, 8 mL). The reaction solution was extracted with DCM recovering an orange/brown liquid.

A portion of the recovered material was purified by flash column chromatography. The column was packed with silica (40-63 μm, Davisil) to the dimensions of 110x35 mm. A gradient solvent system was used (ethyl acetate:petroleum ether (40:60, 400 mL), ethyl acetate:petroleum ether (50:50, 200 mL), ethyl acetate:petroleum ether (70:30, 200 mL), ethyl acetate:petroleum ether (90:10, 200 mL)) to separate and elute the reaction compounds.

4-Acetoxy-γ-valerolactone **(1)** (Rf 0.42 in ethyl acetate:petroleum ether (40:60)): m.p. (DSC) 72-74 °C; ^{1}H NMR (500 MHz): δ 1.77 (s, 3H, H-5), 2.06 (s, 3H, H-2'), 2.31 (ddd, *J* =8.8, 10.6, 18.7 Hz, 1H, H-3), 2.61 (m, 2H, H-2 and H-3), 2.87 (ddd, *J* = 7.8, 10.0, 17.6 Hz, 1H, H-2); ^{13}C NMR (125 MHz) δ 21.6 (C-2',OC(O)*C*H$_3$), 26.1 (C-5, C*C*H$_3$), 28.5 (C-2, C(O)*C*H$_2$) , 32.7 (C-3, C(O)CH$_2$*C*H$_2$), 108.4 (C-4, quat), 169.2 (C-1', O*C*(O)CH$_3$), 175.4 (C-1, *C*(O)O); TOF-HRMS found 181.0472, [$C_7H_{10}NaO_4$]+ calc. 181.0477.

4-Levulinoyl-γ-valerolactone **(2)** (Rf 0.27 in ethyl acetate:petroleum ether (40:60)): ^{1}H NMR (500 MHz) δ 1.77 (s, 3H, H-5), 2.18 (s, 3H, H-5'), 2.26 (ddd, *J* = 8.4, 10.5, 18.8 Hz, 1H, H-3), 2.54 (m, 1H, H-2), 2.55 (m, 2H, H-2'), 2.66 (m,1H, H-3), 2.74 (m, 2H, H-3'), 2.87 (ddd, *J* = 8.4, 10.3, 17.9 Hz, 1H, H-2); ^{13}C NMR (125 MHz) δ 26.2 (C-5, C*C*H$_3$), 28.6 (C-2', Lev OC(O)*C*H$_2$CH$_2$), 28.7 (C-2, *C*H$_2$CH$_2$), 29.8 (C-5', C(O)*C*H$_3$), 32.8 (C-3, CH$_2$*C*H$_2$), 37.7 (C-3', Lev *C*H$_2$C(O)CH$_3$), 108.9 (C-4, quat), 171.2 (C-1', Lev O*C*(O)), 175.6 (C-1, O*C*(O)), 206.5 (C-4', Lev *C*(O)CH$_3$); TOF-HRMS found 237.0744, [$C_{10}H_{14}NaO_5$]+ calc. 237.0739.

β-Angelica lactone **(3)** (Rf 0.55 in ethyl acetate:petroleum ether (40:60)): ^{1}H NMR (500 MHz) δ 1.45 (d, *J* = 6.9 Hz, 3H, H-5), 5.13 (qt, H-3, *J* = 1.8, 6.8 Hz), 6.10 (dd, H-1, *J* = 2.0, 5.7 Hz), 7.46 (dd, H-2, *J* = 1.5, 5.7 Hz); ^{13}C

NMR (125 MHz) δ 18.7 (C-5, CCH3), 79.6 (C-4, quat), 121.3 (C-2, *C*HC(O)O), 157.3 (C-3, *C*HCH), 173.0 (C-1, C(O)O).

The preparation and purification of 4-butyryloxy-γ-valerolactone was completed as follows: LA (5.00 g, 43.1 mmol), butyric anhydride (6.81 g, 43.1 mmol) and concentrated sulfuric acid (11 mg, 113 µmol) were charged to a 50 mL round bottom flask. The solution was heated to 120 °C for 30 minutes with stirring. The reaction solution was allowed to cool to RT, then quenched with $Mg(OAc)_2$ (50 mg) in water (1 mL). The reaction solution was diluted with water and extracted with DCM recovering an orange/brown liquid.

A portion of the recovered material was purified by flash column chromatography. The column was packed with 20.2 g of silica (40-63 µm, Davisil). A gradient solvent system was used (ethyl acetate:petroleum ether (30:70, 100 mL), ethyl acetate:petroleum ether (40:60, 100 mL), ethyl acetate:petroleum ether (60:40, 100 mL), ethyl acetate:petroleum ether (70:30, 100 mL), ethyl acetate (200 mL)) to separate and elute the reaction compounds.

4-Butyryloxy-γ-valerolactone **(4)** (Rf 0.44 in ethyl acetate:petroleum ether (40:60)): ^{1}H NMR (500 MHz) δ 0.95 (t , *J* = 7.4 Hz, 3H, H-4'), 1.63 (tq, *J* = 7.4 Hz, 2H, H-3'), 1.77 (s, 3H, H-5), 2.25 (t, *J* = 7.4 Hz, 2H, H-2'), 2.28 (m, 1H, obscured H-3), 2.57 (m, 1H, H-2), 2.64 (m, 1H, H-3), 2.88 (ddd, *J* = 7.8, 10.1, 18.1 Hz, 1H, H-2); ^{13}C NMR (125 MHz) δ 13.5 (C-4', CH_2CH_3), 18.1 (C-3', CH_2CH_3), 26.3 (C-5, CCH_3), 28.7 (C-2, $C(O)CH_2CH_2$), 32.9 (C-3, $C(O)CH_2CH_2$), 36.7 (C-2', But $C(O)CH_2CH_2$), 108.6 (C-4, quat), 171.9 (C-1', But OC(O)), 175.4 (C-1, OC(O)); TOF-HRMS found 209.0783, $[C_9H_{14}NaO_4]$+ calc. 209.0790.

10.2.3 α-Angelica lactone

A mixture of LA (6.44 g, 55.5 mmol), acetic anhydride (4.25 g, 41.6 mmol) and sulfuric acid (8.5 mg, 86 µmol) was heated at 130 °C under reduced pressure (40 mbar) using a Buchi Kugelröhr (B-585) for 2 hours. One reaction flask and two distillate flasks were used, the last distillate flask was cooled in a water/ice bath and the

reaction and first distillate flask were positioned inside the furnace. The recovered α-AL NMR spectrum was identical to an authentic sample and literature data [221].

10.2.4 Lactone formation from α-AL

- α-AL (100 µL, 93 µmol) in toluene (1 mL) was heated (110 °C) in the presence of catalytic sulfuric acid for 20 minutes. The solvent was distilled giving a 1:2:7 mixture of 4-levulinoyl-γ-valerolactone **(2)**, β-AL **(3)**, and LA. NMR spectra were identical to previously isolated species (Section 10.2.2).
- α-AL (100 µL, 93 µmol) in acetic acid (1 mL) was heated (110 °C) in the presence of catalytic sulfuric acid for 20 minutes. The excess acetic acid was removed under reduced pressure. The reaction exclusively formed 4-acetoxy-γ-valerolactone **(1)**. NMR spectra were identical to previously isolated species (Section 10.2.2).

10.2.5 4-Acetoxy-γ-valerolactone reaction with ethanol

4-Acetoxy-γ-valerolactone **(1)** (100 µL), ethanol (0.5 mL) and catalytic sulfuric acid were heated in a sealed tube at 30 °C for 1 hour. NMR characterisation showed the reaction exclusively formed ethyl acetate and ethyl levulinate in a 1:1 ratio. NMR spectra of the compounds were identical to previously prepared samples (Section 10.2.2) and literature data.

10.2.6 Mixed anhydride reactions

The appropriate carboxylic acid (Table 10-3) was added to acetic anhydride (306 mg, 3 mmol) in a 1.33 acid/Ac_2O mol/mol ratio and the solution was charged to a 50 mL RB flask, before the addition of catalytic sulfuric acid (9.1 mol/L). Evolution of a mild exotherm was only noted for reactions that contained LA. Pre-swollen cellulose (184 mg total mass, contains 130 mg (2.2 mmol) acetic acid) was then charged to the reaction, forming a slurry. This was heated (120 °C) for 45 minutes resulting in a colourless homogeneous solution, except for the levulinyl sample which formed a homogeneous orange/brown reaction solution. The standard work-up procedure

was used, except for samples prepared with valeric and hexanoic acids which were precipitated and washed with a 50:50 ethanol:water solution followed by a final water wash. The DS as defined by NMR analysis is shown in Table 10-3.

Acid	Mass used (g)	DS-Ac	DS-acid group
Butyric	350.7	2.34	0.74
Valeric	408.5	2.42	0.67
Hexanoic	462.6	2.43	0.56
Levulinic	462.4	1.72	1.29

Table 10-3 Acids used in mixed anhydride reaction series and NMR DS data.

10.2.7 Glucosyl-γ-valerolactone

Acetic anhydride (4.25 g, 41.6 mmol), LA (6.44 g, 55.5 mmol) and sulfuric acid (2.3 µL, 4.53 mmol/L) were charged to a 50 mL RB flask, generating a mild exotherm. Glucose (0.50 g, 2.7 mmol) was charged to the reaction solution and stirred at 50 °C for 0.5 hours. The cooled reaction solution was diluted with DCM (100 mL), successively washed with sodium bicarbonate solution (75 mL, 0.1 mol/L), water (75 mL) and brine (75 mL).

A portion of the material was purified by flash column chromatography; the column was packed with silica (40-63 µm, Davisil) to the dimensions of 115x55 mm. The material was eluted isocratically using a methanol:acetone:DCM (5:4:91) solvent system. Unfortunately this method was unable to separate the individual glucose species and isolation of a single penta-substituted glucosyl-γ-valerolactone was not achieved. NMR characterisation of the partially purified material indicated: DS-Lev 0.44, DS-Ac 2.1 and DS-Lactone 2.48.

10.2.8 4-Ethyl-γ-valerolactone

4-Acetoxy-γ-valerolactone (20 mg, 12.6 µmol) and ethanol (7.4 µL) in a 1:1 mol ratio was added to $CDCl_3$ (500 µL) containing sulfuric acid (1 µL/mL). The mixture was heated in a sealed tube at 35 °C for 25 minutes. Following this, the reaction was quenched with 2 eq of triethanolamine with respect to sulfuric acid.

A portion of the material was purified by flash column chromatography. The column was packed with silica (40-63 µm, Davisil) to the dimensions of 70x8 mm. The material was eluted with toluene:DCM (20/80) solvent system with a methanol gradient: 0% methanol (10 mL), 0.5% methanol (10 mL) and 1% methanol (40 mL) gave:

4-Ethyl-γ-valerolactone **(7)** (Rf 0.35 in toluene:DCM (20/80)): ^{1}H NMR (500 MHz) δ 1.18 (t, *J* = 7.0 Hz, 3H, H-2'), 1.62 (s, 3H, H-5), 2.13 (m, 1H, H-2), 2.28 (ddd, *J* = 3.1, 9.5, 13.0 Hz, 1H, H-2), 2.53 (ddd, *J* = 3.0, 9.6, 17.8 Hz, 1H, H-3), 2.75 (td, *J* = 9.6, 17.8 Hz, 1H, H-3), 3.64 (m, 2H, H-1'); ^{13}C NMR (125 MHz) δ 15.4 (C-2', OCH_2CH_3), 22.8 (C-5, CCH_3), 29.0 (C-3, $C(O)CH_2CH_2$), 34.8 (C-2, $C(O)CH_2CH_2$), 58.6 (C-1' OCH_2CH_3), 109.4 (C-4, quat), 176.9 (C-1, O*C*(O)). TOF-HRMS found 167.0685, $[C_7H_{12}NaO_3]$+ calc. 167.0684.

10.2.9 Lactone functional group removal

A portion of LAC (DS-Ac 1.67, DS-Lev 0.83) that contained the lactone functional group (DS-lactone 0.24) was treated to an additional reaction in order to ascertain the reactivity of the lactone moiety:

- LAC (100 mg) was dissolved in glacial acetic acid (2 mL). Sulfuric acid (2 µL) was added and the solution was stirred at RT for 48 hours. The standard LAC reaction work-up procedure was used to purify and recover the sample. NMR analysis revealed DS-Lev 0.85, DS-Ac 1.93 and DS-Lactone 0.00.
- LAC (150 mg) was dissolved in DMF (3.75 mL). Sulfuric acid (3 µL) was added and the solution was stirred at 120 °C for 1 hour. The standard reaction work-up procedure was used to purify and recover the sample. NMR analysis revealed DS-Lev 0.83, DS-Ac 1.67 and DS-Lactone 0.13.

10.2.10 CTA (iodine catalysed)

CTA was prepared following the method of Biswas *et al.* [166]: Cellulose (5.00 g, 30.9 mmol), acetic anhydride (16.7 g, 164 mmol) and iodine (358 mg 1.41 mmol) were charged to a 150 mL RB flask. The flask contents were placed under argon and the reaction slurry was heated to 100 °C with stirring for 10 minutes, forming a dark purple sludge. The reaction was cooled to RT and quenched with a saturated sodium thiosulfate solution (20 mL)

and precipitated with ethanol (300 mL) while stirring for 15 minutes to form an off white/brown solid. The precipitate was washed with ethanol and dried. NMR analysis revealed DS-Ac 2.92.

10.2.11 CTLev

LA swollen cellulose was prepared by stirring acetic acid swollen cellulose in LA at 50 °C for 30 minutes, the cellulose was press filtered using a sintered funnel. The LA solvent exchange process was repeated once. It was assumed that all the acetic acid had been removed with this preparation.

Levulinic anhydride was prepared using a N,N'-dicyclohexylcarbodiimide (DCC) coupling method. LA (50.0 g, 0.43 mol) dissolved in anhydrous ether (200 mL) and DCC (0.5 Eq|LA, 44.4 g, 0.22 mol) dissolved in anhydrous ether (266.6 mL) were combined and the reaction stirred overnight. Cooling the reaction solution on ice precipitated the dicyclohexylurea (DCU) by-product. The solution was filtered and cold ether (100 mL) used to wash the DCU precipitate. The levulinic anhydride[11] (87% yield, containing 5% unreacted levulinic acid) was recovered by distillation. ^{1}H NMR (500 MHz) δ 2.21 (s, 6H, H-5 and H-5'), 2.73 (m, 4H, H-2 and H-2'), 2.85 (m, 4H, H-3 and H-3'); ^{13}C NMR (125 MHz) δ 29.4 (C-2 and C-2', OC(O)*C*H$_2$CH$_2$), 30.1 (C-5 and C-5', C(O)*C*H$_3$), 37.7 (C-3 and C-3', OC(O)CH$_2$*C*H$_2$), 168.9 (C-1 and C-1', C(O)OC(O)), 206.2 (C-4 and C-4', *C*(O)CH$_3$).

LA swollen cellulose (2.13 g total mass, contains 0.73 g (4.5 mmol) dry cellulose) was combined with levulinic anhydride (9.96 g, 46.3 mmol) and sulfuric acid (4.9 µL) in a 50 mL RB flask. The reaction slurry was heated at 120 °C for 93 hours with stirring. The reaction solution was precipitated into a magnesium acetate solution (0.05 mol/L). The precipitate was collected by filtration and then dissolved in hot ethanol (70 °C) and re-precipitated by

[11] The levulinic anhydride / levulinic acid solution on storing for 2 years was observed to convert quantitatively to 4-levulinoyl-γ-valerolactone. It is assumed that levulinic acid in the presence of the anhydride cyclises to α-angelica lactone generating 1 mole of water, that in turn, hydrates one equivalent of anhydride. The reaction of α-angelica lactone and one equivalent of levulinic acid forms the observed species, and the remaining equivalent of levulinic acid from the decomposition of the anhydride propagates the conversion.

cooling the ethanol solution on ice. The precipitate was collected by filtration and dried. Spectral data is reported in Section 3.3; molecular weight analysis by SEC gave 8200 g/mol (M_p). T_g 71°C.

10.2.12 Wood pulp SEC analysis

Wood pulp (BKT, Kinleight pinus) was analysed by SEC[12] as follows: The cellulose (100 mg) was successively swollen in water (3 washings of 10 mL for 1 hour), acetone (3 washings of 10 mL for 1 hour) and DMAc (3 washings of 10 mL for 1 hour). A 10 mg/mL solution of the swollen cellulose was prepared by dissolution of the cellulose in a dry 8% DMAc/LiCl solution, the sample was shaken for 1 hour then stored at 4 °C for 18 hours. Standard SEC conditions were used although an eluent of anhydrous 8% DMAc/LiCl was used. Molecular weight analysis is reported in Section 3.9.2.

10.2.13 CAB (CT-RPa004A and CT-RPa004B)

CT-RPa004A: Acetic anhydride (1.95 g, 19.1 mmol, 2 Eq|OH) and sulfuric acid (1.8 µL, 33.8 nmol) were charged to a 50 mL RB flask. Butyric acid pre-swollen cellulose (1.56 g total mass, contains 0.5 g (3.1 mmol) dry cellulose) was charged to the RB flask and formed a slurry. The slurry was heated with stirring at 120 °C for 50 minutes. Standard work-up conditions were employed. NMR analysis gave DS-But 0.53 and DS-Ac 2.59.

CT-RPa004B: Butyric anhydride (2.65 g, 16.7 mmol, 2 Eq|OH) and sulfuric acid (1.8 µL, 33.8 nmol) were charged to a 50 mL RB flask. Acetic acid pre-swollen cellulose (1.36 g total mass, contains 0.45 g (2.7 mmol) dry cellulose) was charged to the RB flask and formed a slurry. The slurry was heated with stirring at 120 °C for 50 minutes. Standard work-up conditions were employed. NMR analysis gave DS-But 2.78 and DS-Ac 0.41.

[12] The operation of the HPLC was kindly completed by Dr Ian Sims, Science Team leader, Callaghan Innovation.

10.2.14 Solvent extraction

BLAC (CT-x429-1) was vigorously agitated in solvent (15 mL; Table 10-4) for 1.5 hours then centrifuged (4000 rpm). The supernatant was removed, the insoluble pellet was re-suspended in the same solvent (10 mL) and the process was repeated once more. The soluble material was recovered from the supernatant and the pellet (insoluble) was dried at 50 °C for 18 hours. The DS was analysed by HPLC and the results are given in Table 10-4.

Solvent	Mass CT-x429-1 used (g)	Soluble material (g)	DS-Ac	DS-But	DS-Lev
Methanol	462.2	287.3	0.45	1.09	1.14
Toluene	441.4	149.0	0.43	0.98	1.12
MIBK	538.1	403.9	0.42	1.05	1.15

Table 10-4 Extraction solvents, recovered soluble material weights and DS (by HPLC).

10.2.15 Hydrazinolysis (CT-RPa004G)

BLAC (CT-x429-1, 2 g) was dissolved in a 4:1 solution of pyridine:glacial acetic acid (50 mL) and to this 80% aqueous hydrazine (1.56 mL, 25.7 mmol) was added and the reaction stirred for 2 hours at RT. The polymer was precipitated into vigorously stirring DI water (300 mL), stirred for 1.5 hours then filtered through a Teflon membrane (200 µm mesh size) and thoroughly washed. The precipitate was dried in a 50 °C oven for 18 hours to give 842 mg of product. NMR characterisation was carried out in d^5-pyridine. Accurate DS calculations could not be accomplished, although ^{13}C NMR analysis demonstrated the loss of all peaks relating to levulinyl groups.

10.2.16 CT-RPa004G acetylation

CT-RPa004G (489 mg) in a 1:1 pyridine:acetic anhydride (20 mL) solution with catalytic DMAP.HCl was stirred overnight at RT. The solution was precipitated into DI water (200 mL), stirred for 2 hours then filtered through a Teflon membrane (mesh size 200 µm) and dried at 50 °C for 18 hours. NMR analysis revealed DS-But 1.07 and DS-Ac 1.99.

10.2.17 Anhydride content

Acetic anhydride, LA (Table 10-5), and sulfuric acid (6.9 µL, 129 nmol) were charged to a 50 mL RB flask, generating a mild exotherm. Pre-swollen acetic acid wet cellulose (1.71 g total mass, contains 1 g (6.2 mmol) dry cellulose) was charged to the reaction solution forming a slurry. The LA/Acetate (total acetate) ratio was maintained at 0.52. The slurry was heated and stirred at 120 °C for 2 hours. Standard work-up conditions were used. Analysis by NMR was completed and is reported in Table 10-5.

Acetic anhdride (Eq|OH)	Acetic anhydride (mmol)	Levulinic acid (mmol)	DS-Lev	DS-Ac
1.2	22.1	37.8	1.61	3.19
1.5	27.8	43.7	1.56	3.16
2.0	37.0	53.2	1.31	3.13
3.0	55.5	72.5	1.15	3.09
6.0	111.1	130.4	0.87	2.95

Table 10-5 Acetic anhydride and LA reaction quantities and the DS of the resulting LAC (NMR analysis).

10.2.18 Levulinyl ester incorporation with constant anhydride content

Acetic anhydride (5.67 g, 55.6 mmol), LA (Table 10-6) and sulfuric acid (9.06 mmol/L) were charged to a 100 mL RB flask which resulted in a mild exotherm. Pre-swollen acetic acid wet cellulose (1.52 g total mass, contains 1 g (6.2 mmol) cellulose) was charged to the reaction solution forming a slurry. The slurry was heated with stirring at 120 °C for 2 hours. Standard work-up conditions were used. Analysis by NMR was completed and the results are given in Section 4.3.1.

LA/Ac_2O (mol/mol)	Levulinic acid (mmol)	Total reaction volume (mL)	cH_2SO_4 (uL)
0.33	18.5	8.6	4.2
0.67	37.0	10.5	5.1
1.00	55.6	12.4	6.0
1.33	74.1	14.3	6.9
1.67	92.6	16.2	7.8
2.00	111.2	18.1	8.7

Table 10-6 LAC reaction quantities, for the samples produced for the LAC constant anhydride content reaction series.

10.2.19 Levulinyl ester incorporation with constant reaction volume

Acetic anhydride, LA (Table 10-7) and sulfuric acid (9.6 µL, 9.06 mmol/L) with a reaction total volume of 20 mL were charged to a 100 mL RB flask which evolved a mild exotherm. Pre-swollen acetic acid wet cellulose (2.22 g total mass, 1 g (6.2 mmol) dry cellulose) was charged to the reaction solution forming a slurry. The slurry was heated with stirring at 120 °C for 2 hours. Standard work-up conditions were used. Analysis by NMR is reported and discussed in Section 4.3.1.

LA/Ac_2O (mol/mol)	Levulinic acid (mmol)	Acetic anhydride (mmol)
0.33	51.9	155.7
0.67	82.0	123.0
1.00	101.7	101.7
1.33	115.5	86.6
1.67	125.8	75.5
2.00	133.7	66.9

Table 10-7 Production of LAC with a constant reaction volume.

10.2.20 Effect of acetic acid

Acetic anhydride (5.67 g, 55.6 mmol), LA (7.78 g, 66.9 mmol), acetic acid (Table 10-8) and sulfuric acid (9.06 mmol/L) were charged to a 100 mL RB flask and a mild exotherm observed. Pre-swollen acetic acid-wet cellulose (1.52 g total mass, contains 1 g (6.2 mmol) dry cellulose) was charged to the reaction solution forming a slurry. The slurry was heated and stirred at 120 °C for 2 hours. Standard work-up conditions were used. The DS analysis was completed by NMR and the results are given in Table 10-8.

Acetic acid (mmol)	Total reaction volume (mL)	cH_2SO_4 (uL)	DS-Lev	DS-Ac
0.0	13.5	6.5	1.00	2.09
16.7	14.5	7.0	0.92	2.17
33.3	15.5	7.5	0.83	2.28
66.6	17.4	8.4	0.74	2.41
133.2	21.2	10.2	0.62	2.51

Table 10-8 LAC produced with a variation in the proportion of acetic acid (analysis by NMR).

10.2.21 Cellulose ester transesterification

Acetic anhydride, LA (Table 10-9) and sulfuric acid (9.06 mmol/L) were charged to a 50 mL RB flask maintaining a LA/Ac_2O molar ratio of 1.67 and evolved a mild exotherm. The relevant CTA was then dissolved forming a clear homogenous solution reaction solution (CTA; SH-x11-1) remained as a milky solution over the course of the reaction). The solution was heated and stirred at 120 ºC for 1 hour. Standard work-up conditions were used. The DS data, both pre- and post-reaction, are given in Section 4.4.

CTA source	CTA (g)	Levulinic acid (mmol)	Acetic anhydride (mmol)
SH-x11-1	0.5	46.3	27.8
CA 320S	1	92.6	55.6
CA 389-3	1	92.6	55.6

Table 10-9 Transesterification reaction series.

10.2.22 Reaction duration

Acetic anhydride (22.7 g, 222 mmol,), LA (43.0 g, 370 mmol) and sulfuric acid (34.9 µL, 9.06 mmol/L) were charged to a 250 mL RB flask evolving an exotherm. Pre-swollen acetic acid wet cellulose (6.1 g total mass, contains 4 g (24.7 mmol) dry cellulose) was charged to the reaction solution forming a slurry. The slurry was

heated with stirring at 120 °C. From the bulk reaction solution, 10 mL aliquots were sampled at pre-determined reaction times (15, 20, 30, 60 and 120 minutes) and individually worked-up using the standard conditions. NMR DS analysis was completed by NMR and the results are reported in Section 4.5.1.

10.2.23 Reaction temperature

Acetic anhydride (5.67 g, 55.6 mmol, 3 Eq|OH), LA (7.78 g, 66.9 mmol) and sulfuric acid were charged to a 100 mL RB flask and a mild exotherm was generated. Pre-swollen acetic acid-wet cellulose (1.52 g total mass, contains 1 g (6.2 mmol) dry cellulose) was charged to the reaction solution forming a slurry. The slurry was heated with stirring for 2 hours. Six reactions were completed with reaction temperature starting at 90 °C increasing to 140 °C in 10 °C increments. Standard work-up conditions were used. DS analysis was completed by NMR and the results are reported in Section 4.5.2.

10.2.24 Sulfuric acid catalyst concentration

Acetic anhydride (5.67 g, 55.6 mmol, 3 Eq|OH), LA (7.78 g, 66.9 mmol) and sulfuric acid (Table 10-10) were charged to a 100 mL RB flask and a mild exotherm was generated. Pre-swollen acetic acid wet cellulose (1.52 g total mass, contains 1 g (6.2 mmol) dry cellulose) was charged to the reaction forming a slurry. The slurry was heated with stirring at 120 °C for 2 hours. Standard work-up conditions were used. DS analysis was completed by NMR and the results are detailed in Section 4.5.3.

cH_2SO_4 (mmol/L)	cH_2SO_4 (uL)
2.3	1.6
4.4	3.3
9.1	6.5
18.1	13.1
36.2	26.1

Table 10-10 Sulfuric acid catalyst concentration reaction series.

10.2.25 SAIB plasticising

- LBC (CT-x298-3, 100 mg) was dissolved in ethyl acetate (1.3 mL). SAIB was added to 100 mg portions at 5, 10, 20 and 40 wt% additions as a 10% SAIB-ethyl acetate solution. The samples were vigorously mixed and recovered by solvent evaporation. T_g results are given in Section 4.8.1.1.
- BLAC (CT-RPa003K, 100 mg) was dissolved in ethyl acetate (1.3 mL). SAIB was added to individual 100 mg portions at 20, 40 and 80 wt% additions as a 10% SAIB-ethyl acetate solution. The samples were vigorously mixed and recovered by solvent evaporation. T_g results are given in Table 10-11.

CT-RPa003K	
Wt% SAIB	**T_g (°C)**
10	70
20	59
40	41
80	18

Table 10-11 CT-RPa003K plasticised with SAIB.

10.2.26 PEG plasticising

LBC (CT-x298-3, 100 mg) was dissolved in chloroform (1.5 mL) and PEG alkoxy amine[13] was added to individual portions at 6, 12, 18 and 24 wt% additions as a 10 mg/mL PEG solution in chloroform. The samples were stirred for 18 hours and recovered by solvent evaporation. T_g results are given in Section 4.8.1.2.

10.2.27 LA aliphatic mixed esters

Anhydride (55.6 mmol, 3 Eq|OH, Table 10-12), LA (8.6 g, 74.1 mmol) and sulfuric acid (9.06 mmol/L) were charged to a 100 mL RB flask which resulted in a mild exotherm. Pre-swollen LA-wet cellulose (2.21 g total

[13] The author thanks Jenny Mason (Senior Research Scientist, Callaghan Innovation) for the preparation of PEG alkoxy amine.

mass, contains 1 g (6.2 mmol) dry cellulose) was charged to the reaction solution forming a slurry. The slurry was heated with stirring at 120 °C for 2 hours. Standard work-up conditions were used with the follow alterations:

- Cellulose levulinate isobutyrate (LIBC) was precipitated into water (1200 mL).
- Cellulose levulinate propionate (LPC) was precipitated into water (600 mL).
- Cellulose levulinate hexanoate (LHC) was precipitated into water (500 mL) generating a soft amorphous solid. Water was decanted and the sticky material triturated with water (500 mL) at 40 °C for 2 hours then the water was decanted. The CE was dispersed into a 45 °C mixture of methanol and isopropanol (1:1) and upon cooling to 0 °C the polymer was recovered *via* filtration using Whatman number 2 filter paper. Re-precipitation from acetone (35 mL acetone poured into 16.6% aqueous AcOH (400 mL)) gave a solid which was washed with 16.6% aqueous AcOH (200 mL), 8.3% aqueous AcOH (200 mL) and finally water (200 mL).
- Cellulose levulinate valerate (VLC) was precipitated into water (500 mL) generating a soft amorphous solid. Water was decanted and the sticky material triturated with water (500 mL) at 40 °C for 2 hours. With this treatment the CE began to harden. Waste water was decanted and the trituration process was repeated at RT for 16 hours. CE was re-precipitated from acetone (35 mL) into water (500 mL).
- Cellulose levulinate butyrate (LBC) was precipitated into water (1200 mL).

The DS of the samples was analysed by NMR and the results are given in Section 4.7.

Anhydride	Mass used (g)	cH_2SO_4 (uL)
Acetic	5.67	10.8
Propanoic	7.23	9.9
Butyric	8.79	9.0
Isobutyric	8.79	9.1
Valeric	10.35	8.1
Hexanoic	11.91	7.2

Table 10-12 LA aliphatic mixed esters.

10.2.28 LBC ester incorporation

Butyric anhydride (17.58 g, 111.1 mmol), LA (Table 10-13) and sulfuric acid (9.06 mmol/L) were charged to a 100 mL RB flask and a mild exotherm observed. Pre-swollen LA-wet cellulose (7.56 g total mass, contains 2 g (12.3 mmol) dry cellulose) was charged to the reaction solution and a slurry formed. The slurry was heated and stirred at 120 °C for 2 hours. Standard work-up conditions were employed. The DS was assessed by NMR and the results are shown below (Table 10-13).

Sample	LA/But_2O	Levulinic acid (g)	Levulinic acid (mmol)	cH_2SO_4 (uL)	DS-Lev	DS-But	DS-Total
CT-x297-3	3.00	38.70	333.3	25.3	2.26	0.78	3.04
CT-x297-2	2.60	33.54	288.9	23.0	2.13	0.82	2.95
CT-x297-1	2.30	29.67	255.5	21.4	2.04	0.90	2.94
CT-x298-1	2.00	25.80	222.2	19.8	1.97	0.97	2.94
CT-x298-2	1.60	20.64	177.8	17.6	1.76	1.20	2.96
CT-x298-3	1.30	16.77	144.4	15.9	1.52	1.47	2.99
CT-x299-1	1.00	12.90	111.1	14.3	1.10	1.81	2.91
CT-x299-2	0.60	7.74	66.7	12.1	0.46	2.35	2.81

Table 10-13 LBC reaction products with different LA/But_2O ratios (DS calculated by NMR analysis).

10.2.29 Cellulose tributyrate

Butyric anhydride (24.18 g, 152.8 mmol) and sulfuric acid (14.3 µL, 9.06 mmol/L) were charged to a 100 mL RB flask. Butyric acid pre-swollen cellulose (2.13g, 13.1 mmol dry cellulose) was charged to the RB flask forming a slurry which was heated with stirring at 120 °C for 2 hours. Standard work-up conditions were employed. Analysis by NMR gave a DS-But 3.06.

10.2.30 BLAC – levulinyl ester incorporation

Butyric anhydride (17.58 g, 111.1 mmol), LA (Table 10-14) and sulfuric acid (9.06 mmol/L) were charged to a 100 mL RB flask and a mild exotherm generated. Pre-swollen acetic acid-wet cellulose (4.83 g total mass, contains 2.00 g (12.3 mmol) dry cellulose) was charged to the reaction solution and formed a slurry. The slurry was heated with stirring at 120 °C for 2 hours. Standard work-up conditions were employed. NMR analysis was completed and the DS was determined using HPLC, the results of which are given in Table 10-14.

Sample	LA/But_2O	Levulinic acid (g)	Levulinic acid (mmol)	cH_2SO_4 (uL)	DS-Ac	DS-But	DS-Lev	DS-Total
CT-x306-1	3.00	38.70	333.3	25.3	0.32	0.53	1.52	2.37
CT-x306-2	2.60	33.54	288.9	23.0	0.33	0.56	1.48	2.37
CT-x306-3	2.30	29.67	255.5	21.4	0.35	0.62	1.46	2.43
CT-x309-3	2.00	25.80	222.2	19.8	0.41	0.73	1.45	2.59
CT-x309-2	1.60	20.64	177.8	17.6	0.47	0.85	1.37	2.69
CT-x309-1	1.30	16.77	144.4	15.9	0.52	0.98	1.20	2.70
CT-x311-1	1.00	12.90	111.1	14.3	0.61	1.12	0.99	2.72
CT-x311-2	0.60	7.74	66.7	12.1	0.83	1.54	0.52	2.89
CT-x311-3	0.30	3.87	33.3	10.4	1.03	1.81	0.15	2.99
CT-x311-1	0.10	1.29	11.1	9.3	-	-	-	-

Table 10-14 BLAC produced with different LA/But_2O ratios (DS calculated by HPLC analysis).

10.2.31 BLAC acetic acid variation, constant LA/But_2O molar ratio

Butyric anhydride (4.40 g, 27.8 mmol), LA (5.16 g, 44.4 mmol), acetic acid and sulfuric acid (4.8 µL, 90 nmol) were charged to a 100 mL RB flask evolving a mild exotherm. Four reactions were completed in parallel with increasing added acetic acid quantities (0, 6.5, 12.9 and 25.8 mmol of acetic acid). Pre-swollen acetic acid-wet cellulose (0.85 g total mass, contains 0.5 g (3.1 mmol) dry cellulose) was charged to the LA reaction solution forming a slurry. The slurry was heated with stirring at 120 °C for 2 hours. Standard work-up conditions were employed. The DS of the product was calculated from HPLC analysis, the results of which are given in Section 4.9.

10.2.32 BLAC acetone solubility

.For each of the BLAC samples prepared in Section 10.2.30, BLAC (1.2 g) was dissolved in acetone (60 mL) and centrifuged at 4500rpm for 5 minutes. The supernatant was decanted and the pellet was re-suspended acetone (20 mL) and centrifuged at 4500rpm for 5 minutes. The supernatant was collected and this process was repeated once more. The pellet was dried at 50 °C for 24 hours. Distillation of the supernatant recovered the BLAC polymer. Solubility analysis is reported in Section 4.9.

10.2.33 Alpha cellulose preparation

Shredded wood pulp (1 g, BKT, Kinleith bleached pinus) was steeped in a sodium hydroxide solution (12 mL, 17.5% w/v) for 5 minutes. A further sodium hydroxide aliquot (3.5 mL, 17.5% w/v) was added and allowed to steep for 10 minutes. This process was repeated 3 times (total sodium hydroxide solution added 26 mL). The wood pulp slurry was diluted with water (25 mL) and left to stand for 5 minutes. Using a glass sintered filter, the wood pulp was filtered and washed with water (250 mL). The wood pulp was re-slurred in a 10% acetic acid solution (15 mL) and allowed to stand for 5 minutes. The wood pulp was filtered on a glass sinter and washed with water (250 mL). The α-cellulose was dried under vacuum at 55 °C. This methodology was scaled directly for the production of 300 g of α-cellulose.

10.2.34 BLAC LA/But_2O 0.5 (CT-RPa003K)

α-Cellulose (120 g) was stirred in warm water (5L, 40 °C) for 3 hours, then press filtered and this process was repeated. The water swollen α-cellulose was soaked in glacial acetic acid (1.75 L) for 48 hours, and then press filtered. The acetic acid wet α-cellulose was then soaked in butyric acid (1.25 L) for 3 hours and press filtered.

Butyric anhydride (882 g, 5.57 mol), LA (310 g, 2.66 mol) and sulfuric acid (0.7 mL, 9.06 mmol/L) were charged to a 3 L RB flask, evolving an exotherm. The solution was pre-heated to 117 °C. Pre-swollen butyric acid wet α-

cellulose (347.6 g total mass, contains 99.2 g (612 mmol) dry cellulose) which had been pre-heated to 60 °C was charged to the reaction vessel forming a reaction slurry. The slurry was heated with stirring at 117 °C for 2 hours.

The reaction was cooled to 50 °C and DI water (70 mL) added to quench the reactive species followed by 5% magnesium acetate dope solution (500 mL, 1:1 acetic acid water). The doped solution was cooled to RT under continuous gentle agitation before precipitation into water (28 L) with vigorous stirring for 2 hours. The precipitate was filtered through a Teflon membrane (pore size 200 µm) and re-suspended in water (15 L), stirred for 15 hours, filtered, and the plug washed with water (2 L). The process of re-suspending, filtration and plug washing was repeated until washings were of a neutral pH. The material was then dried in a vacuum oven at 65 °C for 24 hours yielding 205 g (91%) of BLAC. HPLC analysis gave DS-But 2.23, DS-Ac 0.34 and DS-Lev 0.35.

10.2.35 BLAC LA/But$_2$O 1.3 (CT-x429-1)

Butyric anhydride (470 g, 2.97 mol), LA (448 g, 3.86 mol) and sulfuric acid (0.47 mL, 9.06 mmol/L) were charged to a 3 L RB flask and an exotherm was generated. Pre-swollen acetic acid wet α-cellulose (91.8 g total mass, contains 53.2 g (328 mmol) dry cellulose) was charged to the reaction vessel forming a slurry. The slurry was heated with stirring at 120 °C for 1 hour. The reaction was cooled to 80 °C, DI water (100 mL) was added and the mixture stirred for 5 minutes. The reaction solution was then cooled on ice, before completing the standard work-up procedure. The product was dried in a vacuum oven at 65 °C for 24 hours to yield 97.5 g (79%) of BLAC. HPLC analysis gave DS-But 1.03, DS-Ac 0.45 and DS-Lev 1.16.

10.2.36 BLAC LA/But$_2$O 1.6 (CT-x416-1)

Butyric anhydride (222 g, 1.41 mol), LA (261 g, 2.25 mol) and sulfuric acid (0.24 mL, 9.06 mmol/L) were charged to a 1.5 L RB flask and an exotherm was generated. Pre-swollen acetic acid wet α-cellulose (37.9 g total mass, contains 25 g (154 mmol) dry cellulose) was charged to the reaction vessel forming a slurry. The slurry was heated and stirred at 120 °C for 1.5 hours. The reaction was cooled to 80 °C, DI water (50 mL) was added and the mixture stirred for 15 minutes. The reaction solution was then cooled on ice, before completing the standard

work-up procedure. The product was dried in a vacuum oven at 65 °C for 24 hours, yielding 53 g (88%) of BLAC. HPLC analysis gave DS-But 0.86, DS-Ac 0.33 and DS-Lev 1.45.

10.2.37 Alternative acid catalysts for the preparation of LAC

Acetic anhydride (2.86 g, 27.7 mmol), LA (6.02 g, 51.8 mmol) and catalytic acid (Table 10-15) were charged to a 50 mL RB flask. Pre-swollen acetic acid wet cellulose (1.2 g total mass, contains 0.5 g (3.1 mmol) dry cellulose) was charged to the LA solution forming a reaction slurry. The slurry was heated and stirred at 120 °C for the duration of the experiment (Table 10-15). Standard work-up conditions were used. The DS of the product was calculated from NMR analysis and the results are reported in Section 5.1.

Catalytic acid	Mass acid used (mg)	Reaction time (hours)
HCl 36 wt%	3.37	20
Phosphoric acid 85 wt%	9.07	20
MSA	8.89	2
pTSA	26.40	2
TFA	10.60	20

Table 10-15 Comparison of acids used in the production of LAC.

10.2.38 Reaction solvent

Acetic anhydride (9.66 g, 55.6 mmol), LA (14.65 g, 126.2 mmol), reaction solvent (Table 10-16) and sulfuric acid (9.8 mmol/L) were charged to a 150 mL RB flask equipped with a condenser and a mild exotherm was evolved. Pre-swollen acetic acid-wet cellulose (3.22 g total mass, contains 1 g (6.2 mmol) dry cellulose) was charged to the levulinic acid solution forming a slurry. The slurry was heated to an oil bath temperature of 65 °C effecting reflux of the reaction mixture with stirring for 18 hours. The reactions were cooled to RT and the solvents removed by distillation where applicable. The reactions where NMP, DMF and DMSO were used were not distilled upon reaction completion, but since these solvents are water-soluble, they were effectively removed

during precipitation of the CE from the crude reaction mixture into water. Samples were worked-up using the standard conditions. NMR analysis is shown in Table 10-17 and is discussed in Section 10.2.1.

Reaction solvent	Density (g/mol)	Volume of solvent used (mL)	cH_2SO_4 (uL)
Acetone	0.79	20.3	21.9
Chloroform	1.48	10.9	17.0
Dimethylformamide	0.94	17.1	20.3
Dimethylsulfoxide	1.10	14.6	19.0
Dioxane	1.03	15.6	19.5
Ethyl acetate	0.90	17.9	20.7
Ethylene dichloride	1.25	12.9	18.1
Methyl isobutyl ketor	0.80	20.1	21.8
Methylene chloride	1.33	12.1	17.7
N-Methyl-2-pyrrolido	1.03	15.7	19.5
Tetrahydrofuran	0.89	18.1	20.8

Table 10-16 Details of reaction co-solvents.

Chlorinated solvents	DS-Ac	DS-Lev	DS-Lactone	DS-Total
Chloroform	1.48	1.33	0.00	2.81
Ethylene dichloride	1.76	1.30	0.00	3.06
Methylene chloride	1.37	1.27	0.06	2.70

Table 10-17 DS data for $CDCl_3$-soluble samples using chlorinated solvents.

10.2.39 LAC reaction calorimetry

LAC calorimetry was completed using an HEL similar reaction calorimeter controlled with winISO using internal power compensation. LA (306 g, 2.64 mol) and cH_2SO_4 (240 µL, 9.1 mmol/L) were charged to a 1 L Buchi glass reactor. The reactor and jacket set point were 60 and 45 °C respectively. The LA solution was stirred at 300 rpm with a 4 blade turbine agitator set at a 45° pitch. A PT-100 1/4" probe and internal wire heating element acted as baffles. Acetic anhydride (244 g, 2.38 mol) was dosed in at 8 g/min and the reaction energy was monitored. Data analysis was completed using HEL winIQ software for internal power compensation. The results are discussed in Section 6.

10.2.40 Scale-up reaction (LAC 500.1, 500 g)

LA (4.3 kg, 38.7 mol) was charged to a 50 L jacketed temperature controlled reactor equipped with a central pneumatic paddle stirrer and the temperature maintained at 35 °C to keep LA in the liquid phase (m.p. 33 °C). Sulfuric acid catalyst (6.36 g, 64.8 mmol) was charged while stirring. Acetic anhydride (2.8 kg, 27.8 mol) was charged slowly over a 20 minute period to the reactor while stirring, and the reaction solution temperature was monitored during this addition to ensure the reaction temperature did not exceed 60 °C. Pre-swollen cellulose was charged to the reactor over a 15 minute period with vigorous stirring. The reactor temperature was raised to 120 °C for 4 hours with vigorous stirring. Once 4 hours had elapsed the reaction solution was cooled to 30 °C over 35 minutes.

A $Mg(OAc)_2$ dope solution (250 g $Mg(OAc)_2$, 3.13 kg water, 3.13 kg acetic acid) was added to the reaction mixture and stirred. The doped reaction solution was precipitated into water (75 L). This precipitated solution was stirred for 1 hour at RT before the precipitate was transferred to a 20 L filter dryer and filtered. Three identical washes were completed: the filter cake was slurred in water (20 L), left for 1 hour for the precipitate to settle, then filtered and followed by a plug wash with water (5 L). The resultant dried LAC polymer was dissolved into acetone (2.1 L) and the LAC polymer solution precipitated into vigorously stirred water (30 L), stirred for 1 hour and left to settle. The recovered precipitate was filtered and washed twice with 12.5 L of water, filtering between washes. The product was dried under reduced pressure at 50 °C for 48 hours to give 891 g of LAC 500.1 polymer (80% yield). Analysis of the LAC 500.1 product is given in Section 6.

10.2.41 Preparation of BLAC phthalate

BLAC levulinyl group removal (DS-Lev 0.87 being removed) was completed as follows: BLAC (CT-x416-1, 23 g) was dissolved in a pyridine:acetic acid (4:1, 500 mL) solution. Hydrazine (80%, 3.15 mL, 51.6 mmol) was added to the BLAC solution at RT and the solution stirred at 60 °C for 3 hours. BLAC was recovered by precipitation into water (1200 mL). The precipitate was stirred for 2 hours then filtered and re-suspended in water (1200 mL)

and stirred for 2 hours and filtered. The precipitate was dried in a 50 °C for 18 hours and yielded 16 g of material. HPLC analysis gave DS-Ac 0.37, DS-But 0.83 and DS-Lev 0.59.

Following hydrazinolysis, BLAC (16.2 g) was dissolved in acetic acid (200 mL) with phthalic anhydride (16 g, 96.3 mmol) and sodium acetate (16 g, 195 mmol) and the solution was heated at 70 °C for 4 hours. The reaction was cooled to RT and precipitated into water (1500 mL) and stirred for 2 hours. The precipitate was recovered by filtration, then re-suspended in water (1200 mL) and stirred for 2 hours and filtered. This process was repeated once more. The precipitate (BLAC phthalate) was dried in an oven overnight at 80 °C. NMR analysis was completed in d^6-acetone, acid number 104 mg KOH/g.

10.2.42 Carboxy methyl cellulose (CMC)-free acid preparation

Three methods were attempted to generate the free acid form of CMC:

- Low viscosity CMC (1 g) was added to a 10% sulfuric acid solution (30 mL) at 60 °C where the CMC quickly formed a gel. The gel was stirred for 30 minutes following addition of 5% sulfuric acid. The gel was filtered and washed with DI water at 75 °C. The gel was then stirred in glacial acetic acid (30 mL) for 45 minutes, filtered and re-suspended in glacial acetic acid, stirred for an additional 2 hours and filtered.
- Low viscosity CMC (1 g) was stirred in an ethanol (19 mL) and sulfuric acid (1.25 mL) solution at 80 °C for 15 minutes, then filtered and washed with 80% hot ethanol until the washings were pH 7. The washed precipitate was stirred in glacial acetic acid for 1.5 hours then filtered and the process was repeated. This method was taken from ASTM D1439-03 [222].
- Low viscosity CMC (10 g) was dissolved in DI water (220 mL), sulfuric acid (22 mL) was added and the solution stirred overnight forming a milky gel. Ethanol (500 mL) was added to the gel and the suspension was stirred for 2 hours and the gel was collected by filtration. The recovered gel was then stirred in glacial acetic acid (250 mL) for 2 hours then filtered and the process was repeated.

The esterification of the CMC-free acid species was as follows:

- Acetic anhydride (1.53 g, 15 mmol), LA (1.74 g, 15 mmol) and sulfuric acid (2 µL, 37.5 nmol) were charged to a 50 mL RB flask, evolving a mild exotherm. Pre-swollen acetic acid wet CMC (0.25 g dry weight CMC) was charged to the reaction solution. The reaction was heated and stirred at 120 °C for 2 hours but the CMC failed to dissolve into the reaction solution. Standard work-up conditions were used. The resultant product was insoluble in the expected solvents (chloroform, acetone or water) and was not characterised further (discussed in Section 7.2).

10.2.43 Levulinyl carboxyl oxime model compound

A model compound for oxime linking was prepared as follows: iso-butyryl levulinate (50 mg, 291 µmol) and carboxymethyl)hydroxylamine hemihydrochloride (32.4 mg, 296 µmol) were dissolved in a mixture of acetonitrile (1 mL), acetic acid (100 µL), DCM (1 mL) and isopropyl alcohol (200 µL). The solution was heated to 50 °C for 1 hour. Following this, the solvents were removed by evaporation to give the model compound **(10)**.

^{1}H NMR (500 MHz) δ 0.93 (d, *J* = 6.7 Hz, 4H, H-3'), 1.90 (s, 3H, H-5, Z), 1.92 (s, 3H, H-5, E), 1.92 (m obscured, 1H, H-2'), 2.54 (m, 2H, H-2, E), 2.54 (m, 2H, H-3, E), 2.61 (m, 2H, H-3, Z), 2.67 (m, 2H, H-2, Z), 3.86 (d, *J* = 6.8 Hz, 2H, H-1', E), 3.88 (d, *J* = 6.8 Hz, H-1', Z), 4.59 (s, 2H, H-6, E), 4.61 (s, 2H, H-6, Z); ^{13}C NMR (125 MHz) δ 14.9 (C-5, CCH_3, E), 19.0 (C-3', (CH_3)$_2$CH), 19.7 (C-5, CCH_3, Z), 25.1 (C-2, OC(O)CH_2, Z), 27.8 (C-2', (CH_3)$_2$CH), 30.1 (C-3, CH_2CH_2, Z), 30.3 (C-2, OC(O)CH_2, E), 30.9 (C-3, CH_2CH_2, E), 69.7 (C-6, OCH_2C(O)O), 70.7 (C-1', CHCH_2), 158.3 (C-4, C=N, E),159.1 (C-4, C=N, Z), 172.8 (C-1, OC(O)), 174.9 (C-7, C(O)OH, Z), 175.1 (C-7, C(O)OH, E); TOF-HRMS found 268.1159, [$C_{11}H_{19}NO_5Na$+] calc. 268.1161.

10.2.44 Carboxylation of BLAC and subsequent carboxyl group methylation

Both CT-x429-1 (23.7 g) and O-(carboxymethyl)hydroxylamine hemihydrochloride (1.57g, 14.3 mmol) were dissolved in a mixture of chloroform:methanol (6:3, 300 mL) and the solution was stirred for 2.5 hours. The product was recovered and dried at 50 °C for 24 hours to yield 25.1 g of material. Theoretical un-methylated

acid number 34 mg KOH/g, actual acid number 3 mg KOH/g. ^{1}H NMR spectroscopy characterisation given in Section 7.4 and ^{13}C NMR spectroscopy assignment shown in Figure 10-6.

^{13}C δ	Assignment
Side chain signals	
13.6	C-4""
14.9	C-5''' (E)
18.2	C-3""
19.7-21.0	C-5''' (Z), C-2'
24.9	C-2''' (Z)
27.8	C-2"
29.3-30.9	C-5", C-3''' (E, Z), C-2''' (Z)
35.8	C-2""
37.8	C-2"
51.8	C-8""
70.2	C-6""
158.0	C-4'''
168-174	C-1' ester[a]
206.5	C-4"
Cellulose signals	
62.2	**C-6**
71.2	**C-2**
72.3	**C-3**
72.6	**C-5**
75.9	**C-4**
100.4	**C-1**

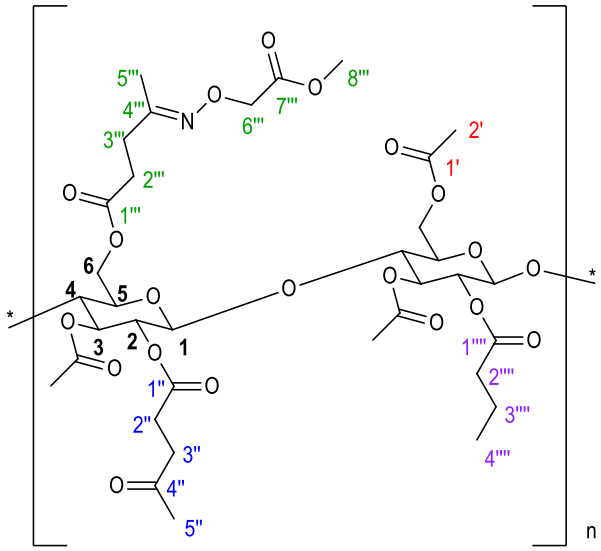

Figure 10-6 ^{13}C NMR assignments of oxime carboxylated and methylated BLAC. [a] A series of complex peaks relating to all of the CE ester carbonyls.

10.2.45 Preparation of CAB phthalate (CT-RPa008A)

Phthalic anhydride (10 g, 67.5 mmol) and anhydrous sodium acetate (10 g, 121.9 mmol) were added to Eastman CAB 553.04 (10 g, 32.6 mmol) stirring in glacial acetic acid (100 g, 1.66 mol) in a 250 mL RB flask. The reaction solution was heated to 60 °C for 15 hours, then cooled and the product precipitated into vigorously stirring water

(800 mL) and stirred for a further 2 hours at a reduced rate. The wet precipitate was recovered on Whatman No.2 paper and re-suspended in water (300 mL) and stirred for 1 hour. This process was repeated before the product was dried in a 50 °C oven for 24 hours. Yield 11.5 g.

To form the free acid, after drying the material, a 5 g portion was re-dissolved in acetone (70 mL) and concentrated HCl (1.14 mL, 13.2 mmol) was slowly added to the solution, then stirred for 1 hour. The CAB phthalate was precipitated into DI water (500 mL), stirred for 2 hours and filtered through a Teflon membrane (200 µm pore size). The precipitate was washed with DI water until the washings were pH neutral, then oven dried at 50 °C for 24 hours. NMR spectroscopy analysis gave DS-But 1.99, DS-Ac 0.08 and DS-Phthalate 0.41. Acid number is reported in Section 8.4

10.2.46 Preparation of CAB succinate (CT-RPa008B)

Succinic anhydride (10 g, 84.7 mmol) and anhydrous sodium acetate (10 g, 121.9 mmol) were added to Eastman CAB 553.04 (10 g, 32.6 mmol) stirring in glacial acetic acid (100 g, 1.66 mol) in a 250 mL RB flask. The reaction solution was heated to 60 °C for 15 hours, then cooled and the product was precipitated into vigorously stirring water (800 mL) and stirred for a further 2 hours at a reduced rate. The wet precipitate was recovered on Whatman No.2 paper and re-suspended in water (300 mL) and stirred for 1 hour. This process was repeated before the product was dried in a 50 °C oven for 24 hours. Yield 11.1 g.

To form the free acid, after drying the material, a 3 g portion was re-dissolved in acetone (40 mL) and concentrated HCl (0.75 mL, 8.7 mmol) was added slowly to the solution, then stirred for 1 hour. The CAB succinate was precipitated into DI water (300 mL), stirred for 2 hours and filtered through a teflon membrane (200 µm pore size). The precipitate was washed with DI water until the washings were pH neutral, then oven dried at 50 °C for 24 hours. NMR spectroscopy analysis gave DS-But 2.01, DS-Ac 0.10 and DS-Succinate 0.60. Acid number is detailed in Section 8.4.

10.2.47 Aqueous dispersion of CAB phthalate

CAB phthalate (CT-RPa008A, 1 g) was dissolved in an acetone (3.75 g) and propylene glycol n-butyl ether (PnB) (250 µL) in a sealed 50 mL RB flask. An aqueous dimethylethanolamine (21.7 µL, DI water 3.75 g) solution was added dropwise over a 2 minute period to the 28 °C CAB solution under mild agitation while the temperature was maintained at 28 °C using a water bath.

On completion of the DI water addition the bath temperature was maintained at 28 °C and the dispersion was put under vacuum starting at 330 mbar ramping down to 150 mbar over 30 minutes then maintaining 150 mbar for 90 minutes. PSD and solids analysis is given in Section 8.4.

10.2.48 Aqueous dispersion preparation of CAB succinate

CAB phthalate (CT-RPa008B, 1 g) was dissolved in an acetone (3.75 g) and propylene glycol n-butyl ether (PnB) (250 µL) solution in a sealed 50 mL RB flask. An aqueous dimethylethanolamine (21.7 µL, DI water 3.75 g) solution was added dropwise over a 2 minute period to the 28 °C CAB solution under mild agitation while the temperature was maintained at 28 °C using a water bath.

On completion of the DI water addition the bath temperature was maintained at 28 °C and the dispersion was put under vacuum starting at 330 mbar ramping down to 150 mbar over 30 minutes then maintaining 150 mbar for 90 minutes. PSD and solids analysis is given in Section 8.4.

10.2.49 BLAC (CT-RPa003K), acid number 32 mg KOH/g

Carboxylation was completed as follows: both CT-RPa003K (180 g) and O-(carboxymethyl)hydroxylamine hemihydrochloride (12.3 g, 113 mmol) were dissolved in DMSO (1000 mL and 50 mL respectively). The two solutions were combined and stirred for 18 hours. The carboxylated BLAC was precipitated into stirring DI water (15 L) and stirred for 2 hours. The precipitate was filtered through a Teflon membrane (200 µm pore size) then re-suspended in DI water (20 L) for 18 hours with gentle agitation before collection by filtration followed by a DI water (2 L) plug wash. The precipitate was dried at 60 °C under vacuum for 48 hours. The acetone-soluble

fraction was recovered by dissolution of the dried product (184 g) in acetone (1.8 L). Separation of the insolubles by centrifugation (4500 g for 20 minutes at 25 °C) gave a pellet which was re-suspended in acetone (1.5 L). The insolubles were again separated by centrifugation (4500 g for 20 minutes at 25 °C) and the supernatant decanted. The re-suspension and centrifugation steps were repeated once more. The acetone-soluble carboxylated BLAC was recovered by vacuum distillation (18 mbar at 50 °C for 3 hours) and finally dried under vacuum at 50 °C for 24 hours to give 184 g of product (87.9% mass recovery). The acid number of this material was 32 mg KOH/g and ^{13}C NMR structural assignment is given in Figure 10-7. The insoluble pellet was dried under vacuum at 50 °C for 24 hours (12.1% mass recovery).

^{13}C δ	Assignment
Side chain signals	
13.6	C-4""
14.9	C-5''' (E)
18.2	C-3""
19.7-21.0	C-5''' (Z), C-2'
24.9	C-2''' (Z)
27.8	C-2"
29.3-30.9	C-5", C-3''' (E, Z), C-2''' (Z)
35.8	C-2""
37.8	C-2"
69.8	C-6'''
158.0	C-4'''
168-174	C-1' ester[a], C-7'''
206.5	C-4"
Cellulose signals	
62.2	**C-6**
71.5	**C-2**
72.3	**C-3**
72.6	**C-5**
75.9	**C-4**
100.4	**C-1**

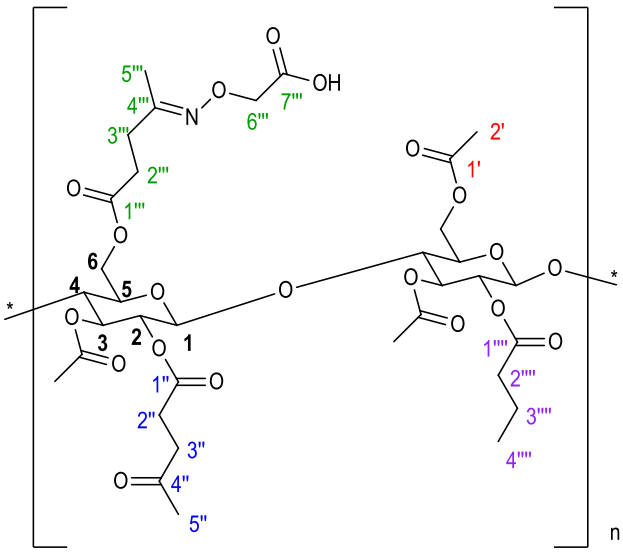

Figure 10-7 Oxime carboxylated BLAC ^{13}C NMR data.

10.2.50 BLAC (CT-x429-1), acid number 63 and 100 mg KOH/g

- **Acid number 63 mg KOH/g**

  Carboxylation was completed as follows; both CT-x429-1 (20.7 g) and O-(carboxymethyl)hydroxylamine hemihydrochloride (2.56 g, 23.4 mmol) were dissolved in DMSO (200 mL and 20 mL respectively). The two solutions were combined and stirred for 2 hours. The carboxylated BLAC was precipitated into stirring DI water (1.3 L) and stirred for 2 hours. The precipitate was filtered through a Teflon membrane (200µm pore size) then re-suspended in DI water (1 L) for 2hours with gentle agitation then collected by filtration. The precipitate was dried at 60 °C under vacuum for 18 hours. This gave 19.7 g of product with an acid number of 63 mg KOH/g.

- **Acid number 100 mg KOH/g**

  Carboxylation was completed as follows; both CT-x429-1 (4 g) and O-(carboxymethyl)hydroxylamine hemihydrochloride (984 mg, 8.97 mmol) were dissolved in DMSO (60 mL and 5 mL respectively). The two solutions were combined and stirred for 2 hours. The carboxylated BLAC was precipitated into stirring DI water (500 mL) and stirred for 2 hours. The precipitate was filtered through a Teflon membrane (200 µm pore size) then re-suspended in DI water (300 L) for 2 hours with gentle agitation then collected by filtration. The precipitate was dried at 60 °C under vacuum for 18 hours. This yielded 4.2 g of product with an acid number of 100 mg KOH/g.

10.2.51 Dispersion of BLAC (acid number 63 mg KOH/g)

BLAC (acid number 63 mg KOH/g, 0.5 g) was dissolved in acetone (3.3 mL) and agitated until a homogenous solution was obtained. DI water (200 µL) and DMEA (25 µL) were added to the polymer solution and thoroughly mixed. The polymer solution was added dropwise to vigorously stirring DI water (3.75 mL) in a 25 mL RB flask. The dispersion was concentrated using a rotary evaporator at 25 °C with a starting pressure of 300 mbar ramping down to 100 mbar over 30 minutes and maintaining 100 mbar for 1 hour. The PSD of the dispersion was analysed and is reported in Section 8.5.1.

10.2.52 Dispersion of BLAC (acid number 100 mg KOH/g)

In a 25 mL RB flask, BLAC (acid number 100 mg KOH/g, 0.5 g) was dissolved in acetone (3.3 mL) and agitated until a homogenous solution was obtained. DI water (200 µL) and DMEA (25 µL) was added to the polymer solution and thoroughly mixed. DI water (3.6 mL) was added dropwise over a 2 minute period to the BLAC acetone solution under mild agitation. The dispersion was concentrated using a rotary evaporator at 25 °C with starting pressure 300 mbar ramping down to 100 mbar over 30 minutes and maintaining 100 mbar for 1 hour. The PSD of the dispersion was analysed and is discussed in Section 8.5.1.

10.2.53 T-mixing and effect of neutralisation using TEA

Dispersions were prepared as follows; Low acid number BLAC (CT-RPa003K, 600 mg) was dissolved in acetone and (3.8 mL) the mixture was agitated until a homogenous solution had formed. To the organic polymer solution triethylamine (TEA; Table 10-18) and DI water (200 µL) were added and thoroughly mixed. The organic polymer solution was primed into a 6 mL syringe and an equal amount of DI water (4.5 mL) was primed into a second 6 mL syringe. Using a pneumatic syringe pump set at 6 bar, the anti-solvent and polymer solution streams were brought together and combined at a T-mixer interface. The dispersion was collected in a 25 mL RB flask and concentrated using a rotary evaporator at 25 °C with a starting pressure of 293 mbar ramping down to 90 mbar over 1 hour and maintaining 90 mbar for 1 hour. The PSD of the dispersion was analysed (see Section 8.6).

Percentage carboxyl neutralisation	TEA (uL)
21	10.0
32	15.0
42	20.0
53	25.0
58	27.5
64	31.0

Table 10-18 TEA content and percentage carboxyl neutralisation.

10.2.54 T-mixing and effect of ram pressure and mixing rate

Dispersions were prepared as follows; Low acid number BLAC (CT-RPa003K, 600 mg) was dissolved in acetone and (3.8 mL) the mixture was agitated until a homogenous solution had formed. To the organic polymer solution TEA (27 µL) and DI water (200 µL) were added and thoroughly mixed. The organic polymer solution was primed into a 6 mL syringe and an equal amount of DI water (4.5 mL) was primed into a second 6 mL syringe. Using a pneumatic syringe pump the anti-solvent and polymer solution streams were brought together and combined at a T-mixer interface. Four dispersions were prepared with increasing pneumatic ram air pressure (2, 3, 4 and 6 bar). The dispersion was collected in a 25 mL RB flask and concentrated using a rotary evaporator at 25 °C with starting pressure 293 mbar ramping down to 100 mbar over 1 hour and maintaining 100 mbar for 1 hour. PSD analysis of the dispersion produced is given in Section 8.7.

10.2.55 Dispersion distillation, increasing % solids

Dispersions were prepared as follows; Low acid number BLAC (CT-RPa003K, 1.2 g) was dissolved in acetone and (7.6 mL) the mixture was agitated until a homogenous solution had formed. To the organic polymer solution TEA (55 µL) and DI water (200 µL) were added and thoroughly mixed. The organic polymer solution was primed into a 12 mL syringe and an equal amount of DI water (8.8 mL) was primed into a second 12 mL syringe. Using a pneumatic syringe pump set at 5 bar the anti-solvent and polymer solution streams were brought together and converged at a T-mixer interface. The dispersion was collected in a 50 mL RB flask and concentrated using a rotary evaporator. The distillation pressure was reduced to 100 mbar over 1 hour and then maintained at 100 mbar for 1 hour. The distillations were preformed between 20-50 °C (Table 10-19). The PSD of the dispersion is reported in Section 8.8.

Distillation temperature (°C)	Distillation pressure range (mbar)
20	250-100
30	300-100
40	350-100
50	450-100

Table 10-19 Distillation temperature and starting pressure.

10.2.56 BLAC dispersion (29.1% solids)

Low acid number BLAC (CT-RPa003K, 7.6 g) was dissolved in acetone (45.6 mL) and the mixture was agitated until a homogenous solution had formed. To the organic polymer solution TEA (330 µL) and DI water (1.2 mL) were added and thoroughly mixed. The organic polymer solution (11 mL) was primed into a 12 mL syringe and an equal amount of DI water (11 mL) was primed into a second 6 mL syringe. Five separate runs were completed to disperse all of the material. Using a pneumatic syringe pump set at 5 bar the anti-solvent and polymer solution streams were brought together and combined at a T-mixer interface. The dispersion was collected in a 250 mL RB flask and concentrated using a rotary evaporator at 50 °C, starting pressure 350 mbar ramping down to 100 mbar over 1 hour and maintaining 100 mbar for 1 hour then ramping down to 80 mbar and maintaining for 30 minutes. The dispersion solids content was 29.1 w/v% and PSD was measured to be 220 ± 170 nm.

10.2.57 BLAC dispersions using increasing polymer solution concentration

Low acid number BLAC was (CT-RPa003K, 600 mg) dissolved in acetone (Table 10-20) and the mixture was agitated until a homogenous solution had formed. To the organic polymer solution TEA (27.5 µL) and DI water (200 µL) were added and thoroughly mixed. The organic polymer solution was primed into a 6 mL syringe and an equal amount of DI water (Table 10-20) was primed into a second 6 mL syringe. Using a pneumatic syringe pump set at 6 bar the anti-solvent and polymer solution streams were brought together and combined at a T-mixer interface. The dispersion was collected in a 25 mL RB flask and distilled using a rotary evaporator at 25 °C, starting pressure 293 mbar ramping down to 100 mbar over 1 hour and maintaining 100 mbar for 1 hour. PSD analysis of the dispersion is discussed in Section 8.8.2.

Volume of DI water (mL)	Volume of acetone (mL)	Polymer solution solids (w/w%)
4.5	3.8	16.7
3.5	2.8	21.3
3.1	2.4	24.3

Table 10-20 Acetone and water content.

10.2.58 Commercial amines

Low acid number BLAC (CT-RPa003K, 600 mg) was dissolved in acetone (3.8 mL) and the mixture was agitated until a homogenous solution had formed. The organic polymer solution was neutralised with an amine (Table 10-21), DI water (200 µL) added and the solution was thoroughly mixed. The organic polymer solution was primed into a 6 mL syringe and an equal amount of DI water (4.5 mL) was primed into a second 6 mL syringe. Using a pneumatic syringe pump set at 5 bar the anti-solvent and polymer solution streams were brought together and combined at a T-mixer interface. The dispersion was collected in a 25 mL RB flask and concentrated using a rotary evaporator at 30 °C with a starting pressure of 300 mbar ramping down to 10 mbar over 30 minutes and maintaining at 100 mbar for 1.5 hours. The dispersions PSD were analysed (Section 8.10).

Base	Volume (uL)
AMP-95	19.7
DMEA	19.6
Aqueous ammonia	27.2

Table 10-21 Commercial amines.

10.2.59 Post addition of coalescing solvents

A BLAC dispersion (18.1% solids, PSD 120 ± 283 nm) was weighed (500 mg ± 1%) into a 2 mL vial. The following solvents in the proportions stated were added to the BLAC dispersion as per Table 10-22 where weighed into the vial in the appropriate quantity and the vials were sealed and mixed for 3 minutes. The dispersion was allowed to rest for 20 minutes then was visually assessed for signs of destabilisation. Films were cast from the dispersions following the method of Section 10.1.7 and the results discussed in Section 8.11.1.

	Amount of solvent present (wt%)					
Solvent	**20.0**	**13.3**	**8.9**	**5.6**	**4.4**	**3.3**
Butyl cellosolve acetate	1	2	4	-	-	-
Butyl levulinate	1	1	1	3	-	5
Cellusolve	-	-	-	-	-	-
Diacetone alcohol	1	3	4	5	-	-
Dibasic ester	-	-	-	-	-	-
Diethylene glycol	1	2	3	-	4	-
Ethyl levulinate	1	1	1	5	-	5
Propylene n-butyl glycol ether	5	-	-	-	-	-

Table 10-22 Effect of coalescing solvents on film properties.

10.2.60 Ethyl levulinate

Ethyl levulinate was prepared as follows; ethanol (42 g, 875 mmol), LA (50 g, 422 mmol) and catalytic pTSA (50 mg, 289 µmol) were added to toluene (100 mL). The reaction was heated to reflux and using a Dean-Stark trap over 4 hours. During that time the ethanol was replenished (90 mL, 50 mL, 50 mL and 75 mL) due to the toluene-ethanol azeotrope. NMR of the crude reaction showed a 5.5:1 ratio of ethyl levulinate and 4-ethyl-γ-valerolactone based on previously isolated compounds. Sulfuric acid (50 µL) was added to the crude reaction mixture and it was heated (60 °C) for 15 minutes. The reaction was worked-up by diluting with chloroform (200 mL) and the solution washed with saturated sodium bicarbonate (100 mL), then twice with water (100 mL). The chloroform was dried over magnesium sulfate and the product recovered by distillation (15.33 g, 25.2%). NMR spectra of the product were identical to literature data [221].

10.2.61 Butyryl levulinate

Butyryl levulinate was prepared as follows; 1-Butanol (120 g, 1.6 mol), LA (49.5 g, 417.7 mmol) and catalytic pTSA (50 mg, 289 µmol) were added to toluene (150 mL). The reaction was heated to reflux and using a Dean-Stark trap water was collected (7.1 mL) over 3 hours. The reaction was worked-up by dilution with chloroform (200 mL) and the solution was washed with saturated sodium bicarbonate (100 mL), then twice with water (100

mL). The chloroform was dried over magnesium sulfate and the product recovered by distillation (56.15 g, 78.1%). The NMR spectra of the final product were identical to literature data [221].

10.2.62 SAIB plasticising of BLAC dispersions

Low acid number BLAC (CT-RPa003K) and SAIB (Table 10-23) were dissolved in acetone and the mixture was agitated until a homogenous solution had formed. To the organic polymer solution TEA and DI water (200 µL) were added and thoroughly mixed. The organic polymer solution was primed into a 12 mL syringe and an equal amount of DI water was primed into a second 12 mL syringe. Using a pneumatic syringe pump set at 5 bar the anti-solvent and polymer solution streams were brought together and converged at a T-mixer interface. The dispersion was collected in a 50 mL RB flask and concentrated using a rotary evaporator at a pre-determined temperature, from a starting pressure 300 mbar ramping down to the final pressure over 30 minutes and maintaining final pressure for the desired time (Table 10-23). PSD analysis of the product is discussed in Section 8.11.2.

Mass of SAIB (mg)	SAIB wrt BLAC (wt%)	Mass of BLAC used (g)	TEA (uL)	DI water antisolvent (mL)	Distillation time (hours) / Pressure (mbar) / Temperature (°C)
54	4.5	1200	55.0	8.8	2 / 100 / 30
108	9.0	1200	55.0	8.8	2 / 100 / 30
216	18.0	1200	55.0	8.8	2 / 100 / 30
216	36.0	600	27.5	4.5	1 / 50 / 40
300	50.0	600	27.5	4.5	1 / 50 / 40
360	60.0	600	27.5	4.5	1 / 70 / 40
480	80.0	600	27.5	4.5	1.25 / 90 / 40
600	100.0	600	27.5	4.5	2 / 100 / 30

Table 10-23 Parameters for BLAC dispersions prepared with SAIB.

10.2.63 Dispersion of BLAC modified with PEG carboxyl functionality

Butyric anhydride (28.3 g, 179.1 mmol), LA (34.3 g, 295.4 mmol) and sulfuric acid (26.3 µL, 9.06 mmol/L) were charged to a 250 mL RB flask and a mild exotherm was generated. Pre-swollen acetic acid-wet alpha cellulose

(8.9 g total mass, contains 3 g dry (18.5 mmol) cellulose, 98.3 mol acetic acid) was charged to the reaction solution forming a slurry. The slurry was heated and stirred at 120 °C for 1 hour. The standard work-up procedure was used. The precipitate was dried in at 50 °C for 24 hours. The analysis as estimated by NMR was DS-But 0.97, DS-Ac 0.64 and DS-Lev 1.38.

Carboxylation was completed as follows; BLAC (4 g) and O-(carboxymethyl)hydroxylamine hemihydrochloride (144 mg, 1.3 mmol) and PEG-alkoxy amine **(8)** (650 mg) were dissolved in a chloroform:methanol (9:1, 50 mL) solution. The solution was stirred for 2 hours. The PEG and carboxyl funtionalised BLAC was recovered by distillation. An acid number was not recorded, although the theoretical acid number was calculated to be 15 mg KOH/g.

PEG and carboxyl-modified BLAC (320 mg) was dissolved in acetone (2 mL) and diacetone alcohol (150 µL). The mixture was agitated until a homogenous solution had formed. A solution of DI water (4 mL) and DMEA (40 µL) was added dropwise to the stirring BLAC solution. The dispersion was distilled for 1.5 hours at 150 mbar giving a product with a solids content of 13.8 wt%.

10.2.64 Water-based SAIB paint

The dispersion was prepared as follows; Low acid number BLAC (CT-RPa003K, 6.2 g) and SAIB (4.96 g) were dissolved in acetone (40 mL) and the mixture was agitated until a homogenous solution had formed. To the organic polymer solution TEA (285 µL) and DI water (1 mL) were added and thoroughly mixed. The organic polymer solution (11 mL) was primed into a 12 mL syringe and an equal amount of DI water (11 mL) was primed into a second 12 mL syringe. Four separate runs were completed to disperse all of the material. Using a pneumatic syringe pump set at 5.5 bar the anti-solvent and polymer solution streams were brought together and combined at a T-mixer interface. The dispersion was collected in a 250 mL RB flask and distilled using a rotary evaporator at 40 °C, starting pressure 350 mbar ramping down to 40 mbar over 1.5 hour and maintaining 40

mbar for 1 hour then ramping down to. Dispersion solids were 46.98 wt% (26.1 wt% BLAC), and the PSD was measured to be 148 ± 210 nm.

10.2.64.1 Low-sheen white paint

The polymer dispersion was weighed in to a flask (2.5 g) and the white gloss mill base (provided by Resene Paints Ltd; Section 8.12) was added (913 mg). The mill base was used at a ratio of 1.4 g of mill base to 1 g of resin solids. The mill base was dispersed by hand shaking over 5 minutes. The paint was applied to an opacity card with a 100 µm draw down bar, pictured in Section 8.12.

10.2.64.2 Low-sheen grey paint

The polymer dispersion was weighed in to a flask (2.5 g) and the white gloss mill base (provided by Resene Paints Ltd; Section 8.12) was added (915 mg, white mill base tinted with black pigment). The mill base was used at a ratio of 1.4 g of mill base to 1 g of resin solids. The mill base was then dispersed by hand shaking over five minutes. The paint was applied to an opacity card with a 100 µm draw down bar, pictured in Section.8.12.

11 References

1. *Licence criteria for paints EC-07-13*. 2013, The New Zealand Ecolabelling Trust.
2. *Licence criteria for paints EC-07-09*. 2009, The New Zealand Ecolabelling Trust.
3. Glenny, M., *Acrylics*. 2011, Resene - R&D Team leader.
4. Keddie, J. and A. Routh, *An Introduction to Latex and the Principles of Colloidal Stability*, in *Fundamentals of Latex Film Formation*. 2010, Springer Netherlands. p. 1-26.
5. *Surface coatings raw materials and their usage*. Vol. 1. 1993: The New South Wales University Press.
6. Bozell, J.J. and G.R. Petersen, *Technology development for the production of biobased products from biorefinery carbohydrates-the US Department of Energy's "Top 10" revisited.* Green Chemistry, 2010. **12**(4): p. 539-554.
7. Hernandez, N., R.C. Williams, and E.W. Cochran, *The battle for the "green" polymer. Different approaches for biopolymer synthesis: bioadvantaged vs. bioreplacement.* Organic & Biomolecular Chemistry, 2014. **12**(18): p. 2834-2849.
8. Keddie, J. and A. Routh, *Particle Deformation*, in *Fundamentals of Latex Film Formation*. 2010, Springer Netherlands. p. 121-150.
9. Schneider, M., et al., *High solids content emulsions. I. A study of the influence of the particle size distribution and polymer concentration on viscosity.* Journal of Applied Polymer Science, 2002. **84**(10): p. 1878-1896.
10. Brown, G.L., *Formation of films from polymer dispersions.* Journal of Polymer Science, 1956. **22**(102): p. 423-434.
11. Klemm, D., H.P. Schmauder, and T. Heinze, *Cellulose*, in *Biopolymers Online*. 2005, Wiley-VCH Verlag GmbH & Co. KGaA.
12. O'Sullivan, A.N.T.O., *Cellulose: the structure slowly unravels.* Cellulose, 1997. **4**(3): p. 173-207.
13. Klemm, D., et al., *Cellulose: Fascinating biopolymer and sustainable raw material.* Angewandte Chemie - International Edition, 2005. **44**(22): p. 3358-3393.
14. Yarsley, V.E., et al., *Cellulosic Plastics*. 1964: Iliffe Books Ltd, London.
15. Gírio, F.M., et al., *Hemicelluloses for fuel ethanol: A review.* Bioresource Technology, 2010. **101**(13): p. 4775-4800.
16. R.Janes, *The chemistry of wood and fibers*, in *The pulping of wood*, J.N.F. R.G. Macdonald, Editor. 1969.
17. Chakar, F.S. and A.J. Ragauskas, *Review of current and future softwood kraft lignin process chemistry.* Industrial Crops and Products, 2004. **20**(2): p. 131-141.
18. Bielecki, S., et al., *Bacterial Cellulose*, in *Biopolymers Online*. 2005, Wiley-VCH Verlag GmbH & Co. KGaA.
19. Zhang, S. and J. Luo, *Preparation and properties of bacterial cellulose/alginate blend bio-fibers.* The Journal of Engineered Fibers and Fabrics, 2011. **6**(3): p. 4.
20. Kroon-Batenburg, L.M.J. and J. Kroon, *The crystal and molecular structures of cellulose I and II.* Glycoconjugate Journal, 1997. **14**(5): p. 677-690.
21. Nishiyama, Y., et al., *Crystal Structure and Hydrogen Bonding System in Cellulose Iα from Synchrotron X-ray and Neutron Fiber Diffraction.* Journal of the American Chemical Society, 2003. **125**(47): p. 14300-14306.
22. Langan, P., Y. Nishiyama, and H. Chanzy, *A Revised Structure and Hydrogen-Bonding System in Cellulose II from a Neutron Fiber Diffraction Analysis.* Journal of the American Chemical Society, 1999. **121**(43): p. 9940-9946.
23. Himmel, M.E., et al., *Biomass Recalcitrance: Engineering Plants and Enzymes for Biofuels Production.* Science, 2007. **315**(5813): p. 804-807.
24. Zobel, H.F., *Molecules to Granules: A Comprehensive Starch Review.* Starch - Starke, 1988. **40**(2): p. 44-50.
25. Zhuojun Meng, X.Z., Keyong Tang, Jie Liu, Shufa Qin, *Dissolution of natural polymers in ionic liquids: A review.* e-Polymers, 2012. **028**.
26. Zhu, S., et al., *Dissolution of cellulose with ionic liquids and its application: a mini-review.* Green Chemistry, 2006. **8**(4): p. 325-327.

27. Wang, H., G. Gurau, and R.D. Rogers, *Ionic liquid processing of cellulose.* Chemical Society Reviews, 2012. **41**(4): p. 1519-1537.
28. Nikitin, N.I., *The Chemistry of Cellulose and Wood*. Vol. 1. 1966: Israel Program for Scientific Translations Ltd.
29. E.Kline, *Xanthates*, in *Cellulose and cellulose derivatives part II*. 1954, Interscience publishers.
30. Bridgeford, D., *Thin-walled low plasticizer content regenerated cellulose sausage casing*. 1981: WO 82/ 02649.
31. Wertz, J., O. Bedue, and J.P. Mercier, *Cellulose science and technology*. 2010.
32. Diener, A. and G. Raouzeos, *Continuous dissolution process of cellulose in NMMO.* Chemical fibers international, 1999. **49**: p. 40-42.
33. Just, E.K. and T.G. Majewicz, *Cellulose Ethers*, in *Encyclopaedia of Polymer Science and Engineering*. 1985, John Wiley and Sons. p. 226-269.
34. O'Driscoll, E., *Personal communication - cellulose ethers*. 2009: Dow Wolff Cellulosics.
35. Balser, K., et al., *Cellulose Esters*, in *Ullmann's Encyclopedia of Industrial Chemistry*. 2000, Wiley-VCH Verlag GmbH & Co. KGaA.
36. Brydson, J.A., *The Historical Development of Plastics Materials*, in *Plastics Materials (Seventh Edition)*. 1999, Butterworth-Heinemann: Oxford. p. 1-18.
37. Brydson, J.A., *22 - Cellulose Plastics*, in *Plastics Materials (Seventh Edition)*. 1999, Butterworth-Heinemann: Oxford. p. 613-634.
38. Bernoulli, A.L., M. Schenk, and W. Hagnebuch, *Vergleichende Untersuchungen über Quellung und Acetylierung von Cellulose.* Helvetica Chimica Acta, 1930. **13**(4): p. 534-571.
39. Fujimoto, T., et al., *Reaction of cellulose with formic acid and stability of cellulose formate.* Journal of Polymer Science Part C: Polymer Letters, 1986. **24**(10): p. 495-501.
40. Rustemeyer, P., *1. History of CA and evolution of the markets.* Macromolecular Symposia, 2004. **208**(1): p. 1-6.
41. *Eastman cellulose -based specialty polymers*. 2009, Eastman chemical company.
42. *Eastman cellulose esters for pharmaceutical drug delivery*. 2005, Eastman chemical company.
43. Saunders, C.W. and L.T. Taylor, *A review of the synthesis, chemistry and analysis of nitrocellulose.* Journal of Energetic Materials, 1990. **8**(3): p. 149-203.
44. Hummel, A., *3.2 Industrial processes.* Macromolecular Symposia, 2004. **208**(1): p. 61-80.
45. Steinmeier, H., *3. Acetate manufacturing, process and technology 3.1 Chemistry of cellulose acetylation.* Macromolecular Symposia, 2004. **208**(1): p. 49-60.
46. *T 203 cm-99 Alpha-, beta- and gamma-cellulose in pulp*. 1999, Tappi.
47. ASTM, *Standard Terminology of Cellulose and Cellulose Derivatives*, in *ASTM D1695 - 07,*. 2012, ASTM International.
48. Shelton, M.C., et al., *Low molecular weight cellulose mixed esters and their use as low viscosity binders and modifiers in coating compositions*. 2006, Eastman chemical company: WO 2006/116367 A1.
49. Saka, S. and H. Matsumura, *2.3 Wood pulp manufacturing and quality characteristics.* Macromolecular Symposia, 2004. **208**(1): p. 37-48.
50. Richter, G.A. and L.E. Herdle, *False Viscosity in Cellulose Acetate Solutions.* Industrial & Engineering Chemistry, 1957. **49**(9): p. 1451-1452.
51. Uchida, M. and H. Yabune, *Process for preparation of cellulose acetate*. 1983, Daicel Chemical Industries, Ltd.: US4415734 A.
52. Rodrigues Filho, G., et al., *Synthesis and characterization of cellulose acetate produced from recycled newspaper.* Carbohydrate Polymers, 2008. **73**(1): p. 74-82.
53. Cheng, H.N., et al., *Synthesis of cellulose acetate from cotton by products.* Carbohydrate Polymers, 2010. **80**(2): p. 449-452.
54. Sczostak, A., *Cotton Linters: An Alternative Cellulosic Raw Material.* Macromolecular Symposia, 2010. **294**(2): p. 151-151.
55. Putz, H.J., *Introduction*, in *Handbook of Pulp*. 2006, Wiley-VCH Verlag GmbH. p. 1147-1152.
56. Dahl, C.F., *Process of manufacturing cellulose from wood*. 1884: US 296935.
57. *North American pulping and bleaching chemicals markets*. 2008, Frost and Sullivan.
58. Smook, G.A., *Handbook for pulp and paper technologists*. 1982: Wiley.
59. Clayton, D.W., *The chemistry of alkaline pulping*, in *The pulping of wood*. 1969.

60. Saka, S., K. Takanashi, and H. Matsumura, *Effects of solvent addition to acetylation medium on cellulose triacetate prepared from low-grade hardwood dissolving pulp.* Journal of Applied Polymer Science, 1998. **69**(7): p. 1445-1449.
61. Lonnberg, B., *Industrial cellulose* in *Regenerated cellulose fibres*. 2001, Woodhead Publishing. p. 22-36.
62. Fidale, L.C., et al., *Cellulose Swelling by Aprotic and Protic Solvents: What are the Similarities and Differences?* Macromolecular Chemistry and Physics, 2008. **209**(12): p. 1240-1254.
63. El Seoud, O., et al., *Cellulose swelling by protic solvents: which properties of the biopolymer and the solvent matter?* Cellulose, 2008. **15**(3): p. 371-392.
64. Klemm, D., et al., *Comprehensive cellulose chemistry volume 1*. 1998: Wiley.
65. Burley, R. and L.S. Slota, *Method for acetylating shredded cellulosic*. 1991, Courtaulds Plc: US 5036900 A.
66. Burley, R. and P. Roche, *Process for the production of cellulose acetate from wood pulp*. 1992: US 5114535 A.
67. Hincke, W. and C. Malm, *Activation of cellulose for acetylation*. 1945, Eastman Kodak Company: US 2478396.
68. Rosenthal, A.J., *The role of acid catalysts in the manufacture of callulose acetate.* Pure and applied chemistry, 1967. **14**(3-4): p. 535-546.
69. Malm, C.J. and G.D. Hiatt, *C. Organic esters*, in *Cellulose and cellulose derivatives part II*. 1954.
70. Vaca-Garcia, C. and M.E. Borredon, *Solvent-free fatty acylation of cellulose and lignocellulosic wastes. Part 2: reactions with fatty acids.* Bioresource Technology, 1999. **70**(2): p. 135-142.
71. Shimamoto, S. and A. Higuchi, *Cellulose ester and process for production method thereof*. 2007: EP 1792981 A1.
72. Bogan, R.T. and R.J. Brewer, *Cellulose Esters, Organic*, in *Encyclopaedia of Polymer Science and Engineering*, J.I. Kroschwitz, Editor. 1985, John Wiley and Sons. p. 158-181.
73. Malm, C.J. and L.J. Tanghe, *Chemical Reactions in the Making of Cellulose Acetate.* Industrial & Engineering Chemistry, 1955. **47**(5): p. 995-999.
74. Malm, C.J., L.J. Tanghe, and B.C. Laird, *Preparation of Cellulose Acetate - Action of Sulfuric Acid.* Industrial & Engineering Chemistry, 1946. **38**(1): p. 77-82.
75. Akim, E.L., *On the mechanism of cellulose acetylation.* Pure and applied chemistry, 1967. **14**(3-4): p. 475-480.
76. Yamashita, M., *Method and apparatus for acetylating cellulose*. 1999: US 5869646.
77. Hiller, L.A., *The reaction of cellulose acetate with acetic acid and water.* Journal of Polymer Science, 1953. **10**(4): p. 385-423.
78. Fordyce, C., *Hydrolyzed cellulose acetate*. 1938, Eastman Kodak: US 2129052.
79. Maim, C.J., et al., *CELLULOSE DERIVATIVES - Far-Hydrolyzed Cellulose Acetates.* Industrial & Engineering Chemistry, 1957. **49**(1): p. 79-83.
80. Cox, M.K. and T.J. Frederick, *Continuous hydrolysis of cellulose acetate*. 1994, Eastman chemical company: US 5364935 A.
81. Malm, C.J., L.J. Tanghe, and B.C. Laird, *Primary Hydroxyl Groups in Hydrolyzed Cellulose Acetate1.* Journal of the American Chemical Society, 1950. **72**(6): p. 2674-2678.
82. Malm, C.J., et al., *Hydrolysis of Cellulose Esters.* Industrial & Engineering Chemistry Process Design and Development, 1966. **5**(1): p. 81-87.
83. Touey, G.P. and J.E. Kiefer, *Method of preparing cellulose esters*. 1957: US2861069.
84. Volberg, F.M. and M.D. Martin, *Powder precipitation of cellulose esters of fatty acids of 3-4 carbon atoms*. 1955: US 2824098.
85. Garetto, G., V. Novara, and C. Canciani, *Method of precipitating and forming granules from cellulose ester*. 1968, Rhodiatoce: US 3414640.
86. Eastman Chemical, C., *Cellulose esters, Eastman Cellulose acetate butyrate CAB-381-2 and CAB-381-20*. 2001, Eastman Chemical, Company.
87. Brewer, R. and R. Bogan, *High temperature bleaching method for cellulose esters*. 1982, Eastman Kodak Company: US 4342865.
88. Edgar, K.J., *Cellulose Esters, Organic*, in *Encyclopaedia of Polymer Science and Technology*. 2004, John Wiley & Sons, Inc.

89. Geurden, J., *Heterogeneous process for acetylation of cellulose.* Pure and applied chemistry, 1967. **14**(3-4): p. 507-522.
90. Malm, C.J., C.R. Fordyce, and H.A. Tanner, *Properties of Cellulose Esters of Acetic, Propionic, and Butyric Acids.* Industrial & Engineering Chemistry, 1942. **34**(4): p. 430-435.
91. Klemm, D., et al., *Comprehensive cellulose chemistry volume 2*. 1998: Wiley.
92. Sealey, J.E., et al., *Novel cellulose derivatives. V. Synthesis and thermal properties of esters with trifluoroethoxy acetic acid.* Journal of Polymer Science Part B: Polymer Physics, 2000. **38**(3): p. 486-494.
93. Painter, P.C. and M.M. Coleman, *Fundamentals of polymer science*. Vol. 299. 1997: Technomic Lancaster, PA.
94. Szcześniak, L., A. Rachocki, and J. Tritt-Goc, *Glass transition temperature and thermal decomposition of cellulose powder.* Cellulose, 2008. **15**(3): p. 445-451.
95. Paes, S., et al., *The glass transition and crystallization of ball milled cellulose.* Cellulose, 2010. **17**(4): p. 693-709.
96. Mandelkern, L. and P.J. Flory, *Melting and Glassy State Transitions in Cellulose Esters and their Mixtures with Diluents1,2.* Journal of the American Chemical Society, 1951. **73**(7): p. 3206-3212.
97. Crépy, L., et al., *Effect of side chain length on structure and thermomechanical properties of fully substituted cellulose fatty esters.* Carbohydrate Polymers, 2011. **83**(4): p. 1812-1820.
98. Vaca-Garcia, C., et al., *Dynamic mechanical thermal analysis transitions of partially and fully substituted cellulose fatty esters.* Journal of Polymer Science Part B: Polymer Physics, 2003. **41**(3): p. 281-288.
99. Sealey, J.E., et al., *Novel cellulose derivatives. IV. Preparation and thermal analysis of waxy ester of cellulose.* Journal of Polymer Science, 1996. **34**: p. 1613-1620.
100. Klarman, A.F., A.V. Galanti, and L.H. Sperling, *Transition temperatures and structural correlations for cellulose triesters.* Journal of Polymer Science Part A-2: Polymer Physics, 1969. **7**(9): p. 1513-1523.
101. Ogura, K., et al., *Infrared spectroscopic studies of polymer transitions, 4. A second-order transition of cellulose triacetate in the vicinity of 30°C.* Die Makromolekulare Chemie, 1975. **176**(4): p. 1173-1178.
102. Vaca-Garcia, C., et al., *Cellulose esterification with fatty acids and acetic anhydride in lithium chloride / n,n-dimethlyacetamide medium.* Journal of the American Oil Chemists Society, 1998. **75**: p. 315-319.
103. Glasser, W.G., U. Becker, and J.G. Todd, *Novel cellulose derivatives. Part VI. Preparation and thermal analysis of two novel cellulose esters with fluorine-containing substituents.* Carbohydrate Polymers, 2000. **42**(4): p. 393-400.
104. Glasser, W.G., et al., *Novel cellulose derivatives. III. Thermal analysis of mixed esters with butyric and hexanoic acid.* Journal of Polymer Science Part B: Polymer Physics, 1995. **33**(14): p. 2045-2054.
105. *Asia Pacific remained the largest consumer of levulinic acid in 2013: Grand view research.* SpecialChem, 2014: p. 1-82.
106. Bozell, J.J., et al., *Production of levulinic acid and use as a platform chemical for derived products.* Resources, Conservation and Recycling, 2000. **28**(3-4): p. 227-239.
107. Rackemann, D.W. and W.O.S. Doherty, *The conversion of lignocellulosics to levulinic acid.* Biofuels, Bioproducts and Biorefining, 2011. **5**(2): p. 198-214.
108. Thomas, J.J. and R.G. Barile, *Conversion of cellulose hydrolysis products to fuels and chemical feedstocks*, in *Energy from biomass and wastes VIII*. 1984. p. 1461-1494.
109. Kuster, B.F.M., *5-Hydroxymethylfurfural (HMF). A Review Focussing on its Manufacture.* Starch - Starke, 1990. **42**(8): p. 314-321.
110. Fitzpatrick, S., *Production of levulinic acid from carbohydrate-containing materials*. 1997, Biofine Incorperated: US 5608105 A.
111. Hayes, D.J., et al., *The Biofine Process - Production of Levulinic Acid, Furfural, and Formic Acid from Lignocellulosic Feedstocks*, in *Biorefineries-Industrial Processes and Products*. 2005, Wiley-VCH Verlag GmbH. p. 139-164.
112. Ghorpade, V.M. and M.A. Hanna, *Method and apparatus for production of levulinic acid via reactive extrusion*. 1999: US 5859263.
113. Moens, L. *Sugar Cane as a Renewable Feedstock for the Chemical Industry: Challenges and Opportunites*. in *Advances in the chemistry and processing of beet and cane sugar*. 2002.
114. Mench, J.W., B. Fulkerson, and G.D. Hiatt, *Valeric Acid Esters of Cellulose.* I&EC Product Research and Development, 1966. **5**(2): p. 110-115.

115. McCormick, C.L., P.A. Callais, and B.H. Hutchinson, *Solution studies of cellulose in lithium chloride and N,N-dimethylacetamide.* Macromolecules, 1985. **18**(12): p. 2394-2401.
116. Heinze, T., K. Schwikal, and S. Barthel, *Ionic Liquids as Reaction Medium in Cellulose Functionalization.* Macromolecular Bioscience, 2005. **5**(6): p. 520-525.
117. Heinze, T., et al., *Interactions of Ionic Liquids with Polysaccharides – 2: Cellulose.* Macromolecular Symposia, 2008. **262**(1): p. 8-22.
118. Heinze, T., et al., *Novel Bulky Esters of Cellulose.* Macromolecular Bioscience, 2007. **7**(11): p. 1225-1231.
119. Vladimirova, T.V., et al., *Structure and properties of cellulose and its derivatives. CLXXII. The synthesis of cellulose esters containing keto-groups.* Polymer Science U.S.S.R., 1965. **7**(5): p. 868-873.
120. Edwards, J.V., et al., *Wound dressings with proteases lowering activity*. 2003: US 6627785.
121. Tsukatani, T., et al., *Method for producing cellulose levulinate*, c. Nicca chemical, Editor. 2003: JP 2003082001.
122. Hassner, A., et al., *Levulinic esters. Alcohol protecting group applicable to some nucleosides.* Journal of the American Chemical Society, 1975. **97**(6): p. 1614-1615.
123. Rasmussen, R.S. and R.R. Brattain, *Infrared spectra of some carboxylic acid derivatives.* Journal of the American Chemical Society, 1949. **71**: p. 1073-1079.
124. Bredt, J., *Ueber Acetyllävulinsäure und die Constitution der γ-Ketonsäuren; Zweite Abhandlung.* Justus Liebigs Annalen der Chemie, 1890. **256**(3): p. 314-340.
125. Suami, T. and A. Day, *Preparation of 5-Chloro- and 5-Bromo-2-acetylethyl benzimidazoles.* The Journal of Organic Chemistry, 1959. **24**(9): p. 1340-1343.
126. R. Lukes and V. Prelog, *Sur Les Arylamides Levuliques.* Collection Czechoslovak Chemical Communications, 1929. **1**.
127. Leonard, R., *Method of converting levulinic acid into alpha angelica lactone*. 1957: US 2809203.
128. Gilmour, R., *Constitution of the methyl pentoses part 1.* Journal of the Chemical Society, 1914.
129. Timokhin, B.V., V.A. Baransky, and G.D. Eliseeva, *Levulinic acid in organic synthesis.* Russian Chemical Reviews, 1999. **68**(1): p. 73-84.
130. D. Langlois, H.W., *Pseudo esters of levulinic acid*. 1950, A.E. Staley Manufacturing Company: US2493676.
131. Shu, C.K. and B.M. Lawrence, *Formation of 4-alkoxy-g-valerolactones from levulinic acid and alcohols during storage at room temperature.* Journal of Agricultural and food chemistry, 1995. **43**: p. 782-784.
132. Kim, T., et al., *Acid-Catalyzed Furfuryl Alcohol Polymerization: Characterizations of Molecular Structure and Thermodynamic Properties.* ChemCatChem, 2011. **3**(9): p. 1451-1458.
133. Marvel, C.S. and C.L. Levesque, *The Structure of Vinyl Polymers. III.1 The Polymer from α-Angelica Lactone.* Journal of the American Chemical Society, 1939. **61**(7): p. 1682-1684.
134. Heinze, T. and T. Liebert, *4.2 Chemical characteristics of cellulose acetate.* Macromolecular Symposia, 2004. **208**(1): p. 167-238.
135. Lowman Douglas, W., *Characterization of Cellulose Esters by Solution-State and Solid-State NMR Spectroscopy*, in *Cellulose Derivatives*. 1998, ACS Symposium Series. p. 131-162.
136. Genung, L. and R. Mallatt, *Analysis of Cellulose Derivatives: Determination of Total Combined Acyl in Cellulose Organic Esters.* Industrial & Engineering Chemistry Analytical Edition, 1941. **13**(6): p. 369-374.
137. Garetto, G. and A. Ruffoni, *Determination of Combined Acetic Acid Content of Cellulose Acetate.* Analytical Chemistry, 1955. **27**(3): p. 400-401.
138. Genung, L.B., *Analysis of Cellulose Derivatives.* Analytical Chemistry, 1950. **22**(3): p. 401-405.
139. ASTM, *Standard Test Methods of Testing Cellulose Acetate Propionate and Cellulose Acetate Butyrate1*, in *ASTM D817-96,*. 2010. p. 1-15.
140. Buchanan, C.M., J.A. Hyatt, and D.W. Lowman, *2D-NMR of polysaccharides: spectral assignments of cellulose triesters.* Macromolecules, 1987. **20**(11): p. 2750-2754.
141. Iwata, T., et al., *Preparation and n.m.r. assignments of cellulose mixed esters regioselectively substituted by acetyl and propanoyl groups.* Carbohydrate Research, 1992. **224**(0): p. 277-283.
142. Goux, W.J., *The assignment of carbonyl resonances in 13C-n.m.r. spectra of peracetylated mono- and oligo-saccharides containing D-glucose and D-mannose: an alternative method for structural determination of complex carbohydrates.* Carbohydrate Research, 1987. **159**: p. 191-210.

143. Tezuka, Y., *13C NMR determination of the distribution of two ester substituents in cellulose acetate butyrate.* Carbohydrate Research, 1993. **241**(0): p. 285-290.
144. Tezuka, Y. and Y. Tsuchiya, *Determination of substituent distribution in cellulose acetate by means of a 13C NMR study on its propanoated derivative.* Carbohydrate Research, 1995. **273**(1): p. 83-91.
145. Usmanov, T.I., et al., *NMR study of constituent unit distribution in cellulose acetates.* Polymer Science U.S.S.R., 1986. **28**(7): p. 1658-1666.
146. Fox, S.C., et al., *Regioselective Esterification and Etherification of Cellulose: A Review.* Biomacromolecules, 2011. **12**(6): p. 1956-1972.
147. Heinze, T. and T. Liebert, *Unconventional methods in cellulose functionalization.* Progress in Polymer Science, 2001. **26**(9): p. 1689-1762.
148. Malm, C.J., et al., *Relative Rates of Acetylation of the Hydroxyl Groups in Cellulose Acetate.* Journal of the American Chemical Society, 1953. **75**(1): p. 80-84.
149. Yu, N. and G.R. Gray, *Analysis of the positions of substitution of acetate and propionate groups in cellulose acetate-propionate by the reductive-cleavage method.* Carbohydrate Research, 1998. **313**(1): p. 29-36.
150. Yu, N. and G.R. Gray, *Analysis of the positions of substitution of acetate and butyrate groups in cellulose acetate–butyrate by the reductive-cleavage method.* Carbohydrate Research, 1998. **312**(4): p. 225-231.
151. Lee, C.K. and G.R. Gray, *Analysis of positions of substitution of O-acetyl groups in partially O-acetylated cellulose by the reductive-cleavage method.* Carbohydrate Research, 1995. **269**(1): p. 167-174.
152. Heinrich, J. and P. Mischnick, *Determination of the substitution pattern in the polymer chain of cellulose acetates.* Journal of Polymer Science Part A: Polymer Chemistry, 1999. **37**(15): p. 3011-3016.
153. Mischnick, P., *Determination of the Substitution Pattern of Cellulose Acetates.* Journal of Carbohydrate Chemistry, 1991. **10**(4): p. 711-722.
154. Arndt, P., et al., *Preparation of Cellulose Oligomers from Cellulose Triacetate (Standard Procedure).* Cellulose, 2005. **12**(3): p. 317-326.
155. Kowsaka, K., K. Okajima, and K. Kamide, *Determination of the Distribution of the Substituent Group in Cellulose Acetate by Full Assignment of Au Carbonyl Carbon Peaks of 13C {1H} NMR Spectra.* Polymer Journal, 1988. **20**(10): p. 827-836.
156. Goodlett, V.W., J.T. Dougherty, and H.W. Patton, *Characterization of cellulose acetates by nuclear magnetic resonance.* Journal of Polymer Science Part A-1 Polymer Chemistry, 1971. **9**(1): p. 155-161.
157. Goux, W.J. and D.S. Weber, *The application of NMR-pattern-recognition methods to the classification of reduced, peracetylated oligosaccharide residues.* Carbohydrate Research, 1993. **240**: p. 57-69.
158. Allavudeen, S.S., B. Kuberan, and D. Loganathan, *A method for obtaining equilibrium tautomeric mixtures of reducing sugars via glycosylamines using nonaqueous media.* Carbohydrate Research, 2002. **337**(10): p. 965-968.
159. William Tindall, G., B.W. Boyd, and R.L. Perry, *Determination of acid substituents and unesterified hydroxyl groups in cellulose esters.* Journal of Chromatography A, 2002. **977**(2): p. 247-250.
160. Sano, A., et al., *Determination of levulinic acid in soy sauce by liquid chromatography with mass spectrometric detection.* Food Chemistry, 2007. **105**(3): p. 1242-1247.
161. Roxin, P., A. Karlsson, and S.K. Singh, *Characterization of Cellulose Acetate Phthalate (CAP).* Drug Development and Industrial Pharmacy, 1998. **24**(11): p. 1025-1041.
162. Yau, W., J. Kirkland, and D. Bly, *Modern size exclusion liquid chromatography*. 1979: Wiley.
163. Knobloch, J. and P. Shaklee, *Analysis of low molecular weight heparin products by SEC/MALLS*. 1996, Scientific protein laboratories
164. Meunier, D., *Molecular weight determinations*, in *Handbook of Instrumental Techniques for Analytical Chemistry*.
165. Greene, T. and p. Wuts, *Protective groups in organic synthesis*. 2nd ed. 1991: John Wiley and Sons Inc.
166. Biswas, A., et al., *Iodine catalyzed esterification of cellulose using reduced levels of solvent.* Carbohydrate Polymers, 2007. **68**(3): p. 555-560.
167. Gibney, K., J. Howard, and R. Evans, *Production of cellulose esters*. 1975, Canadian Cellulose Company: US3870703.

168. Ritter, G.J., *Determination of alpha-cellulose.* Industrial & Engineering Chemistry Analytical Edition, 1929. **1**(1): p. 52-54.
169. Brewer, R.J. and B.S. Wininger, *catalyst for and methods of preparing cellulose esters*. 1982, Eastamn Kodak, company: US 4314056.
170. Wininger, B.S., *Methods of preparing cellulose esters*, c. Eastman Kodak, Editor. 1982: US 4329446.
171. *Methane sulfonic acid (MSA) an ideal catalyst for esterification*. Arkema.
172. Touey, G.P. and J.E. Kiefer, *Method of preparing cellulose esters*. 1958, Eastamn Kodak, company: US 2861069.
173. Takahashi, A. and S. Takahashi, *Study on Acetylcellulose Sulfamic Acid, Ammonium Sulfamate, Hydroxylamine Sulfate as Catalyst of Acetylation.* Kobunshi Kagaku, 1969. **26**(291): p. 485-490.
174. Malm, C. and B. Blanchard, *Manufacture of cellulose esters having a high propionyl or butyryl content*. 1945, Eastman Kodak company: US 2379310.
175. Yan, L., et al., *Solvent-free Synthesis of Cellulose Acetate by Solid Superacid Catalysis.* Journal of Polymer Research, 2006. **13**(5): p. 375-378.
176. Hansen, C.M., *Hansen solubility parameters: a user's handbook*. 2012: CRC press.
177. Saka, S. and K. Takanashi, *Cellulose triacetate prepared from low-grade hardwood dissolving pulp and its insoluble residues in acetylation mediums.* Journal of Applied Polymer Science, 1998. **67**(2): p. 289-297.
178. Shashidhara, G.M. and K.H. Guruprasad, *Effect of concentrated sulfuric acid and nitroethane on insoluble residues in acetylating medium of cellulose acetate prepared from low grade pulps.* Journal of Applied Polymer Science, 2005. **98**(4): p. 1765-1771.
179. Barton, A.F.M., *CRC Handbook of Solubility Parameters and Other Cohesion Parameters, Second edition*. 1991.
180. Enterprises, D., *Surface Tension, Hansen Solubility Parameters, Molar Volume, Enthalpy of Evaporation, and Molecular Weight of Selected Liquids* 2010.
181. Allen, T.C. and J.A. Cuculo, *Cellulose derivatives containing carboxylic acid groups.* Journal of Polymer Science: Macromolecular Reviews, 1973. **7**(1): p. 189-262.
182. Allen, J., et al., *Carboxyalkyl cellulose esters*. 1997, Eastman Chemical company: US 5668273 A.
183. Heinze, T. and A. Koschella, *Carboxymethyl Ethers of Cellulose and Starch – A Review.* Macromolecular Symposia, 2005. **223**(1): p. 13-40.
184. Allen, J., et al., *Process for preparing carboxyalkyl cellulose esters*. 1998, J. Allen,L. Curtis,P. Lucas,A. Wilson: US 5792856 A.
185. J. Posey-Dowty, A.K., L. Curtis, P. Swan, K. Seo, *Carboxyalkyl cellulose esters for use in aqueous pigment dispersions*. 1999, Eastman Chemical Corporation: US 5994530 A.
186. Malm, C.J., et al., *Preparation of Phthalic Acid Esters of Cellulose.* Industrial & Engineering Chemistry, 1957. **49**(1): p. 84-88.
187. Edgar, K.J., et al., *Advances in cellulose ester performance and application.* Progress in Polymer Science, 2001. **26**(9): p. 1605-1688.
188. Clayden, J., et al., *Organic chemistry*. 2001: Oxford University Press.
189. Lambert, J., et al., *Organic structural spectroscopy*. 1998: Prentice -Hall.
190. Liu, J., et al., *Keto-Functionalized Polymer Scaffolds as Versatile Precursors to Polymer Side-Chain Conjugates.* Macromolecules, 2012. **46**(1): p. 8-14.
191. Rao, J.P. and K.E. Geckeler, *Polymer nanoparticles: Preparation techniques and size-control parameters.* Progress in Polymer Science, 2011. **36**(7): p. 887-913.
192. Dieterich, D., *Aqueous emulsions, dispersions and solutions of polyurethanes; synthesis and properties.* Progress in Organic Coatings, 1981. **9**(3): p. 281-340.
193. Vitale, S.A. and J.L. Katz, *Liquid Droplet Dispersions Formed by Homogeneous Liquid−Liquid Nucleation: "The Ouzo Effect".* Langmuir, 2003. **19**(10): p. 4105-4110.
194. Ganachaud, F. and J.L. Katz, *Nanoparticles and Nanocapsules Created Using the Ouzo Effect: Spontaneous Emulsification as an Alternative to Ultrasonic and High-Shear Devices.* ChemPhysChem, 2005. **6**(2): p. 209-216.
195. Wondraczek, H., et al., *Nanoparticles from conventional cellulose esters: evaluation of preparation methods.* Cellulose, 2013. **20**(2): p. 751-760.

196. Hornig, S. and T. Heinze, *Efficient Approach To Design Stable Water-Dispersible Nanoparticles of Hydrophobic Cellulose Esters.* Biomacromolecules, 2008. **9**(5): p. 1487-1492.
197. Kulterer, M.R., et al., *Nanoprecipitation of cellulose acetate using solvent/nonsolvent mixtures as dispersive media.* Colloids and Surfaces A: Physicochemical and Engineering Aspects, 2011. **375**(1–3): p. 23-29.
198. Coney, C.H., *Cellulose acetate butyrate emulsion coating*. 1965, Eastamn Kodak, company: US 3220865.
199. Sastry, S.V., et al., *Aqueous-based polymeric dispersion: preparation and characterization of cellulose acetate pseudolatex.* International journal of pharmaceutics, 1998. **165**(2): p. 175-189.
200. Vaithiyalingam, S., et al., *Preparation and characterization of a customized cellulose acetate butyrate dispersion for controlled drug delivery.* Journal of Pharmaceutical Sciences, 2002. **91**(6): p. 1512-1522.
201. Suryya K. Das, F.C.B., Soner Kilic, Robyn E. McMillan, *Stable aqueous dispersions of cellulose esters and their use in coatings*. 2000, PPG Industries: US 6046259.
202. Quintanar-Guerrero, D., et al., *Pseudolatex preparation using a novel emulsion–diffusion process involving direct displacement of partially water-miscible solvents by distillation.* International Journal of Pharmaceutics, 1999. **188**(2): p. 155-164.
203. *Aqueous coating enteric, Aquacoat CPD*, FMC, Editor. 2006, FMC BioPolymer.
204. Kim, B.K., *Aqueous polyurethane dispersions.* Colloid and Polymer Science, 1996. **274**(7): p. 599-611.
205. Dieterich, D., W. Keberle, and H. Witt, *Polyurethane Ionomers, a New Class of Block Polymers.* Angewandte Chemie International Edition in English, 1970. **9**(1): p. 40-50.
206. Williams, C., F. Brochard, and H.L. Frisch, *Polymer Collapse.* Annual Review of Physical Chemistry, 1981. **32**(1): p. 433-451.
207. Zhang, C., et al., *Flash nanoprecipitation of polystyrene nanoparticles.* Soft Matter, 2012. **8**(1): p. 86-93.
208. J. Nothnagel, M.C., M. He, J. Fletcher, *Stable aqueous polymer dispersions and a process for their preparation*. 2001, McWhorter Technologies: US 6277953 B1.
209. McCreight, K., D. Webster, and L. Kemp, *Aqueous dispersions of carboxylated cellulose esters, and methods of making them*. 2005: US2005/0203278 A1.
210. Nanda, A.K. and D.A. Wicks, *The influence of the ionic concentration, concentration of the polymer, degree of neutralization and chain extension on aqueous polyurethane dispersions prepared by the acetone process.* Polymer, 2006. **47**(6): p. 1805-1811.
211. Lee, S.Y., J.S. Lee, and B.K. Kim, *Preparation and Properties of Water-borne Polyurethanes.* Polymer International, 1997. **42**(1): p. 67-76.
212. C.Browner, *Air Quality: Revision to Definition of Volatile Organic Compounds - Exclusion of Acetone*, U.S.E.P. AGENCY, Editor. 1995.
213. ASTM, *Standard Test Method for Speciation of the Volatile Organic Compounds (VOCs) in Low VOC Content Waterborne Air-Dry Coatings by Gas Chromatography* in *ASTM standard D6886, .* 2009, ASTM International.
214. Blackley, D.C., *Polymer Latices: Science and technology Volume 1: Fundamental principles*. 1997: Springer.
215. Glenny, M., *Paint formulation and technical background*. 2012, Resene - R&D Team leader.
216. Keddie, J. and A. Routh, *Drying of Latex Films*, in *Fundamentals of Latex Film Formation*. 2010, Springer Netherlands. p. 95-120.
217. Leonard, R., *Levulinic Acid as a Basic Chemical Raw Material.* Industrial & Engineering Chemistry, 1956. **48**(8): p. 1330-1341.
218. *Eastman SAIB and Eastman Sustane SAIB (CB-37F)*. 2009, Eastamn Chemical company.
219. ASTM, *Standard Test Method for Volatile Content of Coatings*, in *ASTM D2369 - 10e1,*. 2010, ASTM International.
220. ASTM, *Standard Practice for Testing Low Temperature Film-Formation of Latex Paints by Visual Observation*, in *ASTM D7306 - 07,*. 2007, ASTM International.
221. Sigma-Aldrich, *Online database* http://www.sigmaaldrich.com/new-zealand.html. 2013.
222. ASTM, *Standard Test Methods for Sodium Carboxymethylcellulose*, in *ASTM D1439 - 03(2008)e1* 2008, ASTM International.